TITLE: ELECTROKINETIC AND OTHER TRANSPORT PROPERTIES OF CHARGED MEMBRANES UNDER PRESSURE FORCES: AN IRREVERSIBLE THERMODYNAMIC ANALYSIS

SUBMITTED BY

IAN SHEARER BURKE

FOR THE DEGREE OF

PhD

IN THE

DEPARTMENT OF CHEMISTRY

NOVEMBER, 1974.

This Thesis is dedicated to tho three people.

whose help and encouragement aided most in its completion.

To: Andy Hislop.

My Mother

Margaret

My thanks to my Supervisor, Dr. R. Paterson for his guidance and encouragement during the work and to Mr. J. Walker for a great deal of help, especially during the construction of the Reverse Osmosis system. A special thanks to the Engineering workshop who accomplished a very difficult task most efficiently and to the other University services, especially the glass blowing workshop.
To Mr. Antony Yi Yan of the Mechanical Engineering Department goes my thanks for the use of the high pressure Reverse Osmosis system and for his general help and guidance. Finally, my thanks goes to my colleague Andrew Agnew for much help during the three years of this study.

CONTENTS

CONTENTS

CONTENTS

CONTENTS

TABLES

FIGURES

FIGURES

FIGURES

SUMMARY

In order to obtain an impression of the factors which are significant in the process of desalination by Reverse Osmosis, a series of AMF C_{60} polyethylene-polystyrene sulphonic acid membranes with varying water contents and co-ion capacities were prepared by a heat treatment process. Amongst this series a C_{60} Normal and Expanded membrane were found to be similar to the membranes investigated by earlier workers. In this earlier study, using an irreversible thermodynamic approach, the phenomenological coefficients which define the membrane transport processes were obtained under isothermal and isobaric conditions. Using these original phenomenological coefficients a calculation was evolved in this study which could be used to predict the pressure induced transport properties of the two C_{60} membranes. These predicted Reverse Osmosis characteristics and those measured closely agreed. This calculation can therefore be used to predict these properties for any membrane system for which the appropriate data exists and could thus be usefully used in a preliminary survey of Reverse Osmosis characteristics. However, since a complete irreversible thermodynamic analysis is a lengthy process, the use of the predictive calculation is restricted. This restriction might be, to a degree, overcome if an alternative method of obtaining phenomenological coefficients could be obtained. One means of doing this would be to find an accurate and accessible analogue system.

Results from other work on the C_{60} membrane suggested that the polystyrene-sulphonate matrix has similar kinetic characteristics to chloride ion in aqueous solution. Indeed, the measured transport properties of the membrane, once corrected for tortuosity, were similar to those of a simple binary chloride solution.

In/

In this study it is proposed that the C_{60} membrane is modelled by an equimolal electrolyte solution where co-ions of two types are present, one of which is fixed relative to the membrane matrix. The relationship of these two species is taken to be that between chemically identical, but physically distinguishable isotopes.

Thus, by adapting the phenomenological coefficients of a simple binary solution to apply to a ternary solution of the same electrolyte containing the isotopic co-ion species, a precise definition of the phenomenological coefficients of the model can be expressed.

Once the tortuosity of the membrane matrix was accounted for by a suitable scaling factor, phenomenological coefficients, which represented an experimental membrane, were obtained. This salt model calculation (S.M.C.) also provided transport numbers and specific conductivities for various ionic forms. The phenomenological coefficients obtained were in good agreement with the experimental values as were the transport numbers of several of the different ionic forms.

The phenomenological coefficients from the S.M.C. were used to predict the Reverse Osmosis characteristics of the two C_{60} membranes and the success they achieved increased the application of the predictive Reverse Osmosis calculation.

The application of the Salt Model Calculation is, however, restricted since it would undoubtedly not be applicable to every membrane system since a model salt system would have to be found for each membrane and the complete irreversible thermodynamic data would be required for the binary salt. Therefore, by investigating the range of C_{60} membranes and also a range of XR-170 per-fluoro sulphonic/

sulphonic acid membranes, an impression of those membrane properties which affect the reverse osmosis characteristics was obtained and comparison made with other more commercially viable Reverse Osmosis membranes. The results indicate that a thin-film ion exchange membranes might be very successful in the field of Reverse Osmosis since they might be sculptured to meet a particular requirement. They certainly would provide good desalination and a high water flux.

The application of pressure across a membrane which is permeselective to one ion sets up a membrane pressure potential, one of the constituents of which is the membrane streaming potential. This phenomenon is somewhat ambiguously referred to in the literature and a short review is given in this study.

Using a irreversible thermodyn-mic approach, an equation was derived which defined the membrane pressure potential and each individual contributionto it. This equation separates the membrane pressure potential into contributions from the volume change of the electrodes, the difference in the activity coefficients of water and salt respectively and the streaming potential.

It was perhaps the most challenging part of this work to design and construct apparatus upon which the membrane pressure and streaming potentials could be measured. These were subsequently compared with those determined theoretically and the agreement was found to be excellent.

CHAPTER 1

INTRODUCTION AND AIMS

1.0 INTRODUCTION AND AIMS

Ion exchange membranes are usually considered to be insoluble liquids or solids which carry exchangeable ions. If an ion exchange membrane is allowed to come to equilibrium with a solution of a single electrolyte, four separate species may be distinguished in the membrane phase. These are, counter-ion, co-ion, solvent (usually water) and the fixed charge including matrix. Counter-ions have opposite signs to the fixed charges and co-ions, and, depending on the sign of the fixed charges, the membrane may be either a cation (negative fixed charge) or an anion (positive fixed charge) exchanger.

In the early 1950's synthetic ion exchange membranes which were relatively thin and mechanically strong were first produced. This coincided with the work of C.E.Reid and co-workers, on cellulose acetate membranes, in which the reverse-osmosis process of this membrane was shown to be viable alternative to desalination by distillation. These two advances stimulated much of the present day research into membrane processes.

The reverse-osmosis separation process is one of the most important fields of present day research. The term 'osmosis' is familiarly used to describe the spontaneous flow of water from a less to a more concentrated aqueous solution, when separated by a suitable semi-permeable membrane. If, by application of pressure to the concentrated solution, the osmotic flow is reversed and pore solvent passes from the concentrated solution, through the membrane into the solvent phase, then a process of desalination is taking place. This is called 'reverse-osmosis'. The terms "hyperfiltration" and "ultra-filtration" are often used as equivalent/

equivalent descriptions of this process, although ultra-filtration is now used more to describe the removal of large organic molecules by the reverse osmosis process.

When pressure is applied to the solution maintained on one side of a membrane, both salt and water are driven through the membrane. The emerging salt solution will be desalinated if the permeability of the membrane for water greatly exceeds that of salt. This situation is obtained for charged membranes because of Donnan exclusion of salt. If the Donnan exclusion is complete, no co-ions exist in the membrane phase, consequently the membrane is ideally semi-permeable for water and complete rejection of salt will occur. In real membranes, however, co-ion uptake does occur, although it is generally small. For example, for some of the experimental membranes in this study the ratio of co-ions to counter-ions in the membrane is approximately $\frac{1}{500}$. Nevertheless, under pressure of up to 1,500 lbs.in^{-2} the salt rejection never exceeds 85%. It is, therefore, not purely the equilibra between membrane and solution which determines membrane performances, thus, other membrane properties must be considered. Subsequently, one of the main topics for discussion in this thesis is the relationship between flows, applied forces and ionic concentration, in a series of membranes and how these combine to explain the experimentally observed reverse-osmosis characteristics of water flux and rejection.

In order to investigate these relations a series of membranes with varying water contents and fixed charge capacities were required. This was accomplished by expanding the basic A.M.F. C_{60} polyethylene/polystyrene sulphonic acid membrane, to different degrees by a heat treatment process. This has the effect of considerably increasing/

increasing the water content of this membrane. Since the fixed charge capacity of the A.M.F. C_{60} membrane (per unit weight of dry polymer) is constant, the increasing water content means that the internal molality of these membranes decreased with expansion. As the polymer remains constant, but the geometric distribution changes, the series of C_{60} membranes presents an ideal system for the study of the effects of water content and capacity on reverse-osmosis characteristics. In addition, a new membrane from Dupont was investigated. This was the XR-170 perfluoro sulphonic acid cation exchanger. In the series investigated the fixed charge capacity (per unit weight of dry polymer) varied. These membranes thus presented a series of differing water contents and internal molalities, allowing comparison between the two membrane types. Although both the C_{60} and XR membranes have fixed sulphonate groups, the fluorinated hydrocarbon matrix of the XR-170 membranes might be expected to affect the electron density of the sulphonate group and thus the mobility of the water and ion will be different in these membranes.

In an ion exchange membrane, due to permselectivity for one ion, the mobility of the counter-ion is greater than that of the co-ion. When pressure is applied across the membrane this causes a separation of charge and consequently sets up an electric field, which opposes the counter-ion flow and accelerates the co-ion flow. This electric field is called the streaming potential. The streaming potential is thus an intrinsic property of the membrane and depends on the difference between the interaction of counter-ion and co-ion with the fixed charge.

The practical difficulties involved in making an investigation at moderately high pressures were considerable. However, apparatus was designed and constructed which allowed the measurement of the reverse/

reverse-osmosis characteristics of the membranes, and also the measurement of the total pressure potential set up across the membrane in a reverse osmosis system. One of the two main design features was to construct the apparatus in an electrically non conducting material, in order to prevent the short circuiting of the pressure potential created and to prevent any contributions from stray potentials, which might be set up between the electrodes and any metal incorporated in the apparatus. It was also important to ensure a very high flow of solution across the high pressure face of the membrane, in order to exclude the possibility of a build up of electrolyte concentration (concentration polarization) at the membrane surface, since this would affect both the reverse osmosis characteristics and the pressure potential measurements. Once these features were accounted for, the experimental measurements could be attributed to the membrane characteristics and not to characteristics of the apparatus itself.

With the expected dependence on forces, salt permeabilities and water flow, the obvious analysis tool for this study was non equilibrium thermodynamics, where thermodyanmic forces on salt and water are defined and the flows are in turn defined by linear equations in terms of mobility coefficients and conjugate forces.

From the produced series of C_{60} membranes, two in particular were almost identical in all physical characteristics to a C_{60} normal and C_{60} expanded membrane studied previously. The irreversible thermodynamic parameters of these two original membranes were obtained in a series of experiments in which pressure forces were not applied. Phenomenological coefficients were determined for the two membranes by making a number of necessary approximations, which were considered acceptable/

in that they would not significantly affect the values obtained. With this close correlation between the original membranes and those obtained in this study, a method of calculation was evolved, using the mobility cofficients, which predicted the reverse-osmosis characteristics of these membranes and a comparison was made with the experimental results. The predicted and observed results were in excellent agreement and the method of calculation can be generalised to apply to all membranes for which mobility coefficients are known.

This, however, is a very restricting condition since the experimental determination of mobility coefficients is a lengthy and exacting task.

In previous work the analogy was drawn between experimental observations on membranes and corresponding data on concentrated electrolyte solutions, in particular between the sodium sulphonate matrix and aqueous sodium chloride. In this study this analogy has been examined and developed into a self consistent Salt Model Calculation. In this calculation a suitable model electrolyte is chosen for which a complete irreversible thermodynamic analysis is known. Using an anion fixed frame of reference, first mobility and then measured membrane parameters are predicted. The model calculations are encouraging and suggest that the kinetic interactions in a membrane are fundamentally similar to those in concentrated electrolyte solution. They also indicate the importance of such effects as tortuosity on the membrane properties.

Although the phenomenon of streaming potential has been known for a considerable time, there are very few measurements of this property reported in the literature. Indeed, in the past, there has/

has been a degree of ambiguity in the potentials reported as streaming potentials. It was the aim of this work to establish an equation which would distinguish each contribution to the total pressure potential, including the streaming potential, and to compare the calculated pressure potentials with those measured on the apparatus constructed.

The effect of a Concentration Gradient and a Concentration Plus Pressure Gradient on The Chemical Potentials and Flows of both Salt and Water

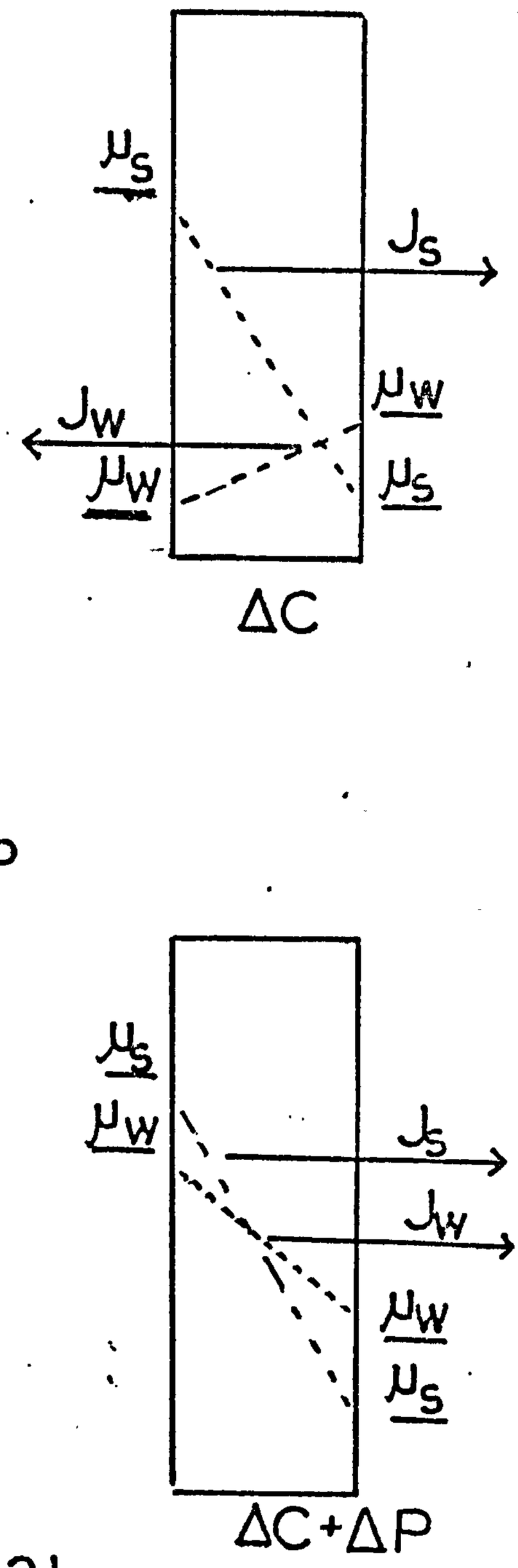

Fig 2.1

CHAPTER 2.

THEORY OF IRREVERSIBLE THERMODYNAMICS

USED IN THIS WORK

2.1 Non Equilibrium Thermodynamics

The theory of classical Thermodynamics deals almost exclusively with equilibrium states and transitions between equilibrium states which occur in a reversible manner within a defined 'system'.

Since the 'world' as a whole is not readily amenable to experimental study, certain parts of it must be isolated from their surroundings and subjected to controlled experimental conditions. These are called Thermodynamic Systems or 'Systems.' One simple method of isolation is to consider the contents of a defined geometric volume, the boundary of which is a mathematical wall which separates the system from the external world. The basis of classical Thermodynamics is contained in two fundamental laws. The first Law of Thermodynamics which defines conservation of energy, and the Second Law of Thermodynamics or Entropy Law. In Thermodynamics the function of state, entropy, is defined by the system as a whole, with mass, volume enthalpy and free energy. These are extensive parameters whereas pressure, temperature and concentration have a well-defined value at every point in the system and are intensive parameters.

A rigorous macroscopic description of non equilibrium processes (irreversible processes) must also be based on these two classical laws. It is, however, necessary to adapt the formalism of the laws to apply to the processes under consideration.

Certainly the most important contribution of irreversible Thermodynamics is that the methods of classical theory may be generalised to include time as a variable. The Thermodynamics of irreversible process has, therefore, a kinetic element which is completely/

completely lacking in classical Thermodynamics.

There exists a number of simple laws which apply to systems in non equilibrium states. In each a flow is defined and related to a 'driving force' by a constant. These laws were discovered experimentally and examples are Fick's Law of Diffusion and Ohm's Law of electrical conductance. In simple systems the flow is proportional to its conjugate force.

Flow $\propto$ Conjugate force examples are:-

Diffusional flow of water $\propto$ -grad(concentration) - Fick

Flow of current $\propto$ -grad(electrical Potential) - Ohm

Flow of heat $\propto$ -grad(T) - Fourier

It was, however, observed by early workers that when two (or more) such phenomena occurred in the same system coupling (or interference) phenomena were observed. One example is, a flow of heat may produce concentration gradients in solution (Soret effect), or conversely, concentration gradients may produce heat flow (Dufour effect). Another is, pressure, applied across a capillary may induce volume flow, but if the capillary is charged then electrical potentials (streaming potential) will be developed. Similarly, under suitable conditions in the same system, applied electrical potentials induce not only flow of electrical current, but also a non-conjugate flow of volume (electro-osmosis). This experimental evidence suggested that the simple dependence of a flow on its conjugate force does not always hold.

In 1854 Kelvin published the first Thermodynamic Study of coupling phenomena. In this he illustrated that for sufficiently slow processes any flow may depend in a direct and linear manner on not only the conjugate force, but also on other non-conjugate forces.

It/

It is this study of coupling which forms the basis of the application of non-equilibrium Thermodynamics to irreversible processes.

2.1.2. The Theory

The second law, or entropy equation forms the basis for the general theory of non-equilibrium Thermodynamics.

In order to evaluate the change in entropy accompanying an isothermal, irreversible process, consider a simple cycle:- a system enclosed by diathermal walls passes isothermally and irreversibly from state I to state II, maintaining contact with a reservoir at constant temperature. Upon reaching state II, the process is reversed and the system is brought back to state I in a reversible manner still in contact with the reservoir applied in step I to II.

For the full cycle

$$\oint dU = 0 = \oint dQ - \oint dW$$

From Kelvin's principle $\oint dW = W \leq 0$

thus $$\oint dQ = \int_1^2 dQ + \int_2^1 dQ \leq 0$$

$\int_1^2 dQ$ is the heat absorbed from the reservoir in the irreversible step.

$$\int_1^2 dQ = \triangle Q_{irr}$$

By applying $dS = dQ/T$ (Clausius equation) to the external surroundings.

$$\int_1^2 dQ = \triangle Q_{irr} = T \triangle_e S$$

$\triangle_e S$ is the entropy change between the system and its surroundings.

For the reversible process $dQ = TdS$ and

$$\int_2^1 dQ = T \int_2^1 dS = T (S_1 - S_2) = -T \triangle S$$

Therefore

$$\triangle Q_{irr} - T \triangle S = T \triangle_e S - T \triangle S \leq 0$$

which can be written

$$\triangle S \geq \triangle_e S$$

or

$$dS \geq dQ/T$$

Therefore, in an isothermal natural process the entropy of the system increases more than can be accounted for by absorption of entropy from the surroundings. A process that creates entropy has, therefore, taken place in the system.

This entropy creation is called the internal production of entropy d_iS.

It is consequently postulated that the total change in entropy is the sum of the entropy exchanged with the surroundings plus the entropy created in the system. so that

$$dS = d_iS + d_eS$$

and the equality may be written

$$d_iS \geq 0$$

thus the internal entropy production is 'positive-definite', it is equal to zero for all reversible changes and greater than zero for all irreversible processes.

The local entropy production σ for a continuous system in which irreversible processes are taking place can be described by

$$\int_V \sigma dV = {}^{d_iS}/_{dt} \qquad (2.1)$$

where σ is the rate and production of entropy per unit volume, per unit time.

In order to evaluate σ certain basic assumptions must be made and limitation applied. Local equilibrium is assumed, (if necessary, by isolating a small part of the system), the gradient of the intensive parameters cannot be large and therefore the system cannot be 'far removed from equilibrium'. Applying these conditions the entropy produced in an irreversible process with no chemical coupling is expressed by

$$\sigma = \sum_i J_i X_i \geq 0 \qquad (2.2)$$

in/

in which X_i is the conjugate force to J_i', the flow, and J_i' and X_i are independent.

It is often convenient to use instead of σ another function the dissipation function such that $\phi = T\sigma$

This has dimensions of free energy per unit time and is a measure of the rate of "Local" dissipation of free energy by an irreversible process. So that in general

$$\phi = T\sigma = \sum J_i' X_i \geq 0 \qquad (2.3)$$

If the flows are defined as those of entropy J_s and matter J_i then equation 2.2 gives

$$\sigma = J_s/T \operatorname{grad}(-T) + \sum_{i=1}^{n} J_i/T \operatorname{grad}(-\hat{\mu}_i) \qquad (2.4a)$$

and using 2.3 becomes

$$\phi = T\sigma = J_S \operatorname{grad}(-T) + \sum_{i=1}^{n} J_i \operatorname{grad}(-\hat{\mu}_i) \qquad (2.4b)$$

where, T is the absolute temperature and μ_i defined by Guggenheim[1] is the electro-chemical potential of the i^{th} ionic constituent which is composed of two parts, a chemical term μ_i and an electrical term $Z_i F \Psi_i$ so that

$$\hat{\mu}_i = \mu_i + Z_i F \Psi_i$$

where μ_i is the chemical potential, Z_i is the signed valency and Ψ_i the internal local electric potential of species i.

The choice of flows thus fixes the thermodynamic forces which have to be employed.

The product of any flow and its conjugate force must have the dimensions of entropy production and for a defined system, the sum of the products must remain the same for any change of flows and forces.

2.13 The Phenomenological Equations and the Onsager Reciprocal Relations

In order to make use of the dissipation function an explicit correlation be tween flows and forces is required. The first of these was obtained by Fourier, and later Ohm and Fick added other laws which indicated the linear dependence of a flow in its conjugate force. Dufour[2] Soret[3] and Peltier[4] showed that for a sufficiently slow process a flow could also be linearly dependent on a non-conjugate force.

In 1931 Onsager[5] proposed that for slow processes occurring not far from equilibrium thermodynamic flows and forces are linearly related by a set of phenomenological relationships of the general type.

$$J_i = \sum_{k=1}^{n} L_{ik} X_k \quad (i = 1,2 \ldots\ldots\ldots n) \qquad (2.5)$$

alternatively

$$X_i = \sum_{k=1}^{n} R_{ik} J_k \qquad (2.6)$$

This expression is obtained from equation (2.5) by Matrix inversion and expresses the forces as linear functions of the flows.

The L_{ik} coefficients of (2.5) are generalised mobility coefficients with units of flow per unit force whereas the R_{ik} coefficients of 2.6 are generalised frictional coefficients with dimensions of force per unit flow.

R_{ik} and L_{ik} coefficients are related by the equation

$$R_{ik} = \frac{|L_{ik}|}{|L|} \qquad (2.7)$$

where $|L_{ik}|$ is the minor of L_{ik} and $|L|$ is the determinent of all L coefficients.

These equations illustrate the possibility of coupling between various irreversible phenomena since each flux J_i may be a linear function of 'n' forces.

To/

To characterise such a system of 'n' forces n^2 mobility or frictional coefficients would be required and consequently n^2 independent experiments would be necessary in order to determine them. Then if $n > 2$ the minimum number of coefficients and subsequent experiments would be nine, making a complete analysis of the whole system very difficult.

Onsager's fundamental theorem states that provided a proper choice is made for the flows J_i and forces X_i, the matrix of phenomenological coefficients L_{ik} and R_{ik} will be symetrical.

i.e. $$L_{ik} = L_{ki} \qquad (i,k = 1,2 \ldots n) \qquad (2.8a)$$

similarly

$$R_{ik} = R_{ki} \qquad (2.8b)$$

Thus the number of independent coefficients required to characterise the system reduces from n^2 to $\frac{1}{2}n\ (n + 1)$

From the O.R.R. and the equation for the dissipation function equation (2.3), applying the requirement for positive entropy production, the further constraints are obtained.

$$L_{ii}L_{kk} \geq (L_{ik})^2 \text{ and } R_{ii}R_{kk} \geq (R_{ik})^2 \qquad (2.9)$$

also $$L_{ii} \geq 0 \qquad R_{ii} \geq 0 \qquad (2.10)$$

i.e. direct coefficients must be positive but cross coefficients may be either positive or negative.

Although these relations were originally proved by a statistical mechanical treatment and are an implication of 'microscopic reversibility' the relations apply to the macroscopic world and have now been proved to hold experimentally in electrochemical systems.

D.G. Miller (6) established that the O.R.R. were obeyed for a large range of experiments on binary electrolytes. The approach used in this work owes a great deal to that of Miller.

2.2 Application of Non Equilibrium Thermodynamics to Membrane Transport Processes.

To date a large number of analysis of membrane transport processes have been reported in the literature.(7) (8) (9) (10) (11) (12)

Whether equation (2.5) or (2.6) is chosen to provide coefficients depends on convenience and many workers have used both for a complete analysis.

Both have their advantages, L_{ik} coefficients are particularly useful in the formulation of equations to predict membrane properties, (2.26) (2.27) (2.28) (2.41) (2.43). whereas frictional coefficients have the advantage of being independent of the frame of reference thus allowing the calculation of the interaction of all species with the fixed charge matrix, species (4). R_{ik} coefficients also allow the comparison of different systems. They are a useful and necessary intermediate in the comparison of mobility coefficients of a membrane with that of an equivalent salt solution (Salt Model calculation). All forces and flows are measured normal to the membrane surface and the thermodynamic forces X_i are defined as the negative gradient of the electrochemical potential of the i^{th} species in the membrane.

The system for analysis is defined as isothermal and has four species:-

(1) Counter-ion

(2) Co-ion

(3) Water molecules

(4) Fixed charge and supporting matrix.

(2.21) The dissipation function then becomes

$$\phi = T\sigma = \sum_{i=1}^{4} J_i X_i \geq 0 \qquad (2.11)$$

where J_i is the flow of species i, in mole $cm^{-2}s^{-1}$ and X_i is the negative gradient of the electrochemical potential

$$X_i = (-d\hat{\mu}_i/dx) = -(d\mu_i/dx + Z_i F\, d\Psi/dx + \hat{V}\, dP/dx) \qquad (2.12)$$

$\hat{\mu}_i$ is the electrochemical potential in Joules $mole^{-1}$

Z_i is the signed valence of species i

F is the faraday in coulombs equivalent $^{-1}$

Ψ is the electrical potential of the phase in volts

P is the hydrostatic pressure in Newtons $metre^{-2}$

$\hat{V}$ is the partial molar volume in $metres^3$

dx is the length in cm across which the force is applied.

(By choosing cm and not metres for dx, $T\sigma$ refers to energy/$(1\ cm^3)$/sec or σ is the rate of production of entropy/1 cm^3.

The Gibbs Duhem Equation states

$$\sum_{i=1}^{n} n_i d\hat{\mu}_i = 0 \qquad (2.13a)$$

where n_i is the number of moles of species i

this becomes $$\sum_{i=0}^{n} c_i X_i = 0 \qquad (2.13b)$$

where c_i is the concentration of species i. From these it is apparent that the four forces are not independent and elimination of X_4 from (2.11) gives (2.14) where

$$J_i^4 = (J_i - c_i\, {}^{J_4}/_{c_4}) \qquad (2.14)$$

equation (2.11) then becomes

$$T\sigma = \phi = \sum_{i=1}^{3} (J_i - {}^{c_i}/_{c_4} J_4) X_i \qquad (2.15)$$

$$\phi = \sum_{i=1}^{3} J_i^4 X_i \geq 0 \qquad (2.16)$$

Thus we have defined the frame of reference for this treatment as "membrane fixed" and J_i^4 in the flow of species 'i' relative to a stationary membrane. This transformation does not alter the value of the dissipation function and preserves the O.R.R.

This/

This frame of reference is different from that used in a solution treatment where it is more convenient to use a solvent fixed reference. Consequently if direct comparison between membrane mobility coefficients and solution mobility coefficients of the same electrolyte system is required then the frame of reference of one must be converted.

On the membrane fixed frame of reference linear phenomenological equations can be written.

$$J_i^4 = \sum_{k=1}^{3} l_{ik} X_i \qquad (i = 1, 2, 3) \qquad (2.17)$$

and

$$X_i = \sum_{K=1}^{3} R_{ik} J_k^4 \qquad (2.18)$$

in which l_{ik} are membrane mobility coefficients and R_{ik} are generalised frictional coefficients. Applying the O.R.R. to equation (2.17) and (2.18) provides six independent phenomenological coefficients, from the three by three matrix, which subsequently characterise the transport properties of the membrane system. From hereafter J_i^4 will be represented by simply J_i and will describe the flow of species i on a membrane fixed frame of reference. Evaluation of the l_{ik} matrix requires the performance of six independent experiments involving electrical, chemical, and pressure potential forces under steady state conditions.

Electric Potential Gradient

Conductivity, Electro Osmosis and transport number are the three experiments in which the external applied force is electrical only.

(2.2.1.1) Conductivity

With an electrical force alone applied across the membrane, the current density in amps cm^{-2} is given by

$$I = (Z_1 J_1 + Z_2 J_2)F \qquad (2.19)$$

where again J_1 and J_2 are the flows of the mobile ionic species and Z_1, Z_2 are the signed valency ofthe ions.

As/

As there is no chemical potential or pressure gradient, X_i is given by

$$X_i = (-d\hat{\mu}_i/dx) = Z_i F\,(-d\Psi/dx) \qquad i = 1,2 \qquad (2.20)$$

and for water

$$X_3 = (-d\mu_3/dx) = 0$$

The phenomenological equations (2.17) then reduce to

$$J_1 = l_{11}X_1 + l_{12}X_2 \qquad (2.21a)$$

$$J_2 = l_{21}X_1 + l_{22}X_2 \qquad (2.21b)$$

$$J_3 = l_{31}X_1 + l_{32}X_2 \qquad (2.21c)$$

therefore substituting for J_1 and J_2 in (2.19) gives for the current density.

$$I = \left[Z_1^2\, l_{11} + Z_1Z_2\,(l_{12} + l_{21}) + Z_2^2\, l_{22}\right] F^2\left(\frac{d\Psi}{dx}\right) \qquad (2.22)$$

by expressing Ohm's law as

$$I = \kappa\,(d\Psi/dx) \qquad (2.23)$$

it is obvious that

$$\kappa = \left[Z_1^2\, l_{11} + Z_1Z_2(l_{12} + l_{21}) + Z_2^2 l_{22}\right] F^2 \qquad (2.24)$$

where κ is the specific conductance.

It proves convenient to further reduce κ to

$$\kappa = \alpha F^2$$

therefore

$$\alpha = \left[Z_1^2\, l_{11} + Z_1Z_2\,(l_{12} + l_{21}) + Z_2^2\, l_{22}\right] \qquad (2.25)$$

(2.2.1.2) Transport Number

The transference number of a species is defined[13] as the number of moles of the species transferred by one faraday of electricity through a stationary cross section in the direction of positive current.

Therefore for water

$$t_3 = J_3 F/I \qquad (2.26a)$$

substituting for I, by equation (2.19) for J_3 by equation (2.21c) a nd X_1 and X_2 by equation (2.20) gives

$$t_3 = (Z_1 l_{31} + Z_2 l_{32}) F^2 / k \qquad (2.26b)$$

Similarly t_i the transport number of an ion, defined as the fraction of total current carried by that ion, can be expressed, for counter-ion as $t_1 = (Z_1^2 l_{11} + Z_1 Z_2 l_{12}) F^2 / k$ (2.27)

and for co-ion $t_2 = (Z_2^2 l_{22} + Z_1 Z_2 l_{21}) F^2 / k$ (2.28)

(2.2.2) Chemical and Pressure Potential Gradients

In the use of concentration gradients to obtain membrane l_{ik} and R_{ik} coefficients there exists the basic objection that as these membrane coefficients are functions of concentration then the values obtained will be mean values. This problem is minimised in salt and water flow experiments by ensuring the gradients of concentration are as small as possible. The application of pressure across the membrane also poses fundamental problems, though of a different nature, in the application and determination of phenomenological coefficients. It must be assumed that the pressure applied causes no structural deformation of the membrane matrix, that is, the membrane under applied pressure is identical to that at atmospheric pressure. Thus l_{ik} and R_{ik} coefficients, and the equations describing membrane processes, may be applied to describe membrane transport processes under both applied pressure and concentration gradients.

When a salt gradient exists across a membrane two flows are observed, those of salt, J_s and of water, J_w (osmotic flow). When the membrane is at atmospheric pressure these flows are in opposite directions due to the opposing gradients of chemical potential for the salt and water. Exceptions occur in certain membranes in which the two flows are concurrent and anomalous osmosis is observed [15][16][17]. If, however, pressure is applied to solution on one side of the membrane, salt and water are caused to flow in the same direction. The applied pressure constitutes an additional force on water which reverses the sign of the water force X_3. This induced flow of water through the membrane

consequently creates (dynamically) a new concentration gradient which will be proportional to the ratio of the fluxes, J_s and J_w. Thus in isobaric and non-isobaric systems the equations describing the salt and water flux will be identical, only the thermodynamic forces will be altered by the inclusion of additional terms:-

For an isothermal system under applied concentration and pressure gradients there is no flow of electric current in the system.

$$\text{i.e.} \quad I = (Z_1J_1 + Z_2J_2)\,F = 0 \tag{2.29}$$

The thermodynamic forces become

$$X_i = (-d\hat{\mu}_i/dx) = \left[(-d\mu_i/dx) + Z_iF\,(-d\Psi/dx)\right] \quad i = 1, 2 \tag{2.30}$$

$$(-d\mu_i/dx) = -\left[RT\,dlna_i/dx + \hat{V}_i\,dP/dx\right] \tag{2.31}$$

$$X_3 = (-d\mu_3/dx) = -\left[RT\,dlna_3/dx + \hat{V}_3\,dP/dx\right] \tag{2.32}$$

From (2.17) the phenomenological equations are

$$J_1 = l_{11}X_1 + l_{12}X_2 + l_{13}X_3 \tag{2.33a}$$

$$J_2 = l_{21}X_1 + l_{22}X_2 + l_{23}X_3 \tag{2.33b}$$

$$J_3 = l_{31}X_1 + l_{32}X_2 + l_{33}X_3 \tag{2.33c}$$

Substituting equations (2.33a) and (2.33b) into the condition for zero current gives

$$(Z_1l_{11} + Z_2l_{12})\,X_1 + (Z_1l_{12} + Z_2l_{22})\,X_2 + (Z_1l_{13} + Z_2l_{23})\,X_3 = 0 \tag{2.34}$$

By applying the equations (2.26), (2.27), (2.28) defining the transport numbers, equation (2.34) reduces to

$$t_1/Z_1 \cdot X_1 + t_2/Z_2 \cdot X_2 + t_3X_3 = 0 \tag{2.35}$$

and from (2.30) by expanding X_i and collecting terms (2.35) becomes

$$F(-d\Psi/dx) = t_1/Z_1(d\mu_1/dx) + t_2/Z_2\,(d\mu_2/dx) + t_3\,(d\mu_3/dx) \tag{2.36}$$

This/

This equation was first given by Plank [18] and by Henderson [19] and later by Staverman[20] using an irreversible thermodynamic presentation. By integration across the membrane the expression for membrane diffusion potential is obtained (2.3.2.1)

(2.2.2.1) Salt Flow J_s

Using the condition for electro-neutrality

$$(Z_1 r_1 + Z_2 r_2) = 0 \qquad (2.37)$$

and $$\mu_{12} = r_1\hat{\mu}_1 + r_2\hat{\mu}_2 \qquad (2.38a)$$

alternatively written $$X_{12} = r_1 X_1 + r_2 X_2 \qquad (2.38b)$$

where r_1, r_2 denoted the number of moles of cation and anion given by one mole of electrolyte, and r_{12} is defined as a number of moles of ions given by one mole of electrolyte so that

$$r_{12} = r_1 + r_2 \qquad (2.39)$$

The flow of salt, J_s, under a concentration and pressure gradient is given by

$$J_s = J_1/r_1 = J_2/r_2 \qquad (2.40)$$

using equation (2.33a), (2.40) becomes

$$J_s = {}^1/r_1 (l_{11}X_1 + l_{12}X_2 + l_{13}X_3)$$

expanding X_i from (2.30) (i = 1, 2) gives

$$J_s = {}^1/r_1 \left[l_{11}(-d\mu_1/dx) + l_{12}(-d\mu_2/dx) + l_{13}(-d\mu_3/dx)\right] + {}^1/r_1\left[Z_1 l_{11} + Z_2 l_{12}\right] F\,(-d\Psi/dx)$$

expressing $(Z_1 l_{11} + Z_2 l_{12}) = {}^{t_1\alpha}/_{Z_1}$ from equation (2.27)

and substituting for $(-d\Psi/dx)$ from equation (2.36) J_s becomes

$$J_s = {}^1/r_1 \left[\left(l_{11} - \frac{t_1^2\alpha}{Z_1^2}\right)\left(\frac{-d\mu_1}{dx}\right) + \left(l_{12} - \frac{t_1 t_2 \alpha}{Z_1 Z_2}\right)\left(\frac{-d\mu_2}{dx}\right)\right] + \frac{1}{r_1}\left[\left(l_{13} - \frac{t_1 t_3 \alpha}{Z_1}\right)\left(\frac{-d\mu_3}{dx}\right)\right]$$

Using the expression (2.37) defining electro-neutrality

$${}^1/r_1\left(l_{11} - {}^{t_1^2\alpha}/Z_1^2\right) = -{}^{Z_1 Z_2}/r_2 \left(\frac{l_{11}l_{22} - l_{12}^2}{\alpha}\right)$$

and $${}^1/r_1 \left(l_{12} - {}^{t_1 t_2 \alpha}/Z_1 Z_2\right) = -{}^{Z_1 Z_2}/r_1 \left(\frac{l_{11}l_{22} - l_{12}^2}{\alpha}\right)$$

Finally applying condition (2.38a) the general equation for the flow

of/

of salt can be expressed as equation (2.41)

$$J_s = -Z_1Z_2/r_1r_2 \left(\frac{l_{11}l_{22}-l_{12}^2}{\alpha}\right)\left(\frac{-d\mu_{12}}{dx}\right)+\frac{1}{r_1}\left(l_{13}-\frac{t_1t_3\alpha}{Z_1}\right)\left(\frac{-d\mu_3}{dx}\right) \qquad (2.41)$$

(2.2.2.2) Water Flow, J_w

From equation (2.33c)

$$J_w = (l_{13}X_1 + l_{23}X_2 + l_{33}X_3) \qquad (2.42)$$

In an expansion similar to that for J_s, above, using equations (2.30) (2.36), equation (2.42) becomes

$$J_w = \left(l_{13}-\frac{t_1t_3\alpha}{Z_1}\right)\left(\frac{-d\mu_1}{dx}\right)+\left(l_{23}-\frac{t_2t_3\alpha}{Z_2}\right)\left(\frac{-d\mu_2}{dx}\right)+(l_{33}-t_3^2\alpha)\left(\frac{-d\mu_3}{dx}\right)$$

Once more employing the condition for electro-neutrality it can be shown that

$$\left(l_{23}-\frac{t_2t_3\alpha}{Z_2}\right) = \frac{r_2}{r_1}\left(l_{13}-\frac{t_1t_3\alpha}{Z_1}\right)$$

Using equation (2.38a) the water flow is given by (2.43)

$$J_w = \frac{1}{r_1}\left(l_{13}-\frac{t_1t_3\alpha}{Z_1}\right)\left(\frac{-d\mu_{12}}{dx}\right)+(l_{33}-t_3^2\alpha)\left(\frac{-d\mu_3}{dx}\right) \qquad (2.43)$$

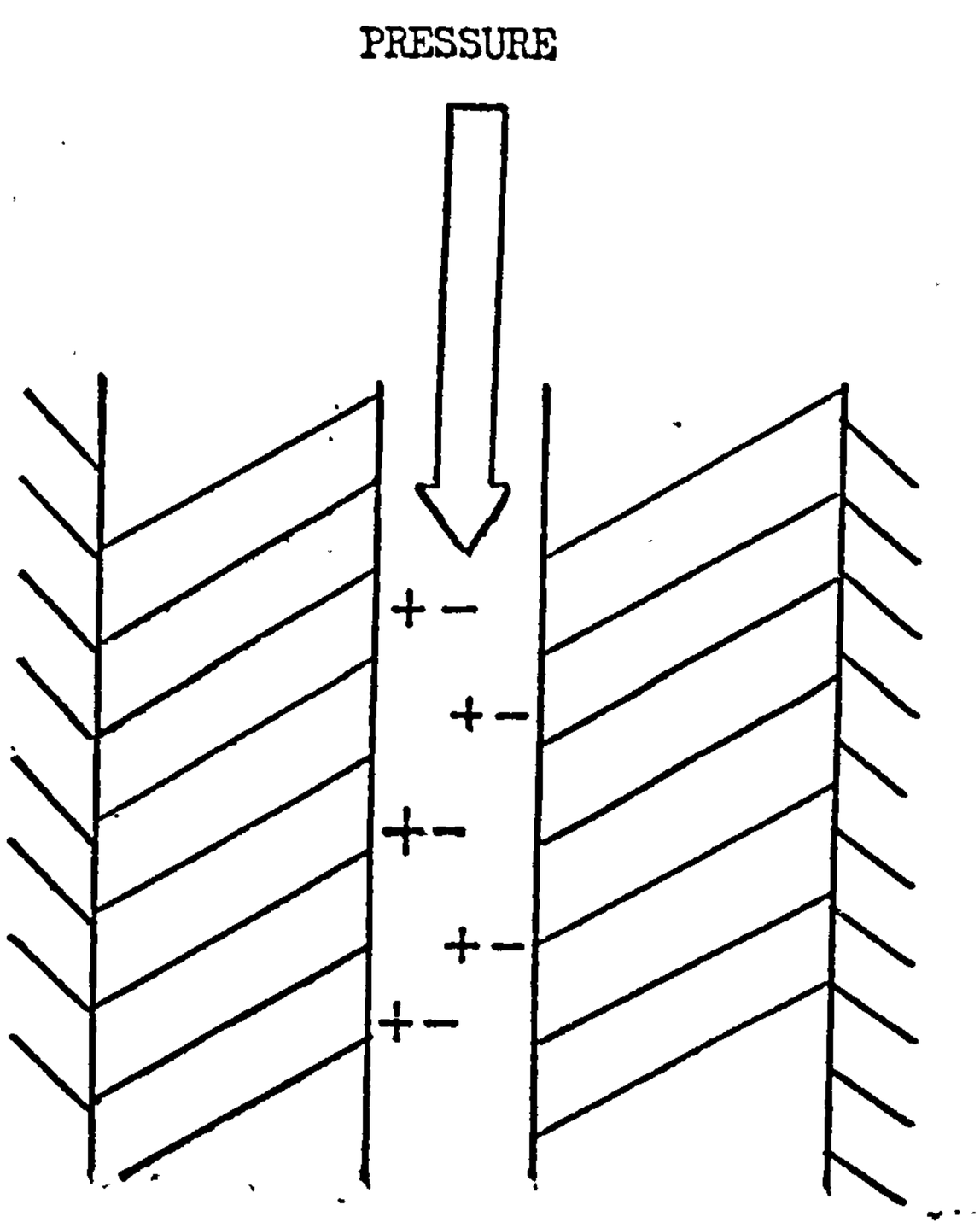

No Fixed charge or difference in mobility of Cation and anion for any reason. Therefore No Streaming Potential.

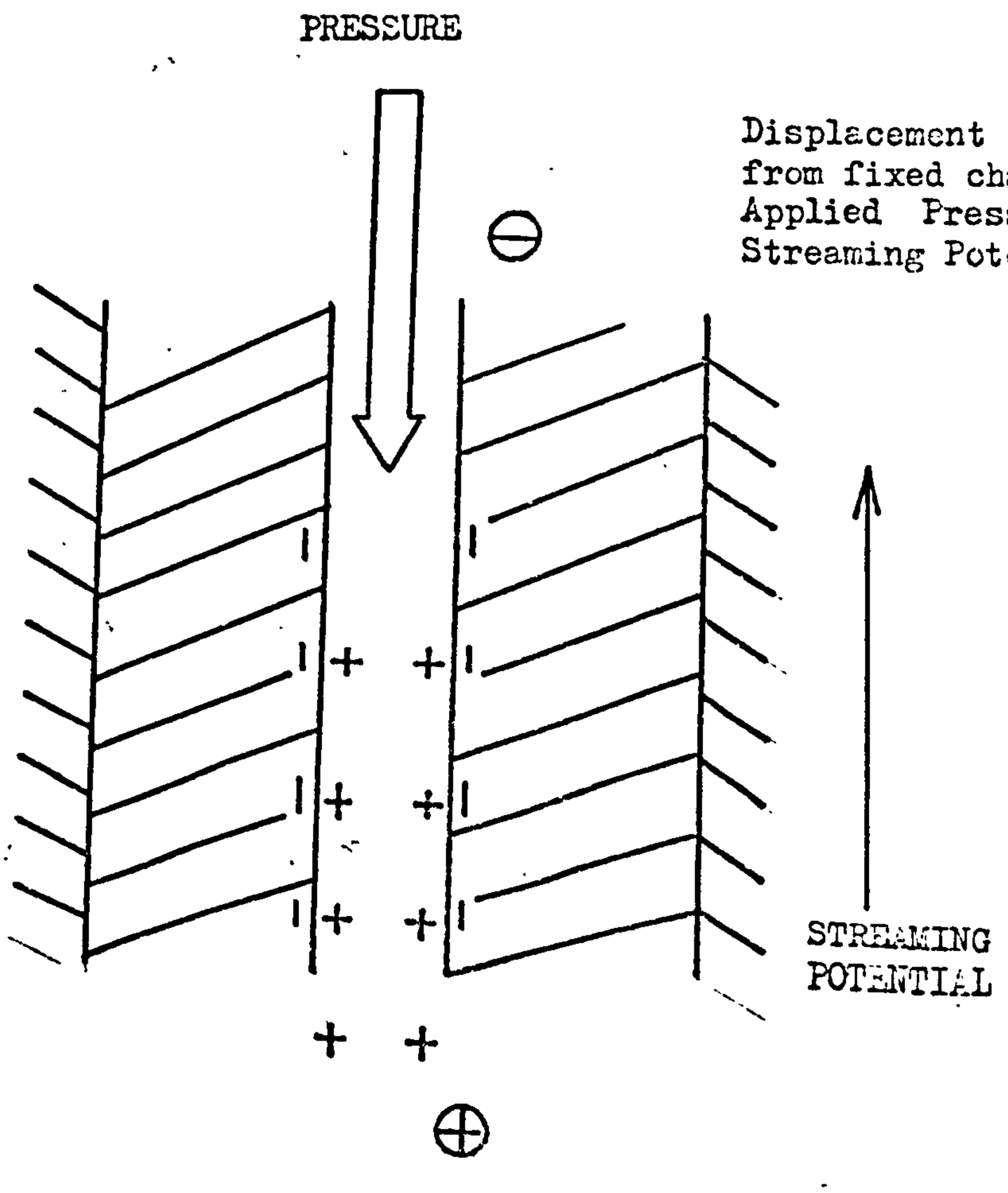

Displacement of counterion from fixed charge by the Applied Pressure causes a Streaming Potential

FIG 2.2

2.2.2.3 THERMODYNAMIC FORCES FOR SALT $\hat{\mu}_{12}$ AND WATER μ_3 UNDER APPLIED CONCENTRATION AND PRESSURE GRADIENTS

From the full expression for X_i equation (2.31) i = 1, 2 and from equation (2.38b) and the equation for electro-neutrality (2.37)

$$X_{12} = -RT\left(\frac{d\ln a_1}{dx} + \frac{d\ln a_2}{dx}\right) - (r_1\hat{V}_1 + r_2\hat{V}_2)\left(\frac{dP}{dx}\right)$$

The activity of salt

$$a_{12} = a_1^{r_1}.a_2^{r_2}$$

and the partial molar volume of salt

$$\hat{V}_{12} = r_1\hat{V}_1 + r_2\hat{V}_2 \qquad (2.44)$$

therefore $X_{12} = -RT\left(\frac{d\ln a_{12}}{dx}\right) - \hat{V}_{12}\left(\frac{dP}{dx}\right)$ (2.45)

This illustrates the additional term included to account for the effect of a pressure gradient on the chemical potential of salt. X_{12} can be calculated from activity coefficients derived at zero pressure, using the term $\hat{V}_{12}\frac{dP}{dx}$ as a correction term accounting for the applied pressure. Alternatively the activity coefficients obtained at specific pressures above 1 atmosphere can be used (14) In practice, however, this consideration need only be made at very high pressures. Appendix I.

The thermodynamic force, X_3, on the other hand contains a major contribution from the applied pressure gradient equation (2.32)

$$X_3 = -\left(RT\frac{d\ln a_3}{dx} + \hat{V}_3\frac{dP}{dx}\right) \qquad (2.46)$$

The influence of pressure on X_3 may be large and if water activity and pressure terms oppose, as they will when pressure is applied to the concentrated solution,(in the direction of the salt gradient) then the pressure force may reverse the direction of X_3. Such conditions are obtained in reverse osmosis (desalination) techniques.

Equations/

Equations (2.43) (2.41) can be expressed in shortened form

$$J_s = L_{ss}X_{12} + L_{sw}X_3 \qquad (2.47)$$

$$J_w = L_{ws}X_{12} + L_{ww}X_3 \qquad (2.48)$$

Therefore, in the full equations for J_s and J_w if $l_{13} > \frac{t_1 t_3 \propto}{z_1}$ and $l_{33} > t_3^2 \propto$ all the mobility coefficients in equations (2.47), (2.48) will be positive. From Fig. (2.1) for an applied concentration gradient, X_{12} and X_3 have opposite signs, consequently J_s and J_w are in opposing directions. Under these conditions it is obvious that the cross effect expressed by the coefficients $L_{sw} = L_{ws}$ (O.R.R.), due to the coupling of the two flows, causes reduction in both the salt and water flow. However, under an additional pressure gradient, X_{12} and X_3 assume the same sign causing J_s and J_w now to be in the same direction. The coupling term in this case contributes to the flow of both. The water flow is a reverse-osmotic-flow and the coupling between the flows causes an increase in the concentration of salt on the low pressure side of the membrane.

Thus, coupling acts against the process of desalination in a reverse osmosis system.

2.2.3 E.M.F. MEASUREMENTS ACROSS THE MEMBRANE IN THE REVERSE-OSMOSIS CELL

When a salt solution is compressed through an ion exchange membrane a portion of the electrolyte is excluded (21) by Donnan rejection. The result of this exclusion is a salt filtering effect. The salt filtering process across ionic membranes can be described in terms of the flux equations of irreversible thermodynamics, for example equations (2.41) (2.43) (22) (23) (24)(25)

Figure (2.2) shows the compression of an electrolyte solution through a cation exchange membrane. The chloride ions (of the electrolyte) are effectively excluded from the membrane because of the high concentration of fixed negative charge (Donnan effect). When pressure is applied, displacement of the Na^+ counter-ions, with respect to the fixed negative charge occurs, because the latter cannot move under the influence of pressure, whereas the former can. The result is a streaming potential with the low pressure side carrying positive charge. This potential enhances the flow of the chloride ions and tends to work against effective desalination. However, if the concentration of chloride ions in the membrane is small, the flow of chloride and hence the total salt flow should remain relatively small compared with the flow of water.

Consider a cation exchange membrane separating two idential salt solutions. An equilibrium situation exists $X_{12} = X_3 = 0$. If a pressure is applied to one solution a non-equilibrium situation is created $X_3 \neq 0$. In consequence water and salt flow through the membrane and in the steady state J_s and J_w are defined, equations (2.41) (2.43). If the high pressure solution is effectively stirred and is of a sufficient volume, its concentration remains constant (effectively) up to the membrane surface. The flows of salt and water into the low pressure solution define the concentrations (and consequently the

chemical/

chemical potentials) at the membrane surface on the low pressure side since

$$\frac{J_s}{J_w} \times C_w = \text{Concentration of product } (C_p)$$

and consequently the salt gradient across the membrane is defined.

If electrodes which undergo a reversible reaction with one of the ions in solution are chosen and inserted on both sides of the membrane the total emf. of the reverse osmosis system can be measured.

The method of Irreversible Thermodynamics provides a complete and elegant determination of the total emf of the system, allowing the origin and form of the different contributions to be distinguished.

The total emf. can be expressed.

$$(2.2.3.1.)\Delta\psi \text{ SYST} = (\psi'_E - \psi'_S) + (\psi'_S - \psi'_M) + (\psi'_M - \psi''_M) + (\psi''_M - \psi''_S) + (\psi''_S - \psi''_E) \quad (2.49)$$

or alternatively

$$\Delta\psi \text{ SYST} = \Delta E_{\text{Electrodes}} + \Delta E_{\text{Donnan}} + \Delta E_{\text{Diffusion}} \quad (2.50)$$

By choosing the silver-silver chloride electrode which reacts reversibly with chloride ion, the equilibrium conditions for the electrodes can be written

$$Agcl + e \rightleftharpoons Ag^{\circ} + cl^{-}$$

and

$$\mu_{Agcl} + \mu_e = \mu_{Ag}{}^{\circ} + \mu_{cl}{}^{-}$$

The electrode potentials are:-

$$(\psi'_E - \psi'_S) = -\frac{1}{F}(\mu^{\circ}_{Ag} + \mu^{\circ}_{cl^-} - \mu^{\circ}_{Agcl}) - \frac{P'}{F}(\hat{V}_{Ag} - \hat{V}_{Agcl} + \hat{V}_{cl^-}) - \frac{RT}{F} \ln a'_2$$

$$(\psi''_E - \psi''_S) = \frac{1}{F}(\mu^{\circ}_{Ag} + \mu^{\circ}_{cl} - \mu^{\circ}_{Agcl}) + \frac{P''}{F}(\hat{V}_{Ag} - \hat{V}_{Agcl} + \hat{V}_{cl^-}) + \frac{RT}{F} \ln a''_2$$

where $\frac{1}{F}(\mu^{\circ}_{Ag} + \mu^{\circ}_{Cl^-} - \mu^{\circ}_{AgCl})$ = Constant = E_o the standard electrode potential.

If Donnan Equilibrium is set up the chemical potential of salt at the solution-membrane interface on each side of the membrane are inequilibrium

$$\begin{aligned} \hat{\mu}'_S &= \hat{\mu}'_M \\ \hat{\mu}''_M &= \hat{\mu}''_S \end{aligned} \qquad (2.51)$$

Therefore

$$(\Psi'_S - \Psi'_M) = \frac{RT}{F} \ln \frac{a'_2}{\bar{a}'_2} + P'(\hat{V}^S_2 - \bar{V}^M_2)$$

$$(\Psi''_M - \Psi''_S) = -\frac{RT}{F} \ln \frac{a''_2}{\bar{a}''_2} - P''(\hat{V}^S_2 - \bar{V}^M_2)$$

where the barred symbols represent the membrane phase. The diffusion of salt due to a concentration gradient creates a diffusion potential which can be expressed by integration of equation (2.36) across the membrane and by substituting for the thermodynamic forces, equations (2.31), (2.32).

$$(\Psi'_M - \Psi''_M) = \frac{RT}{F}\left(\frac{t_1}{Z_1} \ln \frac{\bar{a}''_1}{\bar{a}'_1} + \frac{t_2}{Z_2} \ln \frac{\bar{a}''_2}{\bar{a}'_2} + t_3 \ln \frac{\bar{a}''_3}{\bar{a}'_3}\right) + (P'' - P')\left(\frac{t_1}{F}\bar{V}^M_1 - \frac{t_2}{F}\bar{V}^M_2 + \frac{t_3}{F}\bar{V}^M_3\right).$$

As P' = 1 atmosphere then P'' is the applied pressure which will be denoted hereafter by P

For a 1:1 electrolyte,

$Z_1 = 1$, $Z_2 = -1$ and applying $t_2 = 1 - t_1$ gives for $(\Psi'_M - \Psi''_M)$

$$(\Psi'_M - \Psi''_M) = \frac{t_1 RT}{F} \ln \frac{\bar{a}''_1 \bar{a}''_2}{\bar{a}'_1 \bar{a}'_2} - \frac{RT}{F} \ln \frac{\bar{a}''_2}{\bar{a}'_2} + \frac{t_3 RT}{F} \ln \frac{\bar{a}''_3}{\bar{a}'_3} + \frac{P}{F} t_1(\bar{V}^M_1 + \bar{V}^M_2) - \frac{P}{F}\bar{V}^M_2 + \frac{t_3}{F} P \bar{V}^M_3$$

From/

From equation (2.44) and the assumption that the partial molar volumes of the species in the solution and membrane are identical, i.e.

$$\hat{V}_i^S = \hat{V}_i^M$$

The expression for the total emf of the cell becomes

$$E_{tot} = \frac{P}{F}\left(\hat{V}^{o}_{Ag} - \hat{V}_{AgCl}\right) + t_3 \frac{RT}{F} \ln \frac{\bar{a}''_3}{\bar{a}'_3} + t_1 \frac{RT}{F} \ln \frac{\bar{a}''_1\,\bar{a}''_2}{\bar{a}'_1\,\bar{a}'_2} + \frac{P}{F}\left(t_1\hat{V}_{12} + t_3\hat{V}_3\right)$$

in the case of a 1:1 salt:

$$\bar{a}''_1\,\bar{a}''_2 = (\bar{a}''_{12})^2 \qquad \bar{a}_1\,\bar{a}_2 = (\bar{a}'_{12})^2$$

However

$$a_1 = M_1 \gamma_1 \qquad a_2 = M_2 \gamma_2$$

where $M_i \gamma_i$ are the molar concentration and activity coefficients respectively,

therefore

$$a_1 a_2 = M_1 M_2 \gamma_1 \gamma_2$$
$$= (M_s \gamma_\pm)^2$$

Since equilibrium is assumed at the solution membrane interface

$$\bar{a}''_{12} = a''_{12}, \quad \bar{a}'_{12} = a'_{12}, \quad \bar{a}''_3 = a''_3, \quad \bar{a}'_3 = a'_3$$

therefore

$$E_{tot} = \frac{P}{F}\left(\hat{V}_{Ag} - \hat{V}_{AgCl}\right) + t_3 \frac{RT}{F} \ln \frac{a''_3}{a'_3} + 2t_1 \frac{RT}{F} \ln \frac{M''_s \gamma''_\pm}{M'_s \gamma'_\pm} + \frac{P}{F}\left(t_1\hat{V}_{12} + t_3\hat{V}_3\right) \qquad (2.52)$$

The first term $\frac{P}{F}\left(\hat{V}_{Ag} - \hat{V}_{AgCl}\right)$ is a correction term due to the effect of pressure on the volume change of the electrodes and will be negative for silver-silver chloride electrodes.

$t_3 \frac{RT}{F} \ln \frac{a''_3}{a'_3}$ also makes a negative contribution.

This represents the tendency (osmotic) of the water to diffuse back in the direction of the concentration gradient (of water) thus opposing the applied pressure.

The final two terms both of which are positive for a positive t_3 give the contribution respectively from the concentration cell (due to the salt gradient created by the flows J_s and J_w) and the streaming potential.

(2.2.32) Streaming Potential and Electrokinetic Phenomena

Streaming Potential is a consequence of coupling between irreversible processes, i.e. coupling between flow of electric current, volume flow and hydrostatic pressure; with three other similar electrokinetic effects it makes up the well known Saxen's relationships.

The first theoretical explanation of these phenomena was advanced by Helmholtz, Gouy, and others [26] [27] [28] based on the electric double layer theory.

However this theory reaches a limit where it fails to describe experimental data when the water content of the membrane is very low.

Saxen in later years observed that several relations between coupled phenomena remain valid for dense membranes and Mazur and Overbeck proved they may be deduced from the phenomenological equations of irreversible thermodynamics[29]

From the derivation of the total emf of the reverse osmosis cell equation (2.52) and from the equation itself it is apparent that the streaming potential is derived from the diffusion potential part of expression (2.49) and is a consequence of the movement of pore solution in the membrane, expressed by t_3.

Saxen's relationships can be established under the condition of no concentration gradient across the membrane and it is convenient to choose the flows and forces so that the dissipation function is given by

$$\phi = J_v \Delta P + IE$$

where J_v = volume flow

ΔP = applied pressure

I = electric current

E = potential difference across the membrane (between the reversible electrodes)

The/

The system is then described by two flows and two forces which can be used to establish the Saxen Law equation (2.53). This relates the streaming potential across a membrane to the electro-osmotic flow.

$$\left(E_{ST}/\Delta P\right)_{I=0} = \left(t_v/I\right)_{\Delta P=0} \qquad (2.53)$$

E_{ST} is the streaming potentialin volts, P the applied pressure, t_v the electro-osmotic water transport in $cm^3\ sec^{-1}$ and I the current in amps. Hence Saxen's law implies a comparison of two different experiments involving a membrane separating two electrodes.

1) Application of pressure, and measurement of the resultant streaming potential between the electrodes to give $\left(\Delta \frac{E}{P}\right)_{I=0}$

2) Application of electrical potential difference between the electrodes with P = 1 atmosphere. This yields $\left(\frac{V}{I}\right)_{\Delta P=0}$

Saxen's law holds for all membranes when E and V are proportional to P and I respectively.

The equations (2.27) (2.28) (2.26) for t_1, t_2 and t_3 respectively and for J_s and J_w (2.41) (2.43) have normally in the past been considered under isothermal and isobaric conditions thus giving five equations to determine six unknown mobility coefficients. In order to evaluate the complete l_{ik} matrix various assumptions were made for specific coefficients (30) (31). However, if equations (2.41) and (2.43) are used in a pressure experiment this will provide additional data with which to evaluate the full l_{ik} matrix. This pressure experiment will also allow an alternative evaluation of the various l_{ik} coefficient assumptions made in previous work when the pressure experimental system was not available. Equation (2.52) describing the total E.M.F. of a reverse osmosis cell allows evaluation of all the contributing processes and illustrates the relative value of each.

REFERENCES

CHAPTER 2.

1) E.A. Guggenheim, J. Phys. Chem. 33, (1929) 842.

2) L. Dufour, Ann. Phys. (5) 28, (1873) 490.

3) C.H. Soret, Arch. Sci. Phys. Nat. Geneve. 2. (1879) 48.

4) Peltier, I Priogoine Introduction to the Thermodynamics of Irreversible Processes (Thomas Springfield, Illinois 1955).

5) L. Onsager, Phys. Rev. 37, (1931) 405, 38, (1931)

6) D.G. Miller, J. Phy. Chem. 70, 2639 (1966).

7) A.J. Staverman, Trans. Faraday Soc. 48, 176 (1952)

8) P.L. Lorenz, J. Phys. Chem. 56, 775 (1952).

9) K.S. Spiegler, Trans. Faraday Soc. 54, 1408 (1958).

10) C.H. Hills, P.W.M. Jacobs and J. Lakshmina rayanaiah. Proc. Roy. Soc. (London) A.262. 246 (1961)

11) O. Kedem and A. Katchalsky, J. Gen.Physiol 45, 143 (1961)

12) O Kedem and A. Katchalsky, Trans. Faraday Soc. 59, 1918 (1963).

13) F. Helfferich,"Ion Exchange" McGraw-Hill, New York (1962) 403.

14) Harned and Owen, 'Electrolyte Solutions', Butterworths, 2nd Editicn. 505.

15) E. Grim and K. Sollner, J. Gen. Physiology (1957) vol.40 6 887

16) J. Loeb, J. Gen. Physiology (1922) 4, 463, 621.

17) F.F. Bartel, O.E. Madison. J. Physic. Chem. 1920 44, 244, 593

18) M. Planck, Ann. Physik. Chem. 39 (1890) 161 40 (1890) 561

19) P. Henderson, Z. Physik, Chem. 59 (1907) 118, 63(1908) 325.

20) Same as (7) above.

21) K.S. Spiegler, J. Electro Chem. Soc. 100, 303C (1953)

22) J.W. Lorimer, E.I. Boterenbrod and J.J. Hermans. Discussions Faraday Soc. 21, 141 (1956).

23) P. Mazur and J.G. Overbeek. Rec. Trav. Chim. 70, 33 (1951)

24) K.S. Spiegler. "Ion Exchange Technology" ed. by F.C. Nachod and J. Schubert. Academic Press, New York (1956)

25) A.J. Staverman, Trans. Faraday. Soc.54 1438 (1958)

26) H. Helmholtz, Wied. Ann. 8 (1879) 337.

27) A. Gouy. J. Physique. 9 (1910) 457

28) J. Perrin. J. Chem. Phy. 2. 2(1904) 601.

29) P. Mazur and J.T. Overbeck. Rec. Trav. Chim. 70 (1951) 83.

REFERENCES

CHAPTER 2 (cont'd)

30) R. Paterson and C.R. Gardner. J. Chem. Soc. A.2254 (1971)

31) H. Ferguson, C.R. Gardner, R. Paterson. J.C.S. Faraday I. 68 2021 (1972)

CHAPTER 3

SALT MODEL CALCULATION

3.0 SALT MODEL CALCULATION

The equations describing membrane transport processes formulated in the previous section provide the means by which the phenomenological coefficients describing a particular membrane system may be evaluated. However, in order to do so a great deal of experimentation must be carried out as the transport coefficients cannot be predicted from molecular theory. Therefore any model which might allow quantitative assessment of transfer coefficients and of general membrane properties would short cut a great deal of the practical work, consequently making a useful contribution to the understanding and assessment of membrane properties. One means of accomplishing this would be to find an accurate and accessible analogue system.

The obvious first choice for such a model would be the poly-electrolyte salt solutions from which the membrane matrix is formed. This choice would give a ternary solution system when the imbibed electrolyte in the membrane matrix was considered. Transport processes would be evaluated at equal molalities in the membrane and model. Data on the transport properties of polyelectrolyte solutions and their ternary mixtures with simple salts is however insufficient to allow this model to be useful. This particular system, providing that the polyelectrolyte undergoes no conformational changes would give the most accurate comparison to the exchanger membrane.

A much simpler model system, to the extent of presenting a limiting case, is the analogy to a simple aqueous electrolyte. It is proposed that the membrane is modelled by an equimolal electrolyte solution where co-ion of two types are present,

co-ion/

co-ion species (2) as before and co-ion, species (4) which is fixed relative to the membrane matrix. The relationship of these two species is taken to be that between chemically identical, but physical distinguishable isotopes. In order for this model to function, the aqueous electrolyte must be chosen carefully in such a way that its anion and the fixed charge on the membrane matrix exhibit similar kinetic behaviour. Thus by adapting the phenomenological coefficients of a simple binary solution and making them apply to a ternary solution of the same electrolyte containing the isotopic anion species (2) and (4) , a precise definition of the phenomenological coefficients of the model can be expressed.

As the accuracy of the model depends on the similarity existing between the matrix fixed charge and the solution anion chosen to model it, comparison between them must be examined.

The Salt Model calculation presented was developed from observations made on the A.M.F. C_{60} membrane described in section (3.3) - Paterson & Gardner [1] [2] [3] using the method of Arnold and Koch [4] prepared an expanded form of the A.M.F.C_{60} membrane, C_{60E}, Section(4.1.4.1.) The physical properties of both the expanded C_{60E} and the normal C_{60N}, were obtained in sodium chloride solutions in the concentration range 0.1 - 2.0M, these are shown in Table (3.1). The expanded membrane C_{60E} takes up more salt $\bar{C}_2$ than the normal C_{60N}, at each concentration of external electrolyte and the salt uptake ranges from 0.2% of the total capacity for the 'normal' in 0.1M NaCl (ext.) to 22% for the 'expanded' in 2.0M (ext.) Figures (3.1) (3.2) (3.3) (3.4) show the results of isotope diffusion and electrical studies.

The flows of both ions and water are larger in the more open structure of the expanded membrane and in general decrease as both membranes shrink when equilibrated in more concentrated solutions.

This can be attributed, at least partially, to the increasing obstruction of the polymer matrix as the diffusional pathways become more tortuous and the fractional pore volume decreases.

For electrical conductivity, Fig. (3.3) there is the additional effect of increasing uptake of salt by the membrane, which tends to increase the conductivity. These opposing effects almost cancel for C_{60N} above 0.5M Nacl (ext.), but increased salt uptake in the C_{60E} more than compensates the effect of increasing tortuosity (and decreasing pore volume) and at higher concentrations, specific conductivity increases. In figure (3.2) isotopic diffusion coefficients for counter-ion, co-ion and water (determined using tritiated water) show similar diversity between the C_{60N} and C_{60E} membranes and there is little to suggest the common source of these membranes at this stage. However, when scaled by the tortuosity factor θ_m calculated by Meares [5], for path length tortuosity, the two sets of data for, C_{60N} and C_{60E} coincide and are close to the corresponding values for sodium ion [6] chloride ion [6] and tritiated water [7] in equivalent equimolar aqueous solutions of sodium chloride. Fig. (3.2).

The scaling factor θ_m is used outwith the terms of reference of Meares' original derivation [5], however, using θ_p, Prager's estimate [8] obtained from a more generalised treatment alternative value, $D_{ii}\theta_p$ are some 15% lower.

The mobility, l_{ik} and frictional, R_{ik} coefficients which measure the kinetic interactions of the counter ion and co-ion and water with each other and with the exchanger matrix were obtained for both membranes using irreversible thermodynamics [1] [2] [3].

The matrix-fixed frame of reference is used for the membrane mobility coefficients while solution flows are measured relative to/

to a stationary solvent. Therefore for a direct comparison of membrane and solution the membrane l_{ik} coefficients must be converted to a solvent-fixed frame of reference and designated L_{ik}. By using θ_m these can be corrected for path tortuosity becoming $L_{ik}\theta_m$ and can be compared with the coefficients for sodium chloride solution at closely-corresponding concentrations, Table (3.2).

The agreement between the membranes and an equivalent sodium chloride solution is good and indicates that membranes and solutions are similar when allowance is made for tortuosity. The intrinsic mobility of sodium, $L_{11}\theta/_m$, increases as the internal electrolyte concentration decreases although more markedly in the membrane than in solution. Both sulphonate in the membrane and chloride in solution show larger intrinsic mobilities $L_{22}\theta/_m$, than the sodium (both large order destroying ions).. Although the cation-anion ccupling $L_{14}\theta/_m$ is of the same order of magnitude in the membrane and solution, the correspondence for this coupling is least satisfactory. Overall the best agreement is obtained between the expanded membrane (2.13 internal molality) and the sodium chloride solution of molality 2.09.

In each case the purely geometric scaling factors θ_m, θ_p, bring the C_{60N} and C_{60E} data into good agreement with equimolar solutions for sodium chloride.

The experimental values for the electro-osmotic transport number t_3, equation (2.26), range from 15.77 for C_{60E} (0.1M external) to 5.48 for the C_{60N} (2.0M external) and at each corresponding external salt concentration the transference numbers for the C_{60E} are greater than for the C_{60N}. However, in the plot of t_3 against molality of membrane electrolyte, the data for both C_{60E} and C_{60N} combine in a single curve (Fig.3.4). Spiegler has shown (9) that/

that a large number of exchangers obey the empirical equation $t_3 = \beta \bar{C}_3/\bar{C}_1$ where $\bar{C}_3, \bar{C}_1$ are the respective capacities of water and counter-ion in moles/litre of exchanger and β = 0.50. Fig. (3.5) shows that the ratio t_3/t_1 is a linear function of the concentration gradient and has the slope 0.576.

Once again the properties of normal and expanded membranes are shown to obey a common law and it is of interest to examine the significance of this relationship.

From the equations (2.26a). (2.27) and since $J_i = C_i V_i^4$ where C_i is the concentration and V_i^4 the velocity relative to the membrane t_3/t_1 becomes

$$t_3/t_1 = C_3 V_3^4 / Z_1 C_1 V_1^4$$

The ratio V_3^4/V_1^4 is, therefore, a constant equal to 0.576 for C_{60} membranes in normal and expanded forms under all conditions studied.

To examine the analogue with aqueous electrolyte solutions the velocity V_i^4 must be converted to a solvent fixed frame of reference V_i^3. Then

$$V_3^4 / V_1^4 = -V_4^3 / (V_1^3 - V_4^3) = 0.576$$

which on rearrangement gives that the velocities of sulphonate-matrix to sodium counter-ion

$$- V_4^3 / V_1^3 = 1.36$$

This shows that these two ions have similar velocities relative to water solvent. The sulphonate-matrix ion has therefore much in common with a simple order destroying anion such as chloride, which has slightly greater mobility than sodium ion in aqueous solution (in the same concentration range as the internal electrolyte concentration in the membrane). In concentrated sodium chloride the mobility ratio $V_{Cl}^3/V_{Na}^3 = 1.70$. The fact that increasing concentration of salt in the membrane, up to 22% has no effect upon the mobility ratio is a good indication that from a kinetic standpoint/

standpoint, sulphonate and chloride are to a degree similar. Therefore, as a consequence of this similarity, exhibited between the sulphonate-matrix fixed charge of the membrane and the free chloride ion of the binary solution, the polystyrene sulphonic acid membrane can be modelled by a sodium chloride solution of equal molality to that of the exchanger membrane. It is a basic assumption of this model that the polymer matrix makes no reactive contribution to the membrane transport processes. However, because of the random orientation of the polymer chains, and cross linking, the matrix creates intricate pathways to which the mobile species are restricted. Thus the phenomenological coefficients, obtained from the binary solution system to represent the ternary solution model, have no account taken, in their basic form, for this tortuosity correction imposed by the polymer matrix. Major deviations between the observed transport parameters and those predicted by the model can also be considered as indications of this steric polymer effect, for instance the orientation of the polymer-fixed charge may cause structuring of the pore solution to some extent different from that of the free solution, and might also impose a degree of coupling or ion pairing, especially with di or tri-valent cations. Homogeneous membranes which are not very dense, or membranes with large pore cross-sections would have local ionic distributions which differed greatly from those of the aquecus binary model, thus the polymer matrix would again affect the transport processes to a very great extent. If, however, the aqueous ion permeable regions of the membrane constitute an essentially homogenecus phase, it is conceivable that the distribution of charges might approximately represent those in an aqueous electrolyte solution, and in this range a salt model would predict membrane/

membrane properties in at least a semi-quantitative fashion.

The choice of a salt model based on a ternary isotopic solution allows precise evaluation of model coefficients. The theory of isotopic diffusion and the identification of isotope-isotope coefficients has been developed by Laity [10] and by Kedem and Essig [11]. The theoretical treatment presented owes much to these papers and is developed primarily to express frictional interaction in the isotopic ternary solution in terms of those of the parent binary electrolyte and the isotopic diffusion coefficient for co-ion.

As stated previously frictional coefficients R_{ik} are independent of frame of reference, and are therefore convenient for this presentation as a change in frame of reference is required from solvent fixed, for the binary model to ion-(4)-fixed for the membrane.

3.1 THEORY

From equation (2.6) the phenomenological equations for a simple binarysolution are given by

$$X_1 = R_{11}J_1^3 + R_{12}J_2^3 \qquad (3.1a)$$

$$X_2 = R_{21}J_1^3 + R_{22}J_2^3 \qquad (3.1b)$$

where the flows of both cation and anion are expressed on a solvent fixed frame of reference. Now consider another solution where cation remains unchanged, but a specified number of anions (2) are replaced by a chemically identical species (4) under the condition that the total anion concentration remains unchanged thus

$$c_2 = c_2 + c_4 \qquad (3.2)$$

equation (2.18)

$$X_i = \sum_{k=1}^{4} J_k R_{ik} \qquad (i,k = 1, 2, 4.)$$

gives the phenomenological equations for the ternary system.

$$x_1 = r_{11}j_1^3 + r_{12}j_2^3 + r_{14}j_4^3 \qquad (3.3a)$$

$$x_2 = r_{21}j_1^3 + r_{22}j_2^3 + r_{24}j_4^3 \qquad (3.3b)$$

$$x_4 = r_{41}j_1^3 + r_{42}j_2^3 + r_{44}j_4^3 \qquad (3.3c)$$

Assuming the Onsager Reciprocal relationships for equations (3.1) and (3.3)

$$R_{ik} = R_{ki} \quad \text{and} \quad r_{ik} = r_{ki}$$

By comparing the binary and ternary systems certain relationships become apparent.

As defined, the cation situation is unchanged and as change in anion has no effect on either x_1 or j_1^3 then

$$J_1^3 = j_1^3 \quad \text{and} \quad X_1 = x_1$$

Also/

Also as a condition of the model and from (3.2)

$$J_2^3 = j_2^3 + j_4^3 \qquad (3.4)$$

From the Gibbs-Duhem, equation (2.13) for both binary and ternary solutions

$$C_1X_1 + C_2X_2 = 0$$

and $$c_1x_1 + c_2x_2 + c_4x_4 = 0$$

the expression (3.5) is derived

$$C_2X_2 = c_2x_2 + c_4x_4 \qquad (3.5)$$

the conditions for isotope diffusion of co-ion, i.e.

no electrochemical gradient for species (1) gives that $x_1 = 0$

$j_1^3 = 0$. As no bulk flow of co-ion takes place

$$J_2^3 = j_2^3 + j_4^3 = 0 \qquad (3.6)$$

thus $j_2^3 = -j_4^3$ and from (3.5)

$$c_2x_2 = -c_2x_4 \qquad (3.7)$$

applying these equalities to (3.3a) gives

$r_{12} = r_{14}$ and from the O.R.R.

$$r_{12} = r_{14} = r_{41} = r_{21}$$

Comparing expressions (3.1a) and (3.3a) for $J_1^3 = j_1^3 = 0$ and $J_2^3 = 0$ give respectively $R_{11} = r_{11}$ and $R_{12} = r_{12} = r_{14}$ and comparing (3.1b) with (3.3b)(3.3c) under the condition

$X_2 = x_2 = x_4 = Z_iF\left(\frac{-d\psi}{dx}\right)$ where $Z_i = Z_2 = Z_4$, using $R_{11}X_1 = r_{11}x_1$ gives the equations (3.8) and (3.9)

$$R_{22}J_2^3 = r_{22}j_2^3 + r_{24}j_4^3 \qquad (3.8)$$

$$R_{22}J_2^3 = r_{42}j_2^3 + r_{44}j_4^3 \qquad (3.9)$$

Since co-ions (2) and (4) are chemically identical they have the same/

same electrochemical mobility, v, under an applied electric potential gradient, such that $J_i = C_i v_i$, therefore (3.8) and (3.9) become

$$C_2 R_{22} = c_2 r_{22} + c_4 r_{24} = c_2 r_{42} + c_4 r_{44} \qquad (3.10)$$

Again under the conditions for isotopic diffusion of co-ion, with no gradient of electric potential, salt concentration, or pressure potential, the thermodynamic forces x_i reduce to

$$x_i = \left(\frac{d\hat{\mu}_i}{dx}\right) = RT\left(\frac{d\ln c_i}{dx}\right) = \frac{RT}{c_i}\left(\frac{-dc_i}{dx}\right) \qquad (3.11)$$

(where i = 2,4)

Using equations (3.6) and (3.11) equations (3.3b) (3.3c) give

$$j_2 = \frac{RT}{c_2}(r_{22}-r_{24})\left(\frac{-dc_2}{dx}\right) \qquad (3.12)$$

$$j_4 = \frac{RT}{c_4}(r_{44}-r_{42})\left(\frac{-dc_4}{dx}\right) \qquad (3.13)$$

which on comparison with Ficks Law of Diffusion

$$J_i = D_{ii}\left(\frac{-dc_i}{dx}\right)$$

gives the expression for the diffusion coefficient of co-ion

$$D_{22} = RT/c_2(r_{22}-r_{24}) = RT/c_4(r_{44}-r_{42}) \qquad (3.14)$$

By using equation (3.10) a single equation for D_{22} and D_{44} can be obtained (3.15) expressing the diffusicn coefficients in terms of the direct frictional coefficient of anion R_{22} and the total concentration of anion C_2 in the binary and

r_{24} the isotope-isotope frictional coefficient of the ternary

$$D_{22} = D_{44} = \frac{RT}{C_2(R_{22}-r_{24})} \qquad (3.15)$$

Rearranging (3.15) gives

$$C_2 (R_{22} - r_{24}) = \frac{RT}{D_{22}}$$

and applying (3.2) and equation (3.10) the expressions (3.16) (3.17) and (3.18) for the frictional coefficients r_{24}, r_{22}, r_{44} are obtained.

$$r_{24} = r_{42} = R_{22} + \frac{RT}{C_2 D_{22}} \qquad (3.16)$$

$$r_{22} = R_{22} + \frac{c_4}{c_2} \frac{RT}{C_2 D_{22}} \qquad (3.17)$$

$$r_{44} = R_{22} + \frac{c_2}{c_4} \frac{RT}{C_2 D_{22}} \qquad (3.18)$$

Equations (3.17) (3.18) indicate that the direct frictional coefficients for species (2) and (4) depend on their ratios in the ternary solution,

Finally, by applying the identities

$$\sum_{i=1}^{3} C_i R_{ik} = 0 \qquad k = 1, 2, 3$$

$$\sum_{i=1}^{4} c_i r_{ik} = 0 \qquad k = 1, 2, 3, 4$$

to both binary and ternary solutions the ion-water frictional coefficients can be found by considering X_3 in the former and x_3 in the latter.

$$R_{13} = r_{13} \text{ and } R_{33} = r_{23} = r_{43}$$

$$R_{33} = r_{33}$$

indicating that the ion-water interactions are the same in the model ternary and the simple binary solutions. This completes the evaluation of the model ternary matrix from the binary solution information.

3.1.1
Phenomenological Equations on a Membrane Fixed Frame of Reference.

While comparing the frictional coefficients of the ternary solution model with the simple binary, it was necessary to consider the flows of each species, in the normal solution fashion, with respect to fixed solvent. However, in order to use the ternary solution/

solution system to model an ion exchange membrane, defining the membrane species as (1) counter ion, (2) co-ion (taken up as salt in the imperfect membrane), (3) solvent water, (4) fixed charge (including surrounding polymer), the flows of these species must be measured relative to the membrane matrix, i.e. to (4).

Redefining the phenomenological equations (3.3)

$$x_1 = r_{11}j_1^4 + r_{12}j_2^4 + r_{13}j_3^4 \qquad (3.19a)$$

$$x_2 = r_{21}j_1^4 + r_{22}j_2^4 + r_{23}j_3^4 \qquad (3.19b)$$

$$x_4 = r_{31}j_1^4 + r_{32}j_2^4 + r_{33}j_3^4 \qquad (3.19c)$$

where j_i^4 is defined.

$$j_i^4 = (j_i^3 - \frac{c_i}{c_4} j_4^3)$$

In the model, with the exception of the direct frictional coefficient of co-ion r_{22}, the frictional coefficients are defined directly from the binary solution.

r_{22} is dependent on D_{22} the isotopic diffusion coefficient and the ratio of species (2) and (4) defined by the model. Thus r_{22} is inversely dependent on the salt uptake of the membrane a feature also observed in experimental studies of ion exchange membranes[2]

3.1.2
Scaling Factors due to Membrane Tortuosity

Equations (3.19) represent a model of a membrane in which no account has been taken of the effect of the polymer matrix. This model assumes that the membrane's properties are determined by the fixed ions on the polymer matrix and that these correspond to simple anions in solution. However, membrane processes will be/

be affected by the polymer matrix creating tortuous diffusional pathways through which transport must occur. Because of this a scaling factor must be derived which will change the phenomenological coefficients of the ternary model in such a way as to account for this polymer effect.

Generally membrane concentrations are expressed in moles cm^{-3} of the total membrane volume $\bar{C}$, i.e. polymer matrix and imbibed water where $\bar{C} = VC$ and V is the fractional aqueous volume (pore volume) of the membrane. Similarly flow across the membrane $\bar{J}$ is expressed in units of flow/unit area of exposed membrane, $\bar{J} = jV^1$ where V^1 is the ratio of pore to geometric area at the membrane surface. The membrane is defined as homogeneous in macroscopic terms if $V^1 = V$.

If the geometric thickness of the membrane is represented by $\bar{d}$ then due to the tortuousity of the polymer matrix the diffusional path length will be $d\theta$ which corresponds to a solution which presents a path length d where $\theta > 1$.

Fick's equation for isotopic diffusion of co-ion can be used to illustrate the effects of these scaling factors.

$$j_2 = -D_{22} \Delta c_{2/d} \qquad (3.20)$$

becomes

$$\bar{J}_2/V^1 = - \frac{D_{22}}{\theta} \frac{\Delta \bar{c}_2}{\bar{d}} \frac{1}{V} \qquad (3.21)$$

and if $V^1 = V$ (for a homogeneous membrane)

$$J_2 = - \frac{D_{22}}{\theta} \frac{\Delta \bar{c}_2}{\bar{d}}$$

So that $D_{22}/\theta = \bar{D}_{22}$ (3.22)

The diffusional coefficient of co-ion in the tortuous membrane $\bar{D}_{22} = D_{22}/_{\theta}$ using this salt model calculation and so is smaller than in free solution. Using barred symbols to represent the membrane.

$$\bar{D}_{22} = \frac{RT}{\bar{C}_2 (\bar{R}_{22} - \bar{R}_{24})} \qquad (3.23)$$

and/

and consequently

$$\bar{R}_{22} = r_{22}\frac{\theta}{V} \quad \text{and } \bar{R}_{24} = r_{24}\frac{\theta}{V}$$

Since this analysis can be applied to the forces and flows in the phenomenological equation (3.19) it is generally true that

$$R_{ik} = r_{ik}\frac{\theta}{V}$$

Therefore, due to the inverse relationship between the frictional and mobility coefficients

$$\bar{l}_{ik} = \frac{l_{ikV}}{\theta}$$

θ may be derived by either the method of Prager giving θ_p, or by that of Meares for the path tortuosity θ_m Section (5.2.1) The salt model calculation S.M.C. however defines θ as $D_{22}/\bar{D}_{22}$ and as θ_s will be used in the comparison of experimental membrane parameters with those calculated by the Salt Model Calculation given in the following sections.

The frictional coefficients for the model membrane system and their relation to solution coefficients can thus be shown

$$\begin{vmatrix} \bar{R}_{11} & \bar{R}_{12} & \bar{R}_{13} & \bar{R}_{14} \\ \bar{R}_{21} & \bar{R}_{22} & \bar{R}_{23} & \bar{R}_{24} \\ \bar{R}_{31} & \bar{R}_{32} & \bar{R}_{33} & \bar{R}_{34} \\ \bar{R}_{41} & \bar{R}_{42} & \bar{R}_{43} & \bar{R}_{44} \end{vmatrix} \qquad \begin{vmatrix} R_{11} & R_{12} & R_{13} & R_{12} \\ R_{21} & r_{22} & R_{23} & r_{24} \\ R_{31} & R_{32} & R_{33} & R_{32} \\ R_{21} & r_{42} & R_{23} & r_{44} \end{vmatrix} \times \frac{\theta}{V}$$

S.M.C. Membrane Solution

where r_{22}. r_{24} and r_{44} are defined by equations (3.17) (3.16) (3.18) respectively.

An estimate of the frictional coefficients for an experimental membrane may therefore be obtained from (1) a knowledge of its physical dimensions, (2) the concentration of ions and water in the membrane, and (3) the co-ion diffusion coefficient.

3.2 Application of the Salt Model Calculation

The isotopic model imposes certain basic conditions. Since the co-ion (2) and matrix fixed charge (4) are taken as chemically identical, the transport number of co-ion t_2 will be zero. The change of frame of reference to matrix fixed automatically requires co-ion to be stationary relative to (4) in an electrical experiment.

3.2.1 Specific Conductivity

The specific conductivity K is independent of the frame of reference chosen and as this can be defined by the mobility coefficients equation (2.24) the S.M.C. predicts the specific conductivity of the membrane $\bar{K}$ can be determined from the specific conductivity of the equivalent equimolar sodium chloride solution, K, by equation (3.24)

$$\bar{K} = K\frac{V}{\theta} \qquad (3.24)$$

3.2.2. Electro Osmotic Transport Number

In-membranes the electro-osmotic flow of water is generally measured with respect to the stationary matrix (4).

therefore in the S.M.C.

$$t_3^4 = t_3^2 = {}^{J_3^2 F}/_{I} = {}^{C_3(V_3 - V_2)F}/_{I} \qquad (3.25)$$

In the binary solution the flows of both cation and anion are measured relative to the solvent water. Therefore, the transport number of the anion in the binary is

$$t_2^3 = \frac{Z_2 J_2^3 F}{I} = \frac{Z_2 C_2 (V_2 - V_3)F}{I} = \frac{-Z_2 C_2 (V_3 - V_2)F}{I} \qquad (3.26)$$

Comparing equations (3,25) and (3.26) gives

$$t_3^2 = -\frac{C_3}{Z_2C_2} t_2^3 \qquad (3.27)$$

and since in the binary solution $Z_1C_1 = -Z_2C_2$

$$t_3^{S.M.C.} = \frac{C_3}{Z_1C_1} t_2^3 \qquad (3.28)$$

Therefore if the capacities of both water and counter ion are known for any membrane, in any proportion, the t_3 can be directly determined from the co-ion transport numbers of the corresponding binary solution.

3.2.3. Salt Flow and Water Flow

For a 1:1 electrolyte equations (2.41) and (2.43) give

$$J_s = \frac{1}{\alpha}(l_{11}l_{22}-l_{12}^2)\left(\frac{-d\mu_{12}}{dx}\right) + (l_{13} - \alpha t_1 t_3)\left(\frac{-d\mu_3}{dx}\right)$$

$$J_w = (l_{13} - \alpha t_1 t_3)\left(\frac{-d\mu_{12}}{dx}\right) + (l_{33} - \alpha t_3^2)\left(\frac{-d\mu_3}{dx}\right)$$

However since in the S.M.C. $\bar{t}_2 = 0 \quad \bar{t}_1 = 1$ equation (2.25) gives that $l_{12} = l_{22}$, therefore J_s and J_w become

$$J_s = l_{22}\left(\frac{-d\mu_{12}}{dx}\right) + l_{23}\left(\frac{-d\mu_3}{dx}\right) \qquad (3.29)$$

and

$$J_w = l_{22}\left(\frac{-d\mu_{12}}{dx}\right) + \left(l_{33} - t_3^2 \alpha\right)\left(\frac{-d\mu_3}{dx}\right) \qquad (3.40)$$

therefore in the salt model calculation

$$l_{22} = L_{ss}$$

$$l_{23} = l_{32} = L_{sw} \text{ and}$$

$$(l_{33} - t_3^2 \alpha) = L_{ww}$$

3.3 Comparison of the Phenomenological Coefficients Calculated with those Observed

The frictional coefficients for the binary (sodium chloride) model electrolyte were obtained from Miller's tabulated data [12] and isotopic diffusion coefficients, for chloride co-ion, taken from Mills [6]. Since molarity C, of the species relative to unit volume of aqueous pore solution is not defined unequivocally, this concentration was estimated by assuming the ratio of molarity to molality to be the same in the membrane as in an equimolar aqueous sodium chloride solution at 25°C.

Frictional coefficients obtained from experimental data and from the salt model calculation for 0.1M (external) are given in Table(3.3) The correction factors accounting for the tortuous 'pores' of the matrix $\theta/_{V}$ were estimated using the ratio $D_{22}/\bar{D}_{22}$ as suggested by the model and those of Meares and Prager as discussed in section (5.2.1.). These three methods designated $(\bar{S})$ $(\bar{M})$ $(\bar{P})$ respectively are used in all tabulated data.

Before making a detailed comparison between this simple model calculation and the observed properties of membranes, it is of interest to note that the model predicts that a value of $\bar{R}_{22}$ the direct frictional coefficient of co-ion in the membrane may be directly determined from the isotopic diffusion coefficient of co-ion in the membrane D_{22} providing the ratio of fixed charge to co-ion concentration is large, equations (3.14) (3.16) (3.17).

For most binary electrolytes the function $RT/\bar{C}_2\bar{D}_{22}$ is of the same order of magnitude as R_{22}.

For example in aqueous sodium chloride at 3M the function is some 20% smaller than R_{22}.

If the co-ion to sulphonate friction in the experimental membrane/

membrane is even approximately equal to r_{24} of the S.M.C. then

$$\bar{R}_{22} \approx {}^{RT}/_{\bar{C}_2\bar{D}_{22}}$$

The overall agreement between calculated and experimental coefficients is good; the values calculated follow in detail the trends and magnitudes presented by the data determined from experimental measurements (1) (2).

There is particularly good agreement between calculated and experimental values of $\bar{R}_{22}$ and $\bar{R}_{44}$ (for the C_{60E}, 0.1M external, the correspondence is almost coincident) which largely justifies the basic assumptiom of the Salt Model; i.e. that aqueous chloride and sulphonate-matrix anions have similar kinetic characteristics. For both normal and expanded membranes, i. 0.1M (external) the salt uptake is small and $\bar{R}_{44}$ is given to a good approximation by the solution coefficient $R_{22}/\bar{\theta}_V$ Table (3.3) equation (3.18). Equally the very large values for $\bar{R}_{22}$ are explained by the dominant contribution of the concentration ratio c_4/c_2 in equation (3.17). The lower value of $\bar{R}_{22}$ in the expanded membrane C_{60E} (0.1M external) is caused primarily by the greater uptake of co-ion $\bar{C}_2$, reducing the c_4/c_2 ratio, since the value of the direct frictional coefficient R_{22} in the model solution, is largely unaffected by the change in concentration from 2.87m in C_{60N} (0.1M external) to 2.11m in C_{60E} (0.1M external). The direct frictional coefficients for sodium ion and water, $\bar{R}_{11}$ and $\bar{R}_{33}$, are over-estimated to a similar extent by the S.M.C. particularly in the more concentrated normal membrane C_{60N} (0.1M external). Ion-to-water coefficients $\bar{R}_{13}$ and $\bar{R}_{34}$ indicate that the sodium ion and sulphonate-matrix have similar water interactions to sodium ion and chloride in the solution model. Apart from two striking examples of disagreement, the co-ion to water/

water friction $\bar{R}_{23}$ and the counter ion to co-ion friction $\bar{R}_{12}$ which are difficult to explain, the S.M.C. shows remarkably good agreement with the experimental data, especially so when the simplicity of the basic concept is considered.

Mobility coefficients, $\bar{l}_{ik}$, for the systems C_{60N} 0.1M (external) and C_{60E} 0.1M and 1.0M (external) are shown in tables (3.4) (3.5) respectively. In the S.M.C. for a 1:1 salt $\bar{l}_{12} = \bar{l}_{22}$ (as $t_2 = 0$). Once again the agreement between experimental and calculated coefficients is very good and the tortuosity corrections $(\bar{S})$and $(\bar{M})$ are superior to the Prager value $(\bar{P})$ for all coefficients except $\bar{l}_{23}$ and $\bar{l}_{33}$ both of which are under estimated by the S.M.C. The experimental value of $\bar{l}_{12}$ is small and cannot be determined with confidence for the membranes equilibrated in 0.1M (external) as tbe co-ion uptake is very low. The good agreement between the S.M.C. and observed coefficients l_{22} indicates (from equation (2.28)) that in the membrane the cross coupling coefficient $\bar{l}_{12}$ must be small. However in the expanded membrane C_{60E} (1.0M external) the salt uptake is some 14% (of the total capacity) and cannot be neglected. For this membrane the S.M.C., especially $(\bar{S})$, is in good agreement with the measured experimental values. As mentioned previously the S.M.C. under-estimates the direct mobility coefficient of water, $\bar{l}_{33}$. In the C_{60N}(0.1M external) the disagreement is very small, less than 2.0% (considering $(\bar{P})$). However in the expanded membrane, C_{60E}(0.1M external) and (1.0M external), the degree of under-estimation is close to 50%. This has serious consequences when using the S.M.C. to predict water flow, especially in the desalination predictions of section (6.1.4.) which depend primarily on the magnitude of $\bar{l}_{33}$.

In earlier work on the C_{60} membrane [1] [2] in order to evaluate the/

the full l_{ik} matrix, approximations were made which involved the neglect of certain thermodynamic coefficients further discussed in section (6.1.2.) . In particular neglect of co-ion to water coupling $\bar{l}_{23}$ was found to be valid ($\bar{l}_{23} \ll l_{13}$). The S.M.C. justifies this assumption for the C_{60N} and C_{60E} (0 .1M external) since, by calculation, $\bar{l}_{23}$ is less than 1% of the value of l_{13} and appears only in the expression (2.26a) for electro-osmotic transference number, t_3, which can normally be measured only to an accurary of $\pm$ 1.0%.

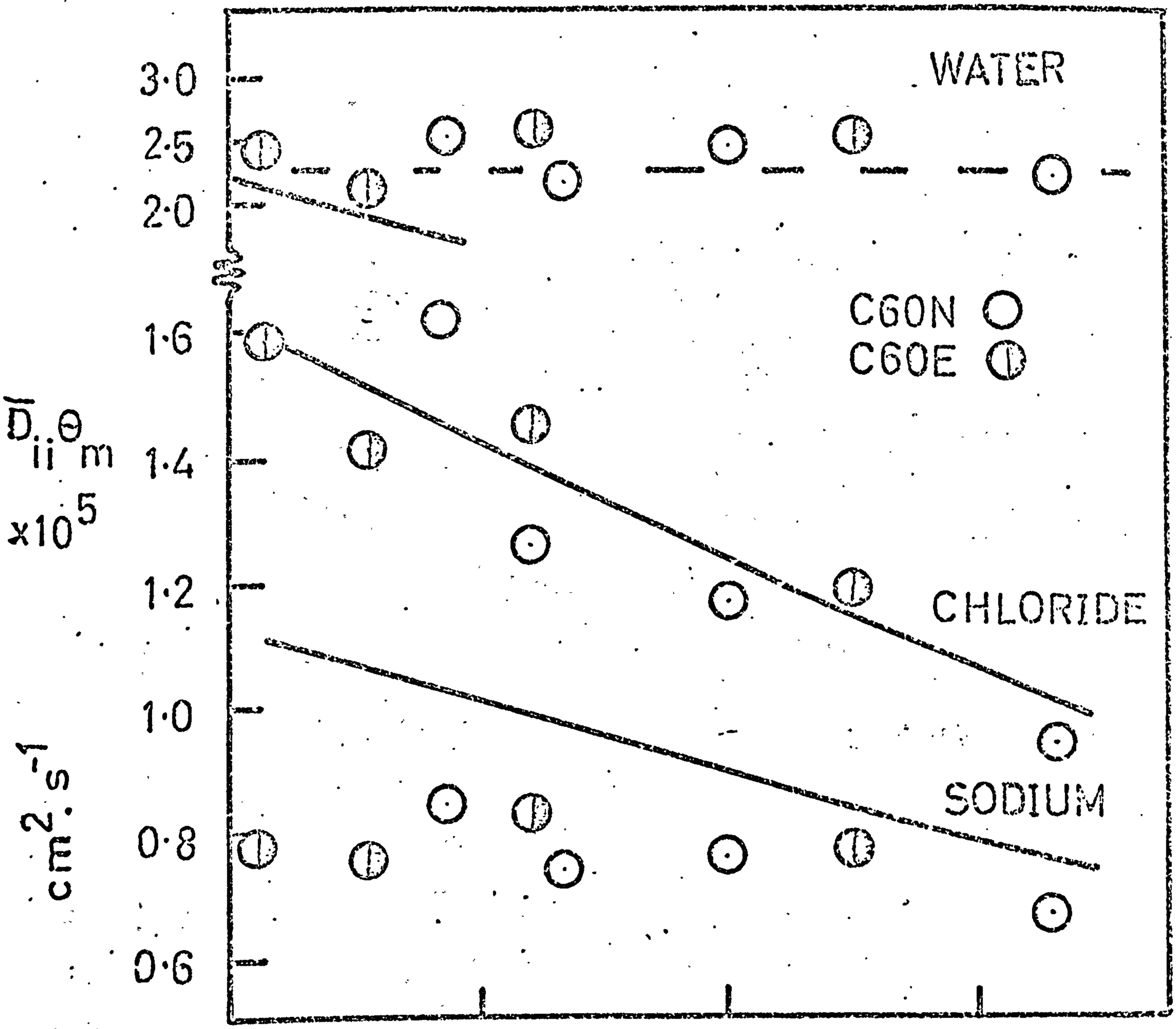
WATER
CHLORIDE
SODIUM
C60N
C60E
3·0
2·5
2·0
1·6
1·4
1·2
1·0
0·8
0·6
$\bar{D}_{ii}\Theta_m$ x10^5
cm^2.s^{-1}
2.0
3.0
4.0
5.0
TOTAL INTERNAL MOLALITY

FIGURE 3.1

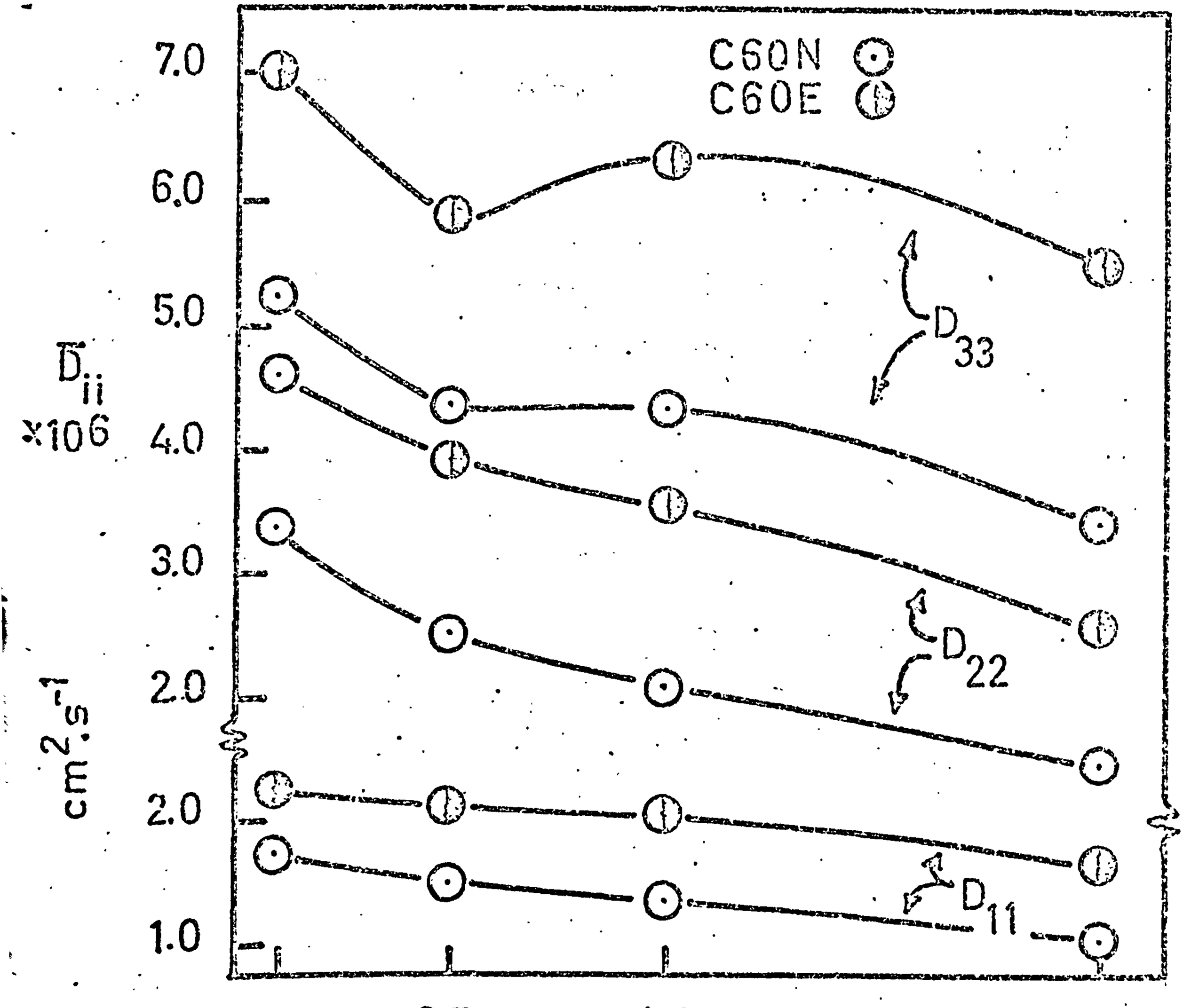
7.0
6.0
5.0
4.0
3.0
2.0
2.0
1.0
D_{ii} x10^6 cm^2.s^{-1}
C60N
C60E
D_{33}
D_{22}
D_{11}
0·0
0·5
1·0
2·0
Molarity NaCl (external)

FIGURE 3.2 -

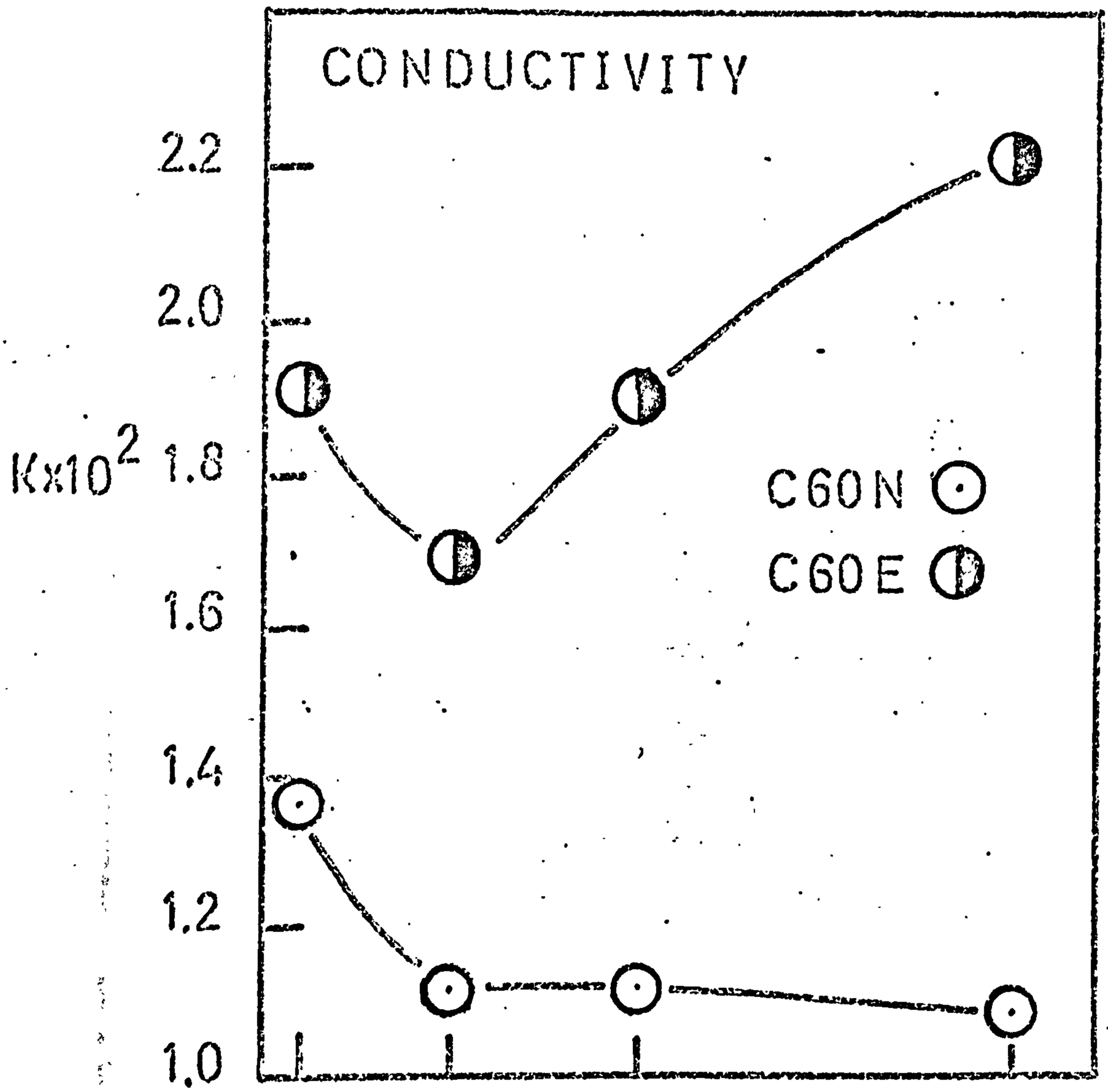
CONDUCTIVITY
2.2
2.0
1.8
1.6
1.4
1.2
1.0
Kx10²
C60N
C60E
.1
.5
1.0
2.0
Molarity NaCl (external)

FIGURE 3.3.

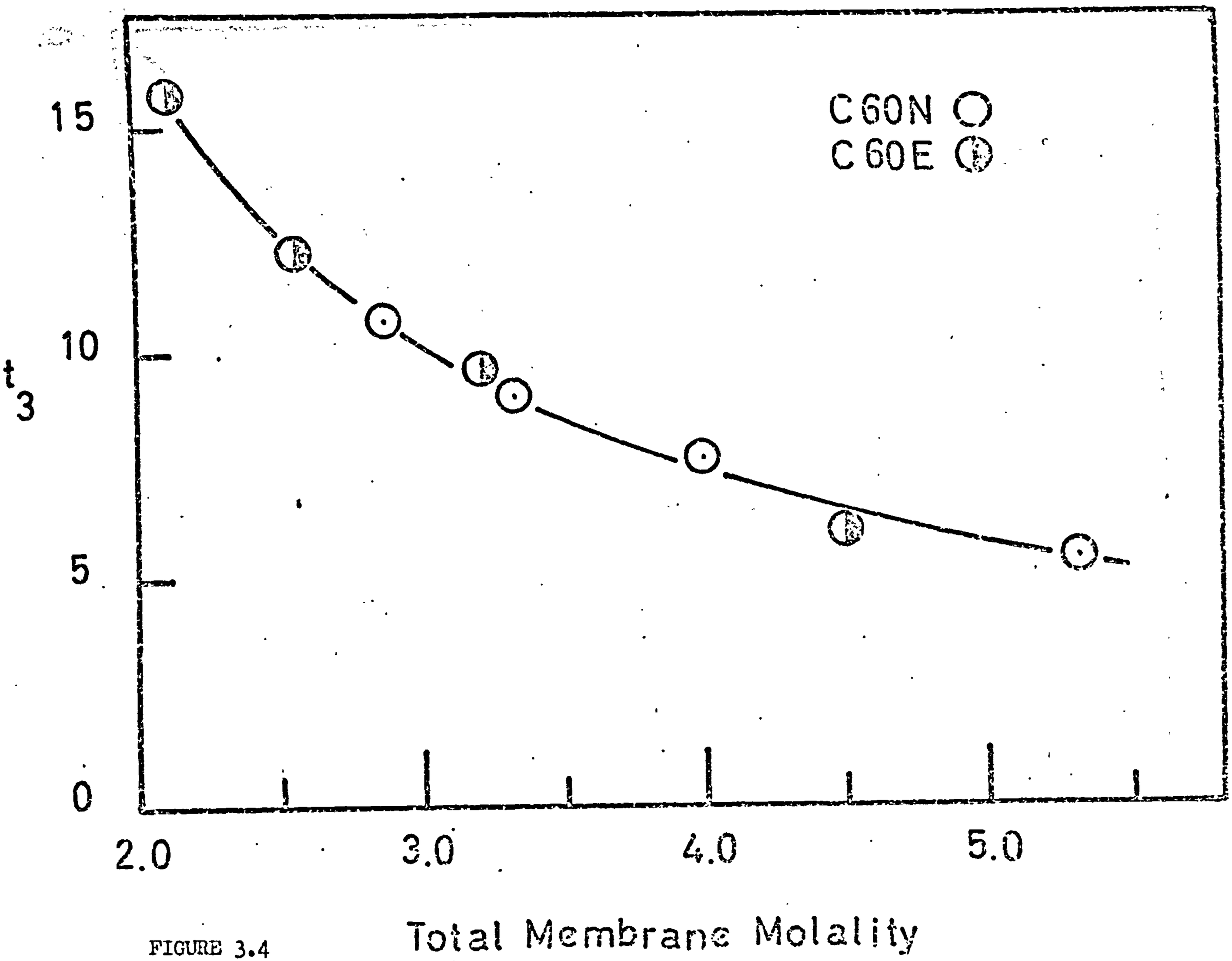

FIGURE 3.4

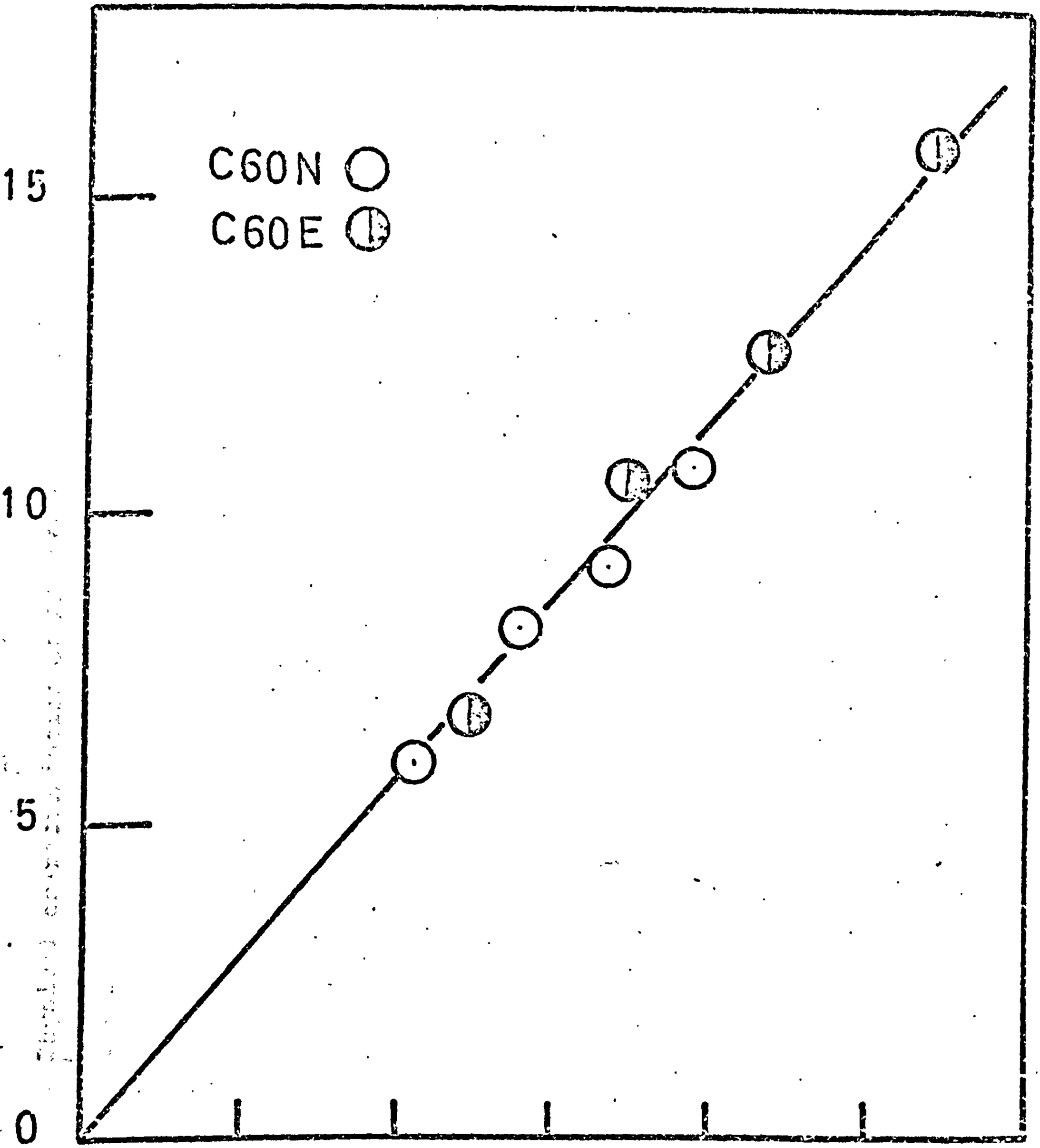

FIGURE 3.5

Table (3.1)

Physical characteristics of AMF C60 membranes[3]

C60N: Dry weight of leached membrane disc in Na form = 0.2345 g, Ion-exchange capacity = 1.57 mequiv. g^{-1} dry membrane

ext.soln. NaCl/M	wet wt./g	% water w.r.t. dry wt.	diameter/ cm	thickness/ cm	volume/ cm^3	$\bar{C}_1$	$\bar{C}_2$	$\bar{C}_3$
						mequiv.cm^{-3}		
0.1	0.3579	52.6	3.698	0.0335	0.360	0.980	0.0024	19.03
0.5	0.3449	46.7	3.655	0.0314	0.329	1.104	0.0360	18.48
1.0	0.3320	40.8	3.611	0.0308	0.315	1.209	0.0946	16.86
2.0	0.3176	33.7	3.551	0.0299	0.296	1.419	0.2312	14.89

C60E: Dry weight of leached membrane disc in Na form = 0.2249 g, Ion-exchange capacity = 1.70 mequiv. g^{-1} dry membrane

ext.soln NaCl/M	wet wt./g.	% water w.r.t. dry wt.	diameter/ cm	thickness/ cm	volume/ cm^3	$\bar{C}_1$	$\bar{C}_2$	$\bar{C}_3$
						mequiv.cm^{-3}		
0.1	0.3998	77.7	3.847	0.0333	0.387	0.960	0.0052	25.07
0.5	0.3807	68.6	3.754	0.0321	0.355	1.112	0.0717	24.11
1.0	0.3629	59.8	3.697	0.0317	0.340	1.270	0.1832	21.94
2.0	0.3470	50.5	3.616	0.0308	0.316	1.621	0.4533	19.95

TABLE (3.2)

A Comparison of L Coefficients for Sodium Sulphonate Membrane and Aqueous Sodium Chloride ($25^{o}C$)

The reference frame for each is stationary solvent

System	C_{60N}	C_{60E}	NaCl	NaCl	NaCl
Internal Molality	2.87	2.13	2.09	2.64	3.20
$10^{12} \times L_{11}$	1.27	2.37	-	-	-
$10^{12} \times L_{44}$	1.45	2.95	-	-	-
$10^{12} \times L_{14}$	0.63	1.64	-	-	-
θ	4.81	3.45	1.0	1.0	1.0
$10^{12} \times L_{11}\ \theta/M$	2.14	3.84	3.75	3.18	3.16
$10^{12} \times L_{44}\ \theta/M$	2.64	4.77	5.79	5.10	5.06
$10^{12} \times L_{14}\ \theta/M$	1.05	2.60	0.873	0.813	0.805
$10^{12} \times t_1$	0.441	0.363	0.362	0.359	0.356

Data for NaCl taken from reference (12)

TEXT BOUND INTO

THE SPINE

Table (3.3)

Comparison of salt model calculations (S.M.C.) with experimental values of R-coefficients for C60N and C60E (a)

Membranes in sodium chloride solutions. (0.1M) at 25°C

Method	$\bar{R}_{22}$	$\bar{R}_{11}$	$\bar{R}_{44}$	P_{22}^*	$\bar{R}_{33}$	$-\bar{R}_{12}$	$-\bar{R}_{14}$	$-\bar{R}_{13}$	$-\bar{R}_{23}$	$-\bar{R}_{43}$
C60N	J cm s mole^{-2} x 10^{-12}									
Exptal.	349	1.01	0.88	-	0.0028	-1.57	0.442	0.030	0.144	0.023
S.M.C. (s)	294	1.30	0.82	0.82	0.0045	0.204	0.204	0.057	0.032	0.032
(m)	329	1.46	0.92	0.92	0.0050	0.229	0.229	0.064	0.036	0.036
(p)	260	1.15	0.72	0.72	0.0040	0.181	0.181	0.050	0.028	0.028
S.M.C. (uncorrected)	24.76	0.1101	0.0691	0.06895	0.000386	0.01725	0.01725	0.0048	0.00267	0.00267
	m_1 m_2 m_4, the molalities of sodium, chloride and sulphonate were 2.87, 7.08 x 10^{-3} and 2.863 respectively, and the concentration ratio m_4/m_2 = 404.38									
C60E										
Exptal.	102	0.83	0.602	-	0.0013	-1.65	0.283	0.0218	0.102	0.0128
S.M.C. (s)	103	0.88	0.619	0.619	0.0019	0.149	0.149	0.0320	0.0181	0.0181
(m)	103	0.98	0.621	0.621	0.0019	0.149	0.149	0.0320	0.0181	0.0181
(p)	82.9	0.79	0.501	0.501	0.0015	0.120	0.120	0.0258	0.0145	0.0145
S.M.C. (uncorrected)	14.024	0.134	0.0848	0.0848	0.000261	0.0203	0.0203	0.00436	0.00247	0.00247
	m_1, m_2 and m_4 are 2.1?$_v$, 11.49 x 10^{-3}, and 2.113 respectively and m_4/m_2 = 183.49									

In salt model calculations, (S.M.C.), (s), (m), (p) refer to scaling factors θ/v calculated using θ_s (experimental), θ_p, and θ_m respectively.

*For the aqueous binary friction coefficient, for chloride is retained for comparison with $\bar{R}$

Table (3.4)

Mobility coefficients, $\bar{\ell}_{ik}$, for C60N and C60E membranes in sodium chloride solutions. (0.1M) at 25°C.

Method		$\bar{\ell}_{11}$	$\bar{\ell}_{12}$	$\bar{\ell}_{22}$	$\bar{\ell}_{13}$	$\bar{\ell}_{23}$	$\bar{\ell}_{33}$
		$mole^2\ J^{-1}s^{-1}cm^{-1} \times 10^{12}$					
C60N							
		1.47	-	0.0029	16.0	0.159	547
S.M.C.	(s)	1.65	0.0034	0.0034	20.7	0.065	475
	(m)	1.49	0.0031	0.0031	18.6	0.059	427
	(p)	1.84	0.0039	0.0039	23.6	0.075	540
S.M.C. (Uncorrected)		19.9	0.0405	0.0405	247.6	0.784	5673
C60E							
		2.05	-	0.0103	33.6	1.07	1930
S.M.C.	(s)	2.25	0.0099	0.0099	33.3	0.257	1152
	(m)	2.24	0.0099	0.0099	33.2	0.256	1149
	(p)	2.78	0.0122	0.0122	46.4	0.328	1425
S.M.C. (Uncorrected)		16.14	0.0722	0.0722	274.3	1.88	8423

TABLE (3.5)

Membrane-fixed Mobility Coefficients for C_{60E} in 1.0 molar Sodium Chloride (25°C) (C_2/C_{Total} = 0.144)

Method	l_{11}	l_{12}	l_{13}	l_{22}	l_{23}	l_{33}
			$\times 10^{12}$ (mole^2 J^{-1} cm^{-1} s^{-1})			
Exptal						
(a)	2.09	0.210	-32.0	0.372	12.3	1010
(b)	2.09	0.199	30.0	0.361	10.0	1076
S.M.C.						
(s)	2.40	0.29	28.6	0.29	5.1	570
(m)	2.48	0.30	20.6	0.30	5.3	591
(p)	3.33	0.41	39.6	0.41	7.1	792

Assumptions made in the evaluation of parameters from experimental data

(a) $\frac{l_{23}}{C_2C_3} = \frac{2l_{33}}{C_3^2} - \frac{l_{13}}{C_1C_3}$ and

(b) $R_{22} = 0$

REFERENCES (S.M.C.)

CHAPTER 3.

1) R. Paterson and C.R. Gardner. J. Chem. Soc. A.2254 (1971)

2) H. Ferguson, C.R. Gardner, R. Paterson. J.C.S. Faraday I. 68, 2021 (1972)

3) C.R. Gardner and R. Paterson. J.C.S. Faraday I. 68, 2030 (1922)

4) R. Arnold and D.F.A. Kock. Aust. J. Chem. 19, 1299 (1966)

5) J.S. Mackie and P. Meares. Prov. Roy. Soc. (London) A.282, 510 (1955)

6) R. Mills. Rev. Pure Appl. Chem. 11. 78, (1961).

7) B. Brun. PhD Thesis. Moltpellier University (1967)

8) S. Prager. J. Chem. Phys. 33, 122 (1960)

9) K.S. Spiegler. Trans. Faraday. Soc. 54, 1409. (1958)

10) R.W. Laity. J. Phys. Chem. 70, 2639 (1966)

11) O Kedem and A. Essig. J. Gen. Physioal 48, 1047 (1965)

12) D.G. Miller. J. Phys. Chem. 70, 2639 (1966)

CHAPTER 4

EXPERIMENTAL

APPARATUS AND PROCEDURES

4.1 EXPERIMENTAL

4.1.1. Reagents

Unless stated to the contrary, all reagents used in this study were AnalaR grade.

Solutions were made up with distilled water from an all-glass still in re-calibrated Grade 'A' volumetric glass-ware at 20°C.

4.1.2. Radio Isotopes and Counting Method

The radio isotopes used, Sodium-22, Chlorine-36 were obtained from the Radio Chemical Centre, Amersham as aqueous solutions of sodium chloride.

The radio activity measurements were made, utilising a dioxan based phosphor suitable for aqueous samples[1], on a Packard Tricarb Liquid Scintillation Spectrometer Model 3003. This instrument had an automatic sample changer and print-out device.

Radio-active samples of between (0.10 - 0.50 ml) were added using a Hamilton micro-litre syringe to 10 ml. aliquots of the phosphor solution contained in polythene phials supplied for that purpose (More Scintillation Service, Interexchange Ltd.)

The Hamilton micro-litre syringes used throughout the work were each fitted with Chaney adaptors which allowed accurate volumes reproducible to $\pm$ 0.1% to be delivered each time.

4.1.3. THE ION-EXCHANGE MEMBRANES

The A.M.F. C_{60} Sulphonated Polystyrene Membranes

A.M.F. C_{60} graft copolymer, polyethylene/polystyrene sulphonic acid cation exchangers were provided and manufactured by the American Machine and Foundry Company, Springdale, Connecticut. The basic membrane is prepared from low-density polyethylene and 35% styrene, the styrene copolymer chains are cross-linked with approximately 2% divinyl benzene.

Chemical free radical initiators are used to polymerise the styrene and the fixed sulphonate groups added by reacting with oleum(2).

This process gives a mechanically strong light brown exchanger consisting of microscopic regions of alternate crystalline polyethylene and polystyrene sulphonate.

Electron micrographs of the thorium form(3) show inhomogeneties consisting of high density fixed charge 200 - 400°A in diameter distributed in an even fashion across the membrane. Thus providing for macroscopic considerations a homogeneous membrane.

In 1966 Arnold & Koch(4) reported that this membrane would expand irreversibly on heating. This was confirmed by later work in this laboratory (5) (6) (7)

The heat treatment alters the physical geometry of the membrane and affects the degree to which it will take up both salt and water consequently altering its properties.

In previous work only two types of this membrane were considered, a normal form designated C_{60N} which had undergone no heat treatment and a single expanded form C_{60E} obtained by heating at one temperature (95°C) for a specific time (½ hour). However, in this presentation the effects of heat treatment upon membrane structure

and/

and transport were investigated more systematically. A number of membranes were heat treated for varying lengths of time thus giving a range of membranes with approximately the same ion exchange capacity per unit weight of dry polymer matrix but possessing different degrees of expansion and consequently different physical properties. From this series of membranes the relative effects of expansion on various membrane parameters and properties were examined and trends and relationships between degree of expansion and membrane transport, especially under an applied pressure gradient, determined.

XR - 170 Perfluoro Sulphonic Acid Membranes

The other membrane used in this study was the Nafion Perfluoro Sulphonic Acid cation exchanger. This is a new membrane produced by Du Pont, the composition is currently called XR and consists of a perfluoro carbon sulphonyl fluoride resin (8) produced by polymerising tetra fluorethylene with a polysulphonyl fluoride vinyl ether.

This resin can be completely saponified with hot caustic and treated with strong acid (nitric) to give the hydrogen form of the exchanger. This membrane thus consists of a 'homogeneous' polymer not a copolymer as does the C_{60}. Unlike the C_{60} these membranes are not cross linked, the polymer chains, however, are intertwined at various points and the sulphonate groups are clustered with associated counterions in the interstitial volume, i.e. between the polymer chains. The membrane matrix possesses good mechanical properties and the polymer is chemically, oxidatively and thermally very stable. In visible light it has a water-clear transparency.

By adjusting the proportions and distributions of the comonomers and varying the length, molecular weight, and molecular weight distribution of the precurser chains the properties of the resin can/

can be altered. Using this procedure Du pont have prepared three 'Nafion' membranes in the XR-170 series each having different fixed charge capacity, with respect to dry matrix. These membranes were investigated in this research.

Cellulose Acetate Membranes.

The cellulose acetate membranes used in this research were supplied by the Atomic Energy Research Establishment, Harwell.

The membranes were obtained in a final cast form, but had undergone no heat treatment. As these cellulose acetate membranes were involved in a research project at Harwell, no definite data on the casting process were available. However, a typical casting process is as follows:-

The casting solution is a mixture of cellulose acetate powder, formamide and an inorganic salt, usually magnesium perchlorate, in the proportions 22:67:10:1.

The solution is cast at 0^{o} to $10^{o}C$ on to a cold glass plate. A uniform film thickness is obtained by passing an inclined knife over the surface.

The casting solvents are allowed to evaporate at low temperatures after which the membrane is immersed in cold water. The product is normally a thin film membrane 100 μ thick.

The casting powder is normally cellulose triacetate, however, in a number of effective monomer units (taken as $C_6H_7O(OH)_3$) acetylation is incomplete, hence all cellulose acetate membranes contain some residual carboxyl groups. These carboxyl groups and the carbonyl groups of the 'acetyl' are thought to be important in the rejection mechanism of these membranes.

The cellulose acetate membrane consists of two layers, a backing layer (which makes up almost the whole membrane thickness) of spongy cellulose acetate. This layer has pores 0.1 μ in diameter On top of this spongy layer is a very dense layer called the active layer some 0.25 μ thick. It is this dense layer which desalinates.

If/

If solution is passed first through the active layer into the backing layer, the membrane rejects. If, however, the concentrated solution is passed in the other direction, i.e. first through the backing layer, the membrane does not apparently reject.

The two cellulose acetate membranes used were each heated in a water bath for thirty minutes, one at 80°C, the other at 85°C. They were then equilibrated in solutions of 0.10M NaCl. The membranes were stored in 0.10M NaCl solution and were taken from these for use.

4.1.4 HEAT TREATMENT AND CUTTING

4.1.4.1. A.M.F. C_{60} Membranes.

The membranes, as obtained from the manufacturers were stored in distilled water to which some sodium benzoate was added to prevent fungal and bacterial growth and the storage vessel was kept sealed. For all scientific purposes discs of membrane were used. The C_{60} normal membranes were cut from sheets of wet membrane sandwiched between layers of hard filter paper.

The cutting tool was manufactured from brass tubing approximately 3.8 cm. in diameter to which a very keen cutting edge was machined. By careful rotation of the cutting tool uniformly circular discs were obtained which had cleanly cut edges and hence were suitable for dimensional measurements.

Six inch square sheets of the normal membrane were heat-treated by immersing in a stirred water bath at 95°C forvarious periods of up to three hours. After which the membranes were cut using the machined die. After this heat-treatment the membranes changed colour to a lighter brown and become mechanically softer. Expansion of the membranes by cutting first followed by heating in a water bath was tried. This would give the same weight of polymer matrix for each membrane. However, using this procedure caused the membrane disc to curl into a cylindrical form which could not be straightened out.

After being cut and expanded each membrane was examined under a projection microscope (Nikon Project Projector, Model 6C) for any imperfections, only those which were visibly uniform and unblemished were kept for study.

4.1.4.2 XR-170 Membranes.

The XR-170 membranes (like the C_{60} membranes) swell in hot water. Unlike/

Unlike the C_{60} membranes this expansion may be reversed and the original form obtained by drying at elevated temperatures ($>100^{o}C$). The degree of solvent water absorbed by this membrane is dependent on the temperature of pretreatment. Consequently, in order to make meaningful comparisons of physical and transport properties a standard pretreatment must be used. Grot & Munn (9) reported that after boiling for 30 minutes in water with the polymer in the sulphonic acid form little further change in the physical dimensions of the polymer could be observed.

Several membranes were heated over a period of three hours. At various times during heating they were removed and their wet weights measured. From this preliminary experimentation an impression of the variation in the water content of the XR membranes with heating time was obtained, thus allowing a standard time of heat-treatment to be decided upon.

Considerable problems arose when cutting discs of this membrane due to its extreme physical toughness. Eventually a tempered steel die with a keen machined cutting edge was implemented which gave precisely defined discs with a clean edge of approximately 4 cm. in diameter.

A number of discs cut from each of the three sheets of differing ion exchange capacity(w.r.t. dry weight) supplied by Dupont were heated at $100^{o}C$ for 60 minutes in a water bath and examined for imperfections using the projection microscope. One disc of each ion exchange capacity was selected for study.

4.1.5. Conditioning processes

The Nafion discs were alternately washed with AnalaR acetone and AnalaR methanol for 30 minutes and finally with distilled water in order to remove any organic surface films.

The/

The discs of both membrane types were then treated in an identical manner. Each was equilibrated in sequence in 1M hydrochloric acid, 1M sodium hydroxide and AnalaR methanol for 24 hours.

Between each of the successive equilibrations the discs were washed for several hours in distilled water. This treatment with strong acid and base removed any heavy metals (especially iron as the metal salt) from the polymer while also conditioning the membrane to function as an ion exchanger in a constant manner. The methanol removed any unreactive monomer or other organic impurity remaining in the membrane. This cycle was repeated several times. The physical dimensions and weight of wet membrane were measured after each cycle. These conditioning processes were continued until constant results were obtained. The discs were then equilibrated in 1 Molar solutions of sodium chloride for several days. The solution was changed each day. Finally they were equilibrated in various 0.10 Molar sodium chloride solutions until once more the physical dimensions and wet weight were constant, indicating that the membrane had assumed a final equilibrium form in which its physical parameters determined its individuality.

4.1.5.2. <u>The Individual Membranes</u>

Since there was a considerable number of A.M.F. C_{60} type membranes used in this work it is necessary to specifically define the treatment applied to each.

The C_{60} membranes willbe designated as $PS_{(n)}$ in the results.

PS_1 - PS_3 are the normal forms of the C_{60} membrane cut and conditioned as described in section (4.1.5).

PS_4 heat treated for $\frac{1}{2}$ hour at 95°C (Similar to the C_{60E} of Gardner and Paterson)

PS_5, PS_6 heat treated for 2 hours at 95°C

PS_7 - PS_9 heat treated for 3 hours at 95°C

PS_{10}/

PS_{10} This membrane was one of several which was heat treated for 2 hours at 95°C (with PS_5, PS_6) but which was not used initially. It was stored for two years in 0.10M NaCl before being investigated.

PS_{11} Once membrane PS_6 had been fully investigated, it was further heat treated for five minutes at 40°C. This brought about further expansion. Each of the expanded membranes was conditioned as described in section (4.1.5)

4.1.6.1. Dry Weights

The leached membrane in the sodium form was placed in a 100 ml. beaker in a desiccator over phosphorus pentoxide and the desiccator evacuated using a water pump. The desiccator was then placed in an oven at 60°C. for two days. Each membrane on removal from the desiccator was placed in a tightly sealed weighing bottle, of known weight, and accurately weighed. The dry weight of each membrane was determined several times by this method until a constant result was obtained.

4.6.2. Wet Weight

The membrane was removed from its equilibrating solution and its surface completely dried between two hardened filter papers. Using dry forceps, it was then placed on a plastic coated wire cradle, of known weight, suspended from the balance pan and weighed. A stop watch was started immediately the membrane was removed from between the filter papers. By measuring the weight of wire cradle plus membrane at specific time intervals over a two-minute period, a plot of weight of membrane against time was obtained. By extrapolating this graph back to time zero the true wet weight of the membrane was determined. The kinetic method of weighing gave wet weights reproducible to $\pm$ 0.1% for both membrane types.

4.1.7 PHYSICAL DIMENSIONS

4.1.7.1. Thickness

The average thickness over the membrane was obtained using a micrometer screw gauge. The thickness was measured with the membrane wet. By using the fine adjustment on the screw gauge the same pressure was applied for each measurement. This method is both simple and accurate. The difference between readings across the membranes was found to be smaller then $\pm$ 1.0% indicating both membranes were cast as very even films and that expansion by heat treatment caused no surface distortion.

4.7.2. Diameter

The membrane was placed wet between two glass plates of sufficient weight to keep it planar but not stretched. The assembly was then placed on the micrometer stage of a travelling microscope. The various 'diameters' were traversed and measured. The average diameter was calculated from a large number of alignments of the membrane. The importance of cutting the disc neatly was apparent when measuring the diameter; membranes with ragged edges were rejected at this stage. The benefit of cutting the disc after expansion of a sheet of membrane was also well illustrated. The C_{60} membranes described a very uniform circle whereas the diameter of the Nafion was more irregular, the recorded value being more obviously an average diameter.

4.1.8 Ion Exchange Capacity.

The number of fixed-charge on the membrane or ion exchange capacity was determined by two methods.

4.1.8.1. Isotope Dilution

This method was used for the C_{60} series only. A stock solution of 0.100 Molar sodium chloride was prepared and used to fill the appropriate number of beakers from a Grade 'A' 10 ml. pipette. Each of these was isotopically labelled with an accurate volume of sodium-22 of a known specific activity, using a Hamilton syringe. The membrane was placed in this solution and allowed to equilibrate for three days at 25°C. After removal, the membrane was washed for one hour in distilled water in order to remove any sodium-22 on the membrane surface or taken up by the membrane as imbibed salt. The membrane was then equilibrated in a further 10 mls. of the inactive stock solution for a further three days.

Triplicate samples were taken after each equilibration using clean Hamilton syringes. These were counted and from the specific activity measured the ion exchange capacity calculated. (Appendix 2.)

4.1.8.2. Direct Titration Method.

This method was used for both C_{60} and Nafion-170 membranes. The hydrogen form of the membrane was obtained by successive equilibrations in 1 Molar hydrochloric acid solutions. The surface film and invading salt were leached out by washing in distilled water. The membrane was then equilibrated in 25 ml. of 0.50 Molar sodium chloride for one day and this procedure was repeated three times. From experience, this was found to be sufficient to exchange all the hydrogen ions, associated with the fixed-charge, by sodium ions. As a check the final solution was always tested with pH paper. The membrane capacity was then determined by direct titration of the released hydrogen ions with 0.05 Molar sodium hydroxide. The acidity of the sodium chloride solution was accounted for by a 'blank titration' of the appropriate volume of salt solution. Reproducibility of each method and agreement between the two methods for each membrane was $\pm$ 1.0%.

4.1.9 Co-ion Capacity.

4.1.9.1. The isotope dilution method can also be used to determine the chloride, co-ion capacity of the membrane using chlorine-36 isotope. The procedure followed is similar to that given above (section 4.1.8) except that as the amount of invading salt in the membrane is to be measured, the washing technique must be changed in order that only the surface film of solution is removed and not the salt imbibed by the matrix. This part of the experimental procedure is critical

as/

as there is a very small amount of salt in the membrane when equilibrated in a 0.100 Molar solution, 400 times less than the amount of fixed charge. Any significant contribution from the surface film would drastically affect the calculated value.

After equilibration in the active solution, the membrane was dipped for five seconds in a large beaker of distilled water, then blotted lightly between two hardened filter papers and finally equilibrated in the inactive solution.

4.1.9.2. An alternative and more accurate method of co-ion determination is by potentiometric titration especially using the linear titration plots of Gran [10].

The membrane, dipped in distilled water and blotted, was equilibrated in two successive 5 ml. solutions of 0.5 Molar sodium nitrate, two equilibrations were found to be sufficient to displace all the imbibed chloride in the membrane. The chloride ion was then titrated. The titrant was a solution of sodium nitrate and silver chloride with the same ionic strength as the equilibrating sodium nitrate solution. This was delivered from a calibrated Agla-syringe. The syringe was fitted with a glass needle which had been drawn out to a capillary tip. Some 4 cm. from the tip a silver wire electrode was fixed with araldite. When carrying out the titration the tip of the syringe was placed in the solution being titrated. The potentiometric cell was completed by inserting a silver/silver chloride electrode in this solution and connecting the electrodes through a Soletron Digital Voltmeter (Model LM.1867). By ensuring the ionic strength of the two solutions was idential and by having a very fine tip on the syringe the liquid junction potential was kept to a minimum.

A teflon coated magnetic stirrer was placed in the solution to be titrated and the titrant added until the end point was reached. This was obvious from the sudden large change in the emf reading.

Thereafter/

Thereafter very small aliquots, 0.005 cm^3 were added from the Agla-syringe until ten readings were obtained of volume added and consequent potential reading.

Of the two methods the latter was found to be the most accurate giving reproducibility of $\pm$ 2% whereas the isotope redistribution method gave for some membranes no better than $\pm$ 10%. In general, over the whole range of membranes reproducibility between successive experiments, and agreement between the two methods was good, however, in some cases, very erroneous answers were obtained. There is little doubt that the factor determining the accuracy of determination of the co-ion concentration is the procedure for removing the surface film of active electrolyte. These measurements of the physical properties of the membrane discussed in the preceding sections were carried out for each membrane at the beginning of the experimental study until consistent results were obtained. They were also periodically repeated throughout the time each particular membrane was being examined, especially when the membranes were being subjected to the more extreme physical conditions of the reverse-osmosis system.

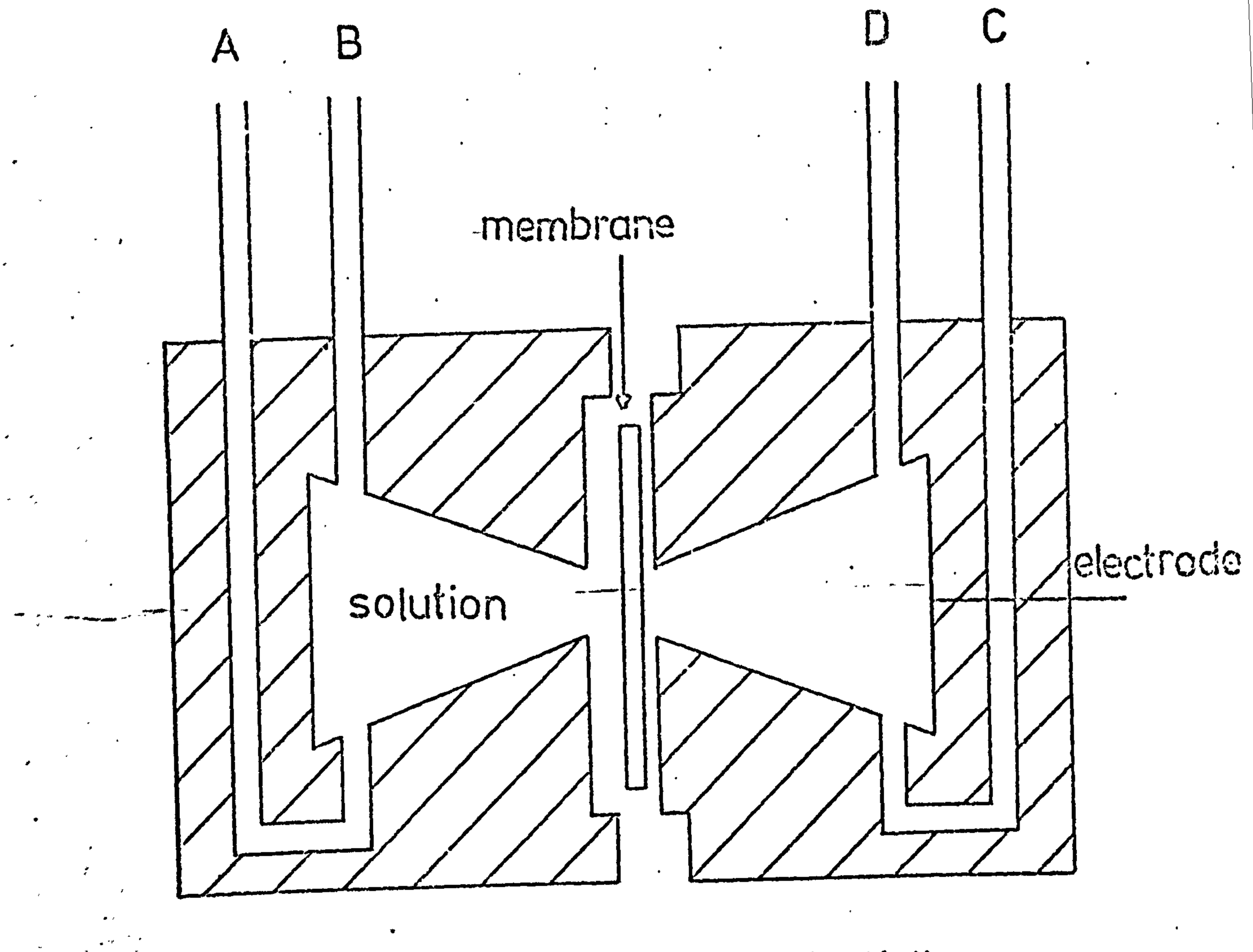

Fig.4.1 Membrane Conductivity Cell

4.1.10 Conductivity

The conductivity of the membrane was obtained using the cell shown diagramatically in figure (4.1). This particular cell was used by previous workers [11] [5] and shown to give accurate and reproducible results.

The filled cell contained in a polythene bag, or covered beaker was positioned in an oil bath, the temperature of which was maintained at $25^{\circ} \pm 0.005^{\circ}C$. A reservoir containing the solution from which the cell was filled was also placed in the oil bath and the two connected, by silicone rubber tubing, in such a way that solution entered by A, circulated via B and C to the other half of the conductivity cell and finally left by D going either to waste, if a gravity flow, or back to the thermostated reservoir if a pumped system was used. In the latter case a Peristaltic pump (Watson-Marlow H.R. Flow Inducer 6C) was used. Care was taken to remove all air bubbles from the system when filling the cell and connecting it to the reservoir.

In order to determine the conductivity of the membrane the cell was first assembled without the membrane and left to equilibrate (thermally). Readings of conductance were taken over several hours until constant. The resistance of the electrolyte in the cell was determined. The cell was then dismantled, a membrane inserted and returned to the oil bath. As before, after an equilibration period, readings were recorded until finally constant. From these two readings the resistance of the electrolyte plus membrane was determined. By subtraction the resistance and conductance of the membrane was calculated. In both measurements, i.e. of resistance of solution and of solution plus membrane, readings were taken with and without

flow/

flow through the system. It was observed that although this affected both measurements, the actual subtracted value, from which the membrane conductivity was calculated, was unchanged.

The conductivity of each membrane was determined a number of times and a reproducibility of $\pm$ 1.0% was obtained. The conductivity measurements were made on a Wayne Kerr B.331 conductivity bridge. Although this indirect method of measuring conductivity has advantages over the direct method used by other workers (4) (12) (13), in dilute solutions, the resistance of the membrane is smaller than that of the solution. Consequently in order that the membranes resistance contributes significantly to the measurements made only a very small area of the membrane, 0.100 cm^2 was exposed. Thus single conductivity measurements may not be representative of the whole membrane disc. Gregor (14) reported variation of 300% in membrane conductances in pieces of membrane cut from the one sheet. In this work this problem of non representative measurements did not arise. Conductivities of a large number of membranes were measured, some having similar physical geometry, but over all providing a range of differing degrees of expansion. This allowed a study of the effect of membrane expansion on specific conductivity.

The measured value of the membrane resistance was corrected for edge effects using the equation derived by Barrer (30). Since the area of membrane exposed in the conductivity cell was small, the edge correction was fairly large, amounting to some .4% of the measured value.

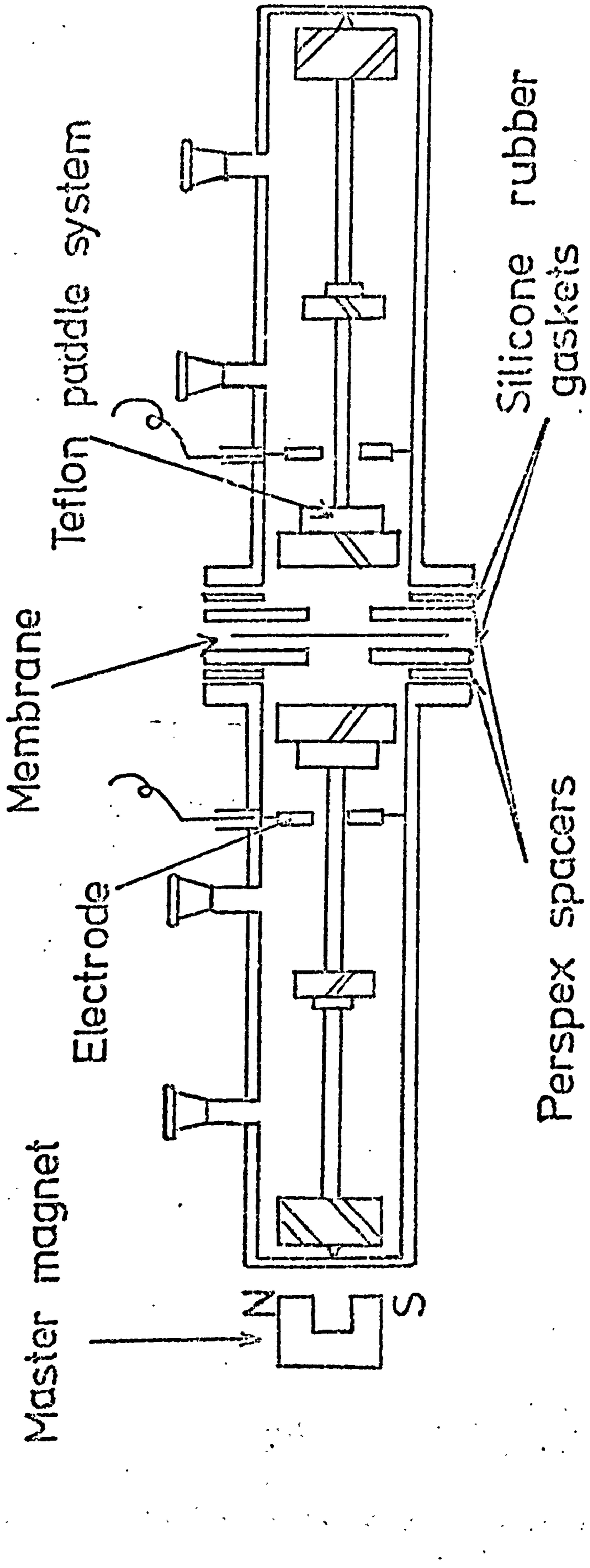

Fig.4.2 Electro-Osmosis Cell

4.1.11 Electro-Osmosis

The electro-osmotic transport number t_3 of the membrane was determined using the glass cell shown in Figure (4.2). This cell is similar to that first used by Mackay and Meares[12] and by previous workers in this laboratory. Identical cells, with the electrodes removed, have been used, under the appropriate experimental conditions, to determine the membrane diffusion coefficient, transport numbers, salt and osmotic flow. In effect this cell of standard design can be used to obtain the transport data from which the phenomenological coefficients characterising the membrane are calculated.

The teflon paddles fixed in both half cells and turned by magnetic coupling agitate the solution at the membrane surface. This coupling was achieved by fixing a small magnet into the end casing of each paddle with araldite. These were driven by larger master magnets outside the cell fixed on a geared assembly and turned by a variable speed Citenco electric motor. The stirring speeds of the paddles were monitored by a Dawe 1200E Stroboscope. A paddle speed of 500 r.p.m. was normally used, However, various speeds between 200 and 600 r.p.m. were also tried.

By measuring the change in volume of each half cell on the passage of a constant electric current across the membrane, the electro-osmotic transference number could be calculated. This current was supplied by a constant current source (Solatron P.S.U. AS1413) and monitored throughout the experiment by measuring the potential drop across a standard resistance in series in the circuit. The silver/silver chloride electrodes were situated three centimetres from the membrane surface. These were prepared from platinum gauze electrolytically silver plated in a dilute solution of silver nitrate, to which a few drops of concentrated nitric acid had been added.

After/

After washing for twenty-four hours in distilled water, one of the electrodes was completely converted to silver chloride and the other lightly chloridised by anodizing in an 0.100 Molar solution of hydrochloric acid. The silver/silver chloride electrodes, produced in this way allowed passage of a 15 m A current for approximately thirty minutes.

In the experimental procedure the membrane was first lightly blotted and mounted between two matched perspex spacers which were kept perfectly aligned by locating pins thus assuring the same area of membrane was exposed during each experiment. This assembly was placed between the two half-cells which were then clamped together. At this stage the 'sandwich' of perspex spacers and membrane was sealed at the edges with paraffin wax and the cell then filled. In order to prevent bubbles forming on the paddles and to aid any trapped bubbles to dissolve, the solutions were thoroughly degassed before use. Horizontal graduated capillaries were attached to each side of the cell employing teflon sleeves to prevent leakage and the cell finally immersed in a water bath maintained at $25 \pm 0.01^{\circ}C$. The paddles were set in motion and the cell allowed to equilibrate for several hours. The capillary readings were monitored during this time in order to determine whether the system was effectively sealed. A constant current was applied and capillary readings taken at regular time intervals over a twenty minute period. The polarity of the cell was then reversed and the procedure repeated. It was discovered that creating a small head of water on one side of the membrane by raising the height of the capillary approximately 2 cm. made the membrane less prone to move during the experiment. The subsequent hydrostatic pressure induced would make a contribution of the order of 10^{-9} to 10^{-10} mls. cm^{-2} sec^{-1} to the electro-osmotic flow. Reducing the area of membrane/

membrane exposed, by changing the centre diameter of the perspex spacers, the membrane could also be made more stable allowing more accurate readings to be taken.

Measurements were made at both 5 and 15 M amps in order to determine the effect of current density on the observed transference numbers. Current was passed three times in each direction at both current densities for each membrane allowing an average value for the volume flow of water to be calculated.

The value of t_3 was determined from equation (2.26a)

$$t_3 = \frac{J_3 F}{I}$$

However, the total volume change ΔV in either compartment in cm^3 per coulomb for an isobaric system is

$$\Delta V = (t_3 \hat{V}_3 + t_1 \hat{V}_{12} + \Delta V_E) \qquad (2.77)$$

where $\hat{V}_3 \hat{V}_{12}$ are the partial molar volumes of water and electrolyte and ΔV_E is the volume change of the electrodes. Rearranging gives (2.78)

$$\overline{t_3} = \left(\frac{\Delta V}{\hat{V}_3} + \frac{t_1 \hat{V}_{12}}{\hat{V}_3} + \frac{\Delta V_E}{\hat{V}_3}\right) \qquad (2.78)$$

where $\frac{\Delta V}{\hat{V}_3}$ is the "apparent" electro-osmotic transport number, which is in effect what is measured experimentally. Therefore, the t_3 calculated by (2.36a) is not the true t_3 but an apparent one in which no account has been taken of the other volume changes occurring in the cell. This correction was applied.

Electro-osmotic transport numbers obtained by this method for a range of membranes were reproducible to $\pm$ 2%.

4.1.12 Determination of the Concentration of the Product Solution from the Reverse Osmosis Experiments.

The product concentration was determined by two methods

1) By measuring the conductivity of a sample or diluted sample

2) By potentiometric determination of chloride ion.

4.1.12.1 Conductivity Method

A standard dip-type conductivity cell (Philips PR.5512/00) which had a 1 cm^3 electrode chamber was used in this method. This cell required approximately two mls. of solution for accurate measurement. Product samples were obtained from the collection vessel Z, Fig. (4.3) and diluted with an known volume of distilled water to cover the electrodes. The conductivity of the resultant solution was measured on a Wayne Kerr conductivity bridge section (4.1.10). Standard sodium chloride solutions were made up in the concentration range 0.01 → 0.10 Molar and their conductivities determined using the dip cell. These results provided a graph of conductance against Molar concentration. Extra points were added to the graph by measuring the cell constant of the dip cell using a 0.100 DEMAL solution [20] and calculating the conductivities from equivalent conductivity data obtained from the literature [21] [22]. The concentration of the product solution was easily determined by measuring the conductance and reading the concentration from the calibration graph. This method gave product concentrations reproducible to ± 2.0%.

However, the indirectness of the method, the need for accurate dilution of each sample and the dependence on temperature made this method/

method impractical for rapid accurate analysis. The very much more precise and rapid method of potentiometric titration was eventually used exclusively.

4.1.12.2 Determination of Product Concentration by the Potentiometric Titration Method of Gran

A Hamilton syringe was used to accurately withdraw 0.08 ml samples of product solution for analysis. Each sample was added to 5 mls. of 0.50M sodium nitrate solution which acted as supporting electrolyte. A silver nitrate/sodium nitrate solution with a concentration and ionic strength sufficient to titrate the samples of product solution was made up and the procedure described in section (4.1.9.2.) used. A minimum of three samples was taken per experiment, at both pressures, for analysis by this method. A reproducibility of $\pm$ 2.0% was obtained for product concentration in repeated experiments.

REVERSE OSMOSIS

4.2 Cell System I

4.2.1 The reverse osmosis cell used in the first part of the experimental study is shown dia grammatically in figure (4.3).

The cell was constructed in Delrin a crystalline thermoplastic polymer of formaldehyde (appendix 3) possessing the mechanical properties required for use in high pressure work. It consisted of two parts E and I, each threaded, which were screwed together and sealed by two o - rings G and J. One o - ring was situated between the top part of the cell and the spacer K, the other between the faces of the top and bottom halves of the cell. The total length of the cell was 20 cm and the diameter 8 cm with 2 cm thick walls to withstand the high applied internal pressure. The internal volume was 150 cm^3.

The cell was filled with solution by removing the threaded plug A and pipetting solution into the connection tube T. Agitation of the solution at the membrane surface was obtained by the teflon paddle R, which was operated by magnetic coupling using the assembly shown in fig. (4.4). This consisted of two large powerful magnets fixed on a rotating stirrup. The stirrup was positioned in order that the magnets were approximately only 0.25 cm. from the cell walls hence allowing maximum coupling with the magnet inside the paddle. The whole assembly was mounted inside a metal glove box, with a perspex front for viewing, which was also used as an air thermostat tank. The temperature inside of this was controlled by a Jumo-Shandon thermo-regulator assembly. The air was circulated by a powerful electric fan. The temperature was kept constant at $25 \pm 0.5^{\circ}C$. The paddles were held in place and centred by the teflon supports V, D, H. V also acted as a bearing on which the head of the paddle turned. Quarter inch internal diameter stainless steel tubing and swage/

swage-lock couplings were used to construct the pressure line which connected the cell to the high pressure nitrogen cylinder. This cylinder supplied the high pressure to the cell.

From the coupling, S, in the cell wall the pressure tubing was bent upwards parallel to the cell for twelve inches where it was then broken and a coupling made. This allowed the cell and the arm of the pressure line to be removed from the air thermostat as a unit rather than disconnect the pressure line from the cell at the metal-plastic coupling in the cell wall. From this coupling, the pressure line was gently bent in a U-shape and led to the nitrogen cylinder . Solution could in this way be contained in the side arm and would not escape down the pressure tubing partially emptying the cell.

The pressure from the cylinder was supplied through a normal nitrogen cylinder valve (P ressure Control Ltd. 31780/1) direct to the solution in the side arm of the pressure line. A Budenburg Standard Test Gauge (10013437 calibrated 0 - 1,000 lbs/in^2) situated between the nitrogen cylinder and the cell was used to monitor the applied pressure, providing an accuracy of $\pm$ 0.25%.

In the cell the membrane was supported by a porous stainless steel disc placed on the bottom of the cell. Beneath the porous disc in the cell bottom concentric channels allowed the desalinated product solution to escape.

The membrane area was defined (5.025 cm^2) by the teflon spacer, K, which fitted perfectly into the bottom of the cell. This spacer and the neopren o-ring, J, above it prevented leakage around the perimeter of the membrane once the top part of the cell was tightly screwed down.

The wet membrane was placed in the bottom of the cell on top of the porous steel backing plate and the teflon spacer and o-ring put in place. The top part of the cell was then firmly screwed down into the bottom part by holding the squared ends with two machined/

machined metal keys. The cell was then unscrewed and the o-ring,J, examined to determine whether this had been pushed into place. This o-ring was pressed by the top part of the cell between the spacer, K, and the cell wall. A fine groove was machined in the cell wall to accommodate the compressed o-ring. Once in this position the o-ring, J, effectively sealed the membrane into the bottom of the cell. When this seal had been checked the cell was again screwed tightly together and filled using degassed solution, from the access port A. The side-arm formed by the pressure line was filled from the coupling, U.

The seal around the perimeter of the membrane was tested by using an impermeable polythene sheet in place of the membrane and pressurising the solution in the cell to 500 lbs/in^2, with the bottom of the cell filled and the capillary in place. Any leak round the polythene sheet, which was of the same thickness as the membrane, was observed as a flow along the capillary. It was critical that no solution should escape round the sides of the membrane as the product fluxes through the membrane were very small, approximately 0.2 cm^3/hour. Great care was also taken to clean and dry the bottom of the cell and the porous steel backing plate. Both of these were washed with distilled water and dried with acetone before each experiment. This removed any possible residue from previous experiments remaining in the bottom of the cell, which would alter the concentration of the product solution.

In early experiments the solutions used were passed through a milli-pore filter to remove dust particles. This was eventually stopped. The milli-pore filters (as supplied by the manufacturers) contain added surfactants. These additives aid the filtering process, but would

be/

be most undesirable in the filtered solutions used in this study. Although a pre-wash with distilled water was usual, the possibility of releasing surfactant and the lack of particulate material in the original solution led to this step being discontinued.

Once filled, the cell was placed in its support inside the air thermostat box and the stirrup assembly adjusted over the cell. The paddle was then set in motion. The cell was left for several hours in this position, to allow trapped air bubbles distrubed by the paddle to rise to the top of the cell and to allow thermal equilibration of the solution inside the cell, before proceeding with the experiment. The cell was continuously topped up with solution during this period. The plug A, was then screwed into place and the pressure line coupled together. Pressure was applied by adjusting the valve on the cylinder head and kept constant by leaving the valve to the high pressure cylinder open, using the cylinder as a pressure reservoir. The rotation speed of the impeller was monitored by a stroboscope section (4.11) and maintained at 500 rpm (usually) although various impeller speeds between 200 - 600 rpm were tried for some experiments.

Using the graduated capillary, N, readings of the volume flow at specific time intervals were taken for periods at the beginning, middle, and end of the experiment at each applied pressure. Samples, for determination of product concentration, were collected using the vessel, Z, at different times, over a number of experiments at each pressure.

At the end of the reverse osmosis experiment the pressure was released by unscrewing coupling, Y.

Information on volume flow and desalination at 200 and 400 lbs/in^2 applied pressure were obtained for two membranes with physical properties/

properties similar to the C_{60} Normal and C_{60} Expanded membranes used by Paterson & Gardner. Feed solutions of 0.10 and 1.00 Molar NaCl were used. Each of the membranes was 'run' four or five times in the pressure cell varying the order in which the pressure was applied. (In some experiments a pressure of 200 lbs/in^2 was applied first. Once the experiment at this pressure was completed the pressure was increased to 400 lbs/in^2. In another experiment on the same membrane, the procedure was reversed). This procedure was intended to show whether the results were in any way altered. by a preconditioning of the membrane which might be brought about by the previously applied pressure.

4.2.2 Discussion of Apparatus

The design of the Reverse Osmosis cell was influenced by other equipment (electro-osmosis and diffusion cells) used in this laboratory. Previous workers had made use of this equipment in the determination of the phenomenological coefficients of various membranes, amongst which were the A.M.F. C_{60} Normal and Expanded. It was a natural progression to design a Reverse-Osmosis cell with an axial paddle system, which would agitate close to the membrane surface and closely resemble earlier cells. This similarity in design was a desirable feature in order to make comparison between the data obtained from the reverse osmosis cell with that predicted from the mobility coefficients obtained by Gardner and Paterson using the original transport cells.

Concentration polarisation at the membrane surface is an obvious problem in the process of hyperfiltration (15) (16) (17) (18) (19).

In any attempt to measure the volume flow, rejection abilities and to compare them with those predicted from mobility coefficients determined/

determined at specific concentrations, this problem must be minimised.

To determine whether the paddle arrangement used, successfully prevented concentration build up at the membrane surface during an experiment, the rotation rate of the paddle was varied for a number of experiments from 200 rpm to 600 rpm with no detectable change in the product flux or concentration.

Experiments were also carried out in which there was no stirring at the membrane, thus generating very high concentration polarisation at the membrane surface. In these experiments the volume flow was significantly reduced and the concentration of the product approximately doubled.

The relatively small volume of the cell, approximately 150 mls., imposed practical restrictions on the length of the experiments conducted. After a period of 24 hours at an applied pressure of 400 lbs/in^2 the concentration of the feed solution would be significantly increased.
(For the normal membrane approximately 4 ml. of solution would be desalinated in 24 hours increasing the feed concentration by 1.5%; in the same length of time the expanded membrane would desalinate approximately 9.5 mls. of solution, increasing the feed concentration by 3.8%)

Fortunately the method used for determination of the product concentration required a very small volume, less than 0.10 mls. Section (4.2.3).

In order to be sure the product concentration was representative of the 0.100 feed solution and not affected by an increase in concentration of the feed, samples were taken during both the early and latter stages of each experiment. Agreement over a number of experiments/

experiments on the two membranes gave reproducibility for product concentration of $\pm$ 2.0%.

The method by which the solution within the cell was pressurised and thus forced through the membrane, created a number of problems and was the most unsatisfactory feature of the apparatus. The procedure of applying high pressure nitrogen gas from a cylinder directly to the feed solution contained in the side arm allowed the solution to absorb nitrogen gas as the experiment proceeded. This was released by the solution as it passed through the membrane substantially affecting the product flux results obtained. In order to account for this the volume flow along the capillary was measured for several hours at the beginning of an experiment and then again for several periods throughout the experiment. By plotting these results the increase in rate of product flow with time could be deduced and the period for which this was unaffected by absorption of gas established. By taking flow readings immediately solution appeared in the capillary, this problem was kept to a minimum and reproducibility of $\pm$ 2% obtained.

REVERSE OSMOSIS CELL I

FIGURE 4.3

A	-	Threaded Plug
B	-	Red Fibre Washer
C	-	Encased Magnet
D, H, V	-	Centr ing Bushes
E	-	Top Part of Cell
F	-	Solution
G, J	-	Rubber O-ring
I	-	Bottom Part of Cell
K	-	Angled Spacer
L	-	Porous Steel Backing Disk
M	-	Capillary Port
N	-	Graduated Capillary
O	-	Gridded Cell Bottom
P	-	Membrane
Q	-	Impeller Blade
R	-	Impeller
S	-	Stainless Steel Coupling
T	-	¼" Stainless Steel Pressure Tube
U, V	-	Swage Lock Coupling
Z	-	Collection Vessels

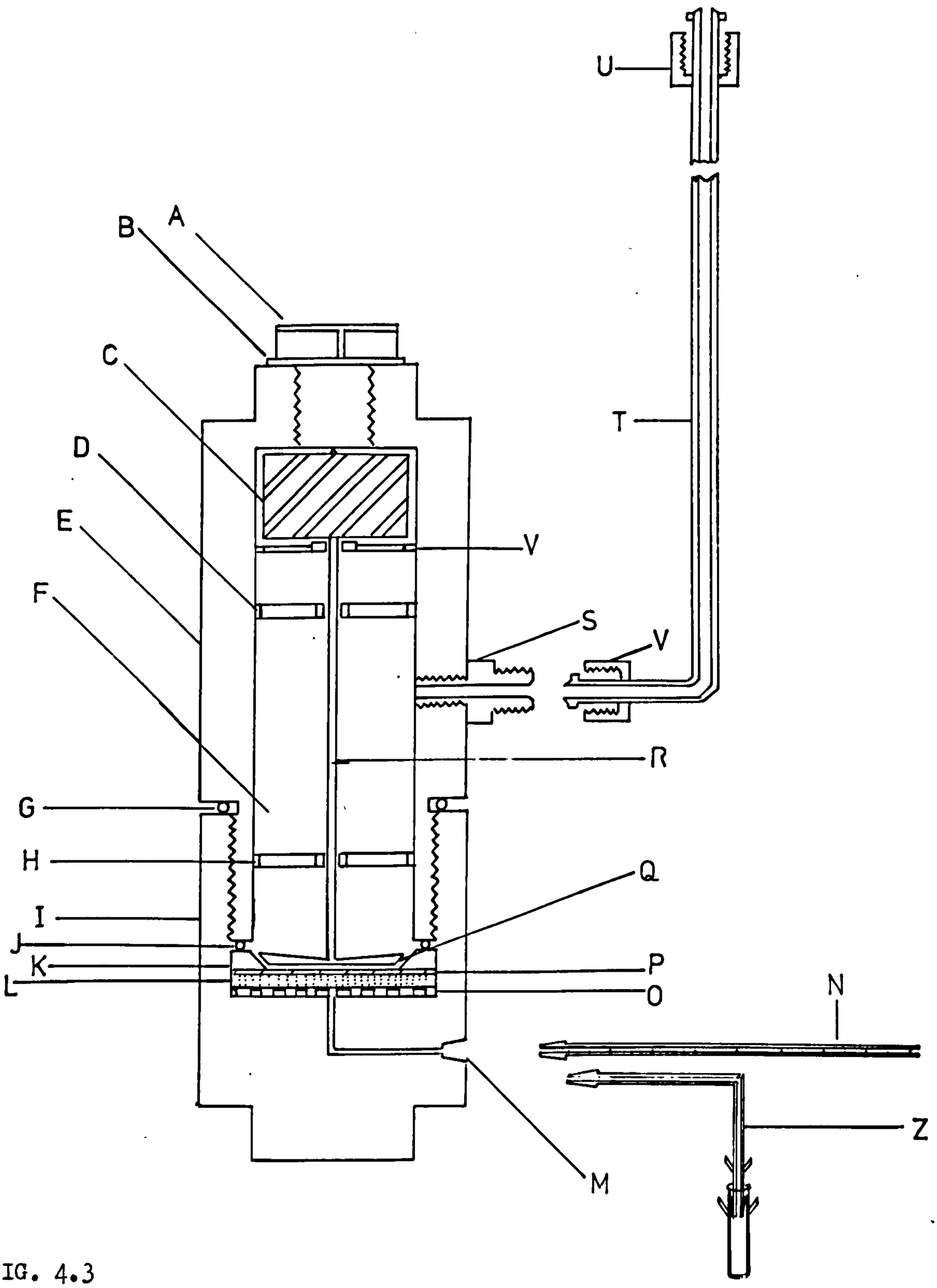

FIG. 4.3

MASTER MAGNET ARRANGEMENT

REVERSE OSMOSIS CELL.

SECTION DIACRAM FIGURE (4.4)

C – Magnet in end casing of impeller

X – Supported stirrup arrangement

W – Master magnets

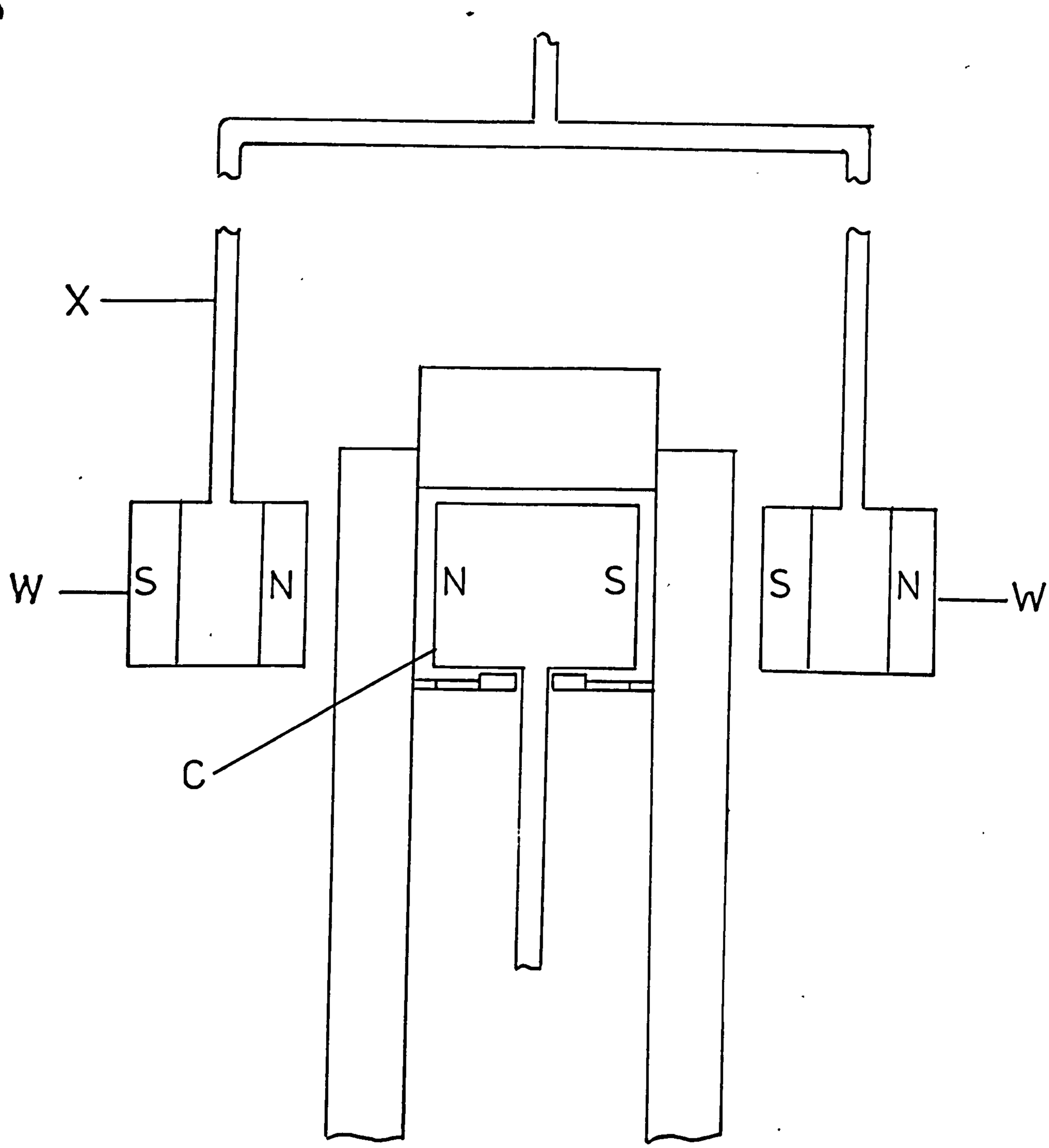

FIG. 4.4

4.3 The Reverse Osmosis System II

The reverse osmosis cell I discussed in the last section was intended to be a prototype cell of simple design which would allow preliminary investigation of the desalination properties of the C_{60} membranes. Certain shortcomings in the design of the system meant that the effective scientific use of the cell, for accurate experimentation was restricted, particularly for emf studies.

However, the experience gained from this proto-type system provided an insight which greatly aided the design and final construction of a more sophistocated, more flexible apparatus, which could be used to obtain measurements of water flux, desalination -ability and pressure potential for a whole range of membranes.

Into this new reverse osmosis system specific features had to be incorporated:-

(1) An effective method of overcoming the build up of concentration polarisation at the membrane surface during the desalination process had to be devised, with the added constraint that in order to make potential measurements across the membrane electrodes would have to be inserted close to the membrane, on both the high and low pressure sides, consequently preventing the use of mechanical stirring at the membrane surface as in cell I. Therefore circulatory pumps causing -an efficient flow past the high pressure side of the membrane were required. From this requirement the design of the new reverse osmosis cell was evolved. This had to be constructed to allow an optimum flow of solution over the whole membrane surface and required to incorporate access ports which would allow probe electrodes to be inserted on both sides of the membrane close to its surface.

(2) A completely new method of applying pressure to the system was needed in order to remove the problem of absorption of nitrogen gas into the solution. The 'usual' method is a 'pressurising and circulatory pump and valve system'. However, these systems are generally constructed in steel. This immediately poses corrosion problems and in general is unsatisfactory for use in a system where potentiometric measurements are to be made. The pumps 'usually' incorporated also create oil contamination problems and heat dissipation problems. Since the pressure is created by a pumping action, pressure pulses are created.

For these reasons no attempt was made to include this method of applying pressure in system II.

An obvious possibility was to use a piston or diaphragm arrangement to separate the solution from the pressure source. This had to be incorporated without interfering with the circulation of the feed solution within the system itself.

(3) In order to prevent the problem of significantly increasing the concentration of the feed solution, as desalination occurred, a reservoir of solution had to be included in the system, sufficiently large, to allow desalination to occur for at least twenty-four hours. This had to be included in such a way that the circulation of solution was not affected.

(4) To make electrical measurements, probe electrodes had to be designed and constructed of a convenient size and with a special housing, which would allow them to be inserted into the high pressure side of the reverse osmosis cell above the membrane/

membrane surface, without allowing leakage when pressure was applied.

(5) Finally, construction of the system in a non metal material was a desirable feature as metal/solution interfaces within the cell would set up "parasitic voltages" with the probe electrodes, thus affecting the accuracy of the potential measurements (23).

4.3.1 CIRCULATORY PUMPS

4.3.1.1. Development.

The importance of obtaining a pump which was both efficient and reliable was realised from the beginning. Numerous designs were considered. Prototype models of pumps with different arrangements of rotors and impellers utilising a mechanical drive were constructed. However, difficulty arose in obtaining non-metallic seals for the drive shaft which required no lubrication and could be sealed into the plastic pump body without leaking when pressure wasapplied. A comprehensive survey of industrial literature provided no information on a suitable seal. Experience obtained with other membrane cells Fig. (4.2), suggested magnetic coupling could be used to rotate an impeller in a circulatory pump. A cylindrical pump housing nine inches in height containing a large five inch high impeller which fitted neatly into the bottom of the cell was constructed. The impeller was fitted with six large perpendicular blades. Into the bottom of the impeller four magnets were fixed with Araldite. The top portion of the "pump" acted as a resevoir for solution. A 'master magnet' assembly was placed beneath the pump and was rotated by an electric motor. The impeller turned successfully in air, but would not turn against the resistance imposed when the housing was filled with solution. An electro-magnet consisting of four pellets of Swedish Iron 1 centimeter cube, wound with cotton covered copper wire, was substituted on the external drive, but without success. This electro-magnet did provide the coupling required to turn the impeller when the pump was full of solution, but only at a very slow speed. When the speed was increased above a few rpm the coupling was broken. Experience gained from this model indicated obvious faults in the design:-

(1)

(1) The concept of a solution resevoir above the impeller was not sound as no pumping action was created from the rotating rotor.

(2) The design of the impeller required to be changed. The area of each blade was too large consequently creating high resistance to movement.

4.3.1.2The Circulatory Pumps.

A diagrammatic representation of the final pumps used is shown in plan and in section figures (4.5) (4.6) respectively and photographic views are shown in figures (4.7)(4.8). The pump body was constructed in two parts, A, B, with 3/8" thick Delrin walls. These were bolted together by six stainless steel bolts, F, and a seal between the top and bottom was effected using a recessed neoprene o-ring, E. An impeller, with twelve 1/8th of an inch deep, 30° pitch teeth, was constructed. This had a hollow centre to receive the slave magnet. A powerful cylindrical magnet, (obtained from a Gallenkamp Magnetic stirrer) was sealed into the hollowed centre of the impeller by a light covering of araldite and a Delrin plate was tightly fitted on top. The impeller assembly was completed by pushing a solid glass pivot I, through the centre of the impeller passing through a hole in the middle of the magnet.

In the top and bottom of the inside of the pump housing teflon "pads", H, were fitted as bearings for the glass pivot. The master magnet used to rotate the impeller was identical to that fitted in the pump rotors. This master magnet was situated 1 mm from the bottom of the pump housing and was directly connected to a variable speed Cetenko motor (KP QS 1200). With this arrangement very effective magnetic coupling was obtained, and the pump rotor could be/

be maintained at 1,000 rpm in air and in solution at 400 rpm. Specifically designed Delrin couplings, G, were threaded into the pump wall at an angle of 60° to each other. The impeller was mounted 1/16" off centre in the pump body, when this was rotated at speed, solution was driven round the edge of the impeller and was drawn in one coupling and forced out of the other causing a circulatory pumping action. The pump was tested at atmospheric pressure, although it would not pump against a head of water (as expected) it circulated solution in a closed system with great efficiency.

Further tests were carried out in situ in the final completed reverse osmosis system, section (4.3.5.).

4.3.2 Reservoir and Pressure Transmitting System.

The reservoir and diaphragm are shown in figure (4.9). This arrangement consists of a relatively large vessel built from Delrin in two sections, A, and B, which were firmly clamped between 1/2" thick Stainless Steel plates, G, using 3/8" Stainless Steel bolts, I. Between the top and bottom sections of the cell a rubber diaphragm was fixed. This diaphragm made an effective seal between the two sections and transmitted the applied external pressure to the solution in the system. The pressure was applied to the small bottom section of the reservoir which was connected to the nitrogen cylinder via a flexible pressure line.

A series of diaphragms were tried; before use each was cleaned with chloroform and carbon tetrachloride and was washed overnight in Decon 75 detergent solution to remove any organic or inorganic impurities, which might dissolve out into solution.

Neoprene rubber 1/32" thick was used, relatively successfully, however, the area exposed to solution tended to discolour after a few days suggesting a reaction with the salt solution, probably leaching out of some material into the solution. Also, if extended to any great extent this rubber easily ruptured. Butyl rubber 1/16" thick was tried next and although this was very strong, it discoloured as before. White silicon rubber 1/16" thick was investigated next. This was very porous to nitrogen gas. It was also extremely soft and easily torn. The edges of the top and bottom of the reservoir cut the silicon rubber diaphragm held between them into a neat circle. A composite diaphragm consisting of silicon rubber on the solution side and butyl rubber on the nitrogen side was an obvious development from these observations. This functioned perfectly, incorporating the inertness of the one with the strength and impermeability of the other. The edges of the top and bottom of the reservoir were rounded to prevent cutting the silicon layer/

layer.

This diaphragm was expanded while fixed in the reservoir by applying a little pressure to the bottom side with no resistance on the solution side. O n releasing the pressure the diaphragm remained in a distended shape which could be inverted and pushed into the bottom of the reservoir in a "cup" shape consequently removing any flexible resistance to pressure. This ensured that none of the applied pressure was used to inflate the diaphragm when the volume of solution in the system decreased as desalination took place.

The reservoir above the diaphragm had a capacity of 400 cm^3. This was filled by removing the threaded plug, H. The walls of the reservoir were made 1/2" thick to withstand the high pressures applied.

This method of transmitting the pressure had many advantages and few disadvantages over the method 'usually' employed. The solution and pressure source in the system were effectively separate. Gas could not be absorbed by the high pressure solution and there was no problem of leakage round the side of the diaphragm, as there would be in the case of a piston arrangement. The feed solution also remained uncontaminated and corrosion and stray potentials obviated.

4.3.3 Reverse Osmosis Cell II

Figure (4.10) gives a diagrammatic sectional representation of the reverse osmosis cell II and figures (4.7), (4.8) display photographically the cell assembled and dismantled.

The cell was constructed from extruded Delrin bar, 10.5 cm. in diameter, in two sections, R, and S, with cell walls 2 cm (minimum) thickness, to withstand the high applied pressures. The two sections were held together by six 3/8" diameter stainless steel bolts. Both the high pressure side, R, and the low pressure side, S, were drilled and tapped to accommodate the probe electrodes which were inserted at positions, O, and G. The membrane was positioned beneath the compartment, K. The high pressure electrode penetrated this compartment above the centre of the membrane. Solution was pumped through this compartment and across the membrane surface, entering and leaving by way of the angled channels, L, and, T, respectively. The compartment, K, was 2.1 cm. long by 1.8 cm. across with a depth of 2.5 mm. The narrow apertures, V, U, where solution entered the compartment, K, were 1.8 cm. long by 2.0 mm. in height. These directed the entering solution at an angle of 60°. As a consequence of this geometry the velocity of the circulating solution was a maximum over the membrane surface. The membrane was sealed at its perimeter edges by a circular silicone rubber gasket, B, 2 mm. thick. In this a rectangular central hole was cut exactly matching the shape defined by the compartment, K. This defined the 'working' area of the membrane and presented no resistance to the flow over the membrane.

The membrane was supported on a wedge shaped piece of porous teflon, C, which fitted flat into the bottom of the cell. The top

and/

and bottom of the cell were sealed with the neoprene o-rings, D. The top of the cell was stepped and the bottom recessed to accommodate the larger outer o-ring and the bottom grooved to hold the smaller inner one. It was of absolute importance to carefully adjust the relative thickness of the o-rings and the silicon rubber gasket, B, in order that the perimeter of the membrane was sealed. If either of the o-rings was too thick when fully compressed, solution would be able to escape round the membrane into the bottom of the cell. Although the porous teflon material used in the backing plate was fairly strong and inflexible, it did compress under the applied pressure. By machining an angled section in the bottom of the cell and cutting the backing plate in a wedge to fit this exactly, the compression was prevented. The backing plate was placed in a channelled bottom section, E, in which very fine holes had been drilled. This allowed the product solution to escape into, H, where a horizontal capillary could be fixed and samples collected. Holes, two millimetres in diameter, F, were drilled through, E, into the backing plate, C, stopping 1 millimetre from the top surface. Into these the low pressure electrodes, I, were screwed penetrating as near to the membrane surface as possible.

Specifically designed, right angled couplings, M, made in Delrin were screwed into the top of the cell and sealed with 'Red Fibre' washers,P . These couplings were threaded in such a way that when fully screwed home they were positioned facing 180^{o} from each other, thus allowing easier coupling with the rest of the system.

4.3.4. HARWELL REVERSE OSMOSIS SYSTEM.

In order to obtain reverse-osmosis data at high applied pressure, experimental time was obtained on a high pressure reverse-osmosis apparatus. This was supplied to the Engineering Department of Glasgow University by the Harwell Atomic Energy Research Establishment.

The system was entirely constructed in stainless steel. Solution was pumped through the system and pressurised by an Air Hydro Pump. An 'Accumulator' was employed in the system to smooth out pressure pulsation and the pressure was maintained constant by a nitrogen filled 'Back Pressure Valve'.

The cell in which the membrane was housed was similar in design to that described in section (4.3.3). A porous steel support was used for the membrane. The exposed area of the membrane was 12.57 cm^2 and the flow rate of circulating solution 500 $cm^3.min^{-1}$. The volume of the system was some 12 litres.

The reverse osmosis characteristics of a C_{60} Normal and C_{60} Expanded membrane for an 0 .10M feed solution were determined at both 1000 and 1500 $lbs.in^{-2}$.

Solution was pumped into the system from a thermostated tank and the first three litres used to clean the system and then discarded.

Once the system was filled with solution the valve from the thermostated tank to the pump was closed and pressure was built up in the system.

Each of the membranes was investigated for twelve hours at both 1000 and 1500 $lbs.in^{-2}$.

The desalinated product solution was run from the low pressure side of the membrane cell into a glass vessel. The flow rate was determined/

determined by weighing the amount of solution which had passed through the membrane in several one-hour periods. The product concentration was determined from samples collected at various stages of a n experiment and was found not to change with time. The potentiometric method section (4.1.12.2) was used to determine the concentration of the product solution. The product concentrations were found to be reproducible to $\pm$ 1.0% and the water flux to $\pm$ 2.0% in separate experiments at each pressure.

4.3.5 The Reverse-Osmosis System

The relative positions of each vessel in the completed reverse osmosis system are shown in figure (4.12). A, is the reverse osmosis cell, on either side of this are the circulatory pumps B^1, B^2. Pressure was applied from a nitrogen cylinder through the metal coupling, J, by the diaphragm, K, situated in the bottom part of the solutions reservoir, C. Each vessel was mounted in an adjustable stand and the whole assembly was contained in a large box made from 1/4" thick perspex. This had a sliding front to allow access to the system. This box served a dual role, providing protection against any accident when the system was under pressure and acting as an air thermostat tank. The temperature was maintained at $25 \pm .05^{\circ}C$ by a platinum thermometer and Haaks relay (TP.32) which controlled a 250 watt heater connected in front of a powerful air blower. Stainless steel couplings to fit into the vessels and flexible hose assemblies to connect the vessels were obtained commercially, (George Boyds Ltd.) and (Palmer Aero Products Ltd). The latter consisting of P.T.F.E. sleeves strengthened by stainless steel mesh and fitted with mild steel cadmium plated ferrules. However, after fourteen days the couplings began to show signs of rust. Nickel plating the couplings and ferrules was tried without success and they had to be discarded. Undoubtedly, a corrosion cell was created between the two different types of steel causing them to rust in the presence of electrolyte. Eventually flexible plastic hose was obtained (Intech Type 100 hose) and Delrin hose couplings were machined and fitted to it. Cell couplings to connect each vessel to the hose couplings were also machined from Delrin, E, Fig.(4,9). By cutting a shoulder in these which flattened against the cell wall a very tight seal was obtained. These machined couplings were generally/

generally very successful. The hose couplings held pressure at 600 lbs/in^2 when only hand tight. They also finally eliminated all metal from the system and with it the problem of corrosion.

Each vessel and length of pressure tubing was pressure tested to 800 lbs/in^2 by directly applying nitrogen gas pressure with the vessel contained under water. Any leaks were immediately indicated by a stream of gas bubbles. At this stage it was discovered, contrary to the manufacturer's information, that extruded Delrin bar from which each vessel was constructed, was porous through the centre. This apparently disastrous information, however, only affected the circulatory pumps as all the other vessels were drilled and 'tapped' in the centre. The central core of the pump bodies was removed and a solid piece of slightly tapered Delrin rammed, using a hydraulic press, into place. This new centre core was machined and new bearings fitted.

The flow created in the final system by the two circulatory pumps and the effect of this flow at the membrane surface was investigated:- With the system completely full of solution the maximum rate of rotation of the pumps was 450 rpm. At this rate the velocity of the solution in the flexible connecting hose was 1.7 feet/second, and the volume flow at the membrane, through the angled channels (1.8 cm. long and 2 mm. high) was 1.0 litre/minute.

The effectiveness of the flow at the membrane surface, which would be impaired by the formation of trapped air in the compartment above the membrane and by an uneven flow over the membrane surface, was investigated by firstly sealing a glass plate in place of the membrane and secondly by adding photographic developer or 'fixer' into the feed solution and replacing the membrane by a piece of exposed photographic film. The glass plate showed there were no air bubbles trapped/

trapped in the compartment and no apparent uneven flow distribution over the surface of the membrane. This was confirmed by the photographic film which was blackened by the developer and cleared by the fixer in a completely uniform way. On the numerous occasions this procedure was carried out, varying the strength of the reagent and the time of 'exposure' to it, no striated or unreacted areas were found. Each time the flow caused the whole exposed area of the film to be completely blackened or cleared.

In order to determine whether the magnetic coupling was intact and the impellers rotating during a pressure experiment, a stirring magnet was placed on the top of the pump casing. This could not be rotated by the master magnet(underneath the pump)if the impeller was stopped. These stirring magnets thus gave a visual indication of the rotation rate (if any) of the impeller.

4.3.6 Pressure Line and Pressure Measurement

A standard nitrogen cylinder was connected to the reservoir vessel 'C' by flexible pressure hose (Tecalan Type 100) through a spun steel two litre bomb (Hoke sampling cylinder) and a series of needle valves (Hoke two-way sampling valve).

Pressure was applied by adjusting the valve on the nitrogen cylinder (Pressure Controll Ltd. 31780/1) to a calibrated position, thus filling the steel bomb to the desired pressure. By releasing the two-way needle valve fixed into the end of the bomb, pressure was slowly leaked into the rest of the system. Applying pressure in this way protected the Delrin vessels against any accidental surge of a destructively high pressure. The pressure was maintained constant at an exact value by having the valves in the nitrogen cylinder and in the pressure bomb open. By this method the nitrogen cylinder acted as a high pressure reservoir feeding pressure into the system thus compensating for any leaks. The pressure bomb acted as a reservoir, at the applied pressure, smoothing out any changes in the volume of the system.

The pressure was measured by a Budenberg Standard Test Gauge to $\pm$ 0.25%. This was calibrated for use on gas and was situated between the pressure bomb and the diaphragm. In order to determine whether the pressure at the membrane corresponded to that recorded on the Budenburg gauge, (no pressure loss across the diaphragm) an electronic pressure senser (Bell & Howell Pressure Transducer 4-366 .000 1-.01MO) was connected in a Delrin mounting next the reverse osmosis cell. This senser was "excited" by a 10 volt D.C. source and functioned in the range 0 - 1000 lbs/in^2 to an accuracy of $>$ $\pm$ 0.25%. The millivolt output was monitored on a Solatron Digital Voltmeter (A.210). The electronic senser indicated there was no pressure loss across the diaphragm. As the senser was made in stainless steel it was not constantly kept in the solution system, but was used at intervals to/

check the pressure in the solution and to act as a double check on the Budenburg gauge.

4.3.7. Desalination Measurements.

Solution was degassed and allowed to thermally equilibrate to 25°C in the air thermostat box before use. The bottom of the cell including the porous teflon supporting plate was thoroughly cleaned and dried before each experiment and the low pressure electrode access ports in the bottom of the cell were sealed with blank screws when not in use.

The membrane was dipped in distilled water, lightly blotted and placed on top of the backing plate in place in the bottom of the cell. The silicone rubber gasket,B, was positioned in the top of the cell with its edges aligned with those of the compartment, K, fig (4.10) thus defining the exposed area of the membrane. The two parts were then fitted together and the stainless steel bolts evenly tightened to 80 in/lb. with a torque wrench.

The cell was filled with solution by a pasteur pipette from the access port,O, figure (4.10) which was then sealed by a blank screw. The cell was then mounted into its holder and connected to the other vessels in the system, which was then filled via the threaded port in the top of the reservoir, K. The whole assembly presents a closed system. As a consequence air pockets tended to be trapped during the filling process. To remove these the couplings on either side of the cell were alternatively loosened allowing solution and trapped air to escape. The system was then left with the pumps running and the port,K, in the reservoir open. The remaining air bubbles trapped in the system were broken up and circulated in a stream by the pumps. These escaped at the open

port/

port,K. When no more air bubbles appeared, the system was finally 'topped up' and the plug, H, figure (4.9) screwed into place sealing the system.

Pressure was applied as described in section (4.3.6) and the capillary fitted into the low pressure side of the cell. The volume flow along the capillary was measured at each pressure

(1) immediately solution appeared in the capillary

(2) at some intermediate time, and

(3) near the end of the experiment.

Since the area of membrane exposed was small (3 cm^2) a considerable time was required for solution to appear in the capillary, consequently, the volume flow, Jv, was generally monitored over a twenty-four hour period. On specifically chosen occasions various membranes were 'run' on this system at 400 lbs/in^2 for forty-eight hours to ascertain if Jv changed with time (due to compaction of the membrane). Samples for the determination of product concentration were taken from just beneath the membrane surface at the low pressure side by inserting a Hamilton syringe through the ports on the low pressure side of the reverse osmosis cell. Samples, 0.08 cm^3, were extracted in this way and the concentrations determined by potentiometric titration of the chloride ion as described in sections (4.2.3.2.). The volume flow and product concentration were investigated at two applied pressures 200 lbs/in^2 and 400 lbs/in^2 on this system. At each of the two pressures, data on volume flow and product concentration were obtained over at least three separate experiments, for a series of membranes and the average values calculated. Reproducibility for volume flow was $\pm$ 1.0% and for product concentration was $\pm$ 2.0%.

4.4 Silver/Silver Chloride Milli-Probe Electrodes

Electrodes of a specific design were required to make potential measurements across the membrane, during the reverse osmosis process. It was necessary thatthese conform to certain requirements imposed by the conditions in which they would be used. The silver/silver chloride electrode is an obvious choice for making potentiometric measurements in a sodium chloride solution these have been used and investigated by many workers. (24) (25) (26) (27). These electrodes have a number of assets in that they are basically relatively small, can be used in any position and will not contaminate the system in which they are immersed. This current application required that the electrodes should be small enough to be incorporated close to the surface of the membrane in the reverse osmosis cell and that they did not interfere with the flow of solution past the membrane. They must be easily mounted into a housing which could be sealed into the reverse osmosis cell and withstand the high pressures applied. Finally, as the potentials to be measured were not large (in the order of 50 mV) the bias potentials between the electrodes used had to be very small <0.05mV

PREPARATION AND DEVELOPMENT

4.4.1. Design I

The first electrode design used is shown diagrammatically in Fig. (4.11A). Both high and low pressure electrodes were made to this design, the former being generally larger than the latter.

The probe consisted of a forged silver billet 3 mm. in diameter, H, into which two 0.75 mm. diameter silver wires A, and G were silver soldered and cut to the required length. The billet was then threaded and the tip of the wire, G, machined to a fine point with a 30° taper. The electrode housing was constructed in Delrin which has excellent insulating properties. Fig. (4.11.A)

A hexagonal bolt head was cut in this housing and the outside threaded to enable the whole electrode assembly to be tightly secured into the reverse osmosis cell. The inside of the housing was threaded to incorporate the silver billet, and the bottom threaded and countersunk to allow the end piece, F, to be fitted.

For assembly the silver billet was lightly covered in casting-Araldite and tightly screwed into the housing. The bottom face of the billet and the thread of the end piece, F, were covered with Araldite and the end piece screwed into place. The excess Araldite was pushed round the edges and through the centre hole of the end piece sealing the whole assembly. The Araldite coating and Delrin housing efficiently insulated the billet.

The tapered tip of the wire, G, was cleaned in ammonia solution and nitric acid solution to remove any surface halides or oxides and finally washed in water. It was then (temporarily) lightly coated in paraffin wax. The rest of the wire protruding from the housing was insulated. Various insulations were tried, the first was a commercially supplied lacquer applied as a fine spray. (Clear Insulation/

Insulation Lacquer, R.S. Components Ltd.) This, however, was brittle and appeared to be attacked by the sodium chloride solution which was also able to penetrate between the lacquer and the silver wire, rendering the insulation valueless. This problem also applied to the various types of araldites used which were also difficult to apply in a thin layer, adding greatly to the diameter of the probe wire. The insulation found to be most successful was a vinyl co-polymer resin coating applied by an aerosol spray (Fison Scientific Apparatus V A/C). This proved to be very satisfactory being easy to apply, very durable and provided good insulation. By using a white vinyl coating any imperfections in the insulation were easily detected. The paraffin wax was removed from the tip of the silver wire and a fresh layer of silver exposed by anodising in a 0.100 Molar solution of silver nitrate. In order to reduce and control the current density at the tip of the silver wire the electrodes were connected in parallel to a two centimetre square piece of silver foil. In this way the current density to the probe electrodes could be easily controlled. The electrodes were washed in distilled water after anodising in the silver nitrate solution. They were then chloridised in an 0.100 Molar hydrochloric acid solution using a platinum gauze cathode, by applying a current of 2.5 milliamps/cm^2 for about 15 minutes. Dry nitrogen gas was bubbled into the hydrochloric acid solution during the chloridising process. This aids in reducing the silver oxide formation on the electrodes. Better bias potentials were obtained when this procedure was used. When the electrodes had been chloridised they were washed overnight in distilled water and then left short-circuited in an 0.100 Molar sodium chloride solution for two to three days. Pairs of electrodes were chosen by selecting/

selecting those with the smallest bias potentials. These were kept, connected together, in a fresh 0.100 Molar sodium chloride solution for one week.

The electrodes produced by this method were found to have bias potentials varying between $\pm$ 0.1 mV and $\pm$ 1.0 mV. In an endeavour to improve this the current density and the length of time the current was applied was varied, but with little improvement. These electrodes were consequently of no use for making accurate potential measurements. They did, however, provide insight into the actual potential range that was finally measured and they demonstrated that the design of the electrode housing was efficient. This withstood the high pressures applied in the reverse osmosis cell, and completely sealed the electrode in place.

Strains 'set-up' in the silver billet during forging and machining were the probable cause of the large bias potentials in these electrodes. In an attempt to prepare better electrodes without using a billet, the tips of 1 mm. diameter platinum wire were electrolytically plated with silver and chlorodised using the method of Brown [29]. Ten 6 cm. lengths of wire were treated in this way, pairs chosen and left shorted for one week. At the end of this time bias potentials were measured. These were found to be no better than before.

4.3.4.2. The electrodes finally used in this work were developed from these platinum wire electrodes. A standard preparation for silver/silver chloride electrodes is the Thermal-Electrolytic method outlined in Ives & Janz [29]. However, the electrodes generally prepared in this way are bulky, usually mounted in a glass support, therefore a means of reducing the size and incorporating them into the/

the electrode housing was required.

Silver wire 0.50 mm. in diameter was cut into 6 cm. lengths and washed alternately in ammonia and nitric acid solutions. Approximately 6 cm. lengths of thick walled pyrex capillaries 1.5 mm. in diameter (internal) were cut. One end of each was sealed and drawn out to a fine point. Dry AnalaR grade silver oxide powder was pushed into the capillaries and tightly packed into the tapered point. The lengths of silver wire were then pushed into each capillary and their ends buried in the silver oxide. These were then placed upright in a muffle furnace (Gallenkamp Scientific Instruments) and the temperature raised, to 450°C and maintained for three hours. In order to prevent any thermal shock which might crack the porous tip the electrodes were left to cool slowly inside the oven. Once cool the wires with the new pointed porous silver tips were easily withdrawn from the capillaries. The wire above the silver tip was insulated with the vinyl co-polymer resin and the electrodes washed overnight in distilled water. They were then chloridised in 0.100 Molar hydrochloric acid solution, as before, section (4.3.4.1) By alternating the polarity of the electrodes, passing a current of 2 m amps/cm^2 for five minutes in each direction, the chloride coating was alternately applied and removed. This procedure helped the final layer of chloride to be applied as a smooth even coating on each electrode. The final chloridisation was accomplished by passing 2.5 m amp/cm^2 for twenty minutes. Nitrogen gas was bubbled into the solution while chlorodisation was taking place and the solutions were degassed before use. The chloride appeared as a dark grey layer.

After chloridising the electrodes were left short-circuited for two days in distilled water and for another two days in 0.100 Molar sodium chloride. The bias potential between selected pairs

was/

was measured and found to be in the range ± 0.15 to ± 0.05 mV depending on the matched pair. The pairs were left shorted for another week, the sodium chloride solutions being changed each day. After this period the bias potentials were remeasured, the maximum discrepancy was ± 0.01 mV and for any pair used in the potential measurements, was never greater than ± 0.005 mV.

Figure (4.11.B.) shows how these were housed. Araldite was mixed and gently heated until it obtained a thinner consistency. The chloridised porous tip of the electrode was protected by soft tissue paper and the wire coated in Araldite and twisted into the Delrin housing, D, through the fine hole drilled in the centre, until it protruded at the top. The length of wire protruding at the bottom was adjusted and the countersunk bottom section, F, filled with more Araldite. The whole assembly was left overnight in an oven at 40°C. Once the Araldite dried the electrodes were firmly fixed in place. The chloridising procedure was repeated for these housed high pressure electrodes each connected to its own group of wire electrodes from which the most compatible were chosen (bias potential<5 μV). The wire electrodes were used without housing in the low pressure side of the cell. When not in use the electrode pairs remained short-circuited in the solution in which they would be used.

P erfect electrical connections to the electrodes were found to be critically important. Many unacceptable bias potentials measured could be attributed to bad electrical connections and not differences in the electrodes. To overcome this, very fine insulated wire was soldered to each of the electrodes and small crocodile clips soldered to the other end.

In preparing the electrodes the solutions used were AnalaR grade and no purification by recrystalisation was found to be necessary. Four pairs of electrodes were used and alternated over a period of

six months. If required, pairs were rechloridised. However, the bias potential of at least two of the pairs remained less than 0.01 mV over this period.

Undoubtedly the success in producing electrodes which could be used in the high pressure system was crucial to the success of this work.

4.5 Pressure Potential Measurements

Potential measurements were obtained by two different procedures:

(1) The reverse osmosis cell was assembled and filled as described in section (4.3.7) The bias potential between probe electrode pairs was measured and the best pair selected (bias potential $< 5\mu$ volts). The housed electrode was screwed into place in the high pressure side of the cell with its tip 1.5 - 2.0 mm from the surface of the membrane. The cell was connected into the complete system which was then filled, section (4.4). The low pressure side of the cell was also filled with feed solution and the wire electrode probe sealed into place with paraffin wax or plasticene. Consequently there was no concentration gradient across the membrane before pressure was applied.

(2) In the second procedure the cell was assembled as before, but the low pressure side was kept completely dry and neither electrode was put into place. Pressure was applied and the desalination process was allowed to proceed until solution was evident in the low pressure side of the cell. The membrane thus created its own concentration gradient; the pressure was released once this was accomplished. The electrodes were fitted in place and the pressure re-established

For both procedures the pressure was maintained until the pressure potential readings were constant for at least two hours and in every case the membrane was investigated over at least a twenty-four hour period.

In the first method, with no concentration gradient at the beginning of the experiment, the complete pressure potential profile

as/

as the membrane reacted to the applied pressure and created its own concentration gradient was obtained.

The effect of short pressure pulses on the membrane (pressure was applied in 50 lbs/in^2 pulses from 0 - 400 lbs/in^2 and released in 50 lbs/in^2 pulses from 400 lbs/in^2 to zero) and the subsequent effect on the potential was measured providing useful data.

The second procedure allowed product samples to be obtained which were not contaminated by traces of the feed solution. Samples were taken from the electrode compartment, on the low pressure side, at the tip of the electrode using a Hamilton syringe. The measured concentration of these determined the 'concentration-cell' contribution to the total reverse-osmosis potential. Section (2.2.3.)

With both procedures the volume flow was measured while the potential was being recorded.

Goldsmith and Lolachi [23] report that flow velocities at Ag/Agcl electrodes slightly affect the electrode potential and this effect was observed in this work as an unstability in the potential reading at the beginning of an experiment using procedure one. To overcome this a guard tube,U, Fig (4.10) was designed and fitted into the topof the compartment, K, fig (4.10) to cover the protruding electrode tip.

The potentials set up were measured in a Solatron Digital Voltmeter (A.210) and were recorded on a Servo Scribe potentiometric chart recorded (IS.R.E.541). The potential signal from the electrodes was passed through a pH meter (E.l.L. M.23A) which had an impedance of $10^6 \Omega$ before connection to the recorder. This prevented the chart recorder drawing current consequently ruining the accuracy of the potential readings.

The total emf measurements determined by both methods closely agreed and over a number of experiments the reproducibility for each membrane was between $\pm$ 0.5 - 1.0 mV.

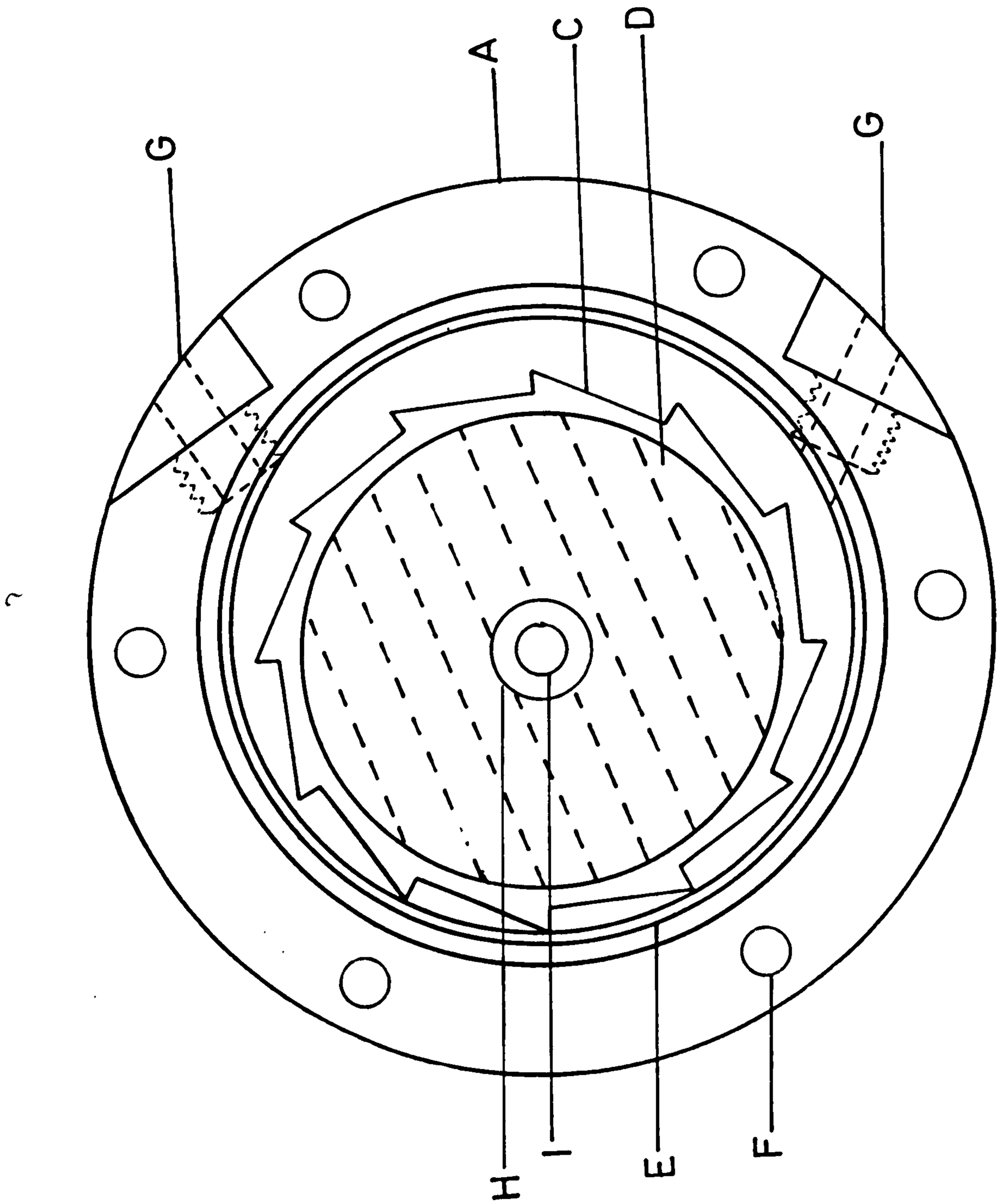

FIG. 4.5

CIRCULATORY PUMP

SECTION DIAGRAM FIGURE 4.6

A - Top section of pump (Delrin)

B - Bottom section of pump (Delrin)

Diameter - 12 cm. Total Height 5½ cm.

C - Impeller (Delrin) Mounted 1/16" of centre twelve teeth, 1/8" deep, 30° pitch.

D - Magnet (from Gallenkamp Magnetic Stirrer)

E - Neoprene o-ring 8 cm. diameter in recession 5 mm. x 5 mm.

F - 3/8" stainless steel bolts torqued to 50 lbs/in.

G - Cell coupling (Delrin) orientated 60° to each other.

H - Teflon bearing cap

I - Glass Centre Pivot

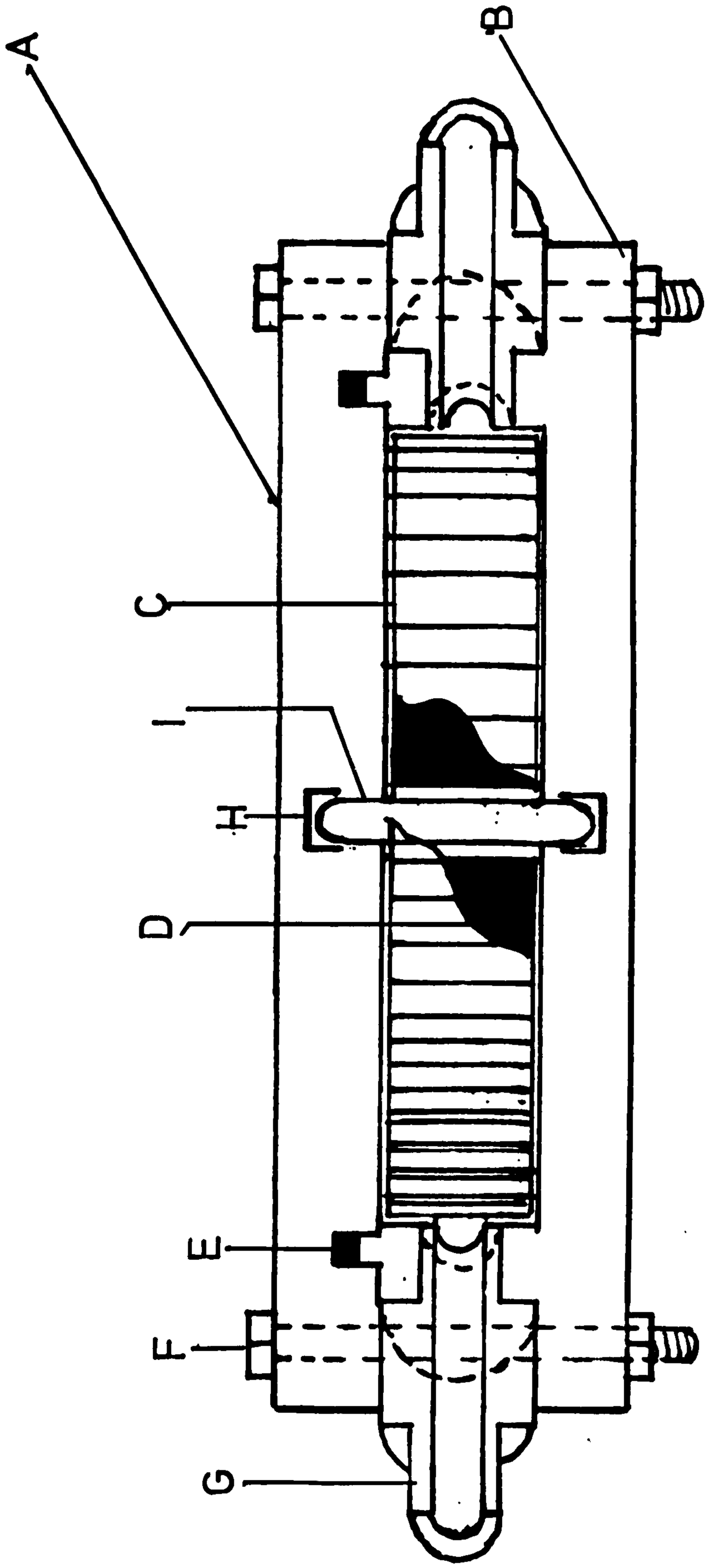

FIG. 4.6

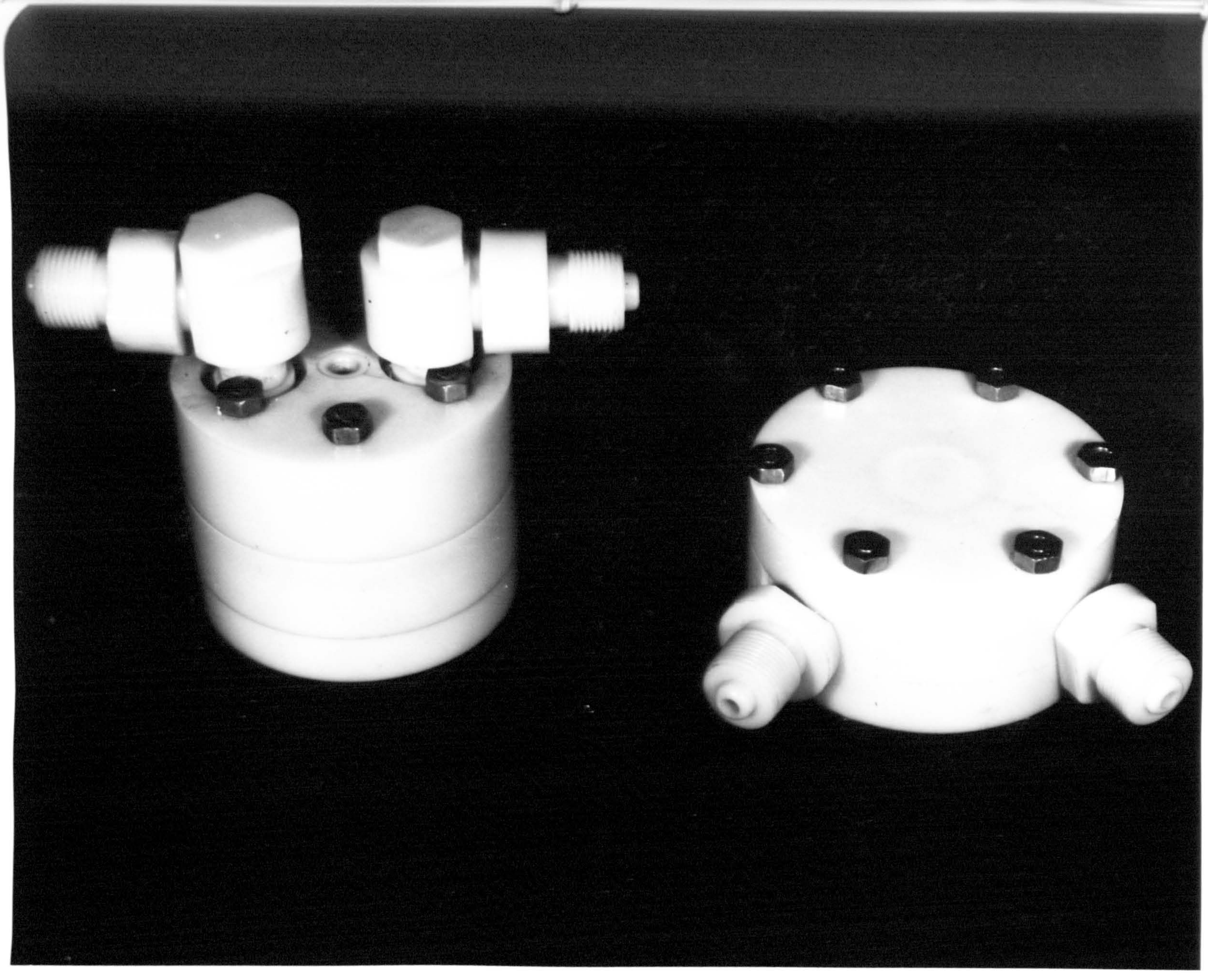

FIG. 4.7

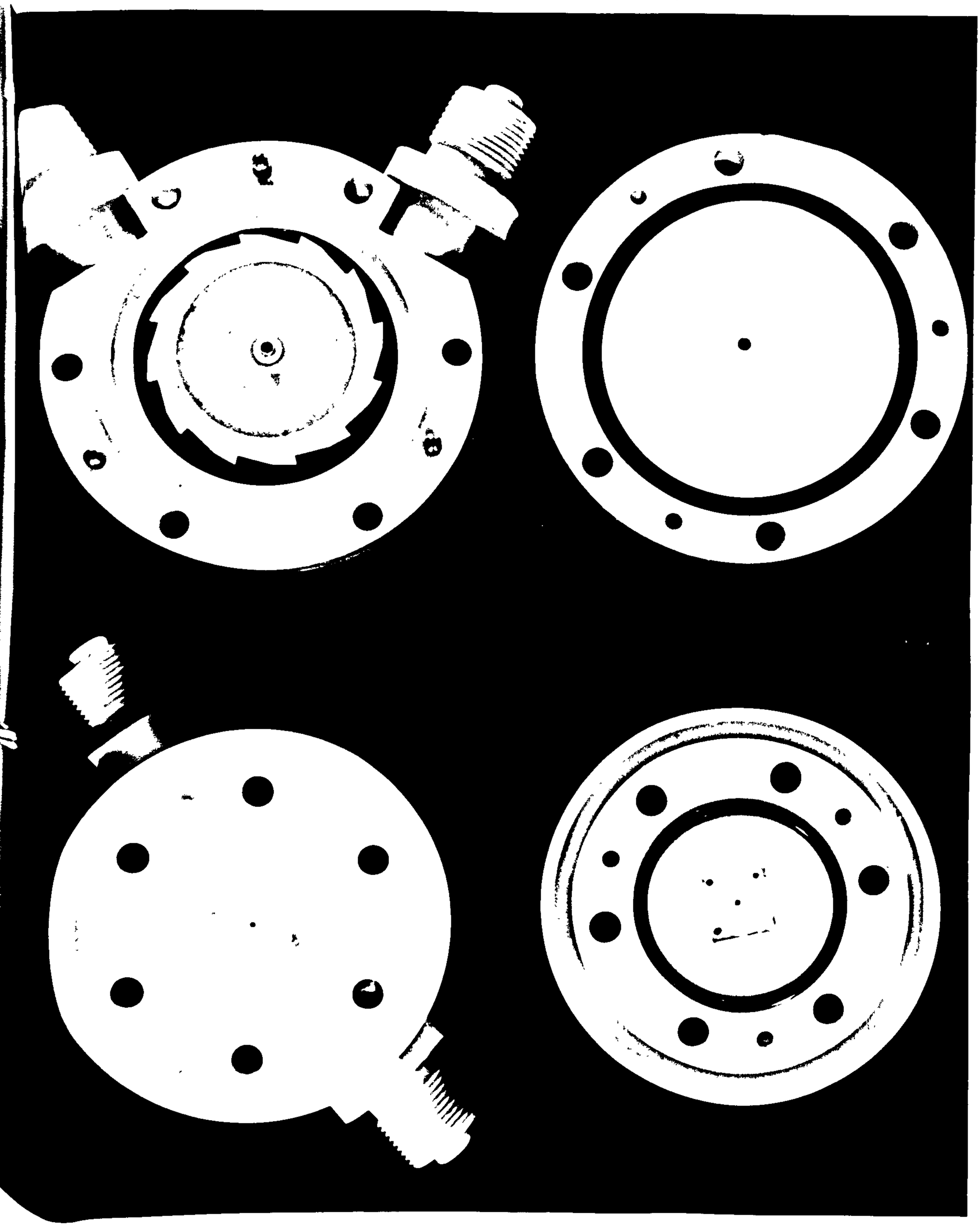

FIG. 4.8

RESERVOIR/PRESSURE TRANSMITTING VESSEL

SECTION DIAGRAM FIGURE 4.9

A - Top section

B - Bottom section.

Overall Diameter 10.5 cm. Overall height 14.5 cm.

C - Rubber Diaphragm 1/16" silicon rubber on top
1/16" butyl rubber on bottom.

D - Stainless Steel Coupling to pressure line.

E - Cell coupling (Delrin) 2½ cm. O.D. head, with 1/10"
shoulder on cell face.

F - Hose coupling (Delrin) 4 cm. Diameter collar 3 cm. tail.

G - Stainless steel plate 1/2" thick.

H - Threaded plug (Delrin)

I - 3/8" stainless steel bolts.

J - Circular steel band (for matching top and bottom section on assembly)

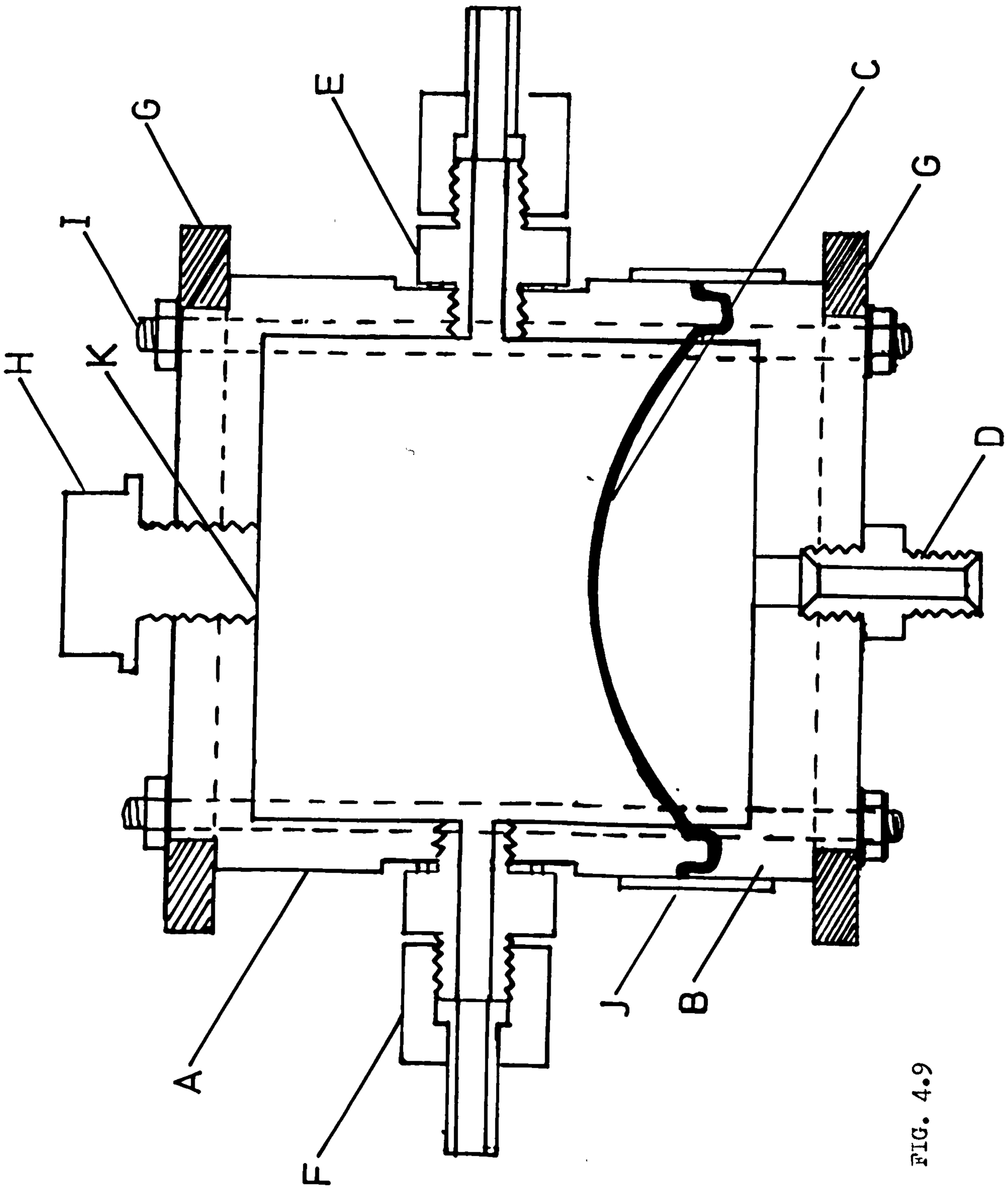

FIG. 4.9

REVERSE OSMOSIS CELL II

SECTIONAL DIAGRAM FIGURE 4.10

A - Membrane

B - Silicone Rubber Gasket

C - Backing Plate (Porous Teflon)

D - Neoprene o-rings

E - Drilled Collection Compartment

F - Low pressure electrode ports 1.5 mm. diameter

G - Threaded port for (early design) low pressure electrode

H - Capillary port

I - Early low pressure electrode

J - 3/8" diameter stainless steel bolts

K - Solution compartment 2.1 cm. x 1.8 cm. x 2.5 mm.

L,T. - Angled solution channels (60°)

M - Right angled cell couplings

N - Pressure hose couplings

O - High pressure electrode access port

P - Red Fibre sealing washers

Q - Stainless steel nuts and washers

R - High pressure section of cell

U,V - Narrow angled aperture into compartment K, 1.8 cm. x 2.0 mm.

Overall diameter 10.5 cm.

Overall height 8.2 cm.

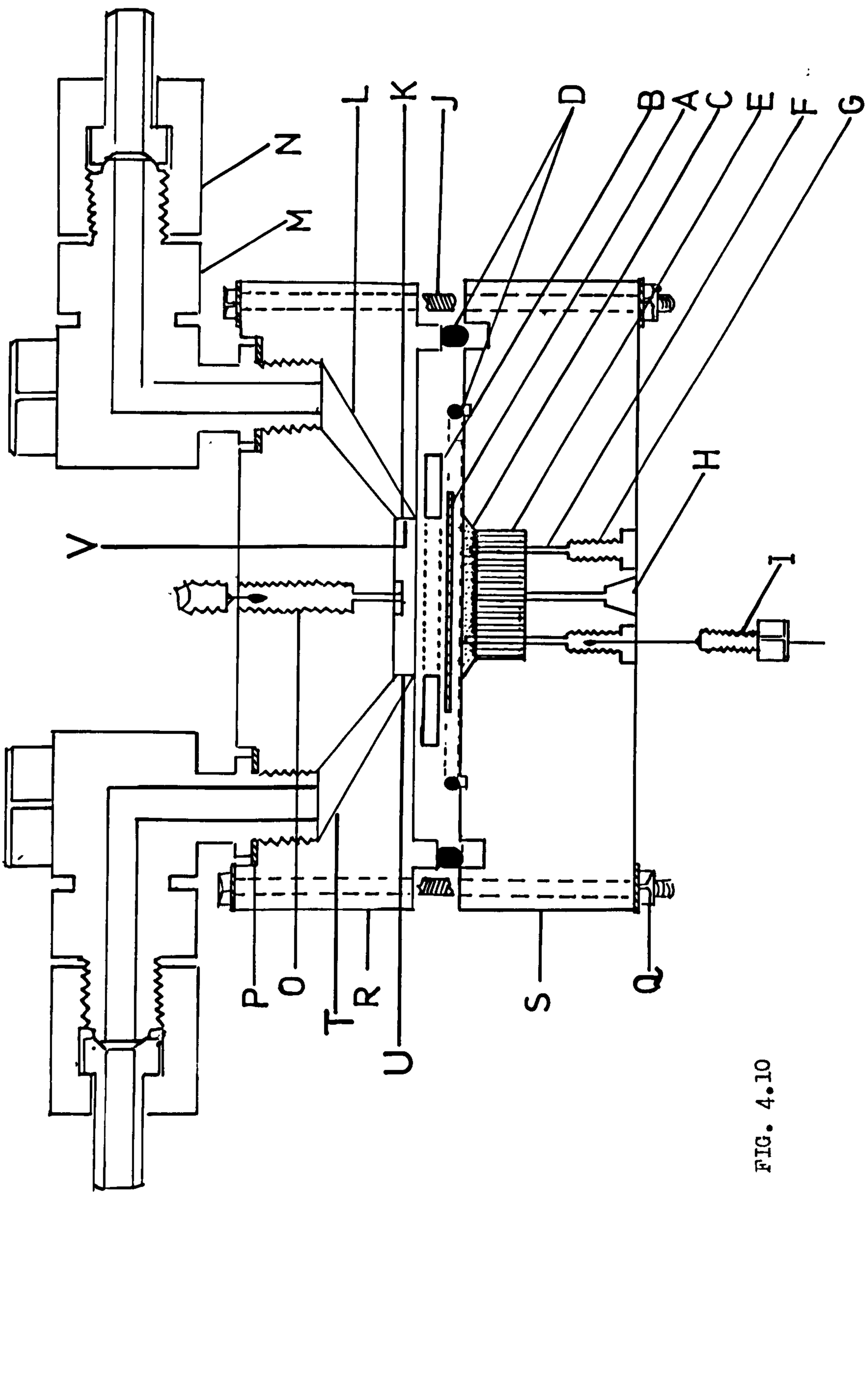

FIG. 4.10

SILVER/SILVER CHLORIDE ELECTRODE

DESIGN I FIGURE (4.11A)

A - Silver wire 1 mm. diameter,for top connection

C - Hexagonal head

D - Threaded high pressure electrode housing (Delrin)

F - Threaded end piece (Delrin)

G - Tapered silver wire 1 mm. diameter (30° taper)

H - Silver billet 1/8" diameter 2.5 cm. long.

DESIGN II FIGURE (4.11.B)

A - Silver wire 1 mm. diameter

B - Araldite

C - Hexagonal Head

D - Threaded High Pressure Electrode Housing (Delrin)

E - Araldite

F - Araldite

G - Porous silver tip

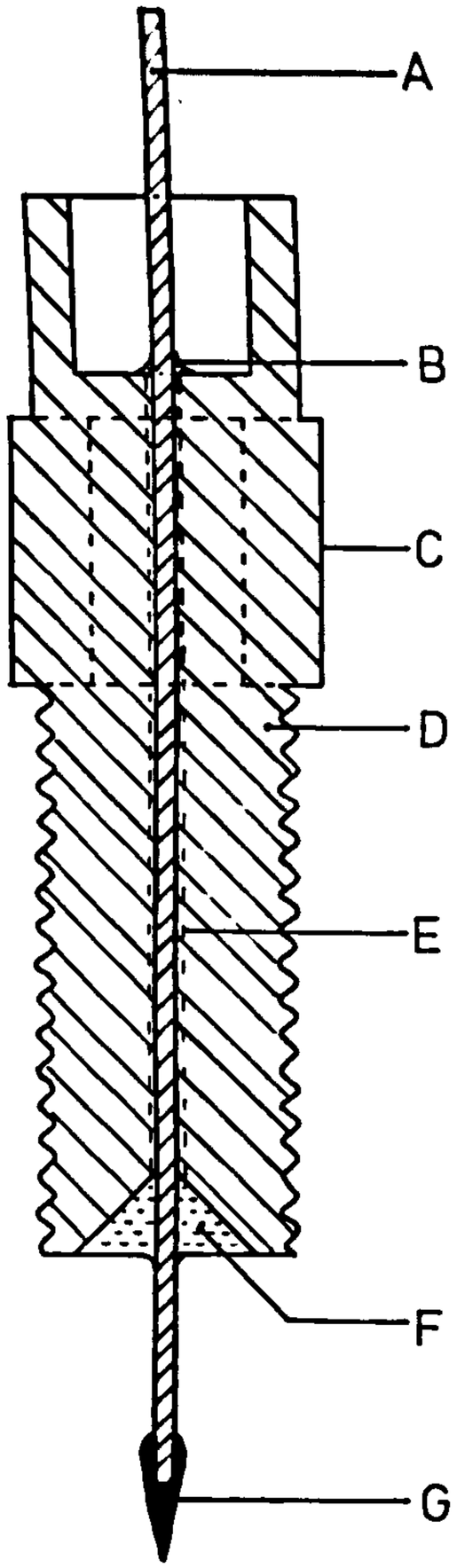

FIG. 4.11B

FIG. 4.11

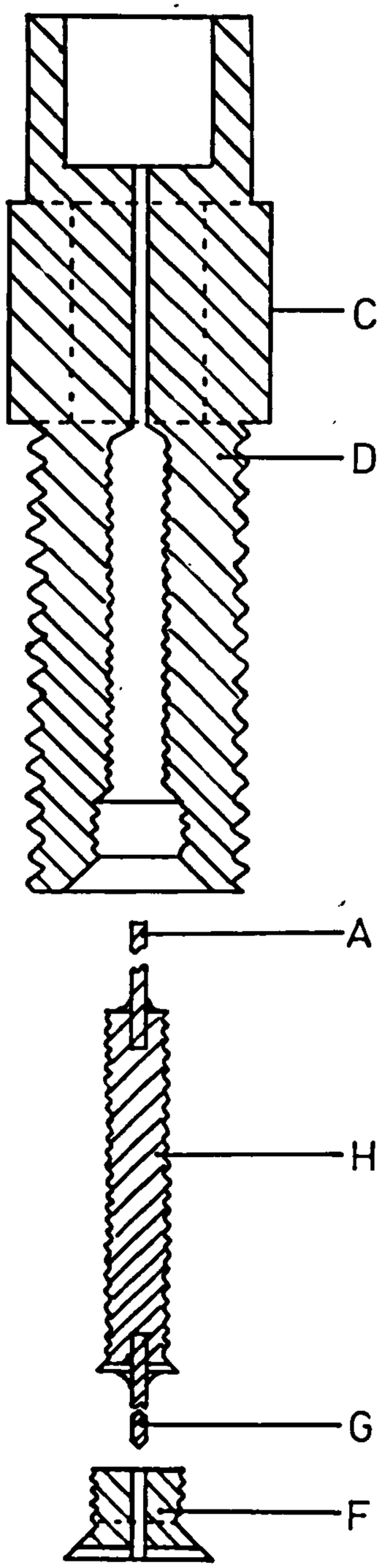

FIG. 4.11A

THE REVERSE OSMOSIS SYSTEM

FIGURE (4.12)

A - Reverse osmosis cell (Delrin)

B^1, B^2 - Circulatory pumps (Delrin)

C - Reservoir/Pressure transmitting vessel (Delrin)

D - Flexible pressure hose. P.T.F.E. inner sleeve reinforced with nylon. Intech Type 100 hose, supplied by George Boyd Ltd.

E - Cetonko Electric Motor (K.P.Q.S. 1200)

F - Master magnet (Gallenkamp Magnetic Stirrer Type)

G - Impeller (Delrin)

H - Angled cell coupling (Delrin)

I - Pressure hose coupling (Delrin)

J - Stainless Steel Coupling to Nitrogen Cylinder

K - Rubber diaphragm consisting of 1/16" silicon rubber on top 1/10" butyl rubber beneath.

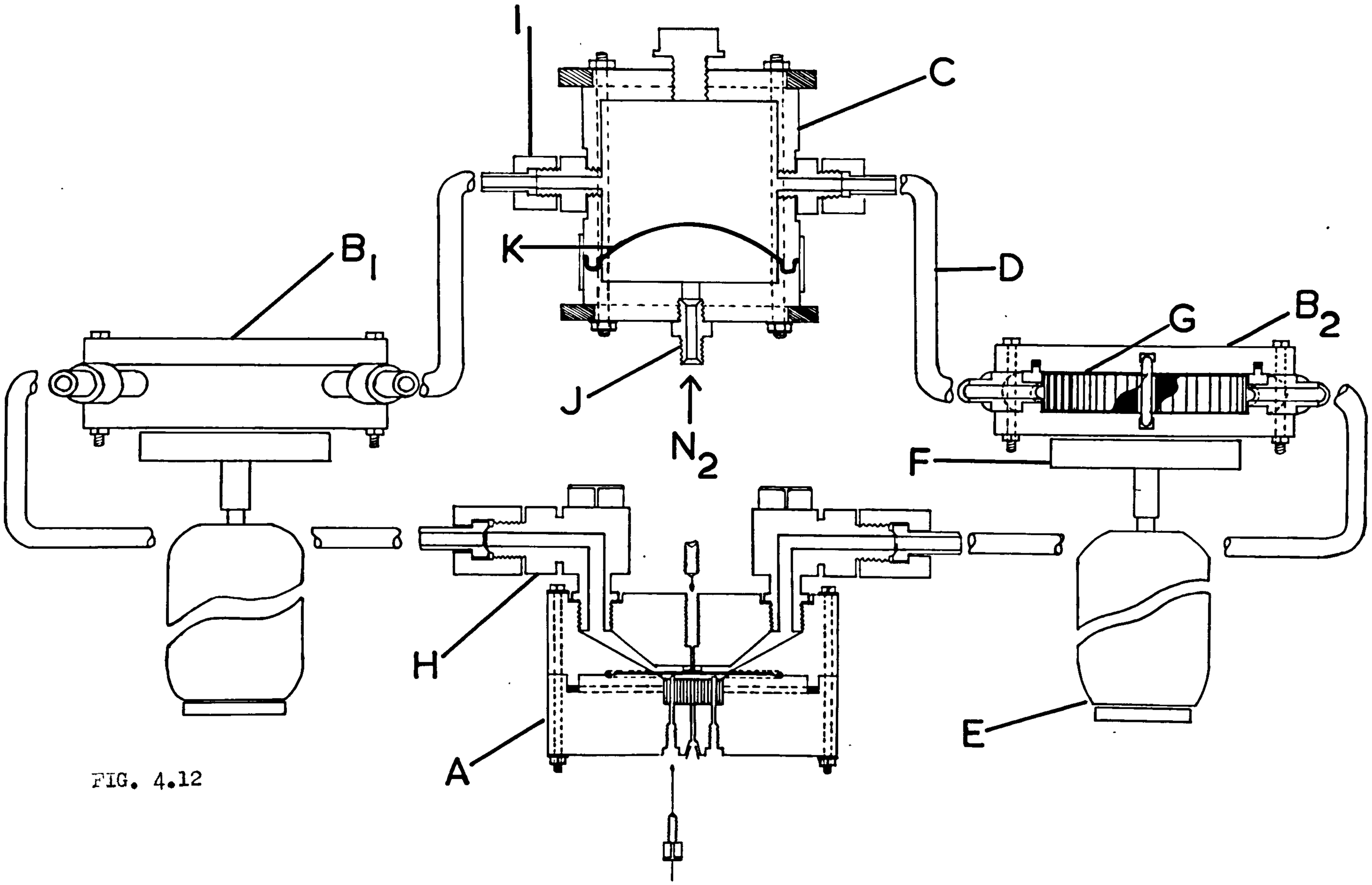

FIG. 4.12

REFERENCES

CHAPTER 4

EXPERIMENTAL.

1) G.A. Bray. Anal. Biochem. 279 (1960).

2) Hefferich 'Ion Exchange'. McGraw-Hill New York (1962)

3) G.R. Gardner and R. Paterson, Diffusion Processes. Proc. of Thomas Graham Memorial Symposium. Univ. of Strathclyde (1969), Gordon & Breach (London) 1970.

4) R. Arnold and D.F.A. Koch. Aust. Journal Chem. V.19 No.8 (1966) 1299

5) C.R. Gardner and R. Paterson. J. Chem. Soc. A. 2254 (1971)

6) H. Ferguson, C.R. Gardner and R. Paterson. J.C.S. Faraday I 63, 2021 (1972)

7) C.R. Gardner and R. Paterson. J.C.S. Faraday I 68, 2030 (1972)

8) Dupont Innovation V.4 No.3 1973.

9) G. Grot and H. Munn. 141 National Meeting American Electro Chem Soc.

10) G. Gran. Analyst 77, 661 (1952)

11) Test Manual for Permselective Membranes. U.S. Office of Saline Water. Research Report.

12) D. Mackie and P. Meares. Trans. Faraday. Soc. 55, 1221 (1959)

13) P. Meares. H. Sutton. J. Colloid. Interface Science 69, 29 116028

14) H.P. Gregor etal, Membrane Evaluation Program , New York, Brooklyn, Polytechnic 1961.

15) J.S. Johnson, J.W. McCutchon, Desalination (1972) 10, 147, 56.

16) C. Forgacs, K.S. Spiegler, Desalination (1972) 10, 181

17) U. Merten 'Desalination by Reverse Osmosis', M.I.T. Press, Cambridge Massachusetts (1966).

18) S. Sourirajin 'Reverse Osmosis', Locos Press Ltd. London, 1970

19) Same as 15 above.

20) R.A. Robinson and R.H. Stokes 'Electrolyte Solutions" Butterworths 2nd Edition (1965) 96, 97.

21) T. Chapman and J. Newman. A compilation of Selected Thermodynamic and transport properties of Binary Electrolytes in Aqueous Solution. Lawrence Radiation Lab. Berkeley California (1968

22) H.S. Harned. B.B. Owen 'The Physical Chemistry of Electrolyte Solutions' Reinhold, New York, 3rd Ed. 1958.

23) H. Goldsmith and H. Lolachie Office of Saline Water Research and Development Progress report No. 527

24) I.B. Grimely and A.F. Mott. Discussion Faraday Soc. 50, 126(1954)

25) G.W.D. Biggs and H.R. Thirsk Trans. Faraday Soc. 48,1171 (1952)

26) D.W. Kennard. Proc. Physical Soc. 39, 20-21 (1963)

27) Kwak J.C. Desalination 11,(1972) 61-69

28) A.S. Brown, Am. J. Chem. Soc. 56,(1934) 645

29) Ives and Janz. Reference Electrodes Ch.4 Ch.11

30) R.M. Borrer, J.A. Barrie and M.G. Roges. Trans. Faraday Soc. 58, 2473 (1962)

CHAPTER 5.

RESULTS AND DISCUSSION.

BASIC EXPERIMENTAL MEASUREMENTS MADE ON THE AMF C_{60} AND XR-170 MEMBRANES.

5. Measured Properties of the Range of C_{60} and XR Membranes

Tables (5.1) and (5.2) show the measured physical parameters of the range of C_{60} membranes studied in this work and demonstrate the effects of heat pretreatment on the membrane, in 0.1M NaCl and 0.0 5M $CaCl_2$. The physical parameters of the XR-170 membranes studied in 0.1M NaCl are shown in Table (5.3) and allow comparison between the two membrane types.

5.1.1. Water Content

The degree of swelling in a fixed charge polymer membrane is determined by the chemical nature and physical structure of the polymer, especially, the degree of cross linking, the fixed charge concentration of the matrix, and the nature of the equilibrating solution. 'Swelling Equilibrium' is a balance of opposing forces. The tendency of the polar and ionic groups in the matrix to solvate and consequently stretch the matrix is opposed by the tension in the extended polymer chains. In the polymer matrix free rotation about chain bonds is sterically hindered, and because of the random nature of the cross-linking reaction some of the lengths of chain between the cross-links will be significantly shorter than average. When the resin swells these may be almost fully extended and their bond angles displaced from the position of minimum internal energy. Since these shorter sub-chains bear a major share of the swelling stress, this increase in internal energy acts as a restoring force. Allowing the coiled polymer chains [1] to assume a more energetically, favourable, less strained, position by heating (kinetic vibration), the tension in these sub-chains is reduced, consequently the primary effect of heating is to allow greater absorption of solvent by the polymer matrix.

This/

This is well illustrated in Table 5.1. The water content (weight per cent. water w.r.t. dry weight of polymer) varies in the range 41 - 150%, depending upon the heat pretreatment process used. The membranes may be divided broadly into three groups. In the range 40-50% the membrane is in its normal condition, essentially unexpanded and in the condition which it would be found in normal use. This group is designated C_{60N} by Gardner & Paterson [2] [3] [4]. By moderate heat treatment the membrane in its usual expanded form containing 80-100% water, i.e. C_{60E} was obtained. With further heat treatment membranes of the third group were obtained. The water content of these was some 120-150%. This suggested a considerable relaxation of the polymer matrix brought about by the heat pretreatment.

Even without considering the two 'super expanded' membranes, of the third group, the water content does not increase linearly with the time of heat treatment, since those heated for two hours, PS_5 and PS_6, showed higher water contents than the membranes heated for either one or three hours. In the latter, which experienced the longest heat pretreatment, some partial transition of the polyethylene substrate from amorphous to crystalline may have occurred, thus increasing the rigidity of the polymer matrix and consequently reducing slightly the water content [5] [6] [7]

5.1.2. In ion exchanger membranes, due to the high concentration of ions in the interior of the membrane there is a tendency to dilute the matrix by additional solvent. This appears as an osmotic pressure difference between the interior of the membrane and the solution. The value of this will be affected by a change in/

in the fixed charge capacity or any change in the concentration or valency of the bathing solution.

Table (5.2) demonstrates the effect of a change of electrolyte solution from 0.10M Nacl to 0.05M $CaCl_2$ on the geometry of the membranes.

The reduction in counter-ion concentration was slightly greater than 50% in each of the three membranes with the change of counter-ions from Na^+ to Ca^{2+}.

The water content of the normal, PS_1 expanded, PS_5 and super expanded, PS_{11} were reduced by some 18%.

The wet volume of the membranes was reduced by some 10-16%.

5.1.3. The effect of variations in fixed charge capacity and consequent change in osmotic pressure difference between membrane and solution is illustrated by the XR-170 membranes in Table (5.3). The water content progressively increases from approx. 13% in XR-A to approximately 26% in XR-C while the capacities increase from 0.68 $m.mol.g^{-1}$ (of dry matrix) to 0.88 $m.mol.g^{-1}$. This shows clearly the very large increase in imbibed water (100%) in the membrane brought about by a relatively small ($\approx$ 22%) increase in the amount of fixed charge and accompanying counter-ion. The increasing water content brought about by increasing the fixed charge capacity is demonstrated in Fig. (5.0). The water content of the homogeneous XR-170 membranes is considerably less than that of the copolymer, C_{60} membranes.

5.2.1. Tortuosity Factor Θ

Experimental evaluation of Θ is usually based upon the assumption that $\bar{D}\,\Theta = D_{soln.}$ but it seems preferable to examine theoretical models, based either upon discrete geometrical assumption, such as configurations of available paths within a medium or upon more abstract mathematical models. One certain outcome is that unless a very detailed statistical picture of the geometry of a membrane is available, the resultant values of Θ cannot be considered to be particularly accurate, (ca $\pm$10%). The correction is, however, very well worth while since only by attempting to remove this geometric factor can membrane functions be resolved in general chemical terms, or comparisons be made with other membranes or ionic media. It should be noted that in expressions which involve ratios of mobility or frictional coefficients, then tortuosity corrections cancel. Thus, for example, t_1, t_3 or predicted product concentrations

$$C_p = \left\{J_s/J_w\right\} \times C_w \quad \text{section } (6.1)$$

are independent of Θ, and allow comparison with Θ corrected data.

Several theoretical estimates for tortuosity exist as functions of the volume fraction of water, V_w, within the membrane. As V_w tends to unity and the corresponding polymer fraction V_p to zero $\Theta \rightarrow 1$. Equally as $V_p \rightarrow 1, \Theta \rightarrow \infty$.

Wheelers' (9) estimate

$$\Theta = \frac{2}{V_w}$$

does not satisfy the first of these boundary conditions and was rejected. Mackie and Meares (10) adapted a regular model for the positions of diffusion sites within a homogeneous polymer. Based upon this idealised model

$$\Theta_m = \left(\frac{2}{V_w} - 1\right)^2$$

Prager discussing the analogous problem of the dielectric constant in a heterogeneous medium containing two distinct components has provided a useful model. Making the reasonable assumption that D_p, the diffusion coefficient in volume of polymer, is zero for ions and water gives

$$\theta_p = \frac{2}{V_w} - 0.5(\ln V_w)^2 / (1 - V_w + V_w \ln V_w)$$

It is worth noting that $\theta_m = \theta_p$ as $V_w \rightarrow 1$.

θ_m has been shown to give good correlation between membrane diffusion coefficients of all membrane species in Zeo-Karb 315 phenol sulphonic acid membranes with diffusion coefficients of corresponding equimolar solutions. However, using different membrane systems other workers have found poor agreement (8) (11) (12) (13). Amongst these were Gardner and Paterson (2) (3) who used

$$\theta_m = \left(\frac{2}{V_w} - 1\right)$$

which they found gave satisfactory agreement for both normal and expanded C_{60} membranes. They also successfully applied θ_p to scale diffusion coefficients in the C_{60} membrane system. The values of θ_m, $\left(\frac{2}{V_w} - 1\right)$, and θ_p were used in thiswork and are shown in Table (5.1).

These scaling factors illustrate quite well the more open structure of the expanded membranes and θ_m indicates that the matrix of the normal membrane PS_1 is approximately three times more tortuous than that of PS_{11}, the most expanded. The values of θ_p for the whole range are smaller than those of θ_m and the effects of this on the phenomenological coefficients and specific conductivities calculated from the salt model will be discussed in section (3.3).

The general decrease in tortuosity of the matrix, as represented by/

by the factors θ_m and θ_p, with increasing dilution of the membrane is shown in Fig. (5.1). This illustrates that a small change in the water content will have an especially large effect for the membranes with a low water content (percentage water). For a change in water content of 10% the tortuosity factor of the normal forms differ by 25%. However, for the more open, more solvated membranes, a change of 30% in the water content causes a much smaller variation of 16% in the tortuosity factor.

In section (3.1.2.) Fick's equation for isotopic diffusion was scaled by θ to apply to the membrane case. Since this is one specific example of a phenomenological equation, the tortuosity factor is therefore a correction to the phenomenological coefficients L and R. Thus since progressive 'expansion' of the membrane influences θ, it may be expected that the fluxes of the different species, through the membrane, will vary with increasing expansion.

5.3 Conductivity.

In ion exchange membranes with large internal ionic concentrations specific conductivities are large, though due to tortuosity effects, observed conductivities are much lower than in corresponding aqueous solutions of equal molality. In appendix (4) the electrical conductivity of an ionic solution is shown to be independent of frame of reference chosen for ionic fluxes, thus the specific conductivity of a salt solution remains unaltered if flows are defined relative to stationary water or if, as in an ion exchange membrane, to a fixed ionic species. This, therefore, allows the comparison of membrane and equimolal solution specific conductivities (once tortuosity has been considered).

Since the measurement of specific conductivity is relatively accessible, many investigators have studied this parameter. In these studies the counter-ions are usually alkali or alkaline earth metal-ions which are important in the desalination processes involving membranes (8) (13) (14) (15) (16), or the membranes are investigated in the acid form (17) (18) (19). However, in general, past workers have investigated either the variation in specific conductivity with increasing concentration of electrolyte or the change in specific conductance effected by various counter-ions. Since for both of these investigations the factor varied causes changes of the membrane which also affect conductivity, the results are sometimes difficult to interpret.

5.3.1. In this work the specific conductivity of several A.M.F. C_{60} membranes was measured, in each of these only the degree of solvation of the matrix was varied thus allowing the effects on conductivity/

conductivity of varying internal molality of exchanger and of changing tortuosity of the matrix to be investigated.

The first feature apparent from the measurements presented in Table (5.4) and Figure (5.2) is that whereas the specific conductivity of the NaCl solutions increases with molal concentration, the conductivity of the various membranes decreases with increasing molality of the membrane. Since the membrane molality increases as the water content decreases, as does the tortuosity, Table (5.1), a reduction in the mobility of the charge carriers in the increasingly tortuous membrane must be the significant factor affecting conductivity and not the internal molality of the exchanger membrane.

Oda [20] has made a comprehensive investigation of the conductivity of a variety of membranes in varying ionic forms. He reports that in membranes of relatively low water content, the specific conductivity falls, due to reduction in ionic mobility as the external electrolyte concentration increases and water content consequently decreases.

Gardner and Paterson [3] have illustrated the additional effect of increasing electrolyte uptake on specific conductivity. In both C_{60N} and C_{60E} the opposing effects of increasing tortuousity and increasing salt uptake decide the final conductivity variation. In C_{60E} the effect on tortuosity of increasing the external electrolyte concentration was small compared with the effect on the C_{60N}, but the salt uptake was more pronounced in the more open structured expanded membrane and thus contributed to a greater extent to the specific conductivity of the C_{60E}.

The/

The increasing resistance to mobility imposed by the tortuous matrix is evident from Tables (5.1) (5.4). As the membrane becomes more expanded and consequently less tortuous, the specific conductivity increases. Membrane PS_1 which contains only 41% water (w.r.t. dry weight) and has a tortuosity factor, θ_M, of 6.01 has a conductivity almost four times less than that of PS_{11} which contains 154% water and has a tortuousity, θ_M, of 2.19. This increase in conductivity is an effect of the increasing fractional pore volume and consequent decrease in tortuosity, which reduces the friction on the ions, thus allowing an increase in the ionic mobility. The largest contribution to the specific conductivity from salt uptake, mentioned previously, should occur in the most expanded membrane, PS_{11}. However, since the amount of imbibed salt makes less than a 1.0% contribution to the total ionic concentration, it is not surprising there is no evidence of salt uptake contributing to specific conductivity in PS_{11}.

5.3.2. The Salt Model Calculation described in chapter 3 demonstrates that specific conductivities of a membrane may be calculated directly from the conductivity of an equimolar sodium chloride solution by using a tortuousity correction.

Since the Salt Model Calculation was based on observations made on the C_{60N} and C_{60E} of Gardner and Paterson, specific conductivities for these membranes in 0.10 and 1.0M NaCl, calculated from equation (3.24) and those observed are given in Tables (5.5) (5.6) In both tables the specific conductivity estimated using the tortuosity corrections (S) and (M) are in particularly good agreement. The values obtained for the expanded membrane are/

are a little better than for the normal. The tortuosity correction (P) over-estimates the specific conductivity of both membranes in 0.10M NaCl and the expanded in 1.0M. However, in general the Salt Model Calculation gives a good estimation of specific conductivity of these two membranes.

The specific conductivities measured for the range of expanded C_{60} membranes, in this work, allowed further investigation into the ability of the Salt Model Calculation togive an estimate of this property. Table (5.4) shows specific conductivities calculated using (M) and (P). Good agreement was obtained between calculated and observed values for the whole membrane range. In each case the calculated values are larger than the observed and the values obtained using (M) are better than those calculated using (P), especially around the intermediate range of expansion (80-100% water). For both (M) and (P) the agreement becomes less satisfactory at PS_{11}, the most expanded C_{60}. However, the Salt Model Calculation gives at least a semi-quantitative estimate of the specific conductance for each membrane and its use for calculating specific conductivity data for the C_{60} membrane is justified.

In fig.(5.3) observed and calculated (S.M.C.) conductivities are shown as a function of V_w. The specific conductivities κ_m (based on θ_m) show the better agreement with the observed values although deviations become more significant as V_w increases. The S.M.C. equation (3.2 4.) indicates that as V_w tends to unity the specific conductivity of the membrane will tend to equal the specific conductivity of the corresponding solution. However, the graph of the observed specific conductivities diverges from the graphs of the calculated values since the former tends to a maximum value. This has also been found by various other workers in similar studies. A. Despic and G.T. Hills [21] found

that/

that the specific conductivities of a series of cross-linked polymethylacrylic acid membranes passed through a maxima at a certain water content. This trend is an effect of the different diffusion mechanisms which occur in an exchanger membrane. These are chain diffusion, in which the counter-ions diffuse parallel to the polymer chains, and volume diffusion, in which the ions jump from the atmosphere around one chain to its neighbour. The relative amount of each mechanism depends on the swelling and salt uptake of the membrane. The relative amount of diffusion taking place by each mechanism will decide the specific conductivity of the membrane.

Several workers have investigated the specific conductivity of the C_{60} membrane in the sulphuric acid form (5) (8) (22).

Fadley and Wallace used the theory of absolute reaction rates to predict the effects of water content on specific conductivity. Both their measured and calculated results and the results of Arnold and Kock were considerably larger than the conductivities measured in this work.

It is difficult to make comparison between specific conductivities measured in the hydrogen form with those measured in the sodium form. However, the larger specific conductivities of the hydrogen form would be predicted by the Salt Model Calculation.

The specific conductivities presented here are in good agreement with those measured by Gardner and Paterson for the C_{60} membrane in 0 .1OM NaCl (Tables 5.4) (5.5)).

5.4 Electro-Osmosis

The convection of the pore liquid in the interior of the membrane and subsequent transference of solvent through the membrane, is the resultant effect of the coupling between the polar water molecules with the charged counter and co-ion and their opposing movement in the applied electric field.

The electro-osmotic transport number, t_3, is independent of the tortuosity, θ, of the matrix. It is, however, affected by the ionic concentration and water content of the membrane.

The relationship $t_3 = \beta \frac{\bar{c}_3}{\bar{c}_1}$ stated in section (3.0) was obtained by Spiegler for a series of exchanger membranes, amongst which were various polystyrene sulphonic acid types, for which $\beta = 0.54$. This implies that the ratio of ions to water in the migrating liquid is approximately half the ratio of ions to water in the membrane.

This relationship was further illustrated by Stewart and Graydon [23] for a large series of polystyrene sulphonic acid membranes with varying degrees of cross-linking and fixed charge capacity who gave $\beta = 0.50$.

The value of $\beta = 0.576$ given in section (3.0) for the C_{60N} and C_{60E} of Gardner and Paterson was determined from t_3 values obtained in sodium chloride solutions of varying ionic concentration (0.1M - 2.0M).

In section (3.0), β was shown to be equal to v_3^4/v_1^4, that is β is the ratio of the velocities of water and counter-ion relative to the membrane.

This is established thus:

By definition:

$$t_3 = {}^{J_3^4}/_{I} = {}^{J_3^4}/_{(Z_1J_1^4 + Z_2J_2^4)F}$$

$$= {}^{J_3^4}/_{(Z_1J_1^4 + Z_2J_2^4)}$$

if J_2 is small compared to J_1 (as it is in the cation exchangers studied in this work) then

$$t_3 = {}^{J_3^4}/_{Z_1J_1^4}$$

$$t_3 = {}^{\bar{C}_3V_3^4}/_{Z_1\bar{C}_1V_1^4}$$

$$t_3 = \frac{V_3^4}{V_1^4}\,\frac{\bar{C}_3}{\bar{C}_1Z_1}$$

5.4.1. In this work the plot of t_3 against $\frac{\bar{C}_3}{\bar{C}_1}$ also defined a straight line, figure (5.4), giving a velocity ratio for the C_{60} series of 0.60. This is similar to that found by Gardner and Paterson even though the membranes were taken from two different batches. This illustrates the consistent quality of the A.M.F. C_{60} co-polymer, without which comparison of results from different membranes (with apparently similar properties) would be impossible. From the plot t_3 against $\frac{\bar{C}_3}{\bar{C}_1}$, β for the XR-170 membranes is 0.73. Thus the velocity ratio of water to counter-ion V_3^4/V_1^4 is considerably higher in the XR membranes. In the XR membrane the per-fluoro carbon chain may tend to inductively withdraw electron-density from the sulphonate fixed charge, consequently reducing the charge density at its surface and fractionally reducing the membrane to water frictional interaction. This will allow easier convectional flow and a subsequently higher t_3.

Since the plot of t_3 against $\frac{\bar{C}_3}{\bar{C}_1}$ for the C_{60} membrane

is linear, the increasing expansion of the membrane and consequent decrease in tortuosity must have an identical effect on the velocity of both water and counter-ion. The effect of expanding the the membranes was to increase t_3. The experimental t_3 values vary from 10.32 - 31.29 over the range of C_{60} membranes in 0.10M Nacl Table (5.7), whereas the t_3 values obtained for the XR membranes increase from 7.7 - 11.8 Table (5.3).

Changing the external solution to 0.05 $CaCl_2$ reduced the electro-osmotic transport number of each of the three membranes. However, this decrease was not consistent for each. Both the membrane in the intermediate range of expansion, PS_5, and the very expanded, PS_{11}, exhibited a decrease in t_3 of some 40%. The normal membrane, however, exhibited a t_3 in the calcium form quite similar to that measured in the sodium form of the membrane.

Tables (5.1) and (5.7) illustrate that the electro-osmotic transport number decreases with molality and Figure (5.5) shows that the plot of t_3 against internal molality of the membrane defines a smooth curve. This relationship allows comparison to be made between different membrane systems. The XR membranes which have smaller t_3 values than the C_{60} membranes have higher internal molalities and fall on the lower part of this curve. Above a molality of 25 the measured t_3 of the C_{60} membranes change almost proportionally with molality, for example, PS_2 has a molality of approximately 3.0M and a t_3 of 11 whereas PS_6 has a molality of approximately 1.5 and a t_3 of 20.6. The XR membranes show an apparentlylinear relationship with molality. Whereas at high internal molalities this (almost) proportional relationship means that a small change in internal molality will have a correspondingly small change in t_3 it is worth noting that as the membrane becomes

more/

more dilute (below 1.5 molal) any small change in internal molality will cause a considerable increase in t_3.

5.4.2.1. Salt Model Calculation Applied to Electro Osmotic Transport Numbers

Electro-osmotic transport numbers were calculated by the Salt Model for the C_{60N} and C_{60E} of Gardner and Paterson, Tables (5.5) (5.6). These are some 10 - 15% larger than the observed, the best agreement was obtained for the C_{60E} in 0.1M NaCl. This agreement is good considering the only data required for the calculation are the water content and fixed charge capacity of the membrane plus t_2^3, the transport number of co-ion in the binary model. The S.M.C. estimation of t_3, therefore, does not take into account the co-ion movement in the membrane which will tend to reduce the electro-osmotic flow. The t_3 values from the S.M. C. and those observed for the range of C_{60} membranes are shown in Table (5.7).

The overall agreement is very good. The calculated values are some 2 - 21% higher than those observed. The best agreement occurs for the normal membranes and the difference between observed and calculated is greatest for the very expanded membranes. For the XR-membranes in the sodium form the calculated t_3 values were 17 - 22% lower than the observed values. This is further demonstrated in fig. (5.4) where Salt Model t_3 values, from aqueous sodium chloride data, are plotted against C_3/C_1. The gradient of this line corresponds to the transport number of co-ion chloride in the binary salt. The close agreement of this line with that defined by the experimental t_3 values for the C_{60} membrane justifies the basic assumption of the S.M.C., that the C_{60} membrane can be modelled/

modelled by an equimolar sodium chloride solution. The values obtained for the XR-170 membranes lie above the sodium chloride line and are in fact nearer to the limiting maximum for t_3 which would occur when $t_3 = \bar{C}_3/\bar{C}_1$ and both ion and water have identical velocities relative to the membrane. In this condition the electrical field would cause the whole pore solution to be transported in electro-osmosis. Again the XR-170 values are consistent with the postulate that the fixed sulphonate in this membrane is of a more order destroying nature than the fixed charge of the C_{60} membranes.

From the basic assumptions of the S.M.C. in the membrane case equation(3.28) can be written $t_3 = \frac{C_3}{C_1} t_4^3$, $(t_4^3 = t_2^3)$, t_4^3 is the transport number of sulphonate relative to water in the membrane. Since the graph of the XR-170 membrane has a gradient $\beta = 0.73$ the sulphonate is acting as a much more mobile anion than chloride. Therefore, a more accurate salt model analogy for this membrane would have to be based on 'ca' sodium hydroxide rather than sodium chloride.

5.4.2.2. Electro-Osmotic coefficients, t_3, for Various Ionic Forms

Since t_3 data on the C_{60} expanded membrane in a variety of ionic forms were available (24) to test the predictions of the S.M.C., calculated values of $t_3 = \bar{C}_3/\bar{C}_1\ t_2^3$ for the corresponding aqueous chloride salts were plotted against $\bar{C}_3/\bar{C}_1$ fig. (5.6). The slopes of these lines correspond to the transport numbers of co-ion chloride in each salt solution. Experimental values of t_3 are shown on the same figure

The S.M.C. gives agreement which is excellent for the hydrogen form/

form and some 10-15% high for the lithium, sodium and potassium forms. For the caesium and rubidium forms the S.M.C. gives results which are much lower than observed. The observed values are much closer to $t_3 = {}^{C_3}/_{C_1}$ hence suggesting that in electro-osmosis these ions tend to move the whole pore solution.

As a further test of the S.M.C. and as a comparison with the C_{60} results the membrane XR-C (the most solvated membrane of this series) was converted into the hydrogen, lithium, sodium, potassium and caesium forms Table (5.8), and t_3 values measured. These were compared with the S.M.C. values as before, fig. (5.6). Again the best agreement was obtained for the hydrogen form. The observed value lies very close to the line defined by the S.M.C.

Of the other ionic forms, the S.M.C. t_3 values are some 25-31% low for lithium, sodium and potassium, and similar to the C_{60} membrane the caesium form of the XR membrane gives an experimental t_3 value much higher than that predicted by the S.M.C. The experimental value again approaches the limiting line $t_3 = {}^{C_3}/_{C_1}$.

Although the S.M.C. is less successful in providing t_3 values for the various ionic forms of both the C_{60} and XR-membranes, the results are in good qualitative agreement and provide a good estimate of the observed value, especially considering the simplicity of the calculation. The calculated values for the XR-membrane which are 25-31% lower than the observed (whereas the calculated for the C_{60} are 10-15% higher than the observed) illustrates further that the perfluoro sulphonic acid membrane is not as successfully modelled by an equimalor sodium chloride solution as is the styrene sulphonic acid, type C_{60} membrane.

Earlier in this section the variation of t_3 with internal molality of the membrane was discussed and fig. (5.5) shows the smooth curve defined by the plot of t_3 against molality.

This plot further demonstrates the success of the S.M.C. to predict t_3. The solid line through the experimental t_3 values in this figure is the plot of $t_3 = t_2^3 \ C_3/C_1$. Thus the S.M.C., via the t_3 - molality relationship, allows comparison between, for instance, the t_3 values of the C_{60} membranes in 0.10M and those obtained in 2.0M and of the t_3 values of different membrane types which exhibit different water content and fixed charge capacity. To further illustrate the ability of the S.M.C. to predict t_3, a very dilute membrane with a large experimental t_3 was chosen.

Data for the Zeo Karb 315 membrane in the sodium form was readily accessible [25]. Using $t_3 = t_2^3 \ \bar{C}_3/\bar{C}_1$ the S.M.C. gives a t_3 value of 54.4 compared with an observed t_3 of 45.7. Thus the S.M.C. over estimates the t_3 by some 20%. This agreement is similar to that obtained for the most expanded C_{60} membranes.

Fig. (5.5) illustrates the success in predicting the electro-osmotic transport number attained by the S.M.C. for three different membrane types, A.M.F. C_{60} (in both normal and expanded form in any external solution in the concentration range 0.1 - 2.0M), XR-170 and Zeo Karb 315, over almost an order of magnitude range from 5 to 50 and to a large extent justifies the idea of a 'salt model'.

5.4.3. A number of workers have found that the electro-osmotic transport of water in ion exchanger membranes is dependent on the current density used in the measurements [26] [27] [28] [29] [30]. Amongst these Lakshminarayanaiah [27] reports that at 0.1M and below the water transference number increases with decreasing current density. Gardner and Paterson [2][3] and others [28][31][32][33] have found no evidence of this. The effect of current density was investigated over the whole range of

C_{60} membranes in both sodium and calcium form and for the XR-170 membranes in the various ionic forms, no evidence of a dependence on current density was observed.

TABLE (5.1)

MEASURED PHYSICAL PARAMETERS OF C_{60} MEMBRANES IN 0.10M NACL

Membrane	Dry Weight gm	Wet Weight gm	Weight Water gm	Water Content %	Diameter cm.	Thickness cm.	Wet Volume cm^3	Fractional Pore Volume V_w	θ_M	θ_p	Internal Molality	C_1	C_2	C_3
												$m.mol.cm^{-3}$		
PS_2=N2	0.2296	0.3446	0.1150	50.09	3.7530	.0300	0.332	0.3466	4.77	3.82	2.99	1.04	0.0023	19.24
PS_4=E2	0.1816	0.3240	0.1424	78.41	3.4454	.0333	.0311	0.3586	3.36	2.78	2.12	0.97	0.0040	25.48
PS_1	0.1936	0.2724	0.0788	40.70	3.5677	0.0277	0.276	0.2855	6.01	4.79	3.32	0.94	0.0022	15.86
PS_3	0.2050	0.3022	0.0972	47.42	3.6261	0.0294	0.304	0.320	5.26	4.189	3.20	1.014	0.0024	17.76
PS_5	0.1675	0.3167	0.1492	89.07	3.5600	0.0322	0.321	0.465	3.30	2.66	2.04	0.93	0.0042	25.82
PS_6	0.1642	0.3222	0.1580	96.22	3.5640	0.0325	0.324	0.488	3.10	2.51	1.98	0.97	0.0044	27.09
PS_7	0.1754	0.3204	0.1450	82.86	3.5404	0.0318	0.313	0.463	3.32	2.68	1.94	0.95	0.0042	25.74
PS_8	0.1735	0.3181	0.1446	83.34	3.5483	0.0320	0.317	0.456	3.39	2.71	1.77	0.80	0.0042	25.34
PS_9	0.1682	0.3100	0.1418	84.30	3.5585	0.0298	0.296	0.479	3.18	2.57	1.81	0.87	0.0042	26.60
PS_{10}	0.1707	0.3765	0.2058	120.50	3.6824	0.0345	0.367	0.561	2.57	2.11	1.47	0.84	0.0052	31.15
PS_{11}	0.1642	0.4169	2.2527	153.9	3.8265	0.0350	0.403	0.627	2.19	1.83	1.24	0.78	0.0058	34.84

$$\theta_M = {}^2/_{V_w} - 1 \qquad \theta_p = {}^2/_{V_w} - \frac{1/2(\ln V_w)^2}{1 - V_w + V_w \ln V_w}$$

Water content = Weight per cent. water w.r.t. dry weight.

TABLE 5.2

MEASURED CHARACTERISTICS OF THE NORMAL AND EXPANDED MEMBRANE IN 0.050M $CACL_2$ AT 25°C.

Membrane	Dry Weight of Polymer gm	Weight gm	Weight of Water gm	% water w.r.t Dry Weight Polymer	C_1 m.mol.cm^{-3}	C_3 m.mol.cm^{-3}	Internal Molality	Diameter cm.	Thickness cm.	Wet Volume cm^3	t_3
PS_1	0.1877	0.2571	0.0646	34.42	0.633 * 0.474	14.34	1.838	3.4101	0.0274	0.2503	9.05
PS_5	0.1606	0.2809	0.1151	71.67	0.814 * 0.488	23.88	1.136	3.3110	0.0311	0.2678	11.93
PS_{11}	0.1570	0.3625	0.2011	127.45	0.858 * 0.370	30.57	0.673	3.6903	0.340	0.3637	17.91

PS_1, PS_5 are a normal and expanded C_{60} membrane respectively, PS_{11} is a super-expanded C_{60}

* Capacity per unit weight of dry matrix.

TABLE 5.3

MEASURED CHARACTERISTICS OF XR-170 MEMBRANES IN 0.100M NACL AT 25°C

Membrane	Dry Weight gm	Wet Weight gm	Weight of Water gm	Percentage Water W.R.T. Dry Weight Polymer	Diameter cm	Thickness cm	Wet Volume cm^3	Internal Molality	C_1 m.mol	C_3 cm^{-3}	t_3 Observed	t_3 Predicted S.M.G.	Difference Between Observed and Predicted
XR-A	0.2294	0.2589	0.0295	12.8%	4.028	0.0118	0.1504.	5.29	1.04 0.68*	10.90	7.7	6.37	17%
XR-B	0.2581	0.3050	0.0469	18.17%	4.396	0.0116	0.1761	4.30	1.15 0.78*	15.65	9.5	7.65	19%
XR-C	0.2592	0.3261	0.0669	25.81%	4.442	0.0130	0.2015	3.42	1.14 0.88*	18.44	11.8	9.43	21%

* Are the fixed charge capacities per dry weight of Membrane as $m.mol.gm^{-1}$

TABLE 5.4

PREDICTED AND OBSERVED SPECIFIC CONDUCTIVITY OF RANGE OF C_{60} MEMBRANES

$10^2 \times$ ohm $^{-1}$ cm^{-1}

Membrane	PS_1	PS_2	PS_4	PS_5	PS_7	PS_9	PS_{12}
Observed	0.68	1.23	2.05	2.00	2.29	2.33	2.67
S.M.C. Predicted θ_m	1.00	1.46	2.14	2.19	2.21	2.21	3.13
S.M.C. Predicted θ_p	1.26	1.59	2.59	2.66	2.56	2.73	3.73

TABLE 5.5

S.M.C. Predictions for Membranes in 0.1M Sodium Chloride

Membrane		Specific Conductivity $k \times 10^2$ $ohm^{-1}\ cm^{-1}$	t_1	t_3
C60N				
	obs.	1.37	0.998	10.75
S.M.C.	(s)	1.55		
	(m)	1.39	1.00	12.47
	(p)	1.76		
C60E				
	obs.	1.92	0.995	15.77
S.M.C.	(s)	2.06		
	(m)	2.06	1.00	16.68
	(p)	2.57		

TABLE 5.6

Observed and Predicted Transport Measurements for C_{60E} (1.0)

		Specific conductivity $K \times 10^2$ ohm^{-1} cm^{-1}	t_1	t_3
Observed		1.90	0.92	9.70
S.M.C.	(s)	1.96		
	(m)	2.03	1.00	11.16
	(p)	2.71		

Salt Model Calculation.

TABLE 5.7

MEASURED AND PREDICTED ELECTRO OSMOTIC TRANSPORT NUMBERS OF C_{60} MEMBRANES IN 0.10M NaCl

Membrane	PS_1	PS_2	PS_3	PS_4	PS_5	PS_6	PS_7	PS_8	PS_9	PS_{10}	PS_{11}
Observed	10.32	11.00	10.92	16.00	16.61	17.51	16.88	16.61	17.54	20.57	31.29
PREDICTED S.M.C.	10.87	11.89	11.27	16.78	17.17	17.82	18.24	20.16	19.50	24.08	28.26
% Difference between Observed and Calculated	5%	8%	4%	5%	3%	2%	8%	21%	11%	17%	10%

TABLE (5.8)

ELECTRO OSMOTIC TRANSPORT NUMBERS, t_3. OF MEMBRANE XR-C IN VARIOUS IONIC FORMS

Form	Observed t_3	S.M.C. t_3	Percentage Difference
Hydrogen	3.45	3.25	6
Lithium	17.07	13.56	25
Sodium	11.84	9.43	26
Potassium	6.36	4.84	31
Cæsium	5.91	3.55	66

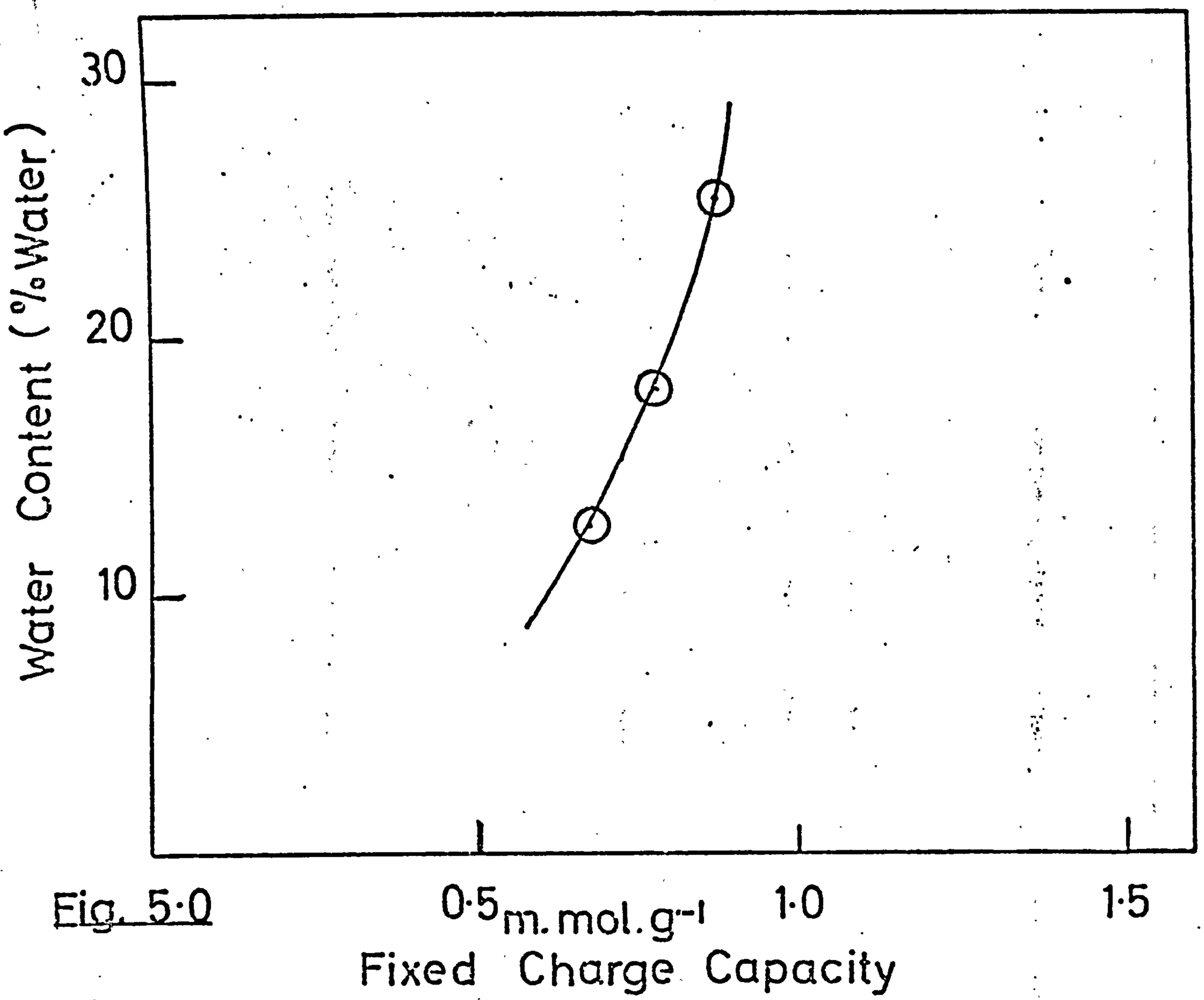
30
20
10
Water Content (% Water)
0·5
m. mol. g⁻¹
1·0
1·5
Fixed Charge Capacity

Fig. 5·0

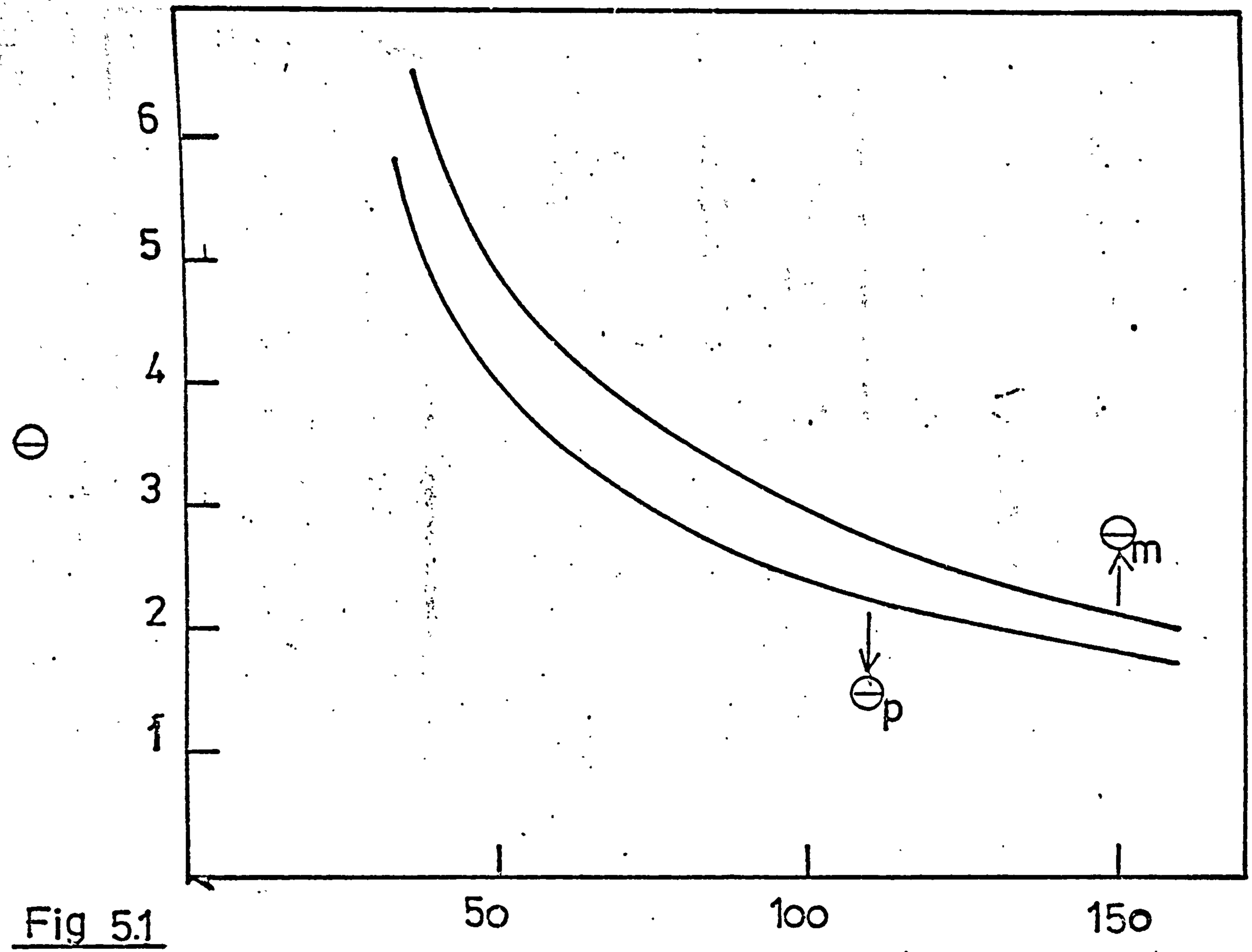

Fig 5.1

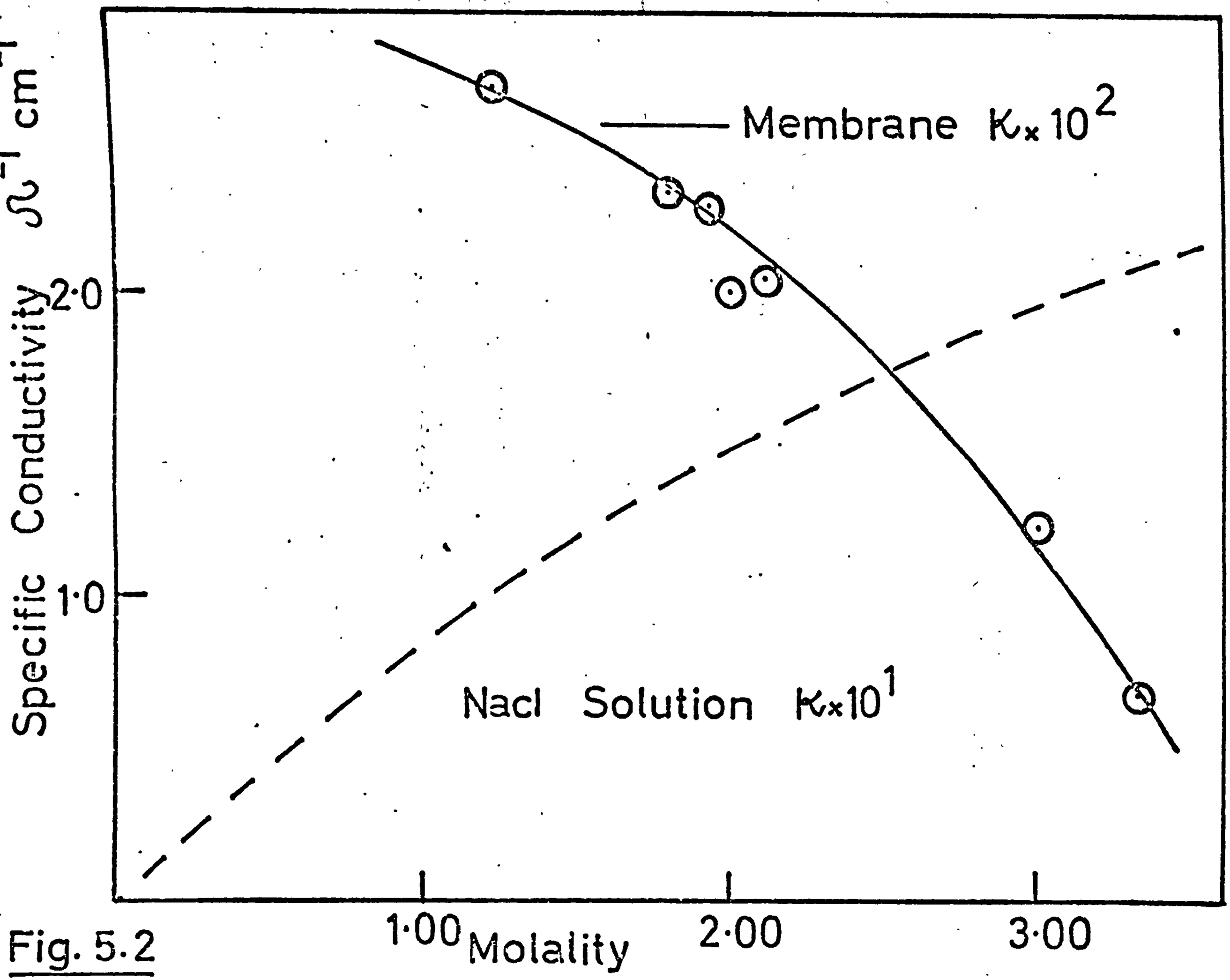
Specific Conductivity Ω^{-1} cm^{-1}
2·0
1·0
Membrane K x 10^2
Nacl Solution K x 10^1
1·00
Molality
2·00
3·00

Fig. 5.2

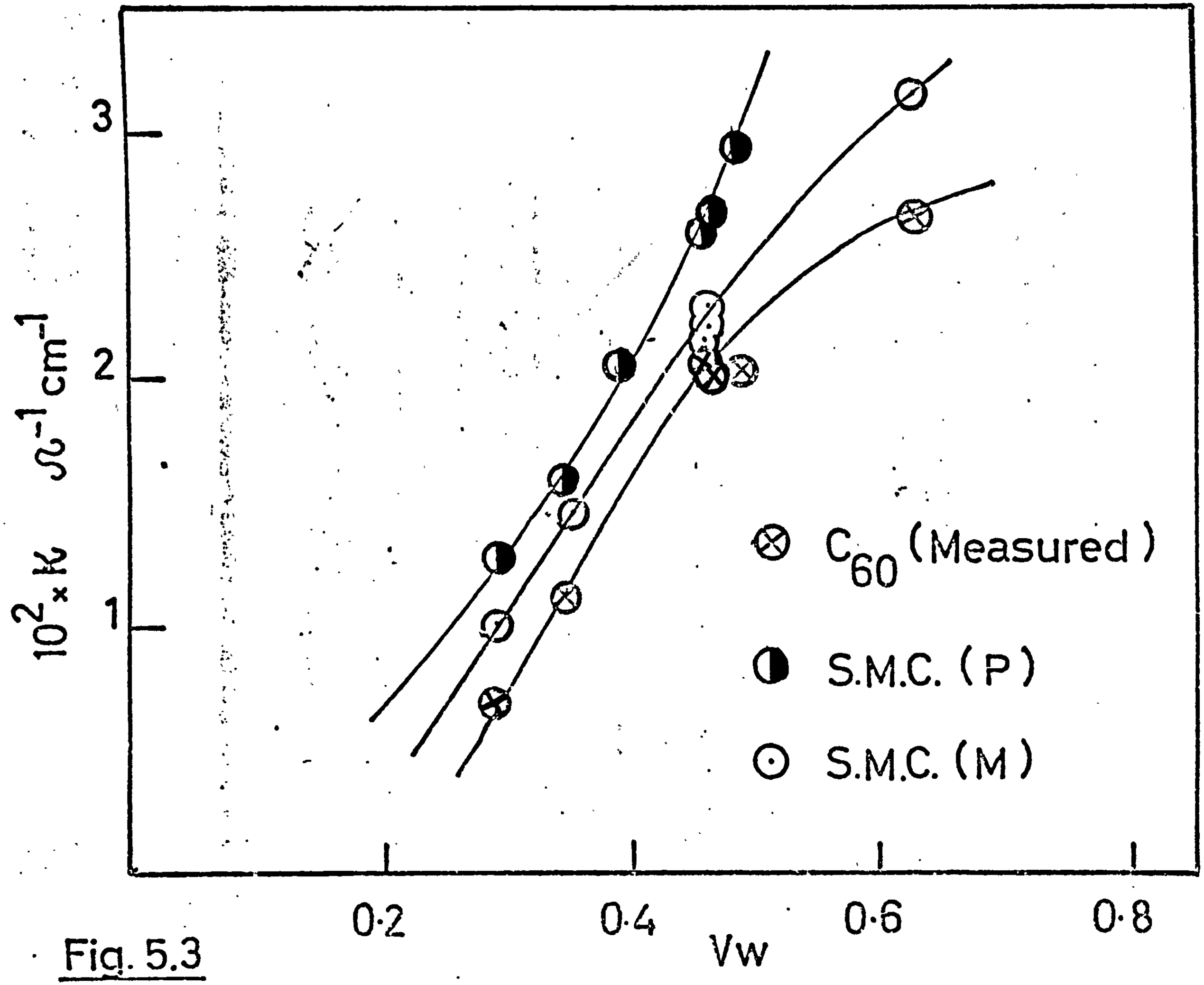
3
2
1
$10^2 \times K \quad \Omega^{-1} cm^{-1}$
0·2
0·4
0·6
0·8
Vw
C_{60} (Measured)
S.M.C. (P)
S.M.C. (M)

Fig. 5.3

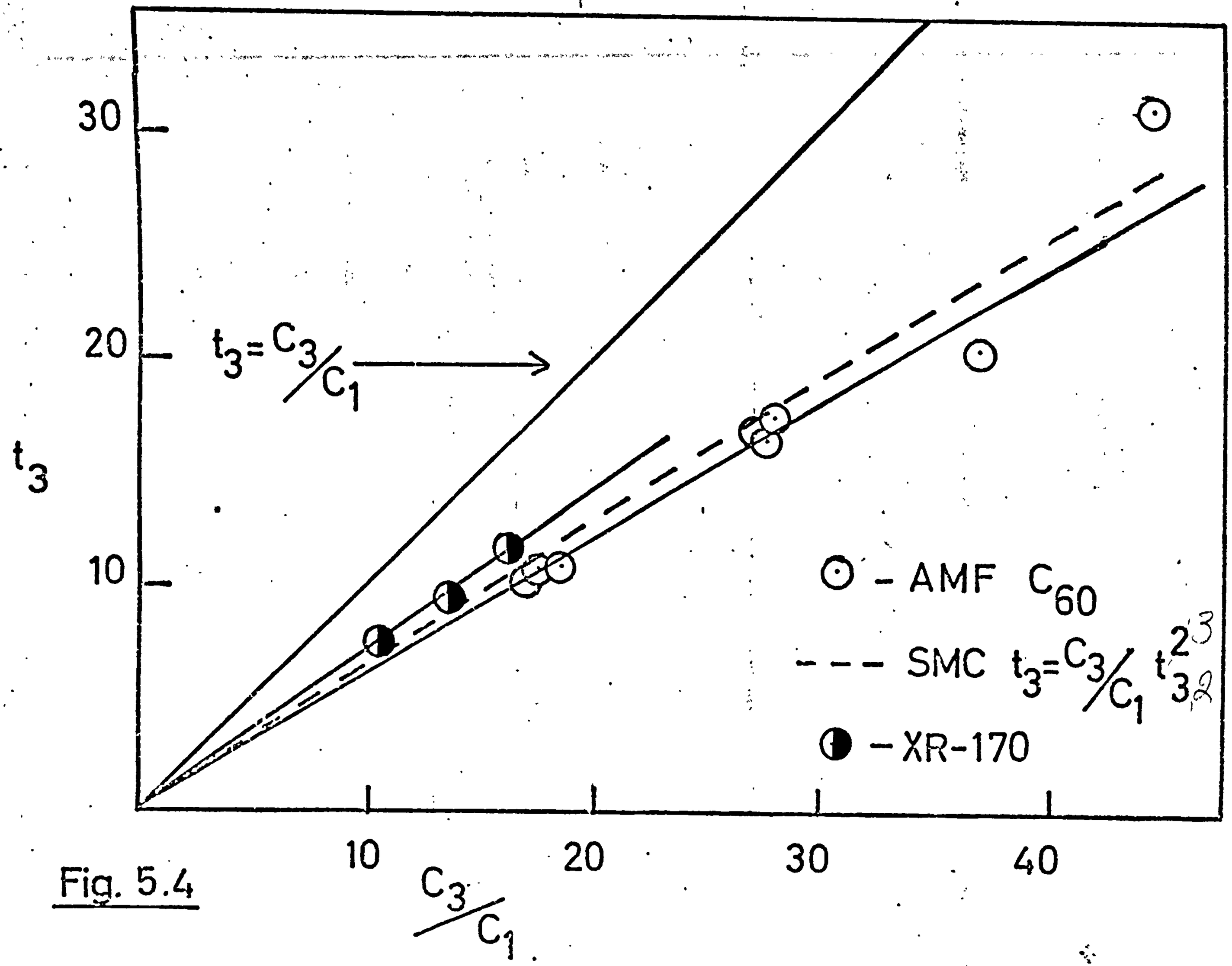
30
20
10
t_3
$t_3 = C_3/C_1$
10
20
30
40
C_3/C_1
⊙ - AMF C_{60}
--- SMC $t_3 = C_3/C_1\ t_3^{2/3}$
◑ - XR-170

Fig. 5.4

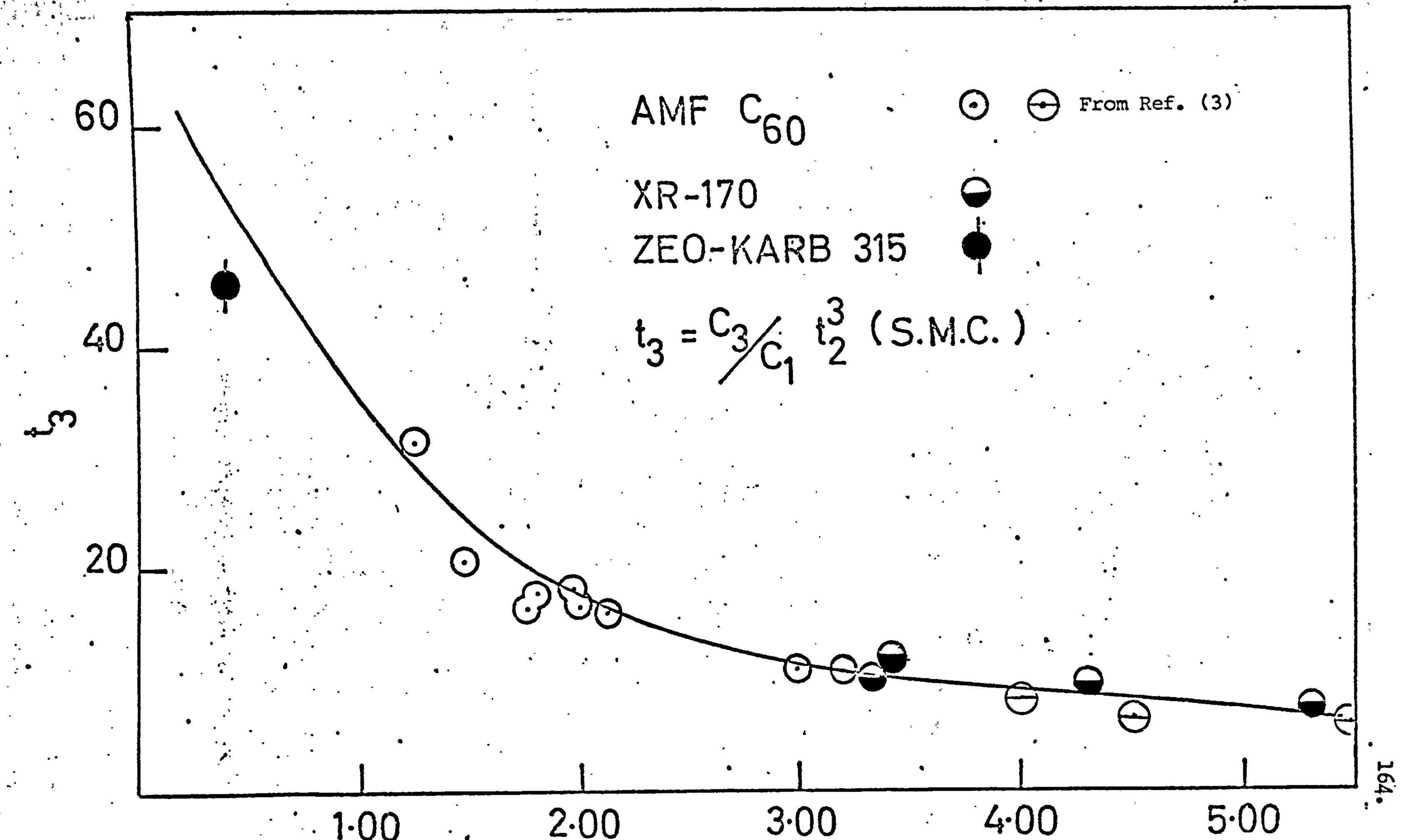
AMF C_{60}
From Ref. (3)
XR-170
ZEO-KARB 315
$t_3 = C_3/C_1\ t_2^3$ (S.M.C.)
60
40
20
t_3
1·00
2·00
3·00
4·00
5·00
Internal Molality

Fig. 5.5

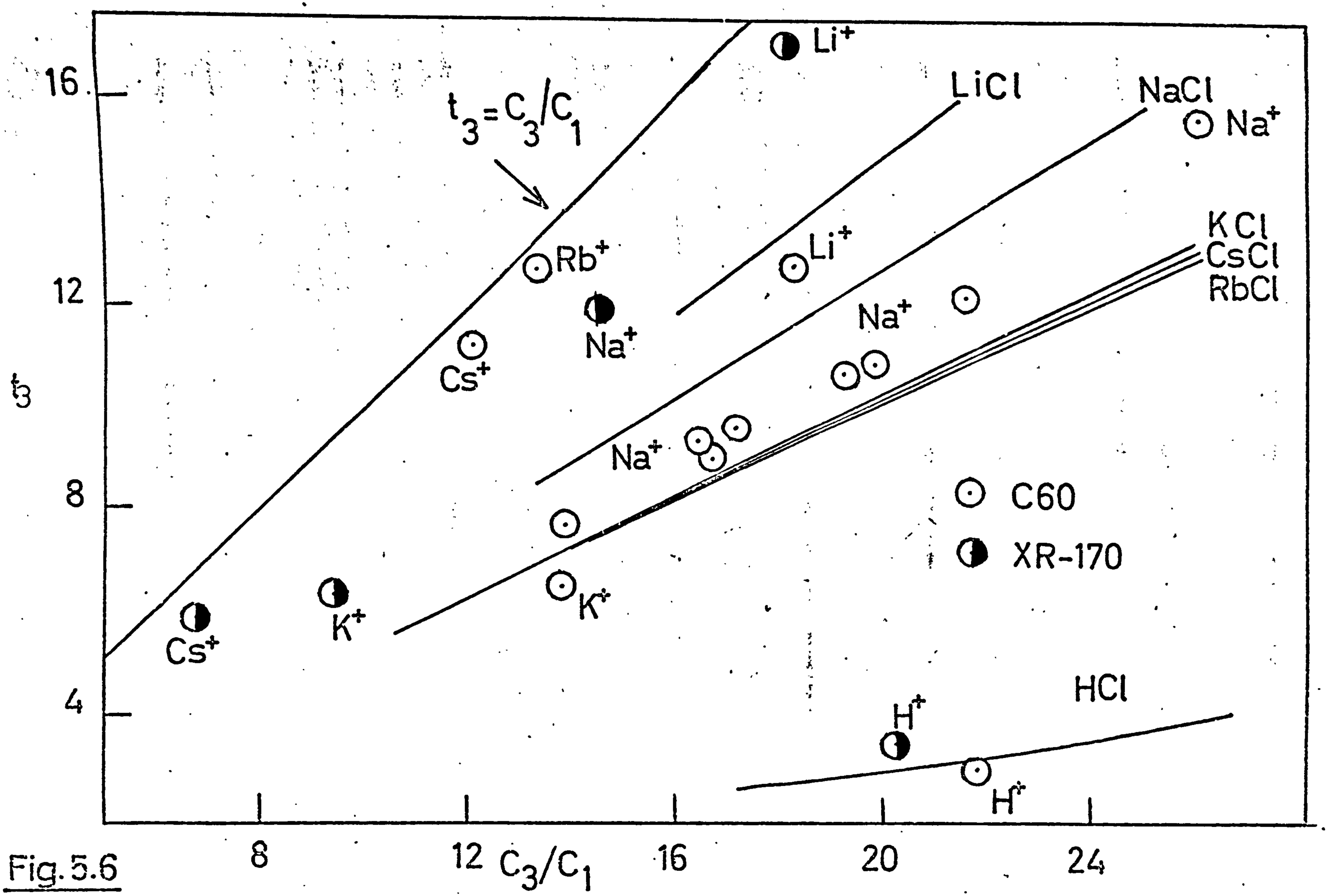
$t_3 = C_3/C_1$
Li+
LiCl
NaCl
Na+
Rb+
Li+
KCl
CsCl
RbCl
Cs+
Na+
Na+
Na+
C60
XR-170
K+
K+
Cs+
HCl
H+
H+
16
12
8
4
t_3
8
12
C_3/C_1
16
20
24

Fig.5.6

REFERENCES

CHAPTER 5.

1) F. Selengy. J. Polymer Science C.4 1455 1963.

2) R. Paterson and C.R. Gardner. J. Chem. Soc. A.2254 (1971)

3) H. Ferguson, C.R. Gardner, R. Paterson. J.C.S. Faraday I. 68,2021 (1972)

4) C.R. Gardner and R. Paterson. J.C.S. Faraday I. 68, 2030 (1922)

5) C. Forgacs. E. Scharf. Israel J. Chem. 34. 269,(1963).

6) R.A. Wallace and B.K. Jindal J. Electro-Chem. Soc.(1971)118,(5) 707

7) A.S. Michaels et al Discussions of the Electro Chem. Soc. 1969 116 (6) 874

8) R. Arnold and U.F.A. Koch. Aust. J. Chem. 19 1299 (1966)

9) A. Wheeler. Advances in Catalysis 3 249(1951).

10) J.S. Mackie and P. Meares. Proc. Roy. Soc. (London) A.232 498(1955)

11) J.M. Crabtree and E.Glueckauf. Trans. Faraday Soc. 59 2639 (1963)

12) A. Despic. G.J. Hills, Trans. Faraday. Soc. 53 1262 (1957)

13) A.O. Jakubovic, G.J. Hills and J.A. Kitchener, J. Chem. Phys. 55 263,(1958)

14) D. Mackie and P. Meares. Trans. Faraday Soc. 55 1221 (1959)

15) O. Kedem. A. Kleinzeller. A. Kotyk. "Membrane Transport and Metabolism" Acad. Press, New York(1960).

16) C. McCallum and R. Paterson. Submitted Trans. Faraday Soc. July,(1974).

17) A.G. Winger, G.W. Badermer R. Kunin. J. Electro Chem. Soc. (1953) 100,178

18) H.P. Gregor. Membrane Evaluation Progrom, New York, Brooklyn Polytechnic (1961)

19) D. Mackay and P. Meares. Trans Faraday Soc.(1959)55, 1221.

20) Y. Oda. Bull. Chem. Soc. Japan 29 673,(1956)

21) A. Despic. G.T. Hills. Trans. Faraday Soc. 51 1260,(1955).

22) C.S. Fadley and R.A. Wallace. J. Electro Chem. Soc. (1968) 115, 1264

23) R.J. Stewart and W.F. Graydon. J. Phys. Chem. 61, 1957, 164

24) I.S. Burke, R.G. Cameron and R. Paterson, N.A.T.O. Advanced Study Inst. Conf. Forges-Leo-Eaux, France. Sept.(1973),in press.

25) D. Mackay and P. Meares. Trans. Faraday Soc. 55 1221 (1959)

26) N. Lakshminarayanaiah and V. Subrahmanyan. J. Polymer Sci. A2. 4491,(1964)

27) N. Lakshminarayanaiah. Desalination, 3, 97 (1967)

28) A.S. Tombalkian, H.J. Borton and W.F. Graydon, J. Phys. Chem.66 1006(1962)

29) N. Lakshminarayanaiah and V. Subrahmanxan. J. Phys. Chem. 72,1253(1968)

30) ibid Current Sci. 29,307,(1960)

31) W.S. McHardy, P. Meares, A.H. Sutton and J.F. Thain, J. Colloid and Interface Science, 145 (1967)

32) C.W. Carr, R. McClintock and K. Sollner, J. ElectroChem. Soc.109,251,1962

33) C. McCallum. PhD, Thesis, University of Glasgow 1971.

CHAPTER 6.

RESULTS AND DISCUSSIONS

6.1 PREDICTION OF THE REVERSE OSMOSIS CHARACTERISTICS OF THE C_{60} MEMBRANE

6.3 THE REVERSE OSMOSIS CHARACTERISTICS OF A SERIES OF C_{60} MEMBRANES

Prediction of the Reverse Osmosis Characteristics For a C_{60} Normal and C_{60} Expanded Membrane, From Mobility Coefficient Data

6.1 In previous studies Gardner and Paterson obtained frictional and mobility coefficients for a Normal, C_{60N} and Expanded, C_{60E} form of the A.M.F. C_{60} Membrane. In this study, in the range of expanded forms of the C_{60} membranes, two membranes have been found to have almost identical physical and transport properties to the original C_{60N} and C_{60E}. Table (6.1) illustrates this similarity.

The original and current membranes have been given the identifiers N1, E1 and N2, E2 respectively. Both N1 and E1 have a slightly more swollen matrix than N2 and E2, however, the parameters are sufficiently similar to justify comparison of the transport properties of the two sets of membranes.

Pressure forces were not used in the original analysis of the transport properties of N1,E1 and it is the aim of this section to consider the methods which may be used to predict the pressure induced transport phenomena of N2 and E2 using the mobility coefficients for N1 and E1 obtained previously.

6.1.1. The Calculation to Predict, Salt Flux, Water Flux and Desalinated Product Concentration

In chapter 2, the full equations (2.41) (2.43) which describe the salt flux, J_s, and water flux, J_w, were established. Since in a defined system the mobility coefficients are constant equations (2.41) (2.43) reduce to

$$J_s = L_{ss}X_{12} + L_{sw}X_3 \qquad (2.47)$$

$$J_w = L_{ws}X_{12} + L_{ww}X_3 \qquad (2.48)$$

where
$$L_{ss} = \frac{-Z_1Z_2}{r_1r_2}\ \frac{(l_{11}l_{22} - l_{12}l_{21})}{\alpha} \qquad (6.1)$$

$$L_{sw} = L_{ws} = \frac{1}{r_1}\ (l_{13} - \frac{t_1t_3\alpha}{Z_1}) \qquad (6.2)$$

$$L_{ww} = (l_{33} - t^2{}_3\alpha) \qquad (6.3)$$

The mobility coefficients of equations (6.1) (6.3) may be obtained either from published data on Nl and El or from the Salt Model Calculation (Chapter 3). Therefore, with the mobility coefficients known only X_{12} and X_3 need be defined to allow J_s and J_w to be calculated from (2.47) (2.48).

In a reverse osmosis experiment the salt force X_{12} and water force, X_3, contain two separate contributions. If the membrane desalinates there will be a salt concentration difference across the membrane, and also each thermodynamic force will have contributions from the applied pressure. These forces are described by equations (2.45) (2.46)

$$X_{12} = RT \frac{-d\ln a_{12}}{dX} + \hat{V}_{12}\left(\frac{-dP}{dX}\right) \qquad (2.45)$$

$$X_3 = RT \frac{-d\ln a_3}{dX} + \hat{V}_3\left(\frac{-dP}{dX}\right) \qquad (2.46)$$

The partial molal volumes of salt and water $\hat{V}_{12}$, $\hat{V}_3$ respectively have units of m^3 $mole^{-1}$ and the units of pressure used are $N\ m^{-2}$. As dX is the distance in cm. across the membrane, then X_{12} and X_3 have the units of Joules $mol.^{-1}$ cm^{-1}.

In (2.45) the contribution from the pressure term is negligible. Appendix (1). However, in equation (2.46) the pressure term is dominant. The first term in equation (2.46) represents the osmotic pressure which works against the applied pressure. This can be calculated from the osmotic coefficient using the expression.

$$\Delta\pi\,\hat{V}_3 = \frac{\vartheta RT}{10^3} W_3 (\phi_f m_f - \phi_p m_p) \qquad (6.4)$$

where $\Delta\,\pi\,\hat{V}_3$ is the osmotic pressure difference across the membrane in Joules $mole^{-1}$

ϕ_f ϕ_p are the osmotic coefficients of the feed and product solution respectively (1)

m_f m_p are the molal concentration of feed and product solutions

∂ is the number of moles of each species obtained from 1 mole of electrolyte.

R is the gas constant in J K^{-1} Mol^{-1}

T is the absolute temperature in K

W_3 is the molecular weight of the water.

On applying pressure across the membrane the solvent water flows through the membrane taking with it an amount of salt by coupling. Therefore in the steady state the ratio of the salt flux and water flux will determine the concentration of the desalinated product solution, Cp.

Since the units of J_s and J_w are moles of salt cm^{-2} $sec.^{-1}$ and moles of water cm^{-2}. $sec.^{-1}$ respectively, the molar concentration of the desalinated product solution is given by

$$J_s/J_w \times C_w = C_p \qquad (6.5)$$

where $C_w = \frac{1000}{18.016} \frac{C}{m}$ (2) and converts the mole ratio to a molarity.

Therefore, since C_p must be known in order to evaluate X_{12} and X_3 before J_s and J_w can be calculated, and C_p is in fact defined by the ratio of J_s and J_w, no direct evaluation of the two fluxes is possible.

In order to calculate J_s and J_w the concentration gradient must be defined by designating some 'guessed' value to the product concentration, C_p^{Guess}. This allows X_{12} and X_3 to be calculated from equations (2.45) (2.46) and J_s and J_w to be evaluated from equations (2.47) and (2.48). By designating several guessed product concentrations a series of (guessed) values of J_s, J_w and

product/

product concentration can be calculated. When C_p^{guess} and $\frac{J_s}{J_w} X C_w$ are coincident, the true predicted product concentrations (for the defined pressure and feed solution) will be obtained. The most practical way of accomplishing this was to graph C_p^{guess} against $\frac{J_s}{J_w} X C_w$ and from the intercept of the line Y = X with this graph the true predicted value was obtained.

Figures (6.0.) (6.1) Tables (6.2) show a typical reverse osmosis calculation (at 400 lbs/in^2) for both normal and expanded membranes. This is a general calculation which is applicable to any membrane system for which the mobility coefficients are known. This calculation will provide an estimate of the reverse osmosis characteristics at (ideally) any applied pressure.

6.1.2. The Mobility Coefficients Used in the Predictive Reverse Osmosis Calculation For the 0.10M NaCl Feed Solution

In their calculation of membrane mobility coefficients Gardner and Paterson [3] were forced to apply several approximations since for six unknown mobility coefficients only five independent experiments were carried out. In this work mobility coefficients from two of these approximations were used. Since the co-ion concentration in the membrane is small (the ratios C_1/C_2 for N_1 and E1 were 408 and 185 respectively), the assumption (a) $l_{12} = 23 = 0$ was made. As co-ion is a minor component, the coupling coefficient l_{12} was assumed to be small compared to l_{11}, thus (b) $l_{12} = 0$ was assumed.

From assumption (a) by neglecting co-ion to counter-ion and co-ion to water interaction, the transport numbers of each membrane species became

$$t_1 = l_{11}\frac{F^2}{K} \qquad t_2 = l_{22}\frac{F^2}{K} \qquad t_3 = l_{31}\frac{F^2}{K}$$

respectively.

Thus equations (2.41) (2.43) can be described in terms of the transport numbers of counter ion, co-ion, water, and the specific conductivity.

$$J_s = \frac{t_2 K}{F^2}(t_1 X_{12} + t_3 X_3) \qquad (6.6)$$

$$J_w = \frac{t_3 K}{F^2}(t_2 X_{12} - t_3 X_3) + l_{33} X_3 \qquad (6.7)$$

Therefore from (6.1) (6.2) (6.3) L_{ss}, L_{sw}, L_{ww} became respectively

$$\frac{t_2 t_1 K}{F^2} \; ; \qquad \frac{t_2 t_3 K}{F^2} \; ; \qquad l_{33} = \frac{t_3^2 K}{F^2} \; ;$$

the significance of which will be discussed later.

The third set of mobility coefficients (designated method (c)) was obtained from the Salt Model Calculation. This supplies an alternative set of l_{ik} coefficients obtained directly from solution data and some basic measurements on the membrane.

The use of the coefficients from the S.M.C. in the predictive calculation provide an impression of the practical application of the S.M.C. and allow further insight into the accuracy of the salt model concept.

Also by using the l_{ik} coefficients from the approximations (a) and (b), an impression of the accuracy of each assumption can be obtained.

6.1.3. The Reverse Osmosis Characteristics of the Normal and Expanded C_{60} for 0.1OM Nacl

Salt Rejection

In this section the rejection characteristics of the membranes at a variety of applied pressures will be discussed.

Rejection is defined by equation (6.8)

$$\text{Rejection} = \frac{C_f - C_p}{C_f} \times 100 \qquad (6.8)$$

where C_f and C_p are the molar concentrations of the feed and product solutions respectively.

(Rejection is normally used as a percentage).

The ability of N2 and E2 membranes to desalinate sodium chloride solutions was studied under a variety of conditions. Pressure differences of 200 and 400 lbs.in^2 were applied using Reverse Osmosis System I, section (4.2) and pressures of 1000 and 1500 lbs.in^2 applied using the Harwell System, section (4.3.4). To investigate the effects of concentration of the feed solution, on desalination properties, solutions of1.0M NaCl were also studied.

For 0.10M NaCl the observed and predicted results for N2 and E2 are presented in Table (6.3). For both N2 and E2 rejection increased (product concentration decreased) as the applied pressure was raised. It is obvious from Table (6.3) that the first achievement of the reverse osmosis calculations is that each method (a - c) predicts this trend in behaviour. Over the whole pressure range the less swollen, N2, which contained 52% water, desalinated slightly better than the more swollen E2, (78% water). Method (a) predicted this observed trend at each pressure, whereas method (b) predicted equal rejection for both membranes. Method (c) predicts better rejection for E2 at 200 and 400 lbs.in^2 and equal rejection at 1000 and 1500 lbs.in^{-2}.

This similar rejection ability of the Normal and Expanded Membranes which was both observed and predicted is not a result which might be reached intuitively, particularly considering that membrane E2 contains more water and is consequently more open structured. It also contains considerably more salt.

The magnitude of the applied pressure has a significant effect on the desalination achieved. For the N2 membrane the salt rejection is 46% at 200 lbs.in^{-2}, but 82% at 1500 lbs.in^{-2}. For the expanded the corresponding rejection figures are 40% rising to 78%. Therefore, with an increase of some seven times in the magnitude of the applied pressure force, the rejection approximately doubles.

Figures (6.2) (6.3) illustrate the success the calculation achieves in predicting the product concentration. The predicted results from each method define a graph which is not only close to the graph defined by the experimental results for both N2 and E2, but each graph is identical in form to that traced by the experimental results. This is a considerable achievement and is a justification of the assumptions(a),(b) made previously to obtain the mobility coefficients and also illustratesthat the Model coefficients accurately describe the intra-membrane interactions. In both figs (6.2) (6.3) the graph defined by method (b) lies closest to the experimental graph and the graphs defined by both (a) and (c) lie below the experimental graph. Although the Salt Model coefficients are least successful in predicting C_p, considering the simplicity of the basic assumption and that the method does not require any transport measurements on a real membrane, the estimate they provide is most satisfactory especially since they clearly show the observed variation of C_p with pressure.

Over the range of pressure the Model coefficients over-estimate C_p by between 0.018 and 0.02M for N2 and by 0.011 and 0 .014M for E2. The best agreement, provided by method (b), predicts for N2 product concentrations almost identical with those observed at each pressure below 1500 lbs. in^{-2}. At this pressure the predicted differs from

the /

the observed C_p of 0.018M, by +0.004M. This is the maximum deviation observed and may well be contributed to by some compaction of the membrane by the very high pressure.

Method (b) also makes the best estimate of C_p for Membrane E2 the graphs of predicted and observed agree almost exactly above 200 lbs in^2. At this pressure the predicted C_p is 0 .004M larger then the observed value of 0.06M, i.e. 6.6%.

For both membranes method (a) provides predicted product concentrations in close agreement with the experimental results although it is not so successful as method (b).

Method (a) gives better agreement for N2 than E2. It over-estimates N2 by some 0.006 - 0.008M and E2 by 0.008 - 0.01M over the range of applied pressures.

It is not surprising that method (a) which is the most simple method, (as it ignores all co-ion in the membrane) is less successful for E2 since E2 contains twice as much salt as N2.

6.1.4. Water Flux, J_w, for Normal and Expanded C_{60} Membranes for 0.10M Nacl.

Table (6.3) and figures (6.4) (6.5) show the effect of increasing pressure on the water flux for the experimental membranes. The water flux increases linearly with pressure until 500 lbs$\cdot in^{-2}$ in the normal and 1000 lbs. in^{-2} in the expanded. Above these pressures deviations from linearity were observed. At 500 lbs, in^{-2} in membrane N2 the water flux was 0.52×10^{-3} ml.cm^{-2} min^{-1} whereas for E2, J_w was 3.7 times larger beihg 1.94×10^{-3} ml.cm^{-2} min^{-1}. This is a consequence of the, "more open", less tortuous, matrix of the expanded membrane. The water flux of N2 reaches a maximum value at 600 lbs.sq.in. after which it levels out to an approximately constant value of 0.60 ml. $cm.^{-2}$ $min.^{-1}$.

Membrane/

Membrane E2 follows a similar trend. J_w begins to level off at 1500 lbs.in^{-2}. At this pressure the maximum J_w value observed of 4.85×10^{-3} ml. cm^{-2}. min^{-1} was reached.

The levelling out of the water flux for both N2 and E2 may be attributed to compaction of the polymer matrix by the high applied pressures. The more rapid and more severe effect in N2 can be explained by considering the polymer structure of the C_{60} membrane.

The mechanical strength of the membrane is derived mainly from the inert impermeable regions of polyethylene which are interconnected with the permeable regions of polystyrene. As a consequence these polyethylene regions support the applied pressure. The membrane can, therefore, be thought of as a series of connected islands of polyethylene and polystyrene.

Under pressure the only means of compaction for the membrane is by collapsing into its own volume and filling the interstitial void between the polymer chains. The compacted membrane will consequently be more dense.

On the application of high pressure the polyethylene 'islands' may distend in such a way as to reduce and restrict the diffusional pathways. This will make the membrane somewhat more tortuous and less permeable. Since the matrix of the expanded membrane is initially more swollen and thus more open, it would seem reasonable that any deformation of the co-polymer would more seriously effect the normal membrane. This conclusion is further confirmed by considering the tortuousity and water flow data for the membranes. Whereas from the normal to expanded the tortuousity factor decreases by only 11%, the water flux increases by some 400%. Therefore, if/

if the tortuousity of both membranes is even slightly increased by compaction, a decrease in J_w might be expected. This increase in tortuousity of the membrane will equally affect each of the individual fluxes and therefore the product concentration will remain unaffected since it depends on the ratio of the salt and water flux. This is as observed.

Since the graphs defined by the predicted values especially method (a) in figs. (6.4) (6.5) show close agreement with the graph from the observed results at low pressures, it may be assumed that the prediction calculations extended to higher pressures represent the performance of an ideal membrane which undergoes no compaction. These plots illustrate that for the ideal membrane water flux is directly proportional to the applied pressure. This is true for the 0.1MNaCl feed solution since the cross term contribution to J_w, $L_{ws}X_{12}$ is very small, (less than 1% of J_w). The osmotic pressure across the membrane is for the 0.10M feed, small. Since there is little change in the osmotic pressure over the range of pressures, this does not affect the change in J_w with applied pressure.

For both N2 and E2 the method (b), which gave the best estimate of C_p, gives the least satisfactory prediction of J_w. In every case J_w is over-estimated. Methods (a) and (c) which tend to predict low values for Cp give good estimates of J_w for both N2 (500 lbs.in^{-2}) and E2 (to 1000 lbs.in^{-2}). For N2 the model coefficients (c) provide a predicted J_w at 200 lbs.in^{-2} which differs from the observed value of 0.20×10^{-3} ml.cm^{-2} min^{-1} by only $0.00\ 5 \times 10^{-3}$ ml.cm.$^{-2}$ min.$^{-1}$. At 400 lbs.in^{-2} the difference, from the observed value of 0.51×10^{-3}, is 0.09 ml.cm^{-2} min^{-1}. The J_w values predicted by method (a) differ by 0.03×10^{-3} and 0.04×10^{-3} ml.cm^{-2} min.$^{-1}$ respectively at these pressures. For the expanded membrane methods (a) (c) slightly underestimate J_w, but the agreement is

good over the whole pressure range and is a major success of both the prediction calculation and also of the Salt Model concept. The estimate from these methods are 0.08 and 0.19 x 10^{-3} ml.cm^{-2}min.$^{-1}$ less than the observed value of 0.76 x 10^{-3} ml.cm^{-2}min.$^{-1}$ at 200 lbs.in^{-2}, and at 1500 lbs.in^{-2} the respective deviations from the observed value of 4.85 x 10^{-3} ml.cm^{-2}min.$^{-1}$ are 0.49 x 10^{-3} and 0.24 x 10^{-3} ml.$cm.^{-2}$min.$^{-1}$.

6.1.5. The Salt Flux, J_s, through N2 and E2 for 0.1N NaCl

The variation of salt flux with applied pressure is shown in figs. (6.6) (6.7). The graph of the observed results for both N2 and E2 are similar to the graphs defined by the experimental J_w values.

Method (a) gives predicted J_s values in good agreement with the experimental values (which were estimated from equation (6.6)). Method (b) over-estimates J_s at each applied pressure. This is as expected, since this method over-estimates J_w, but gives excellent values of C_p. The Model coefficients also over-estimate J_s and they do so in a progressively increasing way which accounts for the large predicted C_p values.

6.1.6. General Conclusions Arising From the Predictive Reverse Osmosis Calculation for 0.10M NaCl.

The relative success achieved by methods (a) and (b) in predicting the fluxes, J_s, J_w and the product concentration can be traced to the approximations used in obtaining each set of mobility coefficients.

Method (b) over-estimates both fluxes. The over-estimation of J_w is caused by the larger value of L_{ww} which is in turn caused by a larger l_{33}. This larger l_{33} can be explained by considering equation (2.43).

$$J_3 = (l_{13} - \frac{t_1 t_3 \alpha}{Z_1}) X_{12} + (l_{33} - \alpha t_3^2) X_3$$

Using equation (2.26) and $t_1 + t_2 = 1$ gives

$$J_3 = \frac{(t_2 t_3 \alpha - Z_2 l_{32})}{Z_1} X_{12} + (l_{33} - \alpha t_3^2) X_3$$

In the original salt gradient experiments to determine l_{33}, if method (a) is used, then l_{33} is under-estimated by the value $l_{32}X_{12}$. This apparently small omission (of $l_{32}X_{12}$) causes a decrease of 24% in L_{ww} (for N2) and thus decreases J_w.

Comparison of the predicted results with those observed shows that the l_{12}=23=0 approximations (method (a)) provides mobility coefficients which give the best estimate of both J_s and J_w for both N2 and E2. It, therefore, appears to be the most accurate assumption and the value of l_{33} which it provides seems to best represent the water - water interaction in the experimental membrane.

The high predicted values of C_p obtained from the Model coefficients are caused by the large values of both L_{ss} and L_{sw} (Table 6.4) (these are caused by the S.M.C. providing large value of l_{11}, l_{22} and l_{13}). These slightly over-estimate J_s. The S.M.C. also under-estimates l_{33} and over-estimates t_3. This in turn causes relatively small L_{ww} values and J_w is slightly under-estimated. The ratio of J_s to J_w is therefore high and "C_p predicted" is larger than observed. The absolute values of J_w (Predicted from (c)) are, however, in good agreement with those observed. Consequently the S.M.C. calculation provides a good estimation of the l_{33} coefficients and thus of the water-water interaction in the membrane. The agreement obtained by method (c) suggests that the factors affecting J_w are θ and V_w since by taking simple solution mobility coefficients and scaling them by θ/V_w, section (3.1.2), accurate values of l_{33}

and consequently of J_w in the membrane are obtained.

The pressure experiments, therefore, confirm the validity of the Salt Model Calculation and illustrate its ability to predict J_s, J_w and C_p to an accuracy which is at least qualitative and which justifies its practical application, especially so since it gives these predicted values requiring the very minimum of information on the membrane.

An impression of the various contributions to J_s, J_w and C_p can be obtained by considering the calculations for each flux using method (a), Table (6.5). The cross term contribution to J_s, $L_{sw}X_3$, in the normal membrane is some 10% of the total salt flux at 200 lbs.in^{-2} and 24% at 1500 lbs.in^{-2}. At these pressures in the expanded membrane this contribution is 17 and 35% respectively. The smaller contribution from the cross term for the normal illustrates the better Donnan exclusion in the more dense membrane. The cross term contribution to J_w, $L_{ws}X_{12}$, in both membranes is very small. The contribution from this term is larger at the low applied pressures. At 200 lbs.in^{-2} it is less than 1% of J_w in the normal membrane and less than 2% in the expanded. Therefore, the term $L_{ww}X_3$ is completely dominant in determining J_w.

$$\text{i.e.} \quad J_w \simeq L_{ww}X_3$$

whereas there is a significant contribution to J_s from both terms in equation (2.47).

The reverse osmosis calculation illustrates that, if a pressure experiment is to be included in the determination of membrane mobility coefficients (and the correspondence between predicted and observed results suggest it should) care must be taken to carry out the experiments at fairly low pressures, otherwise the membrane matrix/

matrix may be altered by compaction.

The reverse osmosis calculation also indicates that any attempt to predict the reverse osmosis characteristics of a membrane by irreversible thermodynamics or otherwise, from membrane data obtained at atmospheric pressure will become less successful at high pressures unless membrane compaction is taken into account.

6.2. The Reverse Osmosis Calculation for a 1.0M NaCl Feed Solution

6.2.1. The variation of the reverse osmosis characteristics of the membrane with concentration were investigated by conducting pressure experiments with a 1.0M NaCl feed solution.

The ability of the reverse osmosis calculation to predict J_s, J_w and C_p at 1.0M was also investigated. Table (6.6) shows the physical characteristics of N2 and E2 in a 1.0M NaCl solution. Comparison of Tables (6.1) and (6.6) shows, in the 1.0M solution the water contents of N2 and E2 are reduced by some 25% and the tortuosity factors of each are increased. From this data alone and from observations made at 0.1M, it could be concluded that J_w for the 1.00M feed will be low. The osmotic pressure difference across the membrane (for even a low rejection) with a 1.0M NaCl feed solution will be considerable. If a rejection of 50% was achieved equation (6.4) gives an osmotic pressure across the membrane equivalent to 350 lbs.in^{-2}. Therefore the force on water, X_3, will also be expected to be small in the 1.0M system. This also will cause J_w to be small.

At 200 lbs.in^{-2} neither N2 nor E2 allowed a flow of water. This is not surprising since a rejection of only 30% would set up an opposing osmotic pressure of approximately 200 lbs.in^{-2}. Even at 400 lbs.in^{-2} the normal membrane would not permit a flow of water. However, the membrane E2 allowed a finite flow at this pressure. The measured product concentration was 0.69M, Table (6.7), giving a rejection of 31%, which is significantly lower than the 56% achieved by the same membrane for the 0.10M feed solution. The measured water flux was 0.54×10^{-3} ml.cm^{-2} min^{-1}, 2.5 times less than that observed at 0.10M. The salt flux of 6.335×10^{-9} Moles salt cm^{-2} sec.$^{-1}$ was almost an order of magnitude higher than the J_s at 0.10M.

6.2.2. The Mobility Coefficients used in the Reverse Osmosis Calculation for a 1.0M NaCl feed Solution and the Results They Predict.

Although in 1.0M NaCl the salt uptake by both membranes increases so significantly that the interaction of the co-ion with the other membrane species cannot be ignored, that is $l_{12} \neq 0$ and $l_{23} \neq 0$, Paterson and Gardner [6], found that equations (2.47) (2.48) gave values of both salt and water flux (in a concentration cell experiment) close to those experimentally observed. The coefficients L_{ss}, L_{sw}, L_{ww} were calculated (I) on the basis of these short equations, (II) from the mobility coefficients obtained using the $l_{23} = C_2(2l_{33}/C_3 - l_{13}/C_1)$ approximation [6] and (III) from the l_{ik} coefficients obtained from the S.M.C. at 1.0M.

The value of product concentration predicted by method (I) was 0.70M, i.e. within 1.4% of the observed concentration of 0.69M. This is, therefore, an excellent method of predicting the product concentration for the 1.0M NaCl system. However, the predictions from (II) and (III) were very high, the former being 0.95M and the latter 0.98M.

Equation (2.48) gave an acceptable estimate of J_w, however, the l_{ik} coefficients from II provided a predicted value of J_w which is almost a factor of three too large. These coefficients also considerably over-estimate J_s. However, in this case the over-estimation of both fluxes is not proportional and consequently the predicted product concentration is unsatisfactorily large. Just as for the 0.10M NaCl feed solution the S.M.C. coefficients give an excellent prediction of J_w which is 0.01×10^{-3} $ml.cm^{-2}\,min^{-1}$ lower than the observed value of 0.54×10^{-3} $ml.cm^{-2}\,min^{-1}$ i.e. within 2.0%. The S.M.C. coefficients also provide a salt flux value closest to that observed experimentally, although each predicted J_s tends to over-estimate the observed value and thus the ratio/

ratio of the fluxes predicts a rather large C_p.

The L_{ss}, L_{sw} coefficients , Table (6.8) are an order of magnitude larger for the 1.0M NaCl feed solution. The increase is caused by the much larger co-ion content of the membrane (in 1.0M) which increases t_2 and consequently increases l_{12}, l_{22} and l_{23}. The direct water coefficients L_{ww} are relatively similar however, for both 0.10M and 1.0M NaCl solutions, since t_3 and l_{33} are less affected by the change in the total molality of the membrane. The effect these changes have on the relative contributions to the fluxes is shown in Tables (6.9)(6.10)Method (I) was chosen as it gives the best estimate of C_p.

The contribution to J_s from the cross term $L_{sw}X_3$ (in 1.0M) was 13% while for the 0.1M system it was 22%, Table (6.11). This decrease is caused by the water force X_3 being reduced by the opposing osmotic pressure. However, the smaller water force means that the cross term contribution to J_w, $L_{ws}X_{12}$ will be more significant. It amounts to some 12%, while for E_2 in the 0.10M NaCl it was only 1.2% . Therefore the change in concentration quite significantly alters the relative significance of each contribution to both J_s and J_w.

6.2.3. General Conclusions from the Reverse Osmosis Calculation for a 1.0M NaCl Feed Solution.

The reverse osmosis calculation confirms that the equations (2.47) (2.48) successfully describe J_s and J_w for 1.0M NaCl solution (where they should not apply). The prediction calculation demonstrates that the approximation (II) over-estimates all membrane mobility coefficient especially those affecting J_s, i.e. l_{11}, l_{22}, l_{13}. The l_{33} coefficient from this approximation was used in method (I) and it gave a good estimation of J_w and thus accurately represents /

represents the water-water interactions in the membrane for the 1.0M NaCl system.

Finally the estimate of J_s and J_w predicted by the model coefficients indicate that these coefficients describe quite accurately the various interactions within the experimental membrane at 1.0M. This further justifies the concept of the salt model and shows that the S.M.C. can be of practical value. Certainly any Model calculation which allows membrane mobility coefficients to be determined, which describe both salt flux and water flux in 0.10M and 1.0M Nacl, to the same degree of accuracy as the experimental mobility coefficients has been successful. Especially so since the model coefficients were obtained from published solution coefficients and a minimum amount of membrane data.

It must be noted that the mobility coefficients from the approximation (II) used in the reverse osmosis calculation for 1.0M NaCl are the only set which gave sensible predicted values of C_p (i.e. less than 1.0M). The other sets [6] gave C_p values greater than 1.0M and consequently were not reported.

Comparison of the Physical Characteristics of the Normal and Expanded C_{60} Membranes used by Gardner and Paterson with the Normal and Expanded used in this Work.

TABLE (6.1)

	% Water	10^2K	t_3	m.mol. cm^{-3} C_1	C_2	C_3
N1	52.6	1.37	10.75	0.98	0.0024	19.03
N2	50.09	1.23	11.00	1.04	0.0023	19.24
E1	77.7	1.92	15.77	0.96	0.0052	25.07
E2	78.41	2.05	16.00	0.97	0.0040	25.48

N1, E1 are the membranes used by Gardner and Paterson

N2, E2 are the membranes from this work.

TABLE (6.2a)

REVERSE OSMOSIS CALCULATION

Membrane C_{60N} =N2 Feed Solution 0.100M NaCl Pressure = 400 lbs.in^{-2}

L_{ss} L_{sw} L_{ws} L_{ww} from $l_{12} = 23 = o$ approximation

C_p Guess Molarity	X_{12} Joules mole cm^{-1}	X_3 Joules mole cm^{-1}	J_s Moles cm^{-2} Sec^{-1}	J_w Moles cm^{-2} Sec^{-1}	$J_s/J_w \times 55.5$ Molarity
0.040	1.400×10^5	14.89×10^2	4.588×10^{-10}	4.304×10^{-7}	0.0592
0.043	1.285×10^5	14.975×10^2	4.252×10^{-10}	4.322×10^{-7}	0.0546
0.045	1.220×10^5	15.030×10^2	4.063×10^{-10}	4.336×10^{-7}	0.0520
0.047	1.152×10^5	15.085×10^2	3.865×10^{-10}	4.349×10^{-7}	0.0490
0.050	1.1053×10^5	15.168×10^2	3.576×10^{-10}	4.370×10^{-7}	0.0454
0.054	0.941×10^5	15.27×10^2	3.2496×10^{-10}	4.395×10^{-7}	0.0410

$C_p^{Guess} = J_s/J_w \times 55.5 = 0.048M$

$J_s = 3.7655 \times 10^{-10}$ moles cm^{-2} sec.$^{-1}$

$J_w = 4.355 \times 10^{-7}$ moles cm^{-2} sec.$^{-1}$

$= 0.47 \times 10^{-3}$ mls cm^{-2} min^{-1}

TABLE (6.2b)

REVERSE OSMOSIS CALCULATION

Membrane C_{60E} = E2 Feed Solution 0.100M NaCl Pressure = 400 psi.

L_{ss} L_{sw} L_{ws} L_{ww} from $l_{12} = 23 = 0$ Approximation

C_p^{Guess} Molarity	X_{12} Joules $Mole^{-1}$ cm^{-1}	X_3	J_s Moles cm^{-2} $sec.^{-1}$	J_w	$J_{s/J_w} \times 55.5$ Molarity
0.040	1.273×10^5	13.54×10^2	1.500×10^{-9}	10.71×10^{-7}	0.078
0.043	1.170×10^5	13.61×10^2	1.395×10^{-9}	10.75×10^{-7}	0.072
0.047	1.048×10^5	13.71×10^2	1.272×10^{-9}	10.87×10^{-7}	0.065
0.050	0.959×10^5	13.79×10^2	1.1817×10^{-9}	10.856×10^{-7}	0.0604
0.055	0.835×10^5	13.91×10^2	1.0566×10^{-9}	10.932×10^{-7}	0.0536
0.060	0.720×10^5	14.04×10^2	0.94072	11.016×10^{-7}	0.0474

$$C_p^{Guess} = J_{s/J_w} \times 55.5 = 0.054M$$

$$J_s = 1.08 \times 10^{-9} \text{ mole cm}^{-2} \text{ sec.}^{-1}$$

$$J_w = 1.082 \times 10^{-6} \text{ mole cm}^{-2} \text{ sec.}^{-1}$$

$$= 1.17 \times 10^{-3} \text{ MLS CM}^{-2} \text{ MIN}^{-1}$$

TABLE 6.3

Membrane	Product Concentration Molar: Observed	Product Concentration Molar: Predicted I $l_{12}=0$	Product Concentration Molar: Predicted II $l_{12}=23=0$	Product Concentration Molar: Predicted III S.M. C.	10^3 x Water Flux $ml.cm^{-2}min^{-1}$: Observed	10^3 x Water Flux: Predicted I $l_{12}=0$	10^3 x Water Flux: Predicted II $l_{12}=23=0$	10^3 x Water Flux: Predicted III S.M.C.	10^{10} x Salt Flux $mol.cm^{-2}sec^{-1}$: Observed	10^{10} x Salt Flux: Predicted I $l_{12}=0$	10^{10} x Salt Flux: Predicted II $l_{12}=23=0$	10^{10} x Salt Flux: Predicted III S.M.C.
200 lbs.in^{-2}												
N_2	0.054	0.057	0.062	0.072	0.20	0.29	0.23	0.205	1.801	2.751	2.372	2.405
E_2	0.060	0.056	0.068	0.071	0.756	1.00	0.57	0.676	7.568	9.210	6.629	8.015
400 lbs in^{-2}												
N_2	0.041	0.042	0.048	0.060	0.510	0.613	0.468	0.420	3.480	4.372	3.665	4.210
E_2	0.044	0.042	0.054	0.058	1.330	2.130	1.170	1.380	9.770	14.600	10.800	13.600
1000 lbs.in^{-2}												
N_2	0.025	0.027	0.032	0.043	0.482	1.610	1.222	1.080	2.084	7.270	6.363	7.820
E_2	0.028	0.027	0.038	0.044	3.920	5.500	3.050	3.560	18.31	24.520	19.620	25.500
1500 lbs.in^{-2}												
N_2	0.018	0.022	0.026	0.038	0.644	2.450	1.860	1.614	1.934	8.760	7.928	10.270
E_2	0.022	0.022	0.032	0.038	4.860	8.370	4.619	5.352	17.840	13.400	25.250	34.140

TABLE 6.4

Mobility Coefficients for Salt and Water Used In The Reverse-Osmosis Calculation

Feed Solution 0.10M NaCl

Membrane	Method	L_{ss}	$L_{sw} = L_{ws}$	L_{ww}
C_{60} Normal	(a)	2.94×10^{-15}	3.167×10^{-14}	2.859×10^{-10}
	(b)	2.94×10^{-15}	3.167×10^{-14}	3.768×10^{-10}
	(c)	3.68×10^{-15}	7.46×10^{-14}	2.471×10^{-10}
C_{60} Expanded	(a)	1.025×10^{-14}	1.626×10^{-13}	7.772×10^{-10}
	(b)	1.025×10^{-14}	1.626×10^{-13}	1.417×10^{-9}
	(c)	1.220×10^{-14}	3.180×10^{-13}	8.991×10^{-10}

In methods (a) and (b) $L_{ss} = \left(\frac{l_{11}l_{22} - l_{12}^2}{\alpha}\right)$; $L_{sw} = L_{ws} = t_2 t_3 \alpha$

$$L_{ww} = l_{33} - \alpha t_3^2$$

In (a) the l_{33} value was taken from the $l_{12} = 23 = 0$ approximation

In (b) the l_{33} value was taken from the $l_{12} = 0$ approximation.

In (c) the mobility coefficients from the S.M.C. were used

$$L_{ss} = l_{12}^{SMC} \qquad L_{sw} = l_{23}^{SMC} \qquad L_{ww} = l_{33} - \frac{\left(l_{31} - l_{32}\right)^2}{l_{11} - l_{12}}$$

TABLE (6.5)

The Calculations for the Prediction of J_s and J_w for a 0.10M Feed Solution

$$J_s = \bar{L}_{ss}X_{12} + \bar{L}_{sw}X_3$$
$$J_w = \bar{L}_{ws}X_{12} + \bar{L}_{ww}X_3$$

MEMBRANE N2

MEMBRANE E2

PRESSURE = 200 lbs.in^{-2}

Method (a)

$X_{12} = 0.729 \times 10^{-5}$ $X_3 = 8.24 \times 10^{-2}$

$J_s = 2.143 \times 10^{-10} + 2.293 \times 10^{-11}$

$= \underline{2.372 \times 10^{-10}}$ 10%*

$J_w = 2.308 \times 10^{-9} + 2.071 \times 10^{-7}$

$= \underline{2.0937 \times 10^{-7}}$ 1.1%

$X_{12} = 0.54 \times 10^{-5}$ $X_3 = 6.73 \times 10^{-2}$

$J_s = 5.535 \times 10^{-10} + 1.094 \times 10^{-10}$

$= \underline{6.629 \times 10^{-10}}$ 16.5%*

$J_w = 0.88 \times 10^{-8} + 5.23 \times 10^{-7}$

$= \underline{5.319 \times 10^{-7}}$ 1.6%

Method (c)

$X_{12} = .503 \times 10^{-5}$ $X_3 = 7.55 \times 10^{-2}$

$J_s = 1.942 \times 10^{-10} + 5.632 \times 10^{-11}$

$= \underline{2.505 \times 10^{-10}}$ 22%

$J_w = 3.62 \times 10^{-9} + 1.866 \times 10^{-7}$

$= \underline{1.902 \times 10^{-7}}$ 2.0%

$X_{12} = 0.48 \times 10^{-5}$ $X_3 = 6.79 \times 10^{-2}$

$J_s = 5.86 \times 10^{-10} + 2.159 \times 10^{-10}$

$= \underline{8.802 \times 10^{-10}}$ 27%

$J_w = 1.526 \times 10^{-8} + 6.105 \times 10^{-7}$

$= \underline{6.258 \times 10^{-7}}$ 2.5%

Method (a)

PRESSURE = 1500 lbs.in^{-2}

$X_{12} = 2.05 \times 10^{-5}$ $X_3 = 60.01 \times 10^{-2}$

$J_s = 6.027 \times 10^{-10} + 1.901 \times 10^{-10}$

$= \underline{7.928 \times 10^{-10}}$ 44%

$J_w = 6.492 \times 10^{-9} + 1.716 \times 10^{-6}$

$= \underline{1.722 \times 10^{-6}}$ 0.04%

$X_{12} = 1.596 \times 10^{-5}$ $X_3 = 54.7 \times 10^{-2}$

$J_s = 1.636 \times 10^{-9} + 8.894 \times 10^{-10}$

$= \underline{2.525 \times 10^{-9}}$ 35%

$J_w = 2.595 \times 10^{-8} + 4.253 \times 10^{-6}$

$= \underline{4.277 \times 10^{-6}}$ 0.61%

Method (c)

$X_{12} = 1.500 \times 10^{-5}$ $X_3 = 60.05 \times 10^{2}$

$J_s = 5.79 \times 10^{-10} + 4.480 \times 10^{-10}$

$= \underline{10.270 \times 10^{-10}}$ 44%

$J_w = 11.190 \times 10^{-9} + 14.838 \times 10^{-7}$

$= \underline{14.95 \times 10^{-7}}$ 0.74%

$X_{12} = 1.375 \times 10^{-5}$ $X_3 = 54.59 \times 10^{-2}$

$J_s = 1.678 \times 10^{-9} + 1.736 \times 10^{-9}$

$= \underline{3.414 \times 10^{-9}}$ 51%

$J_w = 4.373 \times 10^{-8} + 49.08 \times 10^{-7}$

$= \underline{49.55 \times 10^{-7}}$ 0.9%

* The percentages opposite each value of J_s and J_w are the contribution to the flux from the cross term $\bar{L}_{sw}X_3$ or $\bar{L}_{ws}X_{12}$

Units of X_{12} and X_3 = Joules mol.$^{-1}$cm^{-1} Unit of J_s and J_w = mol. cm^{-2} sec.$^{-1}$

TABLE (6.6)

PHYSICAL CHARACTERISTICS OF N2 and E2 IN 1.00M NACL

	Wet Weight gm	Weight Water gm	% Water	Diameter cm	Thick -ness cm	Wet Volume cm^3	V_w	e_m	C_1	C_2 m. mol. cm^{-3}	C_3
N_2	0.3196	0.0900	39.23	3.6740	.0278	0.295	0.305	5.57	1.22	0.0922	16.95
E_2	0.2940	0.1124	61.9	3.2719	.0313	0.263	0.427	3.68	1.410	0.1475	23.74

TABLE (6.7)

REVERSE OSMOSIS RESULTS FOR E_2

Applied Pressure = 400 lbs.in^{-2} 49.6 Joules mole^{-1}

Feed solution = 1.0M NaCl

PRODUCT CONCENTRATION				SALT FLUX				WATER FLUX			
	Predicted				Predicted				Predicted		
Observed	(I)	(II)	(III)	Observed	(I)	(II)	(III)	Observed	(I)	(II)	(III)
	Molar			Moles cm^{-2} sec^{-1}				Mls. cm^{-2} Min^{-1}.			
0.69	0.70	0.95	0.98	6.23×10^{-9}	9.25×10^{-9}	22.92×10^{-9}	9.18×10^{-9}	0.54×10^{-3}	0.77×10^{-3}	1.40×10^{-3}	0.55×10^{-3}

I = $l_{12} = 0$

II = $l_{12} = 23 = 0$

III = S.M.C.

TABLE (6.8)

COMPOUND COEFFICIENTS FOR SALT AND WATER USED IN REVERSE OSMOSIS CALCULATIONS

Feed Solution 1.00M Nacl

MEMBRANE	METHOD	L_{ss}	$L_{sw} = L_{ws}$	L_{ww}
C_{60} Expanded	I	1.48×10^{-13}	15.6×10^{-13}	8.181×10^{-10}
	II	3.6×10^{-13}	137.8×10^{-13}	8.181×10^{-10}
	III	3.03×10^{-13}	52.7×10^{-13}	3.19×10^{-10}

In Method (I) equations (2.47) (2.48) are used to calculate J_s and J_w.

Therefore $L_{ss} = t_1 t_2 \alpha$, $L_{sw} = L_{ws} = t_2 t_3 \alpha$, $L_{ww} = l_{33} - t_3^2 \alpha$

l_{33} is taken from the $l_{23} = C_2(2l_{33}/C_3 - l_{31}/C_1)$

In Method (II) equations (2.41) (2.43) are used.

$$L_{ss} = \frac{l_{11}l_{22} - l_{12}^2}{\alpha} \qquad L_{sw} = L_{ws} = (l_{13} - t_1 t_3 \alpha)$$

$$L_{ww} = l_{33} - \alpha t_3^2$$

l_{33} is taken from the $l_{23} = C_2(2l_{33}/C_3 - l_{31}/C_1)$

In Method (III) the l_{ik} coefficients from the S.M.C. are used.

TABLE (6.9)

THE CALCULATIONS FOR THE PREDICTION OF J_s AND J_w FOR A 1.00M NaCl FEED SOLUTION

PRESSURE = 400 psi

METHOD

(I) $X_{12} = 0.544 \times 10^5$ $X_3 = 7.665 \times 10^2$

$J_s = 8.05 \times 10^{-9} + 1.196 \times 10^{-9}$

$= 9.245 \times 10^{-9}$ mol. cm^{-2} s^{-1} 13% *

$J_w = 8.474 \times 10^{-8} + 6.27 \times 10^{-7}$

$= 7.12 \times 10^{-7}$ mol. cm^{-2} s^{-1} 12%

(II) $X_{12} = .843 \times 10^4$ $X_3 = 14.43 \times 10^2$

$J_s = 3.83 \times 10^{-9} + 19.89 \times 10^{-9}$

$= 22.92 \times 10^{-9}$ mol. cm^{-2} s^{-1} 87%

$J_w = 11.18 \times 10^{-8} + 11.81 \times 10^{-7}$ 9%

$= 12.93 \times 10^{-7}$ mol. cm^{-2} x^{-1}

(III) $X_{12} = 0.369 \times 10^4$ $X_3 = 15.28 \times 10^2$

$J_s = 1.118 \times 10^{-9} + 8.053 \times 10^{-9}$

$= 9.171 \times 10^{-9}$ mol. cm^{-2} s^{-1} 88%

$J_w = 1.945 \times 10^{-8} + 4.874 \times 10^{-7}$ .4%

$= 5.069 \times 10^{-7}$ mol. cm^{-2} s^{-1}

* The percentages opposite each flux are the contributions from the cross terms $L_{sw}X_3$ and $L_{ws}X_{12}$ to the respective Salt flux and Water flux.

Units of J_s J_w mol. cm^{-2} s^{-1}

Units of X_{12} X_3 Joules $mole^{-1}$ cm^{-1}

TABLE (6.10)

THE CALCULATION FOR THE PREDICTION OF J_s and J_w USING $l_{12} = 23 = 0$ COEFFICIENTS WITH FEED SOLUTION 0.10M AND PRESSURE 400 psi.

$$X_{12} = 0.86 \times 10^{5} \qquad X_{3} = 13.76 \times 10^{2}$$

$$J_s = 0.8806 \times 10^{-9} + 1.9938 \times 10^{-11}$$

$$= 1.080 \times 10^{-9} \text{ mol. cm}^{-2} \text{ sec}^{-1}$$

$$J_w = 1.240 \times 10^{-8} + 10.69 \times 10^{-7}$$

$$= 10.82 \times 10^{-7}$$

Units X_{12} J mol^{-1} cm^{-1}

Units J_s and J_w mol. cm^{-2} sec.^{-1}

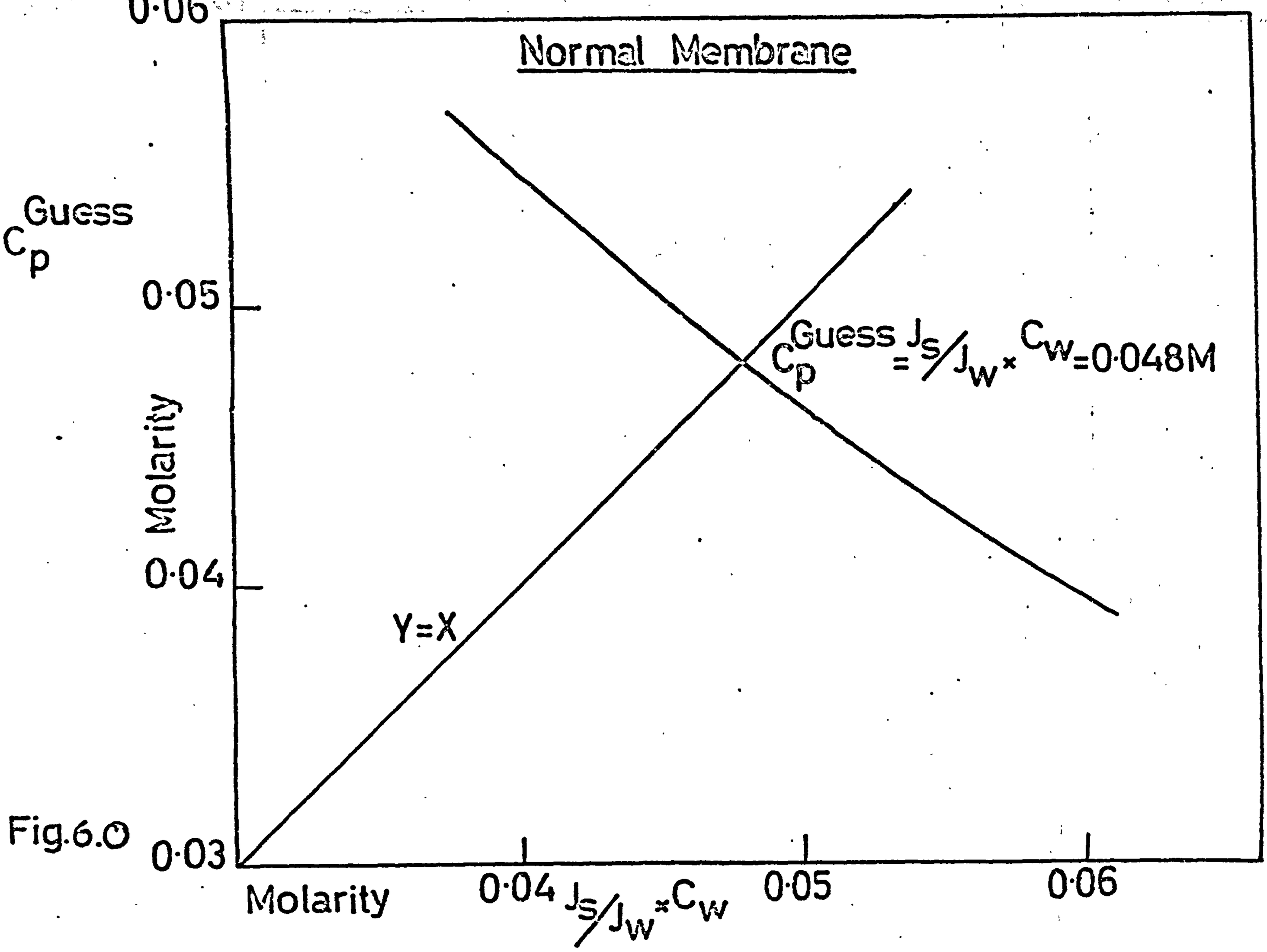
Normal Membrane
0·06
0·05
0·04
0·03
C_p^{Guess}
Molarity
$C_p^{Guess} = J_s/J_w \times C_w = 0{\cdot}048M$
Y=X
Molarity
0·04 $J_s/J_w * C_w$
0·05
0·06

Fig.6.0

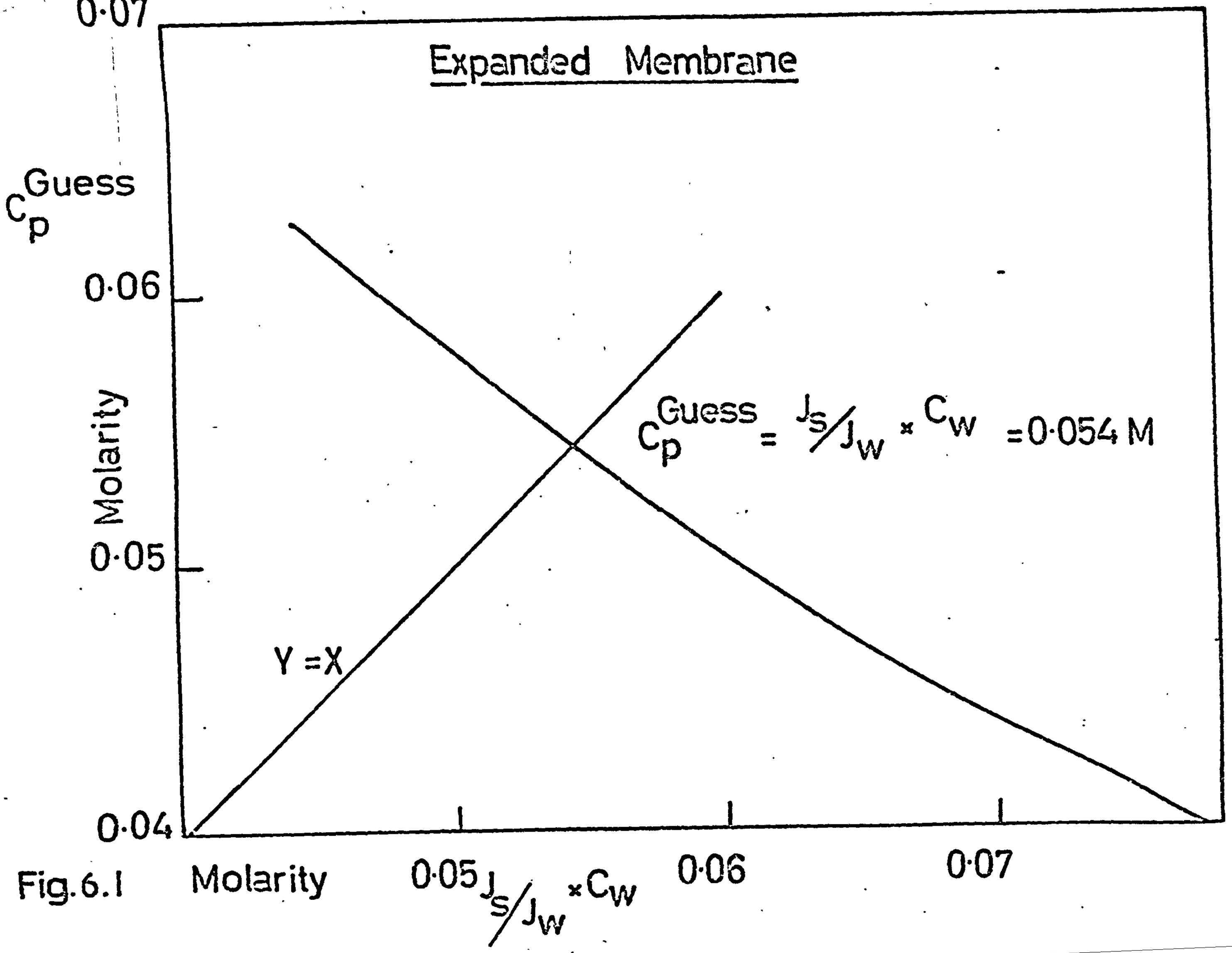
Expanded Membrane
C_p^{Guess}
Molarity
0·07
0·06
0·05
0·04
$C_p^{Guess} = J_s/J_w \times C_w = 0{\cdot}054\,M$
Y = X
0·05
$J_s/J_w \times C_w$
0·06
0·07
Molarity

Fig.6.1

SUPPLEMENTARY LEGEND FOR THE FIGURES OF CHAPTER 6.1

For figures 6.2 - 6.7

The points ● represent experimental data

⊙ represents data from the $L_{12=0}$ approximation

◐ represents data from the $L_{12=23=0}$ approximation

⊗ represents data from the S.M.C. mobility coefficients.

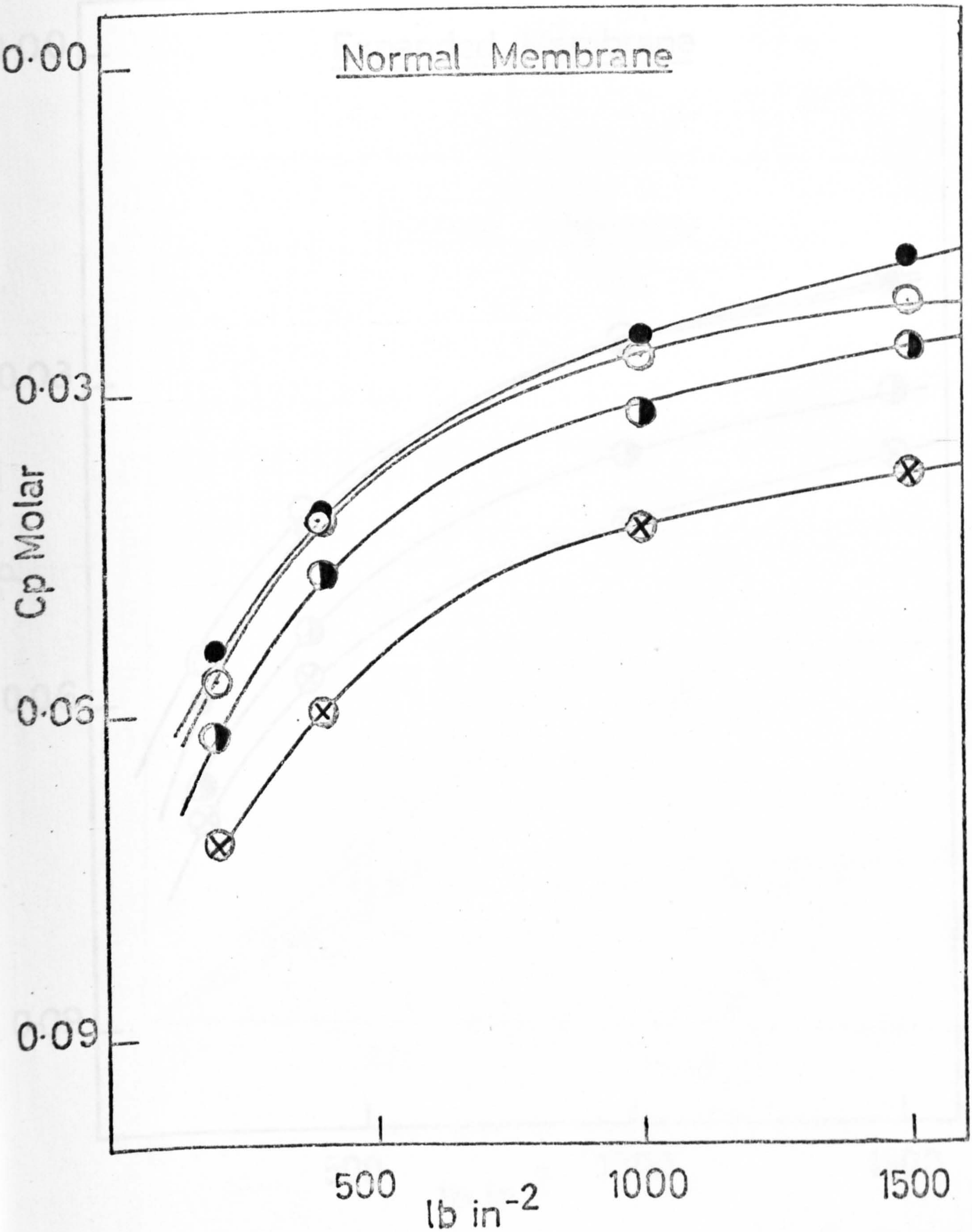
Normal Membrane
0·00
0·03
0·06
0·09
Cp Molar
500
1000
1500
lb in^{-2}
Applied Pressure

Fig. 6.2

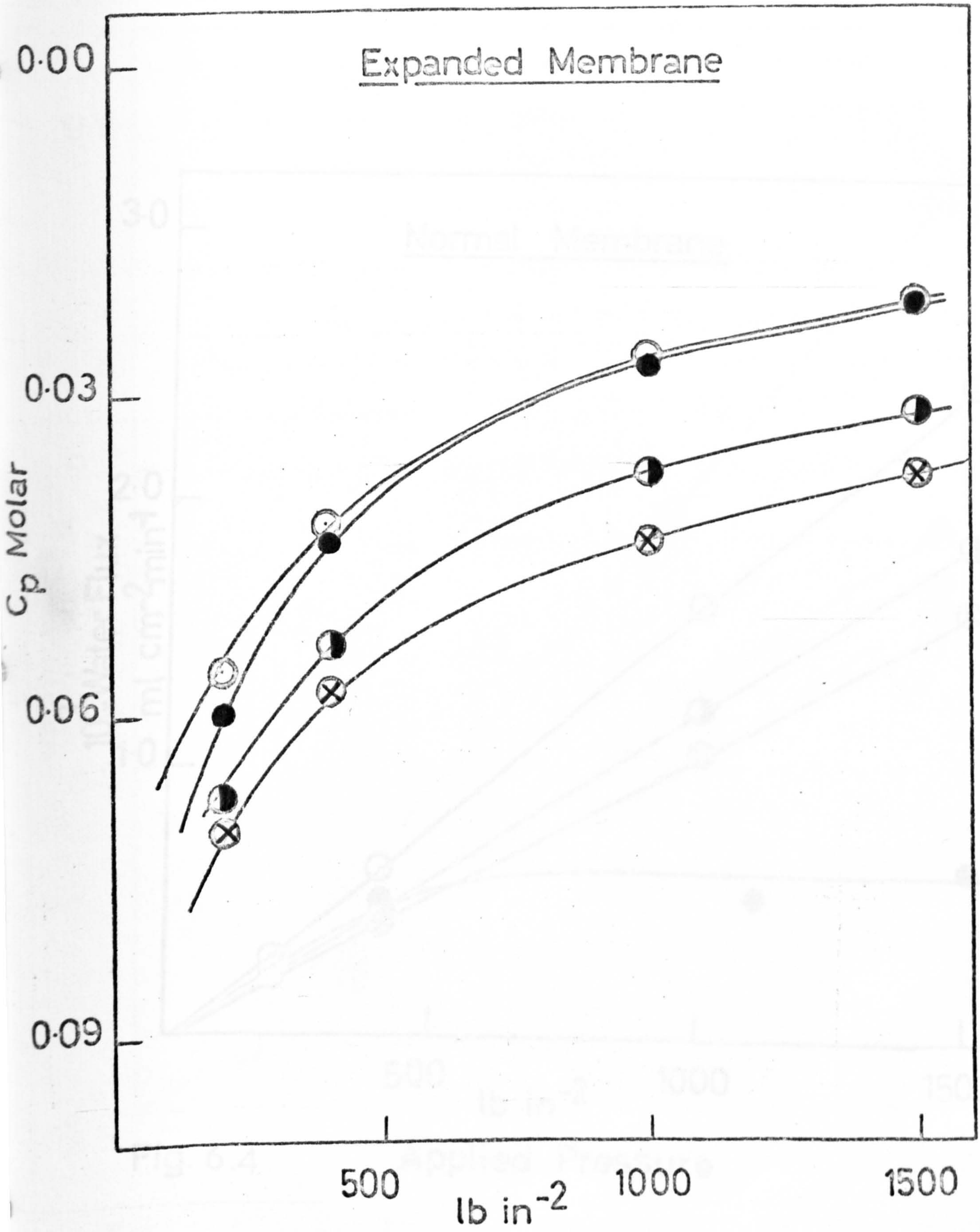
Expanded Membrane
0·00
0·03
0·06
0·09
c_p Molar
500
1000
1500
lb in^{-2}
Applied Pressure

Fig. 6.3

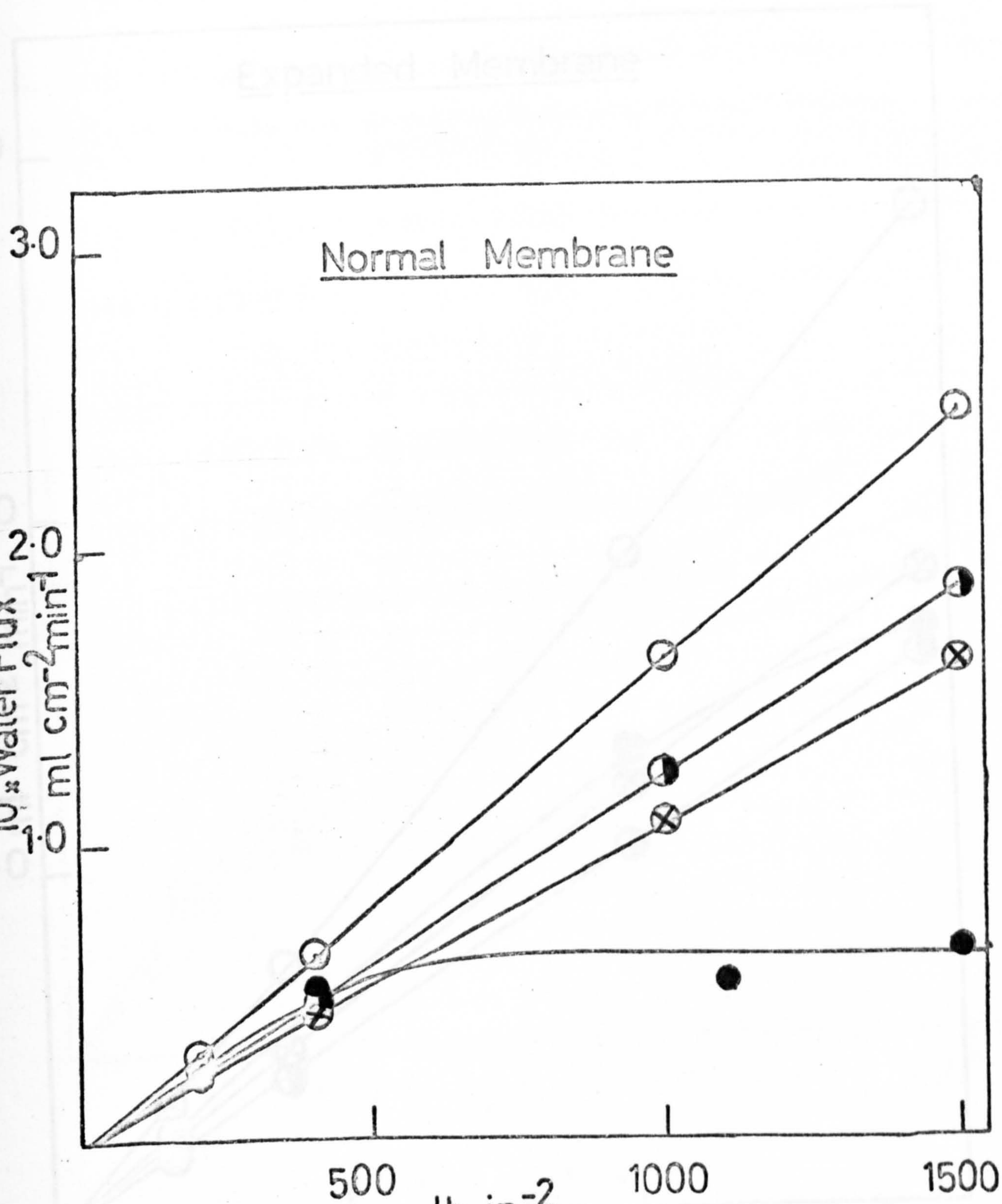
Normal Membrane
3·0
2·0
1·0
10^3 * Water Flux
ml cm^{-2}min^{-1} at
500
1000
1500
lb in^{-2}
Applied Pressure

Fig. 6.4

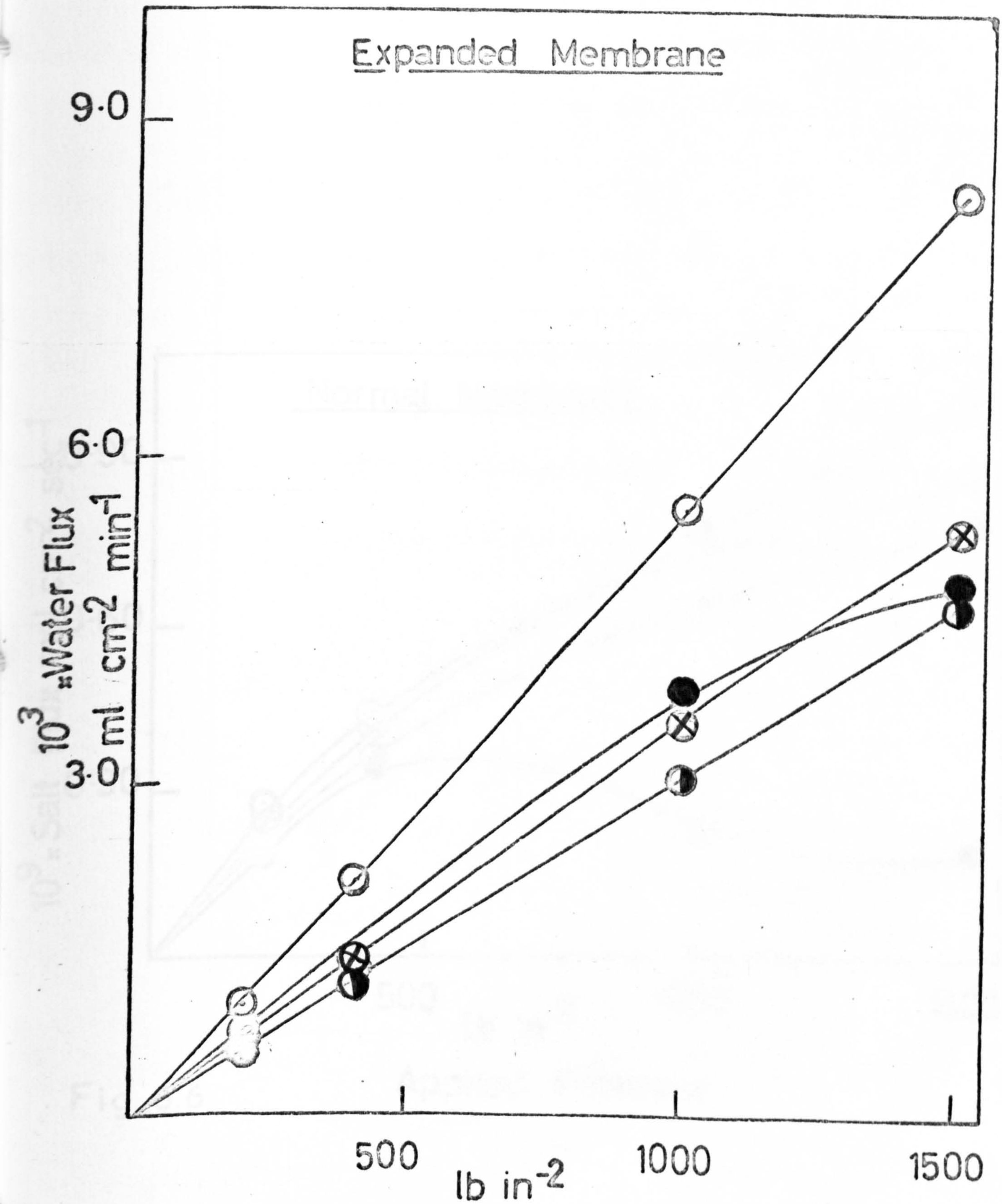
Expanded Membrane
9·0
6·0
3·0
10^3 *Water Flux
ml cm^{-2} min^{-1}
500
1000
1500
lb in^{-2}
Applied Pressure

Fig. 6.5

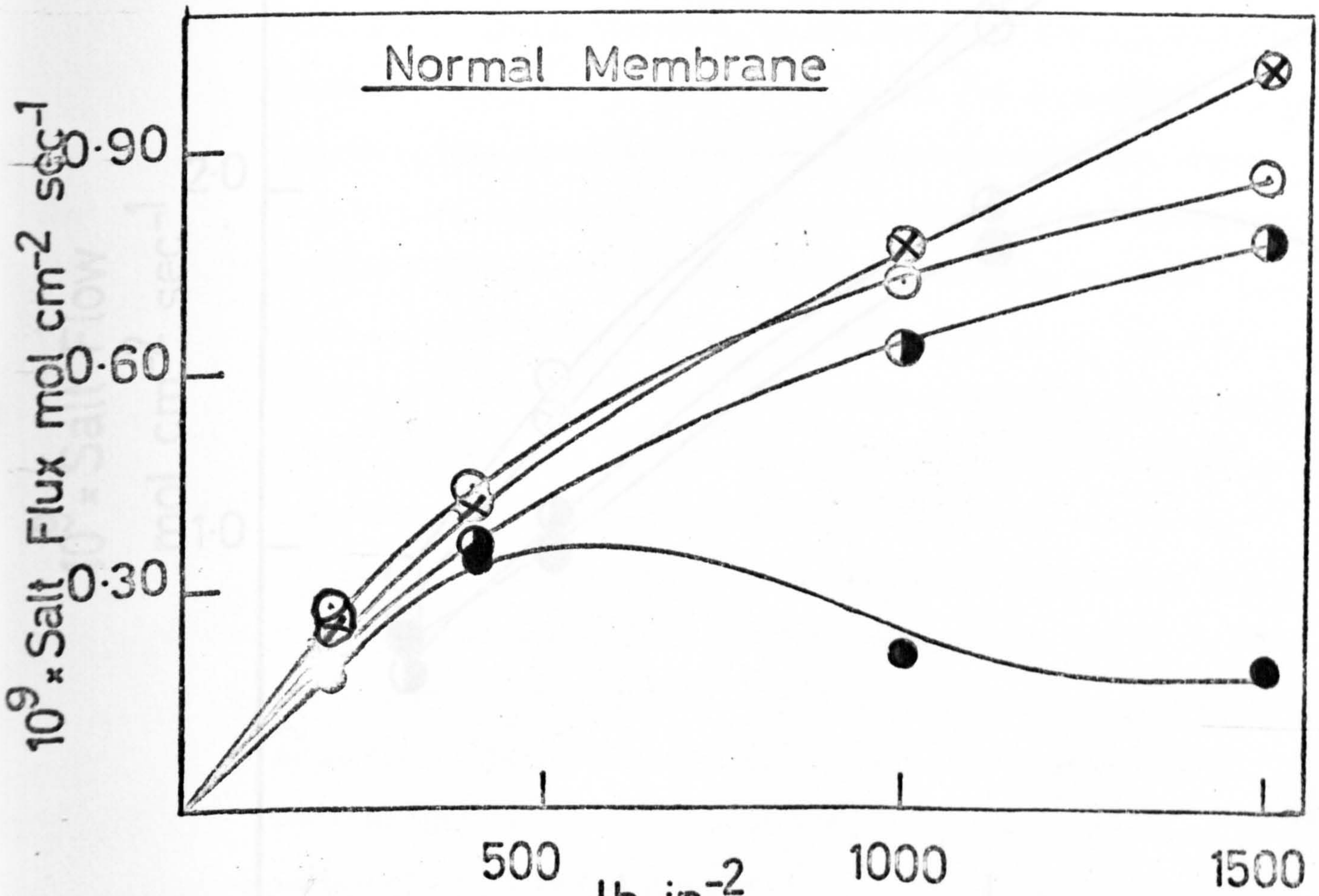
Normal Membrane
10^9 × Salt Flux mol cm^{-2} sec^{-1}
0·90
0·60
0·30
500
1000
1500
lb in^{-2}
Applied Pressure

Fig.6.6

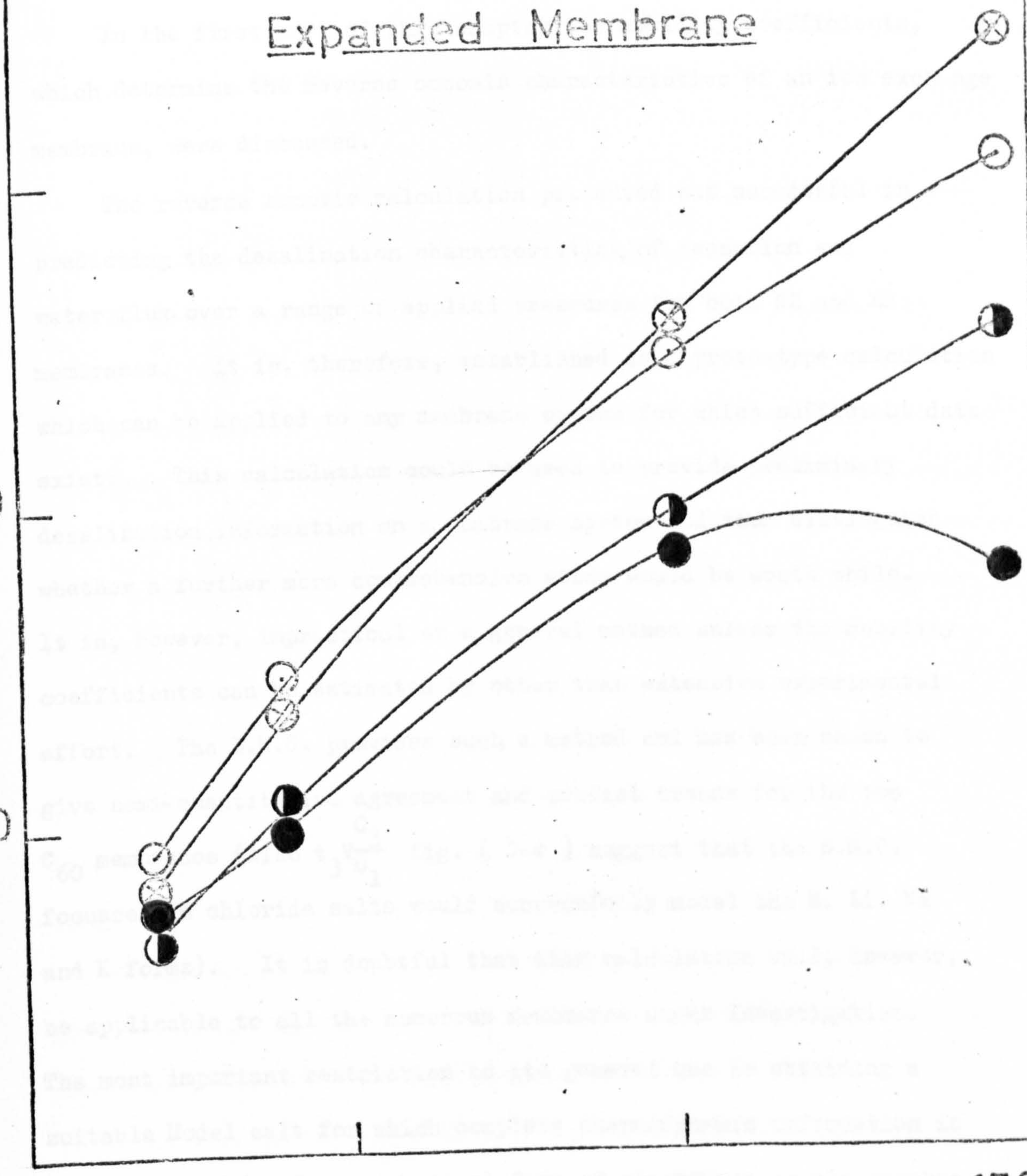
Expanded Membrane
10^9 * Salt Flow
mol cm^{-2} sec^{-1}
3·0
2·0
1·0
500
1000
1500
Applied Pressure
lb in^{-2}

Fig. 6.7

6.3. Reverse Osmosis Characteristics of a Series of Expanded C_{60} Membranes and of Perfluro Sulphonic Acid Membranes with Varying Capacities and Water Contents.

In the first part of this chapter the mobility coefficients, which determine the reverse osmosis characteristics of an ion exchange membrane, were discussed.

The reverse osmosis calculation presented was successful in predicting the desalination characteristics, of rejection and water flux, over a range of applied pressures for both N2 and E2 membranes. It is, therefore, established as a proto-type calculation which can be applied to any membrane system for which sufficient data exist.. This calculation could be used to provide preliminary desalination information on a membrane system and thus distinguish whether a further more comprehensive study would be worth while. It is, however, impractical as a general method unless the mobility coefficients can be estimated by other than extensive experimental effort. The S.M.C. provides such a method and has been shown to give semi-quantitative agreement and predict trends for the two C_{60} membranes (Also $t_3 V\frac{C_3}{C_1}$ fig. (5.4) suggest that the S.M.C. focussed on chloride salts would successfully model the H, Li, Na and K forms). It is doubtful that this calculation will, however, be applicable to all the numerous membranes under investigation. The most important restriction to its general use is obtaining a suitable Model salt for which complete thermodynamic information is available. Therefore, practical data of the effect on the reverse osmosis characteristics of changing various membrane parameters will give an indication of which membrane properties are most important in the hyper-filtration process.

Using the membranes N2 and E2 it was found that when the water content was increased (by expansion) from approximately 50 to 80% both the salt and water flux increased while the rejection remained

almost constant. In order to observe whether these trends continue with increasing expansion and to investigate the general effects of membrane expansion on the reverse osmosis characteristics, the series of expanded C_{60} membranes (discussed in chapter 5) was studied.

6.3.1. Rejection Characteristics of the Range of C_{60} and XR Membranes

The reverse osmosis data for the full range of C_{60} membranes (0.10M) at 200 and 400 lbs.in^{-2} applied pressure are presented in Tables (6.11), (6.12) and for the XR membranes in Table (6.13).

The decrease in rejection with expansion, first observed with membranes N2and E2 is confirmed. The rejection decreases (and product concentration increases) with increasing water content of the membranes. Since the fixed charge capacity of the C_{60} membranes (w.r.t. dry weight of matrix) is constant, the increased water content has the effect of decreasing the internal molality of the membrane. In the range of C_{60} membranes rejection decreases from 70 - 46% (at 400 lbs.in^{-2}) as the membrane molality decreases from 3.3m to 1.23m and from 46 - 28% (at 200 lbs.in^{-2}) as the molality decreases from 2.99m to 1.24m.

For the XR membranes the decrease in rejection is from 60 - 54% at 400 lbs.in^{-2} and 50 - 41% at 200 lbs.in^{-2}. The molality decreases from 5.29m to 3.42m in these membranes.

Other work on the C_{60} membranes has suggested that the internal molality affects the membrane transport properties (e.g. the t_3 - molality relation discussed in section (5.4.1.)). The rejection data for both C_{60} and XR membranes was plotted against internal molality, fig.(6.8). The first and perhaps most remarkable feature is/

is that at both applied pressures, the rejection results of both the C_{60} and XR membranes trace smooth curves which although separate, have identical shapes. This relationship is made more significant by the fact that while for the C_{60} membranes the change in internal molality is caused by a change in the water content, in the XR membranes the molalities vary because the fixed charge capacities are different in each of the three membranes. Thus the relationship of rejection with internal molality may be a general one. It certainly is not one which might be predicted intuitively.

This decrease in rejection with decreasing molality is an effect of the Donnan rejection potential.

The effect of salt uptake on rejection was also investigated. Since C_2 is small in the C_{60} membranes (at 0.10M) to a good approximation $l_{12} = 23 = 0$, section (6.1.2) . This reduces equation (2.41) to equation (2.47) which shows the dependence of J_s on t_2.

$$\text{By definition } t_2 = \frac{Z_2 J_2 F}{I}$$

$$\therefore \quad t_2 = \left(\frac{Z_2 t_2}{Z_1 J_1 + Z_2 J_2}\right)$$

(for a 1:1 salt)

$$t_2 = \left(\frac{-C_2 V_2}{C_1 V_1 - C_2 V_2}\right)$$

$$\text{since } V_1 = V_2 \quad \text{(in the membrane)}$$

$$t_2 = \frac{-C_2}{C_1 - C_2} \cong \frac{-C_2}{C_1} \quad \text{(for low salt uptake)}$$

$(C_1 - C_2)$ is the total ionic concentration of the membrane and is approximately constant for the range of C_{60} membranes. Therefore, J_s and consequently rejection will be (approximately) proportional to C_2.

In the C_{60} membranes the co-ion capacity increases from 0.0022 m.mol.cm^{-3} in PS_1 to 0.0058 m.mol.cm-3/

m. mol.cm^{-3} in PS_{11}. For this increase the rejection decreases by 21% at 400 lbs.in^{-2} and 12% at 200 lbs.in^{-2}. The graphs of the rejection results plotted against C_2 are linear at both 200 and 400 lbs.in^{-2}. fig. (6.9). Therefore, from a knowledge of C_2. the rejection of any membrane in the C_{60} series could be predicted.

6.3.2. Water Flux Characteristics of the Range of C_{60} and XR Membranes. The membrane E1, of Gardner and Paterson, and E2 used in this work have been shown to give larger water fluxes than the C_{60} normal membranes, under both applied concentration (3) and pressure gradients.

Further heating of the membrane which continues the expansion and increases the amount of absorbed water has the effect of further increasing the water flux, Tables (6.11) (6.12). The water flux of the most expanded membrane at 400 lbs.in^{-2} was 3.06×10^{-3} ml.cm^{-2}min.$^{-1}$, which is an increase of some five times on the value measured for E2 (Table (6.3)) and is an order of magnitude greater than the water flux for the least permeable normal membrane, PS_1. The plot of J_w against internal molality, Fig.(6.8) for both the C_{60} and XR membranes defines individual smooth curves which are of similar shape. The graph defined by the C_{60} membranes at 200 lbs.in^{-2} perfectly parallels the graph obtained from the results at 400 lbs.in^{-2}. Fig. (6.8) therefore indicates that both rejection and water flux are functions of the internal molality of the membrane. However, while the rejection decreases very slightly with a decrease in membrane molality, the water flux increases tremendously. For example (at 400 lbs.in^{-2}) for a C_{60} membrane with a molality of 3.9m the rejection is some 65% and J_w is 0.4×10^{-3} ml.cm^{-2}.min^{-1}. However, in a more dilute membrane with a molality of ca 1.5m, the rejection is reduced to only 50%, but J_w is considerably increased to

1.4×10^{-3} mls. cm^{-2} $min.^{-1}$, i.e. by some 350%.

The dependence of water flux on tortuosity suggested by the S.M.C. is demonstrated in Fig. (6.10). Each of the water flux results when plotted against θ_m (and θ_p) fall on a smooth curve. The results at each pressure trace individual graphs which are identical in form.

A significant feature illustrated by these plots is that, while at high values of Θ, (in the 'tighter', least permeable membranes) a change in Θ will have a relatively small effect on J_w. In the more 'open' and thus more permeable membranes, a change in Θ of ca from 3 to 2 will change J_w by a factor of two. Fig. (6.10) shows that the tortuosity factor gives a reasonably good indication of the permeability of a membrane to water, under an applied pressure force.

The XR-170 membranes, which have considerably lower water contents than the C_{60} membranes and hence have large tortuosity factors, give relatively high fluxes. The plot they provide of J_w against θ_m, Fig. (6.10). indicates that Θ gives an impression of permeability relevant to only one specific membrane type and comparison from one membrane system to another cannot be made with confidence. This is probably due to the different character of the host polymer matrix.

The increase in J_w with expansion of the membrane can be explained by considering L_{ww}. In section (6.1.4) it was shown that for 0.1Cm NaCl (to a good approximation)

$$J_w = L_{ww} X_3$$

$$\text{i.e.} \quad J_w = (l_{33} - t_3^2 \alpha) X_3$$

In/

In the previous experimental determination of the mobility coefficients [3] it was shown that l_{33} increases with dilution of the membrane. The S.M.C. also demonstrates that l_{33} increases as the internal molality decreases since the uncorrected l_{33} for E2 is greater than that for N2Table (3.4).Further, since θ is smaller in the more diluted membrane the correction factor used in the S.M.C. will also give a larger l_{33} for the more expanded membrane. However, both the experimental measurements and the S.M.C. indicate that t_3 and α increase with dilution and that α increases with decreasing θ, Chapter 5. Therefore, J_w increases in the range of expanded C_{60} membranes-because l_{33} increases with dilution, and does so to a greater degree than $t_3^2 \alpha$

An effective reverse osmosis membrane must combine a high rejection with a larger water flux. The high molality required to provide the former (in an ion exchange membrane) will, however, tend to create a smaller J_w. These opposing properties are well illustrated in Fig. (6.8) and must be optimized in any ion exchange membrane being used for reverse osmosis. These opposing properties are further demonstrated by figs. (6.11) (6.12). In fig. (6.11) the variation in rejection with the ratio of water to counter-ions in the membrane is shown. The experimental results define a graph which is approximately linear for values of the C_3/C_1 ratio above 25. However, below this, especially between 10 - 20, a decrease in this ratio more significantly increases the rejection capacity of the C_{60} membrane. This suggests that one requirement for high rejection in a desalination membrane, is a low C_3/C_1 ratio.

Fig. (6.12) shows the increase in water flux with increasing C_3 for the C_{60} and XR membranes. Therefore, an efficient desalination membrane/

membrane requires a low C_3/C_1 ratio and a high C_3. These requirements might well be satisfied by a membrane with a very low degree of cross-linking and a high fixed charge capacity.

The normal C_{60} membrane, therefore, provides quite good desalination with a low water flux. Expansion of this membrane slightly decreases the desalination, but increases the water flux by a factor of ten to 7.0×10^{-3} cm. hr^{-1} at^{-1} or 0.042 gal. ft^{-2} day^{-1} at^{-1}.

(which are the units normally used to describe J_w in reverse osmosis).

6.3.3. It is of interest to compare these desalination characteristics with other data on ion exchange membranes used in hyper-filtration studies, and also with the cellulose acetate membranes which are produced as commercial desalination membranes.

Since the discovery of the effectiveness of cellulose acetate membranes for hyper-filtration of saline solutions, relatively little work has been done on the apparently less attractive ion exchange membranes.

Baldwin, Johnston and Halcomb prepared a cation exchanger by grafting poly-acrylic acid onto cellophane (7). This membrane rejected 35% salt from a 0.5M NaCl feed and 80% from a 0.01M feed at 2500 lbs. in^{-2}. These membranes produced a water flux of between $3 - 6 \times 10^{-3}$ cm hr^{-1} at^{-1}. The same workers prepared a strongly acidic cation exchanger by grafting polystyrene sulphonate on to cellophane. This gave similar salt rejection and flow rates to those above.

Michaels and Bixler have reported that membranes prepared by reacting polyelectrolytes based on styrene sulphonate and vinyl-benzyl-trimethyl ammonium chloride (8) (9), rejected 50% salt from a 0.7M NaCl solution at 1500 lbs. in-2. This membrane provided a/

a water flux of 3.4×10^{-3} cm. hr^{-1} at^{-1}. These membranes were 0.0025 cm. thick.

Spiegler [10] has measured the hyper-filtration characteristics of a number of ion exchange membranes and reports for a Pera flux C-10 and Nal-film-1, both of which are sulphonic acid cation exchangers, rejection of 19 and 90% respectively for a 0.10M NaCl feed, at 1000 lbs. in^{-2}. The water flux rates of these membranes were 17×10^{-3} and 0.4×10^{-3} $cm.hr^{-1}.at^{-1}$. The thicknesses were 0.075 and 0.015 cm. respectively. The desalination characteristics of the A.M.F. C_{60} membranes are thus very similar to those exhibited by these other ion exchange membranes. The degree of rejection they provide and their flux rates, are, if anything, slightly better than most. Work by Reid,[11] Breton[12] and McKelvey [13] in the early fifties established that a membrane cast from cellulose acetate would reject 98% or more of salt from salt solutions of salt water concentrations.

Later work by Loeb [14] and Sourirajan [15] developed cellulose acetate membranes of greatly enhanced flow by casting the membrane from solutions containing perchlorate salts (usually $Mg(ClO_4)_2$ and heat treating the cast membrane at temperatures of 60° - 90°C. This membrane combines the two basic requirements for a reverse osmosis membrane and consequently a great deal of research has been carried out on all aspects of desalination using this membrane [16] [17] [18] [19] [20] [21] [22] [23] [24] [25]

The basic membrane is generally about 100μ thick. The active

layer/

layer, which is responsible for the salt rejection, is, however, only 0.25 μ thick. At the normal working pressure of 1500 lbs.in^{-2}, the Loeb-Sourirajan membrane gives a rejection of between 90 - 98% at feed concentration of up to 1.0M NaCl and a flux of approximately 12 gal. ft^{-2} day^{-1}. (i.e. 0.02 cm. hr^{-1} at^{-1}).

In these very high flux membranes the rejection is very sensitive to any concentration polarisation at the membrane surface (high pressure side) which may be created by inefficient flow past the membrane. Rejection may, therefore, vary from apparatus to apparatus.

In section (6.1.4) the variation in both J_s and J_w caused by compaction of the C_{60} membranes was discussed. Since compaction is also a problem in cellulose acetate membranes (14) (15) (26) it is difficult to compare data obtained on the C_{60} membranes at 400 lbs.in^{-2} with data obtained on the cellulose acetate at 1500 psi. For this reason cellulose acetate membranes were investigated on the reverse osmosis system II.

The experimental data obtained for the two cellulose acetate membranes used is given in Table (7.6). The cellulose acetate membranes are denoted CA(80) and CA(85). The bracketed number denotes the temperature of heat treatment.

The effect of the different heat treatments on rejection was slight. CA(80) rejected some 90% of the salt from the 0.10M NaCl feed solution at 400 lbs.in^{-2}, whereas CA(85) rejected 94% salt at 300 lbs.in^{-2}./

300 lbs.in^{-2}. The rejection was relatively unaffected by the applied pressure. The effect of the different temperatures of preheat-treatment was more pronounced in the J_w values of the two membranes. For CA(80) the water flux was 16.3 x 10^{-3} ml.cm^{-2}.min^{-1} (0.048 cm. hr^{-1} at^{-1}). This was significantly larger than the water flux of 10.58 x 10^{-3} ml. cm^{-2}.min^{-1} (0.031 cm.hr^{-1}.at^{-1}) measured for CA(85). These flux rates are 1.5 - 2.0 times larger than the Loeb-Scourirajan values. They are considerably larger than the flux for the most permeable C_{60} membrane, although not quite an order of magnitude. The C_{60} membranes, however, have a thickness of 0.03 cm. whereas the cellulose acetate membranes have an active layer thickness of approximately 1000 times thinner. Equations (2.47) and (2.48) can be written.

$$J_s = \frac{t_2 K}{F^2} \frac{1}{d} \left| t_1(-\Delta\mu_{12}) + t_2(-\Delta\mu_3) \right|$$

$$J_w = \frac{1}{d}\left\{ \frac{t_3 K}{F^2} \left| t_2(-\Delta\mu_{12}) - t_3(-\Delta\mu_3) \right| + l_{33}(-\Delta\mu_3) \right\}$$

where $(-\Delta\mu_{12})$ and $(-\Delta\mu_3)$ are the signed difference in chemical potential of both salt and water across the membrane and 'dx' is the thickness of the membrane in cm.

Therefore both the flux of salt and water are inversely proportional to the membrane thickness. The concentration of product solution, which is defined by the ratio of the two fluxes equation (6.5), is however, unaffected by the thickness of the membrane, only the rate of the desalination process changes with thickness. If the C_{60} membranes were cast as thin films with a thickness of ca 3μ (i.e. 100 times thinner) the consequent rejection and water flux (at 400 lbs.in^{-2}) could be expected to be in the region of 50-70% and 0.03 - 0.30 ml. cm^{-2} min^{-1} or 4.0 gal.ft^{-2} day^{-1} at^{-1}

(assuming/

(assuming the membrane molality and tortuosity remained unchanged). This flux rate is equivalent to some 40-400 gals. $ft.^{-2}$ day^{-1} at 1500 $lbs.in^{-2}$, which is a very considerable flow rate. It is 30 times faster than the Loeb- Sourirajan membranes and more than an order of magnitude higher than the Harwell CA(80) and CA (85).

Therefore, although the C_{60} membranes do not desalinate as effectively as the commercially used cellulose acetate membranes, there is little doubt that ion exchange membranes of this general type may be of use in desalination, if used as thin films.

Since J_w is a function of molality, tortuosity and thickness and C_p is a function of molality and is independent of both tortuosity and thickness, then it may be possible by manipulating these properties to produce a membrane which would perform one specific function. This might be accomplished by varying the type of polymer matrix, the packing of the polymer chains and the fixed charge capacity. In this way membranes could be produced either with a very large flow rate and relatively poor desalination or the inverse, a high desalination and low flow rate. The membrane could then be sculptured to fit a particular need.

By adding ZrO_2 to the NaCl feed solution which was pushed (under pressure) through a porous plate, Kraus (26) (27) produced dynamically formed ion exchange membranes. These are formed by the ZrO_2 partially blocking the porous plate and acting in an equivalent way to the fixed charge of an ion exchange polymer. By using poly-electrolytes rather than inorganic electrolytes, thin film membranes with a high degree of close packing of the polyelectrolyte might be obtained. If the polyelectrolyte was also highly charged then the internal molality would be high and rejection would be good. The water flux would depend on the

thinness of the films and to a lesser degree on the tortuosity (which would be high). As an alternative, extremely high fluxes might be obtained for low charge polymers by having a very 'loose' structured membrane. Although poor desalination could be expected, membranes of this type could be of use to desalinate brackish water (1,000 - 10,000 p.p.m. dissolved material) and also could be used for ultrafiltration. Gregor [29] has used membranes of this type for colloid separation. Since most naturally occurring colloids are negatively charged by using a cation exchange membrane, successful separation is effected with a very high flow rate without fouling.

TABLE 6.11

HYPERFILTRATION CHARACTERISTICS OF C_{60} MEMBRANES FOR FEED SOLUTION OF 0.10M NACL AT 400 lbs.in^{-2}

Membrane	PS_1	PS_3	PS_5	PS_6	PS_8	PS_9	PS_{10}	PS_{11}
Product Concentration (Moles)	0.033	0.035	0.044	0.045	0.045	0.046	0.052	0.054
Rejection $1 - \frac{C_p}{C_f}$ %	67	65	56	55	55	54	48	46
$10^3 \times J_w$ mls.cm^{-2} min.$^{-1}$	0.31	0.37	1.11	1.27	1.29	1.12	1.90	3.06

Units of Water flux of MLS. CM^{-2} MIN^{-1} have been used rather than the units of CM MIN^{-1} as these suggest the measurement of a linear velocity.

The unit gals. ft.$^{-2}$ day^{-1} have also been used in chapter (6) a useful conversion is

$$1 \text{ cm/hr} = 5.9 \text{ gals ft}^{-2} \text{ day}^{-1}$$

TABLE (6.12)

HYPERFILTRATION CHARACTERISTICS OF C_{60} MEMBRANESFOR FEED SOLUTION OF 0.10M NACL AT 200 lbs.in^{-2}

Membrane	PS_5	PS_6	PS_9	PS_{10}	PS_{11}
Product Concentration (Molar)	0.061	0.061	0.065	0.067	0.072
Rejection $1 - \frac{C_p}{C_f}$ %	39	39	35	33	28
$10^3 \times J_w$ ml. cm^2 Min^{-1}	0.70	0.77	0.67	0.13	1.87

For Data for N2 and E2 under Similar Conditions see Table (6.3)

TABLE 6.13

HYPERFILTRATION CHARACTERISTICS OF XR-170 MEMBRANES FOR FEED SOLUTION OF 0.10M NACL

	Pressure 400 lbs.in^{-2}			Pressure 200 lbs.in^{2}		
Membrane	XR-A	XR-B	XR-C	XR-A	XR-B	XR-C
Product Concentration (Molar)	0.040	0.041	0.046	0.05	0.05	0.059
Rejection $1 - \frac{C_p}{C_f}$ %	60	59	54	50	50	41
$10^3 \times J_w$ ml. cm^2 min.$^{-1}$	0.52	0.72	1.57	0.24	0.48	0.76

SUPPLEMENTARY LEGEND FOR THE FIGURES OF CHAPTER 6.3

Figure 6.8

Graph of both rejection and water flux at 200 and 400 lbs.in^{-2} for the C_{60} and XR-170 membranes where solid lines represent the rejection data, broken lines the water flow data. The points $\Phi, \odot$, represent the data for the C_{60} membrane at 200 and 400 lbs.in^{-2} respectively.

Φ $\odot$ represent respectively the data for the XR-170 membranes at 200 and 400 lbs.in^{-2}.

Figure 6.9

Rejection data for membranes N_2 and E_2 at both 200, Φ, and 400 $\odot$ lbs.in^{-2}.

Figure 6.10

Graph of water flow data $10_3 \times J_w$, against Tortuosity for both the C_{60} (solid lines) and XR-170 membranes (broken lines).

Figure 6.11

Graph of Rejection data against C_{3/C_1} for the C_{60} membranes at 200, Φ, and 400, $\odot$, lbs.in^{-2}

Figure 6.12

Graph of water flow data, $10^3 \times J_w$, against the water capacity of the C_{60} membrane, C_3, Φ, 200 lbs.in^{-2}, $\odot$, 400 lbs.in^{-2}, and the XR-170 membrane, Φ.

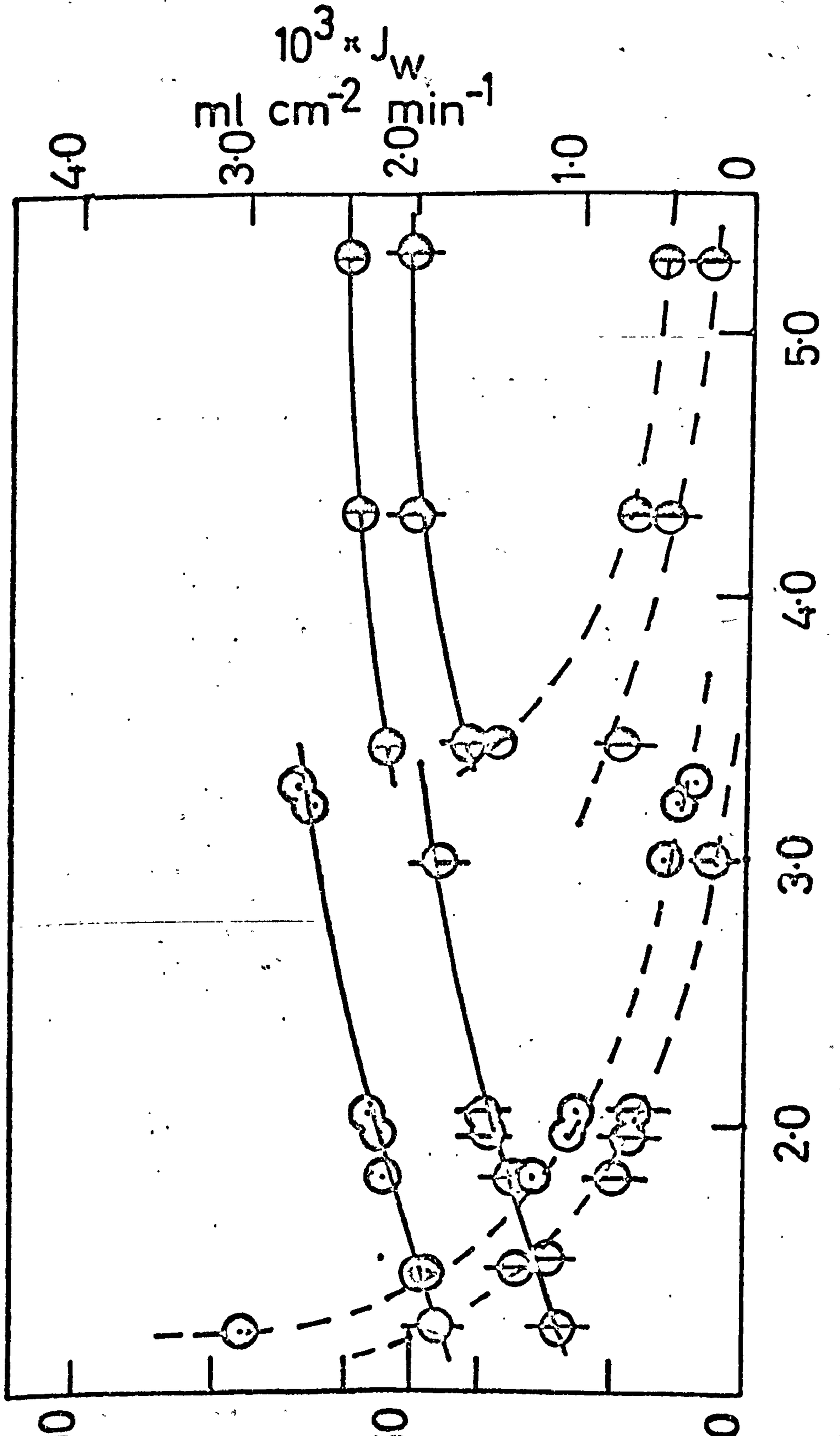
$10^3 \times J_w$
ml cm^{-2} min^{-1}
4.0
3.0
2.0
1.0
0
5.0
4.0
3.0
2.0
Internal Molality
100
50
0
Rejection

Fig.68

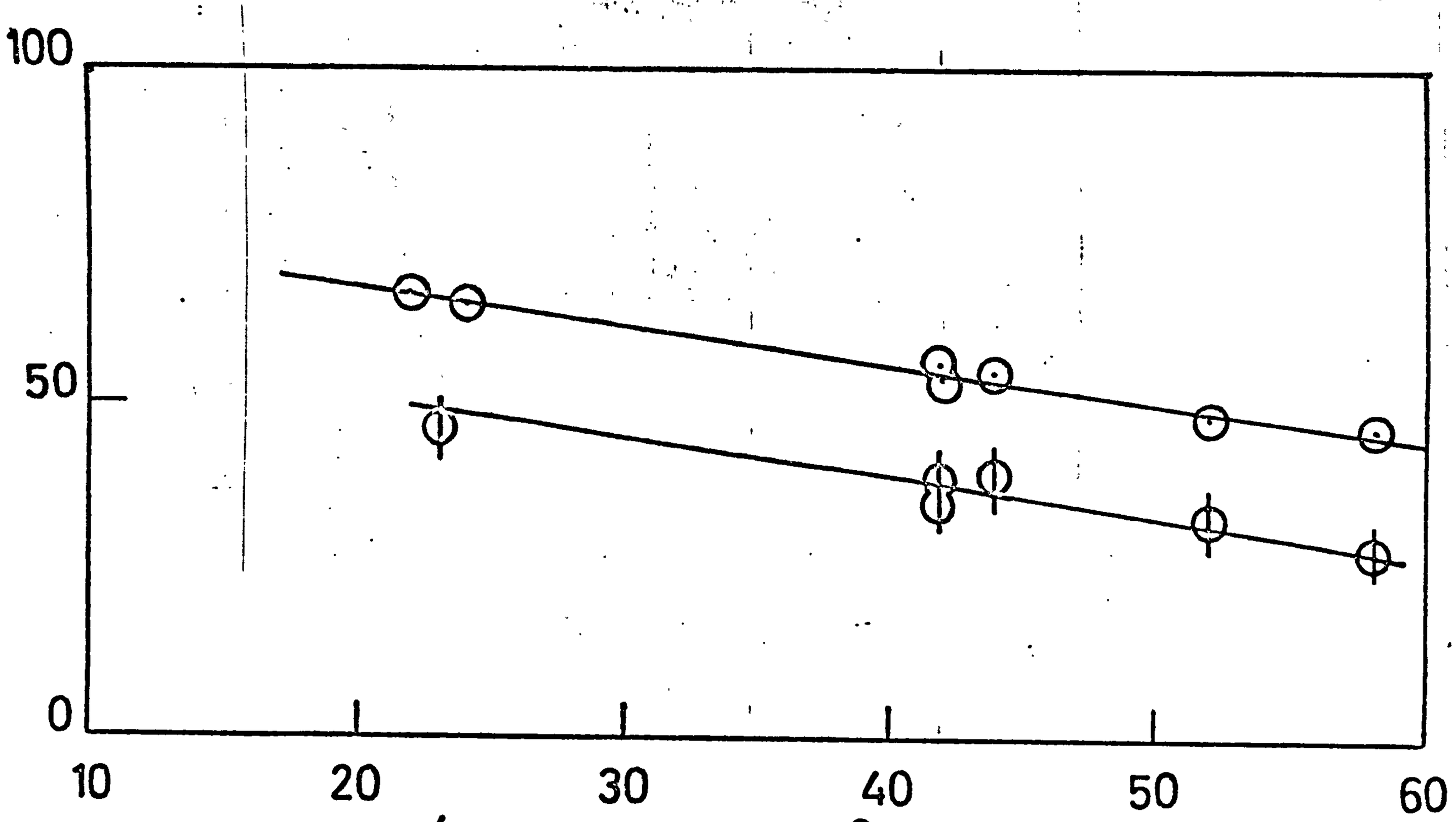

Fig. 6.9

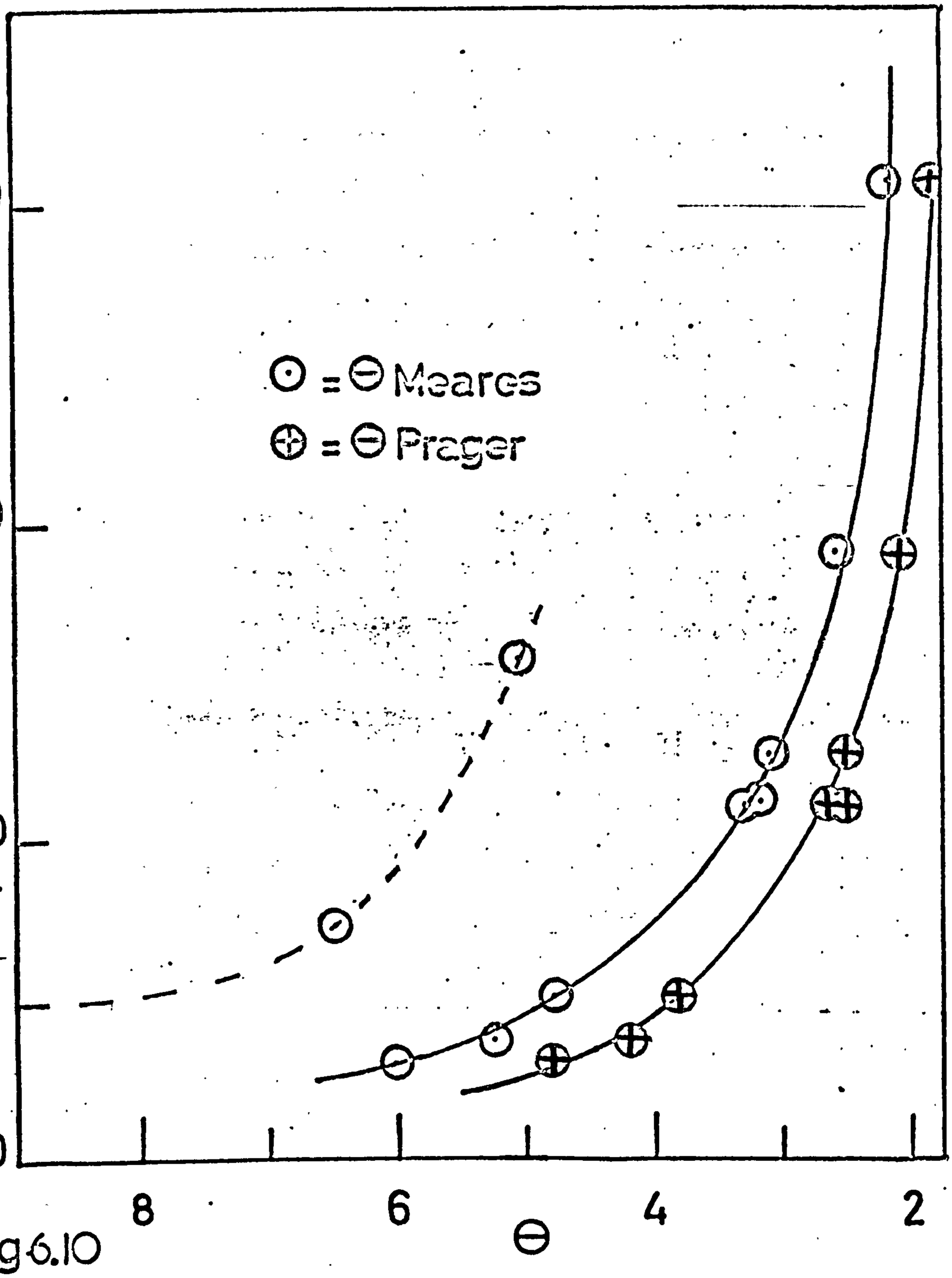

Fig 6.10

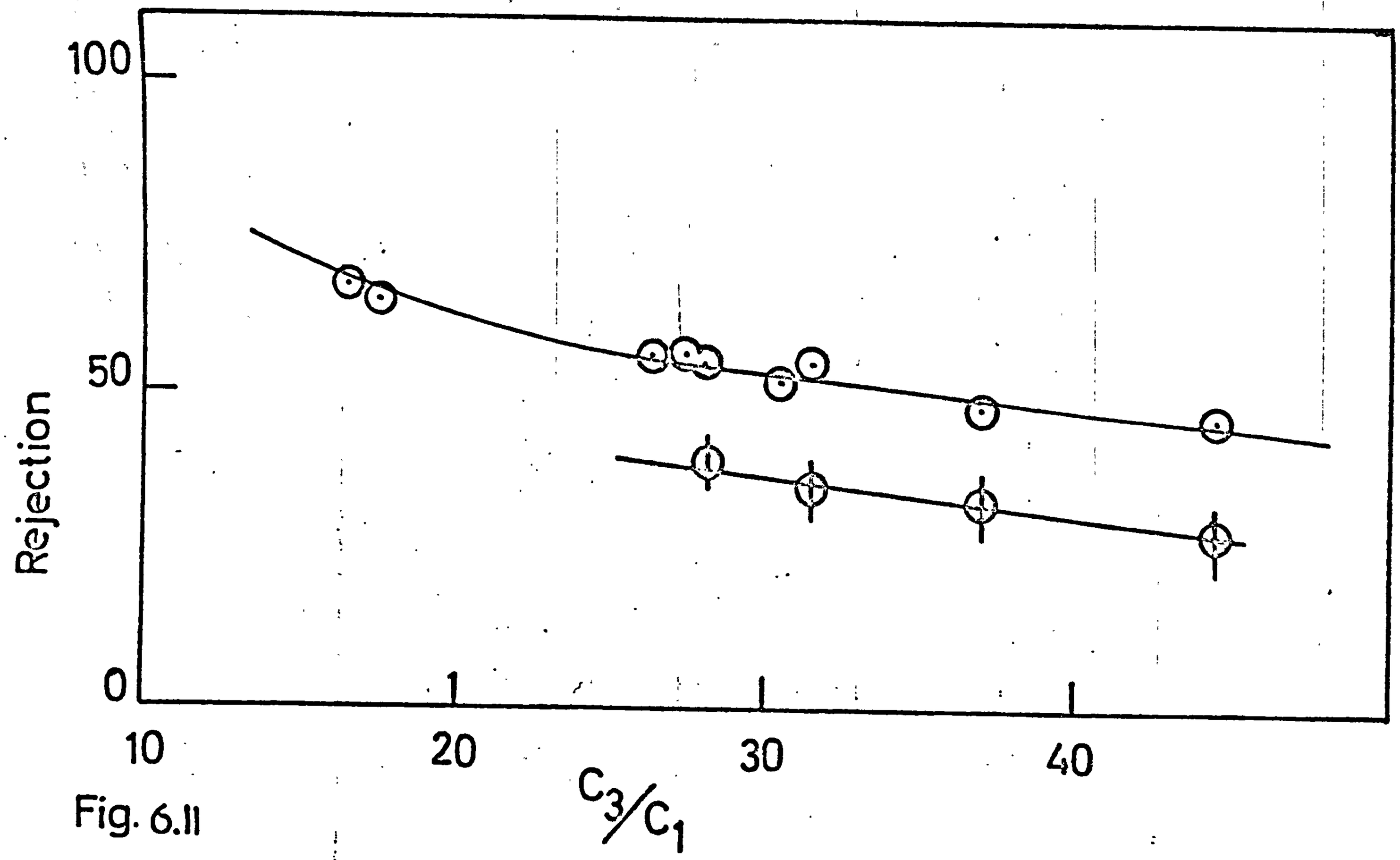

Fig. 6.11

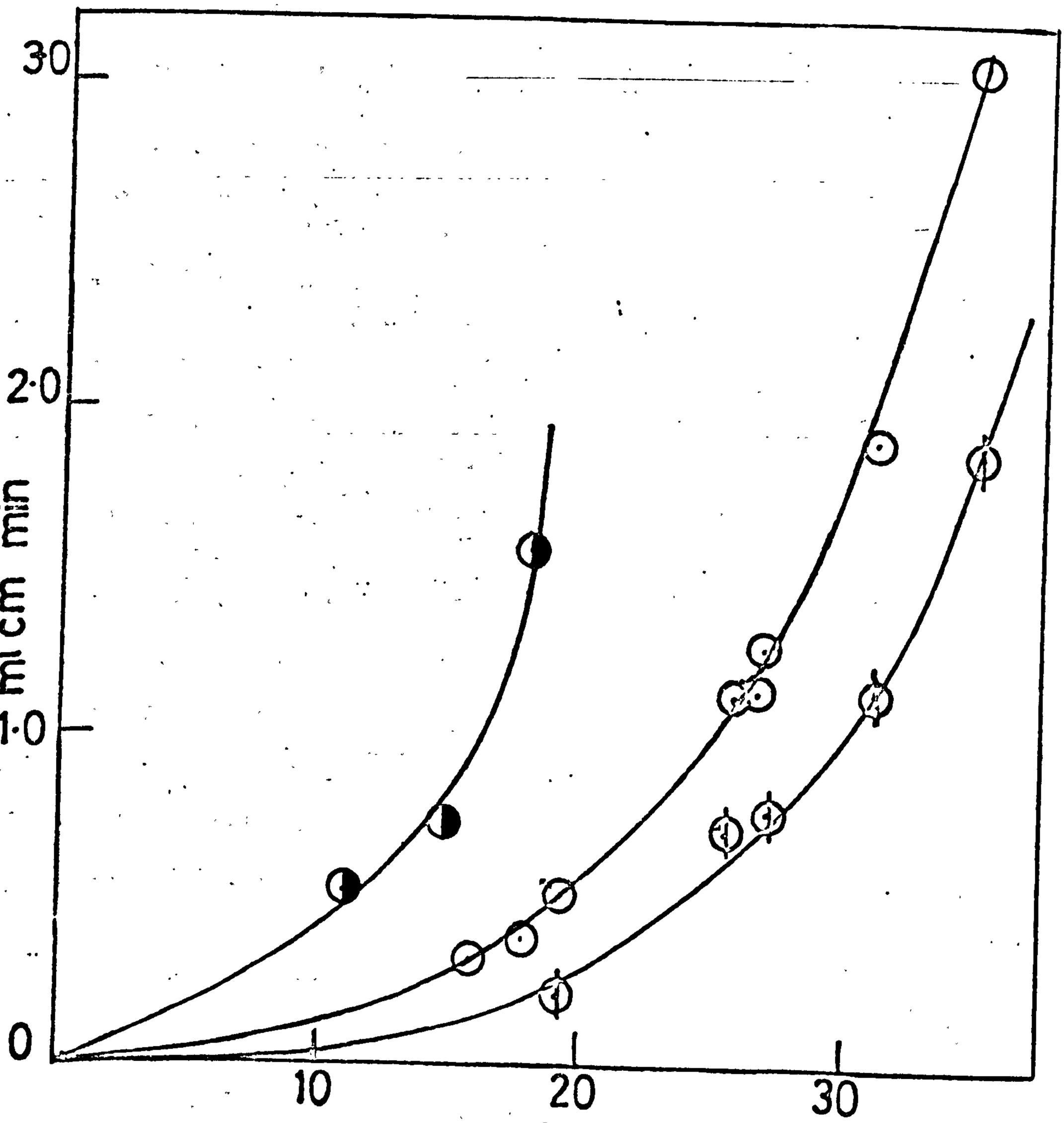

Fig. 6.12

REFERENCES

CHAPTER 6.

1) J. Janz and R. Gordon. J. Am. Chem. Soc. 65,(1943,)228.

2) D.G. Miller. J. Phys. Chem.(1966,)70, 2639.

3) C.R. Gardner and R. Paterson. J. Chem. Soc. (A)(1971.)2254

4) C.R. Gardner and R. Paterson. Diffusion Processes, Proc. Thomas Graham Memorial Symposium (Gordon and Breach, London, 1970).

5) K.A. Kraus, A.J. Shor and J.S. Johnson. Desalination (1967) 2, 243.

6) C.R. Gardner and R. Paterson. J. Chem. Soc. Faraday, I.(1972)Vol.68,2031.

7) W.H. Baldwin, D.L. Holcomb and J.S. Johnson. J. Polymer Science A.3,833 (1965)

8) A.S. Michaels et al. J. Phys. Chem. 69, 1456 (1965).

9) A.S. Michaels and H.J. Bixler. Mass. Inst. Tech. Rept. 315-1. DSR.9407 (1965).

10) K.S. Spiegler, J.G. McKelvey and M.R.J. Wyllie. Chem.Eng. Prager Symp. 55 No.24,(1959.)

11) C.E. Reid and E.J. Breton. J. App. Polymer Science 1, 133, (1959)

12) E.J. Breton, Office of Saline Water, Res. Devel Prager. Rept. 16 P.B. 161391,(1957.)

13) J.G. McKelvey, K.S. Spiegler and M.R.J. Wyllie. J. Phys. Chem.61.174 (1957)

14) Reviewed - Desalination by Reverse Osmosis. Ed. Merten. M.I.T. Press(1966)

15) Reviewed-Reverse Osmosis. Ed. S. Sourirajan. Logus Press,(1970.)

16) J.S. Johnson, L. Dresner and K.A. Kraus.- Review of Reverse Osmosis, Principles of Desalination ed. by K.S. Spiegler. pp.345 - 439 Academic Press. Inc. New York (1966).

17) D.V. Mehta and F. Meinecke, Desalination (1972) 10 (4) 369.

18) L. Dresner, Desalination (1972) 10, 1, 27.

19) C.P. Bean. Office of Saline Water. Res. and Devel.Progress Rept. No. 465. (1969).

20) E. Glueckauf, D.C. Sammon. 3rd International Symposium in Fresh Water from the Sea. Vol. 2. 397 — 422. (1970).

21) J. Kopecek and S. Sourirajan. Ind. Eng. Chem. Process design Development (1969).

22) W.S. Gillam. H.E. Podall. Desalination(1971) 9.201.

23) O. Kedem and A. Katchalsky. J. Gen. Physiol. 45, 143 (1961)

24) O. Kedem, R. Black and G. Thom. Desalination (1966), 129.

REFERENCES

CHAPTER 6 (Continued)

25) K.A. Kraus, A.J. Shor, and J.S. Johnson. Desalination (1968) 68,53 166U

26) H.K. Lonsdale, U. Merten and R.L. Riley. J. App. Polymer Science 9, 1341, (1956).

27) K.A. Kraus et al. J. Am. Chem. Soc. 88, 5744 (1966).

28) K.A. Kraus et al. Proc. Second International Conference on the Peaceful Users of Atomic Energy. Geneva 28. 3 (1958)

29) H.P. Gregor. Advanced Study Institute on Charged Gels and Membranes Forges-Les-Eaux. France(1973.)

CHAPTER 7.

MEASUREMENT OF TOTAL PRESSURE POTENTIAL AND STREAMING POTENTIAL IN A REVERSE OSMOSIS EXPERIMENT

7.1. Pressure Potential and Streaming Potential Measurements.

In a reverse osmosis experiment an electrical potential is developed between the concentrated feed and partially desalinated product. It is the aim of this section to review the published literature in this field and to examine theoretically how this potential may be predicted in terms of accessible membrane parameters.

Using the theory of irreversible thermodynamics, an equation describing the total pressure potential developed between two reversible electrodes on each side of the membrane has been derived, equation (2.52). Few if any approximations have been made and the equation may be considered rigorous. It depends upon two definite assumptions. The first is fundamental to all applications of linear theory, namely, that the O.R.R. are obeyed. On a more trivial level the equation as written may be applied and used to predict observed potentials if the chemical potential gradients across the membrane are linear. This test is trivial from a theoretical point of view since non-linearity in chemical potential gradients could be allowed for by suitable integration procedures across the membrane.

Until very recently there were very few reported measurements of streaming potential in membranes. Amongst the first published data are those of Schmid and Schwartz [1] [2] who measured the potentials set up by applying very low pressures (63 mm Hg) across a collodion membrane which separated two KCl solutions of equal concentration (2×10^{-4}M KCl). These workers illustrated the difficulty of obtaining quantitative measurements of streaming potential by a direct method. Streaming potential, in membranes, is set up by the displacement of the counter-ion from the fixed charge/

charge. This displacement is caused by the coupling between the counter-ions and the moving pore solution (under an applied pressure). The streaming potential, therefore, contains no contribution from any concentration differences across the membrane. The experimental system used by Schmid and Schwartz might, therefore, be expected to provide streaming potentials. However, since the collodion membrane will to some degree act as a reverse osmosis membrane, a concentration gradient across the membrane will be created. A diffusion potential will, therefore, be set up and the measured potential will contain contributions from it.

Stewart and Graydon [3] using a series of sulphonic acid exchangers with varied fixed charge capacity and cross-linking, measured the effect on the diffusion potential (set up by solutions of 0.05 and 0.1M on either side of the membrane) of applying pressures up to 3 atmospheres. Their attempts to predict the change in the measured potential, which they attributed to the streaming potential, was again made difficult by the concentration potential created by the permselective membrane.

By employing a pressure pulse method Brun and Vaula [4] determined electro-osmotic transport numbers of phenol sulphonic acid formaldehyde membranes from the measured streaming potentials. However, the values of the cross coefficients L_{EP} and the hydrodynamic permeability, σ, obtained from the potential measurements, differed considerably from the values obtained by direct measurement. The discrepancy was accounted for by the failure of the equation used to describe the diffusion potential created by the membrane.

In early work Speigler [5] reports measuring the streaming potentials of several ion exchangers. The method employed was similar/

similar to that used in this work, although Speigler used thermal convection and not a flow system to prevent concentration polarization at the membrane surface. He initially maintained identical solutions on both sides of the membrane and high pressures of up to 1,500 lb.in^{-2} were applied. Since no attempt was made to separate the various contributions to the pressure potential Speigler, in fact, measured the total potential change with pressure and not the true streaming potential.

Therefore, to date no attempt has been made to accurately measure the true streaming potential across an ion exchange membrane. It was thus an integral and equally challenging part of this work to design, construct and operate a high pressure apparatus which was suitable for such precise potentiometric measurements.

7.1.1. The Pressure Potential Equation

In section (2.2.3) the pressure potential equation was developed. It represents the potential difference between two reversible (Ag./Agcl) electrodes placed one on each side of a reverse osmosis membrane. The conditions are those of the steady state and the potential is thustime invariant.

The final equation for the pressure potential is given below.

$$E_{tot} = \underbrace{\frac{P}{F}\left(\hat{V}_{Ag} - \hat{V}_{Agcl}\right)}_{I} + \underbrace{t_3^I \frac{RT}{F} \ln \frac{a_3''}{a_3'}}_{II} + \underbrace{2t_1^I \frac{RT}{F} \ln \frac{M_s'' \gamma_\pm''}{M_s' \gamma_\pm'}}_{III} + \underbrace{\frac{P}{F}\left(t_1^I \hat{V}_{12} + t_3^I \hat{V}_3\right)}_{IV} \quad (2.52)$$

where $E_{tot} = E_{LP} - E_{HP}$ and is the total pressure potential across the membrane in mV.

$\hat{V}_{Ag}, \hat{V}_{Agcl}$ are the partial molar volumes of silver and silver chloride respectively in m^3 mol^{-1}.

P is the pressure difference across the membrane, i.e. the applied pressure.

$\therefore$ $\frac{P.\hat{V}_i}{F}$ has units of volts.

F is the Faraday.

R is the gas content in J, K^{-1} Mol^{-1}

T is the temperature in K

$\frac{RT}{F}$ has units of volts.

a_3'', a_3' are the activities of water on the high and low sides of the membrane.

$M_s'' \gamma_{\pm}''$, $M_s' \gamma_{\pm}'$ are the molarities and activity coefficients of electrolyte on the high and low pressure side of the membrane.

$t_1^I + t_3^I$ appear in equation (2.52) from the integration of the Henderson equation, section (2.2.3).

They are defined as $t_1^I = \frac{Z_1 l_{11} + Z_1 Z_2 l_{21}}{\propto}$

$$t_3^I = \frac{Z_1 l_{13} + Z_2 l_{23}}{\propto}$$

For a finite difference in concentration across the membrane t_1^I and t_3^I are integral transport and transference numbers respectively.

If the O.R.R. are assumed then $l_{12} = l_{21}$, $l_{23} = l_{32}$ and $l_{13} = l_{31}$.

Under such condition the integral transport and transference numbers are equivalent to those determined directly, with no concentration gradients across the membrane, section (4.1.11), that is

$$t_1^I = t_1^D \quad \text{and}$$

$$t_3^I = t_3^D$$

This is also the case in solution systems, vis a vis Hittorf and concentration cell emf transport and transference numbers.

Terms II and III of equation (2.52) represent the potential across the membrane with P = 0, i.e. with a concentration gradient alone. These two terms make up the well established membrane diffusion potential.

Under the conditions of $\Delta C = 0$, that is, no concentration gradient existing across the membrane, equation (2.52) reduces to I and IV

$$E_{\Delta C = 0} = \frac{P}{F}\underbrace{(\hat{V}_{Ag} - \hat{V}_{AgCl})}_{I} + \underbrace{\frac{P}{F}(t_1\hat{V}_{12} + t_3\hat{V}_3)}_{IV} \qquad (2.52a)$$

Term I is the potential set up by the effect of pressure on the volume change of the electrodes.

Term IV comes from the integration of the Henderson equation and this represents the effect of pressure on the pore solution in the membrane. This, by definition, is the true membrane streaming potential.

In section (4.1.II) it was shown that for an electro-osmosis experiment using Ag/AgCl electrodes, ΔV, the change in volume per Faraday on the Cathodic side, is given by equation (2.77)

$$\Delta V = t_3\hat{V}_3 + t_1\hat{V}_{12} + \hat{V}_{Ag} - \hat{V}_{AgCl}$$

In the usual terminology of membrane studies $\frac{\Delta V}{F}$, the volume change per coulomb of electricity, is equivalent to the volume flow per area of membrane per unit time, J_v, divided by the current density I, so that

$$\left(\frac{\Delta V}{F}\right)_{\Delta P=\Delta C=0} = \left(\frac{J_v}{I}\right)_{\Delta P=\Delta C=0} = \frac{t_3\hat{V}_3}{F} + \frac{t_1\hat{V}_{12}}{F} + \frac{\hat{V}_{Ag} - \hat{V}_{AgCl}}{F} \qquad (7.1)$$

From equation (2.52a)

$$\left(\frac{E}{P}\right)_{\Delta C=I=0} = \frac{t_3\hat{V}_3 + t_1\hat{V}_{12}}{F} + \frac{\hat{V}_{Ag} - \hat{V}_{AgCl}}{F} \qquad (7.2)$$

Combining equations (7.1) and (7.2) gives

$$\left(\frac{\Delta E}{P}\right)_{\Delta C=I=0} = \left(\frac{J_v}{I}\right)_{P=\Delta C=0}$$

which are the Saxen Relationship, given in section (22.3.2) . Only if the O.R.R. hold are these relationships valid. (The direct transport and transference numbers will be referred to as t_1 and t_3 unless a comparison with the integral values is being made.) Terms I and IV, therefore, constitute the direct pressure contribution to E_{tot}, equation (2.52). This would be the pressure potential measured across a membrane, where no concentration gradient was created, either as a condition of the experiment or by the reverse osmosis property of the membrane. Although this potential was defined by Saxen as the streaming potential, the true streaming potential of the membrane is defined by term IV of equation (2.52) that is

$$E_{\text{Streaming}} = \frac{P}{F}(t_1\hat{V}_{12} + t_3\hat{V}_3) \qquad (7.3)$$

The streaming potential referred to in this work will be that defined by equation (7.3).

7.1.2 The Magnitude of the Individual Terms, and Souces of Thermodynamic Data.

From ref[6] the specific gravity and molecular weight of silver are 10.5 $g.cm^{-3}$ and 107.88 $g.mol^{-1}$ respectively. From the same source these properties for silver chloride are 5.56 $g.cm^{-3}$ and 143.34 $g.mol^{-1}$ hence

$$\hat{V}_{Ag} = 10.28 \times 10^{-6} m^3\ mol^{-1}$$
$$\hat{V}_{Agcl} = 25.8 \times 10^{-6} m^3\ mol^{-1}$$

Term I, therefore, makes a negative contribution of some 0.0163 mV $at.^{-1}$ (-0.111 mV/100 $lbs.in^{-2}$). Thus, although this term is small/

small, it would be greater than 1.0 mV at 1000 lbs.in^{-2} and consequently must be included for an accurate analysis, especially if the pressure and streaming potentials are small.

In term IV the partial molar volume of salt and water, $\hat{V}_{12}$ and $\hat{V}_3$, were calculated in the following way.

The apparent molar volume of the electrolyte was calculated from the expression.

$$\phi = \phi^{o}_{v} + S_v\sqrt{C} \qquad (7.4)$$

values of ϕ^{o}_{v} and S_v were taken from (7) (8).

The partial molar volume was determined from the Masson equation (9)

$$\hat{V}_{12} = \phi_v + \frac{m^{\frac{1}{2}}}{2} \frac{d\phi_v}{d\sqrt{m}} \qquad (7.5)$$

Using these equations a value of 17.61 x 10^{-6} $m^3.mol^{-1}$ was obtained for 0.10M Nacl.

Equations (7.4) (7.5) were used to evaluate the partial molar volumes of the various concentrations of desalinated product solution.

The partial molal volume of water was taken to be equivalent to the apparent molar volume and calculated from molecular weight and density data to be 18.07 x 10^{-6} $m^3.mol.^{-1}$.

The electro osmotic transference numbers, t^{D}_{3}, were measured for each membrane, section (4.1.11) The transport number of counter-ion t_1 was taken to be 0.998 for the normal C_{60} membranes and 0.996 for the expanded C_{60} membranes (20). For the XR series the transport number of counter-ion was taken to be unity.

An experimentally determined t_1 value was not required for each membrane due to a combination of two factors.

(1)/

(1) Past work by Gardner and Paterson on the C_{60} membrane, has shown that even with an increase in the external electrolyte concentration from 0.10M to 1.0M NaCl, which increases the salt uptake of the membrane from 0.002- 0.090 m.mol.cm^{-3}, t_1 only changes from .990 to .951.

(2) Since 10 is a typical value of t_3, the contribution from $t_1\hat{V}_{12}$ to the calculated streaming potential is at most some 10%.

Therefore, a change in t_1 of, for example, 5% over the range of C_{60} membranes would have a very small effect on the calculated streaming potential.

As $\hat{V}_{12}$ and $\hat{V}_3$ have similar magnitudes but $t_1 \gg t_3$, term IV and, thus, the streaming potential will depend almost entirely on the electro-osmotic transference number. This means that the true streaming potential, equation (7.3) depends on the difference between the coupling of counter-ion with water, and co-ion with water, i.e. l_{13} and l_{23}.

By considering only $t_3\hat{V}_3$, for a membrane with an electro-osmotic transport number of 10, the streaming potential would increase by approximately 0.2mV at^{-1} (1.45 mV/100 lbs.in^{-2}).

If under an applied pressure gradient the membrane is permselective and rejects salt on the high pressure side and allows solvent water to pass through, the contribution from the concentration gradient is described by terms II and III.

Term II, $t_3 \frac{RT}{F} \ln \frac{a_3}{a_3'}$ describes the contribution from the osmotic pressure set up across the membrane. This can be re-written as $\frac{t_3}{F}(\Pi' - \Pi'')\hat{V}_3$ where Π' and Π'' are the osmotic pressures of the product and feed solutions. Since the activity of water in the dilute (low pressure) solution will be greater than that in the

more concentrated feed solution, this term will also make a negative contribution to the total pressure potential. Its magnitude will depend on t_3 and C_p. Fig. (7.1) illustrates that term II (for 0.10M NaCl) is small. For a typical ion exchange, with a t_3 of 10 and a rejection of 50% this contribution will amount to less than 0.5 mV. The water activity data for 0.10M NaCl, were obtained from references (10)(11).

The contribution from the electrolyte activities in the high and low pressure solutions is given by

$$2t_1 \frac{RT}{F} \ln \frac{M_s'' \gamma_{\pm}''}{M_s' \gamma_{\pm}'}$$

Figure (7.2) shows that this term increases with increasing rejection (decreasing product concentration) and makes a considerable contribution to the total pressure potential. For example, at a rejection of 90% this term predicts a contribution of greater than 100 mV ($t_1 = 1$).

In equation (2.52) this term will, therefore, make the largest single contribution to the total potential measured (as long as $t_1 = 1$) and will thus be the dominant term.

7.1.3. The Measured Pressure Potentials for the C_{60} and XR-170 Membranes in 0.10M NaCl.

Using the reverse osmosis system II, total pressure potential measurements were made across a number of membranes and values of volume flow and product concentration obtained in the same experiment.. Equation (2.52) allowed comparison between these measured pressure potentials and the predicted values.

The measured pressure potentials for the range of C_{60} membranes at applied pressures of 200 and 400 $lbs.in^{-2}$ are shown in Tables (7.1) (7.2).

The/

The dependence of the observed pressure potentials on the applied pressure is well illustrated. At 200 lbs.in^{-2} the pressure potential of each membrane is approximately half that at 400 lbs.in^{-2}.

For both applied pressures the pressure potential decreases as the membrane becomes more dilute and the molality thus decreases. The total potential decreases from 57.64 mV, in the C_{60} with the highest molality, to 42.0 mV in the membrane with the lowest internal molality. The variation in pressure potential with total membrane molality is illustrated in Fig. (7.3). The results obtained for the C_{60} membrane (at 400 lbs.in^{-2}) defined a smooth curve when plotted against the internal molality of the membrane.

The measured pressure potentials obtained for the three XR membranes at 400 lbs.in^{-2}, are very similar in magnitude to the C_{60} values. Table (7.3 However, at 200 lbs.in^{-2}, the values obtained for the XR membranes were larger than those for the C_{60} membranes. These larger values are caused by a larger diffusion potential term. The XR membranes did not exhibit the progressive decrease in pressure potential with decreasing molality. At both 200 and 400 lbs.in^{-2} the pressure potential passed through a maxima at membrane XR-B.

Equation (2.52) is very successful in predicting the pressure potentials at both pressures for the two membrane types investigated and the excellent agreement establishes the validity of the equation.

For the C_{60} membranes, at 400 lbs.in^{-2} the maximum deviation between calculated and observed pressure potentials occurs for the most expanded membrane, and is 2.15mV in a measured potential of 42.0 mV. This is anomously high. Each of the other calculated values agrees to within $\pm$ 1.0 mV of the observed pressure potentials and the majority agree to better than $\pm$ 0.5 mV. At 200 lbs.in^{-2} the/

the agreement for the range of C_{60} membranes is $\pm$ 1.0 mV. For the XR-membranes the agreement between the experimentally observed and calculated pressure potentials was not quite so good. At both pressures the observed potential was greater than the calculated value.

7.1.3.1 The Individual Contribution to the Pressure Potential.

The collective negative contribution to the total pressure —potentials obtained from the electrode term I, and the water osmotic term II, is small. This contribution ranges from approximately 1 mV in 57.6 mV to $\approx$ 1.7 mV in 42 mV in the C_{60} membranes at 400 lbs.in^{-2}. that is, between 2-4% of the measured pressure potential. In the C_{60} membranes at 200 lbs.in^{-2} this contribution is a maximum of $\approx$ 1mV in a pressure potential of 21 mV. The contribution from these terms is of similar consequence in the three XR membranes at both 200 and 400 lbs.in^{-2}, Table (7.3).

As predicted by equation (2.52) the contribution from term III makes the largest single contribution to the total potential measured. At 400 lbs.in^{-2} this contribution ranges from 91% - 80% of the measured pressure potential in the XR membranes, and 91-70% in the C_{60} series. This contribution decreases because the rejection achieved by the membranes becomes less efficient as the internal membrane molality becomes lower.

The contributions from term IV range from 5.88 to 14.49 mV for the C_{60} membranes, at 400 lbs.in^{-2}, and from 5.8 to 9.74 at this pressure for the XR series. The contribution to the total pressure potential from this term becomes of increasing significance as the total internal molality of the membrane decreases, and t_3 consequently

becomes larger. Indeed for the most expanded C_{60} membrane (lowest internal molality) the contribution from term IV to the measured pressure potential is 33%.

Since term I is a constant at a defined pressure, and the diffusion potential contribution, terms (II + III), decreases while the true streaming potential, term IV, increases, with decreasing membrane molality, the magnitude of the measured pressure potential is a balance between these two opposing trends, Fig. (7.3)

7.1.3.2. The estimated Streaming Potential for the C_{60} and XR Membranes in 0.1OM NaCl.

Once terms I, II and III of equation (2.52) are evaluated from the appropriate data, an estimated membrane streaming potential can be obtained by subtraction of these three terms from the observed total pressure potential. That is

$$\text{Estimated Streaming Potential} = E_{obs.} - \frac{P}{F}(\hat{V}_{Ag} - \hat{V}_{Agcl}) - \frac{t_{3RT}}{F} \ln \frac{a_3''}{a_3'} - 2t_1 \frac{RT}{F} \ln \frac{M_s'' \gamma_{\pm}''}{M_s' \gamma_{\pm}'} \quad (7.6)$$

Table (7.1) shows that the streaming potentials, calculated from term IV of equation (2.52), are in relatively good agreement with those estimated from equation (7.6) above. At 400 lbs.in^{-2} the agreement for the C_{60} membranes was $\pm$ 1.0 mV, apart from the most expanded membrane, where thecalculated streaming potential was 2.2 mV larger than the estimated. At 200 lbs.in^{-2} the agreement was $\pm$ 1.3 mV. For the XR series the agreement was less satisfactory, the measured values being greater than those calculated. At 200 lbs.in^{-2} the difference was some 1.3 mV, whereas at 400 lbs.in^{-2} it was a maximum of 3.9 mV for XR-C. The differences between

observed/

observed and calculated streaming potentials may, to some degree, be caused by slight inaccuracies in the estimate of Cp. Any error in the value of the diffusion potential would considerably change the estimated streaming potential.

7.2. Pressure and Streaming Potentials in 0.05M $CaCl_2$ for a Normal and Expanded C_{60} Membrane.

As final proof of the ability of equation (2.52) to predict the pressure potential which is generated in a reverse osmosis system, and of its ability to evaluate each contribution, some experimentation on a normal (PS_1) and expanded (PS_5) C_{60} membrane was carried out in 0.05M $CaCl_2$, at 400 lbs.in^{-2} applied pressure.

Changing the counter-ion to the divalent calcium ion alters equation (2.52). This became

$$E_{rev} = \frac{P}{F}(\hat{V}_{Ag} - \hat{V}_{AgCl}) + t_3 \frac{RT}{F} \ln \frac{a_3''}{a_3'} + \frac{3}{2} t_1 \frac{RT}{F} \ln \frac{M_s'' \gamma_\pm''}{M_s' \gamma_\pm'} + \frac{P}{F}\left(\frac{t_1}{2}\hat{V}_{12} + t_3\hat{V}_3\right)$$

The partial molar volume of the $CaCl_2$ was calculated from equations (7.4)(7.5). Water activity coefficient and salt activity coefficients were obtained from reference (10).

The measured and calculated pressure potentials and the different contributions are shown in Table (7.4).

The pressure potentials of both normal and expanded membranes were considerably lower (some 3.5 - 4.0 times) than those measured in the 0.1M NaCl solution. The main reason for this is the much smaller diffusion potentials which are a consequence of the poorer rejection (36 and 20% respectively). The t_1 values for the normal and expanded C_{60} membrane in 0.05 $CaCl_2$ were taken as 0.989 and 0.982 respectively (11).

The pressure potentials calculated from equation (2.52) are in good agreement with those measured. For both membranes

the calculated values are slightly larger than those observed. The values differ by 1.3 mV and 0.6 mV respectively in the normal and expanded membranes.

The negative contributions from terms I and II are very small being-0.64 mV and -0.58 mV in PS_1 and PS_5 respectively. Because of the small concentration gradients and relatively small t_3, the contribution from term II is small, and thus the electrode correction, term I, is by far the most significant of the two.

The estimated (true) streaming potentials are smaller than in the 0.1M NaCl and this decrease is more pronounced in the expanded C_{60} membrane.

The estimated (true) streaming potentials of the PS_1 and PS_5 are plotted against total internal molality, Fig. (7.3). Both are below the line defined by the results for 0.10M NaCl. This suggests that the reduction in streaming potential observed in the Ca^{2+} form is a consequence of not only the reduced internal molality, but also of the increased association of the divalent counter-ion with the fixed charge.

The streaming potentials calculated from term IV are in good agreement with those estimated ($E_{obs.}$ - (terms I + II + III). For both normal and expanded membranes the calculated value is approximately 1.0 mV larger than the observed.

Equation (2.52), therefore, successfully describes the pressure potential, and the various contributions to the pressure potential, for the C_{60} series in both 0.10M NaCl and 0.05M $CaCl_2$, and for the XR-170 series in 0.10M NaCl. The equation allows the true streaming potentials to be estimated from the observed pressure potential and the values obtained agreed well with those calculated. Since the accuracy of term IV to provide streaming potentials is established/

established, by using the S.M.C. to obtain t_3 value (for 0.1M NaCl) the true streaming potential could be calculated entirely theoretically. Indeed by using the prediction calculation described in section (6.1) the pressure potential across the C_{60} membranes could be at least qualitatively established by a completely theoretical method. However, the information which could be obtained from a simple pressure potential value is limited, since the contribution from the individual terms varies with the applied pressure and molality of the membrane.

7.3.1. Determination of Integral Electro-Osmotic Transference Numbers from the Total Pressure Potential Measurements.

Once the desalinated product concentration was determined, by equating the observed(steady state) total pressure potential of each membrane with equation (2.52) values of the integral electro-osmotic transference number t_3^I were obtained, Table (7.1).

For the C_{60} membranes (at 400 lbs.in^{-2} in 0.10M NaCl) the t_3^I values were in good agreement with the directly obtained electro-osmotic transference numbers, t_3^D. The agreement was especially close for the two normal membranes, (PS_1) and (PS_3). The t_3^I value determined for the most expanded C_{60} membrane, PS_{11}, deviated most from the value obtained directly. However, the former was much closer to the electro-osmotic transference number predicted from the S.M.C. Table (5.7). The t_3^I value obtained for PS_{11} was confirmed by the experiments conducted at 200 lbs.in^{-2}, as was the t_3^I value for PS_5. The t_3^I values obtained for the other C_{60} membranes at this pressure varied considerably from the/

the integral values obtained at 400 lbs.in^{-2} and from the direct electro-osmotic transference numbers.

For the expanded C_{60} membrane (PS_5) in 0.05 $CaCl_2$ the t_3^I value of 10.19 was in good agreement with the value of 11.93 obtained directly, Table (7.4). However, the t_3^I value of 6.6 obtained for the normal C_{60} membrane (PS_1) was considerably lower than the t_3^D value of 9.05.

For the XR-A at both 200 and 400 lbs.in^{-2}, the t_3^I values are in good agreement. The average of these two values is idential to the t_3^D value. However, each of the t_3^I values for the other XR membranes is in poor agreement with the direct electro-osmotic transference numbers. At both pressures the t_3^I values are considerably larger than the t_3^D values. However, in general, this indirect method provides an alternative procedure for the determination of electro-osmotic transference numbers which could be used with confidence to provide t_3 values for membranes which were not amenable to investigation by the direct method.

7.3.2. Investigation of a Pressure Pulse Method for determination of Electro-Osmotic Transference Numbers

By maintaining 0.10M NaCl on both sides of the membrane at the beginning of an experiment and applying pressure in short (20 second) pulses (of 50 or 100 lbs.in^{-2} from 0 - 400 lbs.in^{-2}) a plot of ΔE_{pulse} against ΔP_{pulse} was obtained for several C_{60} membranes. If it is assumed that the initial potential jump is due solely to the pressure terms of equation (2.52), then t_3^I may be estimated. That is

$$\Delta E_{pulse} = \frac{\Delta P_{pulse}}{F} (t_1\hat{V}_{12} + t_3\hat{V}_3 + \hat{V}_{Ag} - \hat{V}_{AgCl}).$$

This/

This assumption assumes that on the time scale of the pressure jump the membrane does not have sufficient time to establish new internal concentration gradients which extend to the low pressure side. Figures (7.4) (7.5) show examples of the effect of pressure pulses across a normal (PS_1) and expanded (PS_8) membrane. On every occasion the pressure pulse method was employed, the electrode response was immediate. The potential jumps become slightly larger towards the end of the pulse experiment, almost certainly because in the time elapsed between the first pulse, 0-50 lbs.in^{-2} and the last, 350 - 400 lbs.in^{-2}, a diffusion potential contribution begins to increase the potential measured.

Table (7.5) shows the t_3^I values obtained by the pressure pulse method for four C_{60} membranes.

The t_3^I values obtained for PS_1 and PS_{10}, especially the latter, are in good agreement with those obtained by the direct method. However, the values of 14.5 for PS_2 and 32.3 for PS_8 are in poor agreement with the direct values. They are considerably larger than the electro-osmotic transference values obtained by either of the other methods.

Thus the pressure pulse method as used in this study provides only qualitative estimates of the electro-osmotic transference number.

It may, however, be possible to obtain accurate t_3^I values by this method, if very small pressure pulses are applied and the potentials created are amplified.

It can, therefore, be concluded from the evidence of this work that the pressure pulse method provides no advantages over the direct method nor over the indirect method of section (7.3.1.).

7.4 Pressure Potentials and Streaming Potentials Measured Across Cellulose Acetate Membranes.

The method of obtaining t_3^I values from the total pressure potentials (section (7.3.1.)) would be especially useful for obtaining information on membranes of the cellulose acetate type.

Since these membranes have a porous backing layer very much thicker than the active layer, in a direct experiment to determine an electro-osmotic transference number, this porous supporting layer will cause surface concentration polarization. However, in the reverse osmosis cell the flow of desalinated solution through the porous backing layer will prevent concentration polarization. Thus, the concentration gradient across the membrane can be identified and equation (2.52) can be applied to the cellulose acetate membrane.

Although there is an enormous amount of research being carried out on the reverse osmosis characteristics of the cellulose acetate membrane, to date, the reasons for salt rejection by hyperfiltration membranes of this type are not fully understood. A number of theories explaining the rejection abilities of these membranes have been expounded.

1) A sieve mechanism which is an obvious (simple) choice of explanation has been proposed by some workers[12].

However, the removal of salt from water is unlikely to be caused by a simply steric mechanism since there is little substantial difference in the size of water molecules and of inorganic ions.

2) Several workers [13] [14] using a variation of the sieve mechanism have related desalination to a decrease in the salt concentration in the surface layer of solution adjacent to the/

the membrane. This they propose is caused by a difference in surface tension of the salt solution and water. Neither of these mechanism has been particularly successful in explaining the measured properties of the cellulose acetate membrane.

(3) Until recently the most widely held theory of salt rejection in these membranes was evolved by Reid (15) (16) (17) and co-workers. They postulated that permeation occurs in the non crystalline portions of the membrane and is much faster for molecules which can form hydrogen bonds with the matrix. Flow is pictured as migration of water molecules from one hydrogen bond site to the next and the salt is rejected since it is incapable of forming hydrogen bonds and thus passing through the membrane. The carbonyl groups of the acetate matrix can be thought of as ordering the water into a Quasi-Ice Lattice, in the membrane.

Very recently work by Speigler and Kedem (18) (19) has suggested that in cellulose acetate membranes there exists a small amount of fixed charge and that Donnan exclusion may be at least a contributory mechanism to rejection in these membranes.

In this study a preliminary investigation on the cellulose acetate membrane was carried out. On the basis of the successful results obtained for the ion exchange membranes the pressure potential was measured across two cellulose acetate membranes at various applied pressures.

From the potential results an attempt was made to establish a value of t_1^I and t_3^I by equating the measured pressure potentials with equation (2.52).

The/

The (true) streaming potential was also determined and compared with Speigler's value.

The results for the two cellulose acetate membranes CA(80) and CA(85) are shown in Table (7.6). At each pressure the pressure potential for CA(85) is larger than that for CA(80). At both 200 and 400 lbs.in^{-2} the pressure potentials for CA(80) are smaller than those obtained for either of the C_{60} or XR membranes.

The rejection and thus the concentration gradient is much larger in both the cellulose acetate membranes. Since the rejection is relatively unaffected by the pressure applied, the diffusion potential for both membranes in the limiting case of t_1=1, would be greater than 100 mV at each applied pressure. Therefore, from experience obtained with the C_{60} membrane, a preliminary conclusion is that the relatively small pressure potentials are caused by a combination of t_1^I being considerably less than unity and the electro-osmotic transport number being large and negative.

Both the pressure potential and water flux of CA(80) and CA(85) vary proportionally with the applied pressure, Fig. (7.6) (7.7)

Equation (2.52) can be solved for t_1^I and t_3^I at each applied pressure for both membranes.

For CA (80) values of 0.06 and 33.2 were obtained for t_1^I and t_3^I respectively and for CA(85) the respective values were 0.11 and 22.5.

The effect of heating the cellulose acetate membranes to 85°C (rather than 80°C) was to make it less permeable to solvent and by analogy with the C_{60} membranes this 'tighter' membrane would be expected to have the smaller t_3. Thus the t_3 values estimated are in the order expected.

The/

The t_1 values obtained are very difficult to interpret. If the true t_1 values in the cellulose acetate membranes are 0.06 and 0 .11 then the respective t_2 values must be 0.94 and 0.89. This implies that the co-ion is the more mobile species in these membranes. If this is true then the streaming potential would be expected to be negative as would the electro-osmotic transference numbers.

The streaming potentials obtained are very similar to the values determined for the ion exchange membranes investigated, although they are lower than the 0.91 to 1.17 mV atm^{-1} reported by Speigler and Minning (obtained in 0.5 and 0.01M NaCl solutions).

There are no sources of comparison for the electro-osmosis transference numbers obtained for the cellulose acetate membranes. However, by analogy with the C_{60} membrane, the determined values are of the approximate magnitude expected.

A complete explanation cannot be forthcoming from the few measurements made, but the results indicate that further work of this kind on this membrane might be fruitful.

TABLE (7.1)

MEMBRANE PRESSURE POTENTIALS OF A.M.F. C_{60} MEMBRANES IN 0.10M NACL AT 400 lbs.in^{-2}

			Contributions to $E_{Calc.}$							
			Electrode	Diffusion Potential		True Streaming Potential				Estimated Streaming Potential
Membrane	E,Obs. mV	E.Calc mV	I mV	II mV	III mV	IV mV	Product Conc. Molar	Estimated t_3^I	Measured t_3^D	mV
PS_1	57.64	54.25	-0.443	-0.595	52.52	5.77	0.033	10.93	10.32	6.15
PS_3	54.47	54.70	-0.443	-0.603	49.64	6.11	0.035	10.44	10.92	6.07
PS_5	46.10	46.70	-0.443	-0.790	38.89	9.04	0.044	15.41	16.61	8.44
PS_6	46.92	46.05	-0.443	-0.819	37.81	9.50	0.045	19.13	17.51	10.34
PS_8	46.75	45.82	-0.443	-0.777	38.00	9.04	0.045	18.36	16.61	9.92
PS_9	45.64	45.16	-0.443	-0.806	36.90	9.51	0.046	18.39	17.54	9.98
PS_{10}	41.98	41.66	-0.443	-0.850	31.88	11.07	0.052	21.12	20.57	11.39
PS_{11}	42.00	44.09	-0.443	-1.23	29.12	16.64	0.054	27.22	31.39	14.11

$$E_{Calc.} = \underbrace{\frac{P}{F}(\hat{V}_{Ag}-\hat{V}_{AgCl})}_{\text{I}} + \underbrace{t_3\frac{RT}{F}\ln\frac{a_3''}{a_3'}}_{\text{II}} + \underbrace{2t_1\frac{RT}{F}\ln\frac{M_s''\gamma_\pm''}{M_s'\gamma_\pm'}}_{\text{III}} + \underbrace{\frac{P}{F}(t_1\hat{V}_{12}+t_3\hat{V}_3)}_{\text{IV}}$$

I: Electrode; II, III: Diffusion Potential; IV: True Streaming Potential

TABLE (7.2)

MEMBRANE PRESSURE POTENTIALS OF A.M.F. C_{60} MEMBRANES IN 0.10M NACL AT 200 lb.in^{-2}

			Contributions to $E_{Calc.}$						
Membrane	E.Obs. mV	E.Calc. mV	Term I mV	Term II mV	Term III mV	Term IV Streaming Potential mV	Product Concentration Molar	Estimated t_3^I	Estimated Streaming Potential
PS_5	26.70	27.08	-0.222	-0.549	23.33	4.52	0.061	15.10	4.14
PS_6	28.29	27.23	-0.222	-0.579	23.33	4.75	0.061	21.50	5.80
PS_9	24.94	24.34	-0.222	-0.520	20.32	4.76	0.065	19.80	5.36
PS_{10}	22.66	23.62	-0.222	-0.575	18.88	5.54	0.067	15.82	4.58
PS_{11}	21.25	22.23	-0.222	-0.769	14.90	8.30	0.072	27.42	7.32

$$E_{Calc} = \underbrace{\frac{P}{F}\left(\hat{V}_{Ag} - \hat{V}_{AgCl}\right)}_{\text{I}} + \underbrace{t_3 \frac{RT}{F} \ln \frac{a_3''}{a_{3'}}}_{\text{II}} + \underbrace{2t_1 \frac{RT}{F} \ln \frac{M_s'' \gamma_{\pm}''}{M_{s'} \gamma_{\pm'}}}_{\text{III}} + \underbrace{\frac{P}{F}\left(t_1\hat{V}_{12} + t_3\hat{V}_3\right)}_{\text{IV}}$$

I: Electrode; II, III: Diffusion Potential; IV: True Streaming Potential

TABLE (7.3)

MEMBRANE PRESSURE POTENTIALS OF XR-170 MEMBRANES IN 0.1M NACL

Membrane	E.Obs.	E. Calc.	Contributions to $E_{Calc.}$				Measured		Estimated	Estimated Streaming Potential
			Electrode I	Diffusion Potential II	III	Streaming Potential IV	Product Conc.	t^p_3	t^I_3	
400 lbs.in^{-2}	mV	mV	mV	mV	mV	mV	Molar			mV
XR-A	47.64	46.91	-0.443	-0.393	43.20	4.45	0.040	7.72	8.90	5.08
XR-B	48 .31	46.64	-0.443	-0.476	42.19	5.38	0.041	9.48	12.60	7.00
XR-C	45.45	42.38	-0.443	-0.542	36.81	6.56	0.046	11.84	17.90	9.74
200 lbs.in^{-2}										
XR-A	34.09	34.38	-0.222	-0.338	32.71	2.23	0.050	7.72	6.57	1.94
XR-B	36.04	34.76	-0.222	-0.417	32.71	2.69	0.050	9.48	14.50	3.98
XR-C	28.41	27.54	-0.222	-0.410	24.89	3.28	0.059	11.84	15.20	4.16

TABLE (7.4)

MEMBRANE PRESSURE POTENTIALS OF A.M.F. C_{60} MEMBRANES IN 0.05 $CACL_2$ AT 400 lbs.in^{-2}

Membrane	E.Obs. mV	E.Calc. mV	Calculated Contributions to $E_{Calc.}$: Terms (I + II) mV	Term III mV	Streaming Potential Term IV mV	Product Conc. Molar	Measured t_3	Estimated t_3	Estimated Streaming Potential mV
PS_1	16.60	17.86	-0.64	13.25	5.29	0.032	9.05	6.60	3.99
PS_5	12.33	12.90	-0.58	7.07	6.41	0.040	11.93	10.91	5.84

PS_1 is a Normal C_{60} Membrane

PS_5 is an Expanded C_{60} Membrane

TABLE (7.5)

Membrane	$\Delta E/\Delta P$ mv/100 lbs.in^{-2}	t_3^I (Estimated)	t_3^D (Observed)
PS_1	1.2	8.3	10.32
PS_2	2.00	14.5	11.00
PS_8	4.30	32.3	16.61
PS_{10}	2.70	20.0	20.57

TABLE (7.6)

MEMBRANE PRESSURE POTENTIALS OF CELLULOSE ACETATE MEMBRANES.

Membrane	Pressure lbs.in^{-2}	E. Obs. mV	10^3 x Water Flux ml cm^{-2} min^{-1}	Product Concentration Molar	Estimated t_3	Estimated t_1	Estimated Streaming Potential mV/at.
C-80	100	14.80	3.50	0.012	33.23	0.057	4.29 /100 PSI
	200	19.10	9.67	0.012			0.63
	300	23.15	16.30	0.010			
	400	27.50	22.57	0.010			
C-85	100	25.60	2.36	0.012	22.50	0.113	2.91 /100 PSI
	200	32.1	6.44	0.008			0.43
	300	38.2	10.58	0.006			

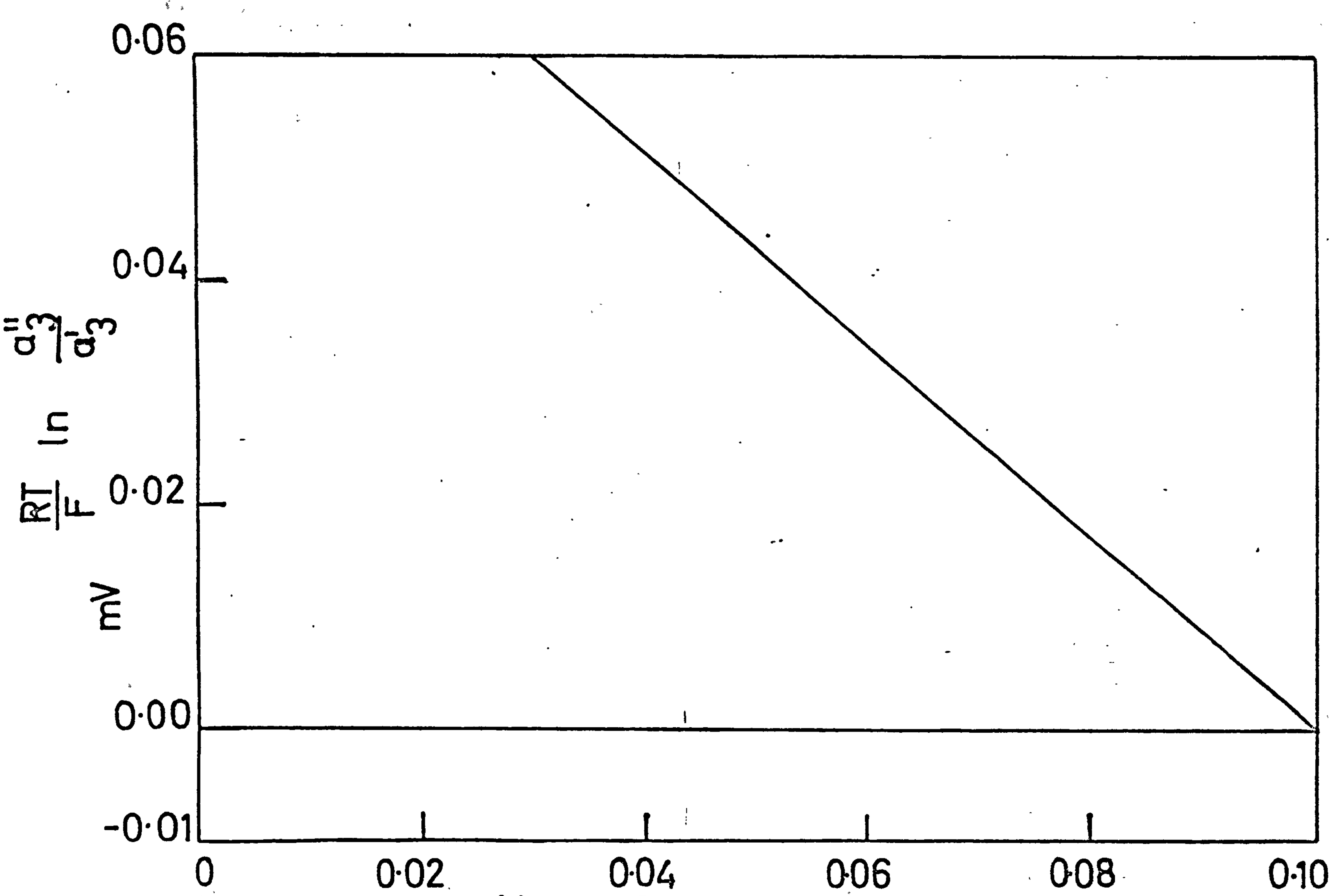

Fig. 7.1

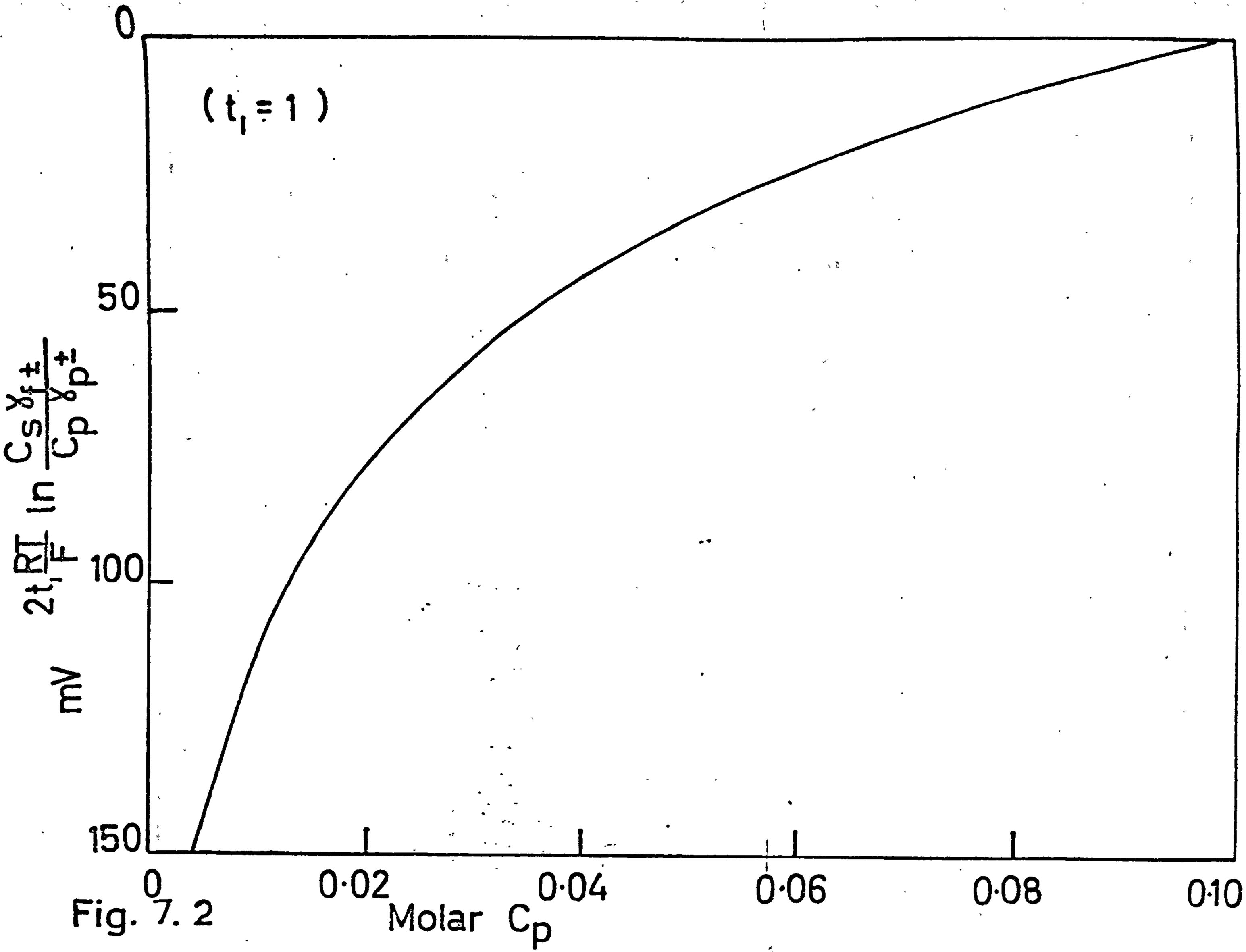
0
50
100
150
$2t_1\frac{RT}{F}\ln\frac{C_s\gamma_{f\pm}}{C_p\gamma_{p\pm}}$
mV
$(t_1 = 1)$
0
0·02
0·04
0·06
0·08
0·10
Molar C_p

Fig. 7. 2

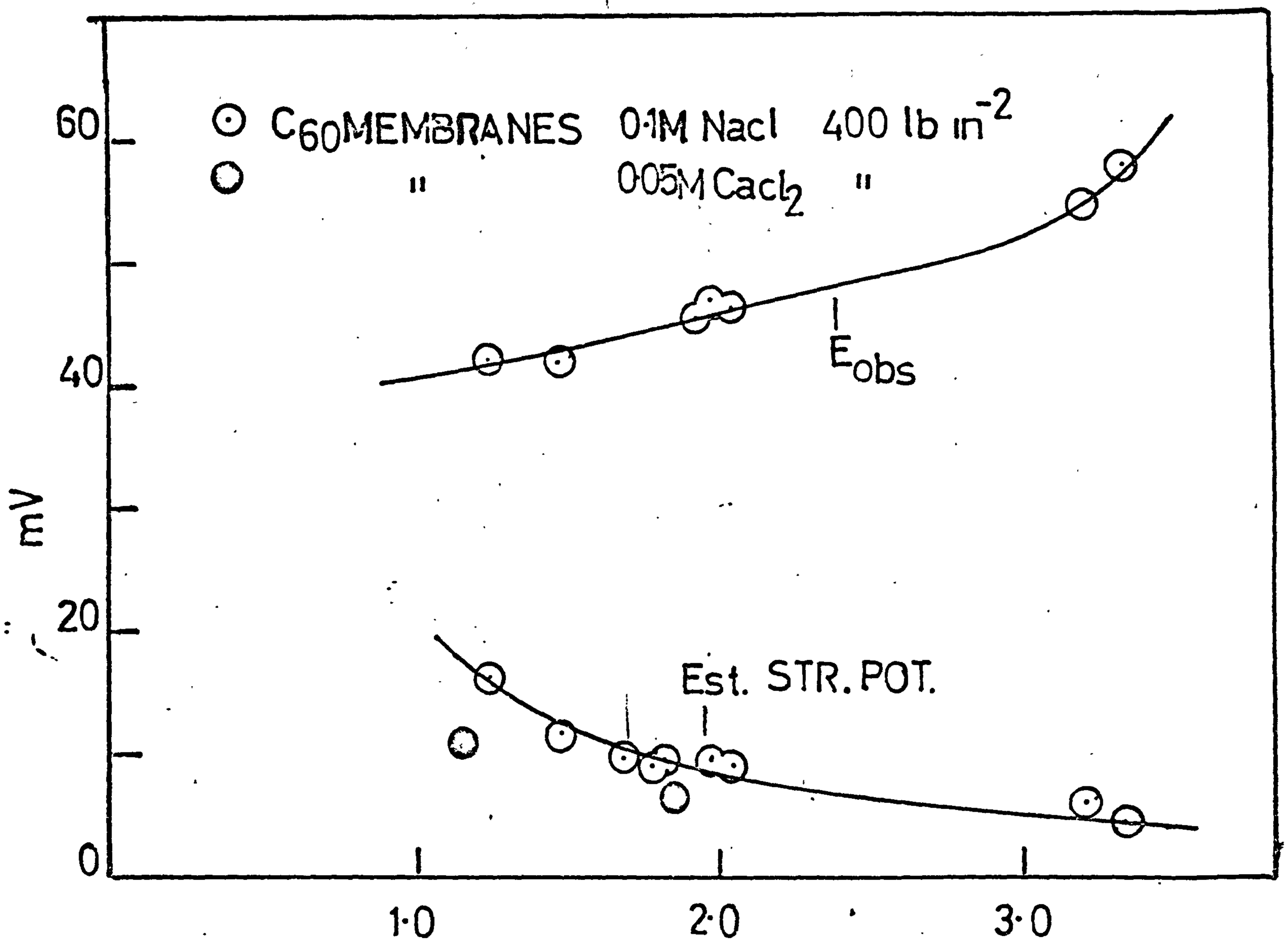
60
40
20
0
mV
⊙ C_{60} MEMBRANES 0·1M Nacl 400 lb in^{-2}
○ " 0·05M $Cacl_2$ "
E_{obs}
Est. STR. POT.
1·0
2·0
3·0
INTERNAL MOLALITY

Fig 7.3

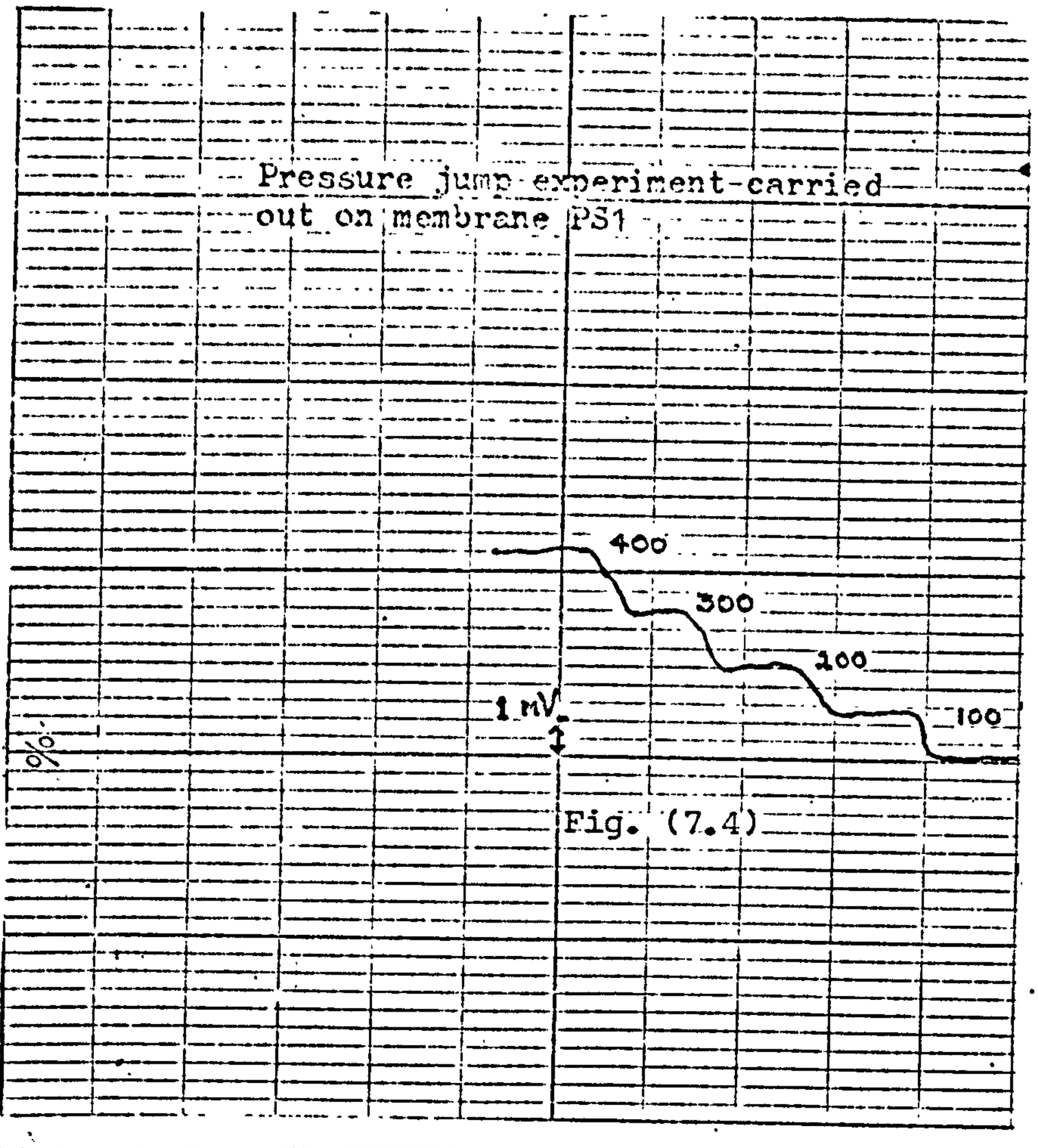
Pressure jump experiment-carried out on membrane PS1
400
300
200
100
1 mV
%

Fig. (7.4)

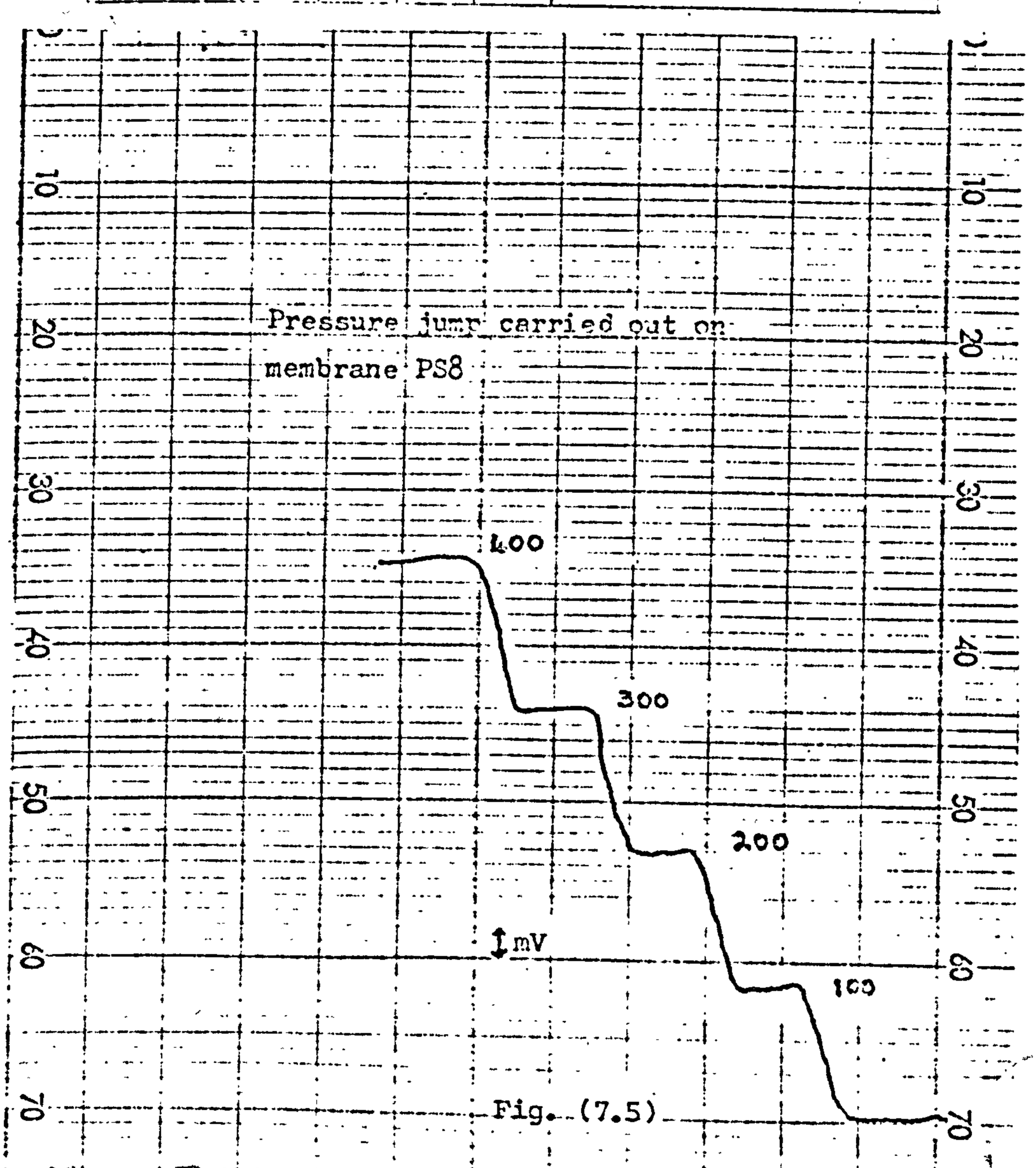
Pressure jump carried out on membrane PS8
400
300
200
100
1 mV

Fig. (7.5)

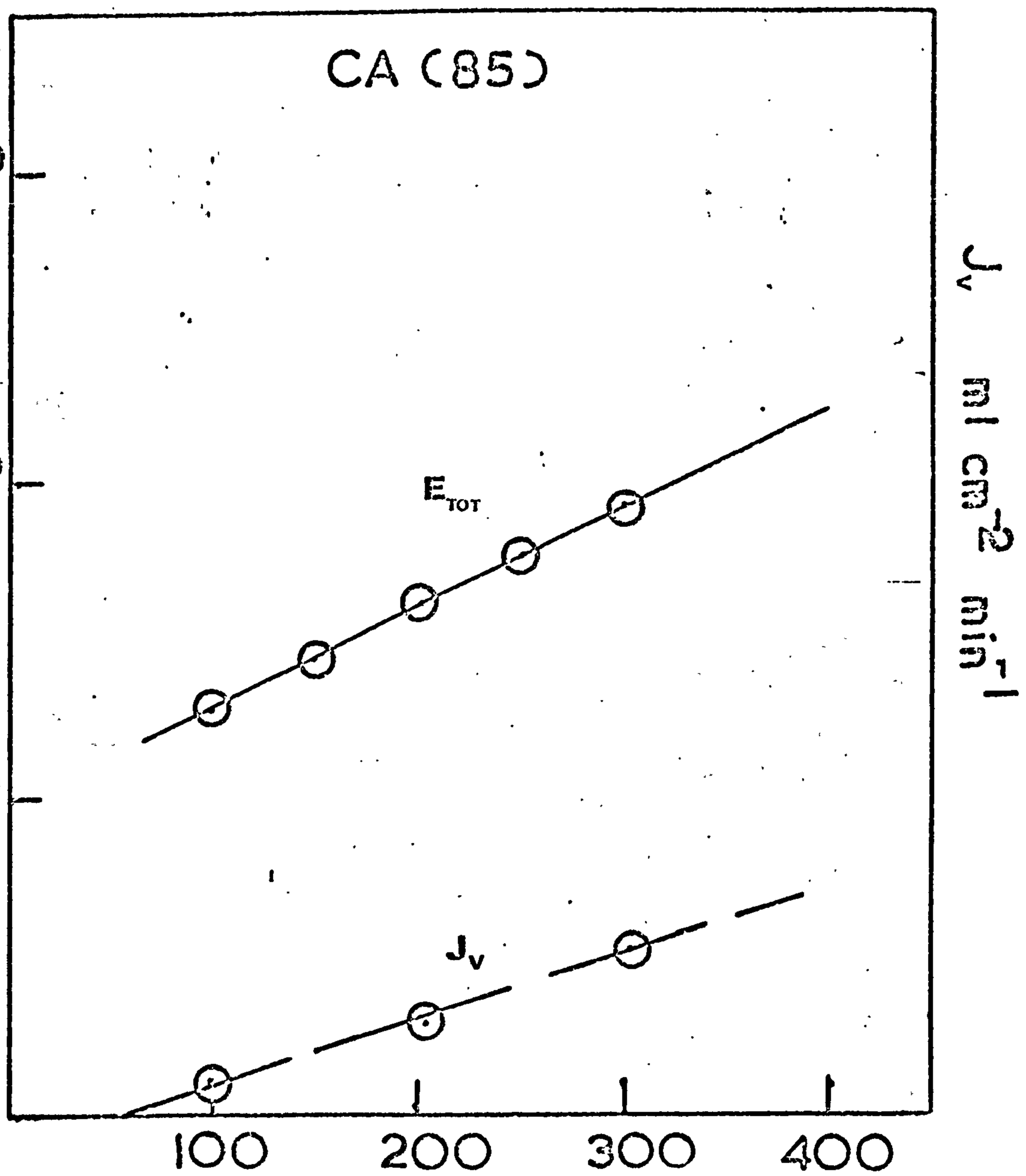
CA (85)
60
40
20
E mV
E_{TOT}
J_V
100
200
300
400
Pressure lb in^{-2}
J$_V$ mA cm^{-2}

Fig. 7.6

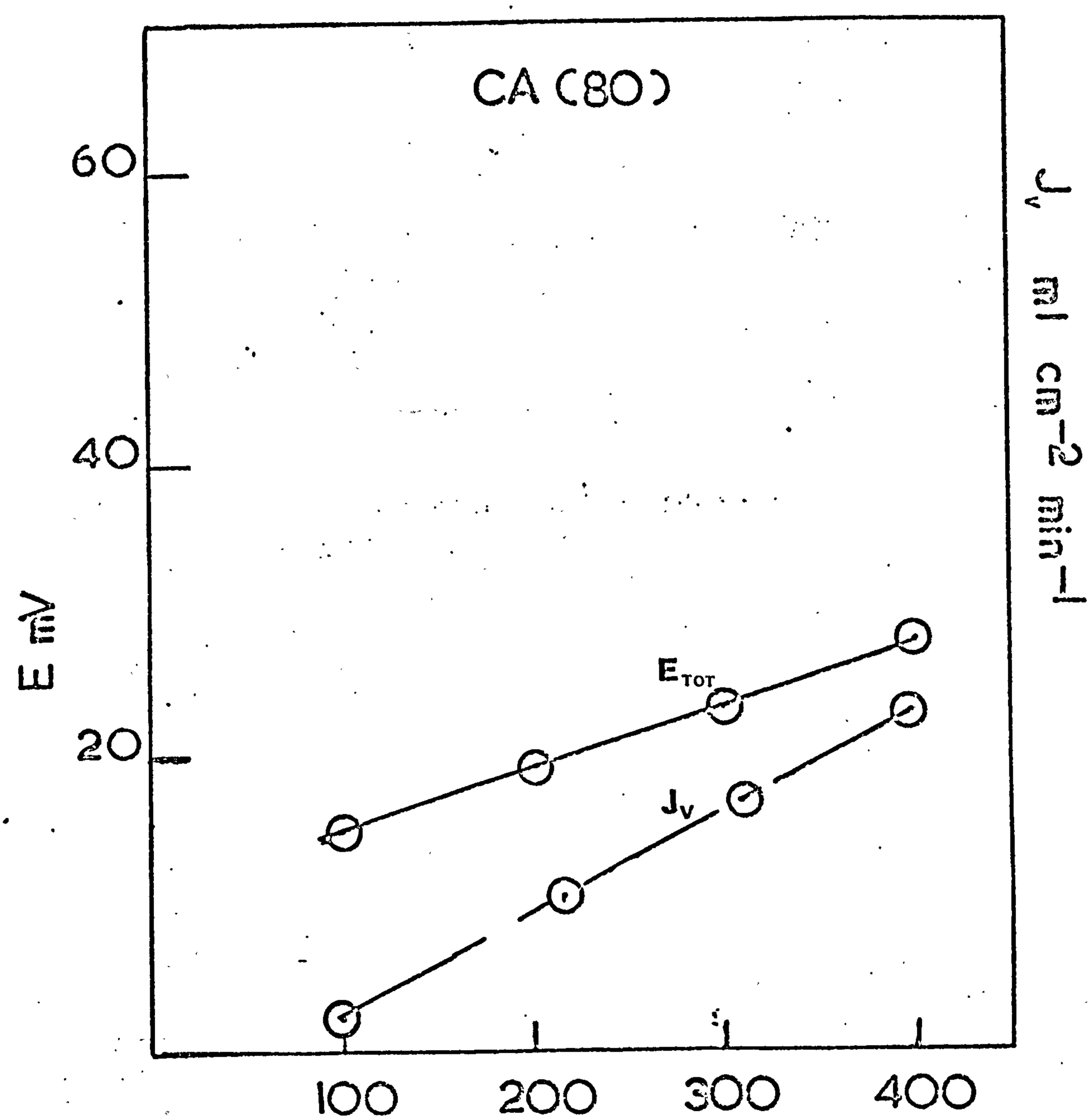
CA (80)
60
40
20
E mV
J_v ml cm^{-2} min^{-1}
E_{TOT}
J_V
100
200
300
400
Pressure lb in^{-2}

Fig. 7.7

CHAPTER 7

REFERENCES.

1) G. Schmid and H. Schwarz. Z. Electrochem. angew. Physik, Chem. 54, 424 (1951).

2) Ibid. , 56, 35 (1952)

3) R.J. Stewart and W.F. Graydon. J. Physic. Chem. 61, 164 (1957)

4) T.S. Brun and D. Vaula. Berichte der Bunsengesell Schaft 71, NF.8 (1967) (Eng.)

5) K.S. Speigler. Chem. Eng. Prog. Symp. V.55 N.24 (1959).

6) Handbook of Chemistry and Physics. 53rd edition. CRC Press.

7) Wen-Yang Wen in "Water and Aqueous Solutions" ed. R.A. Horne Wiley Interscience, New York, (1972)

8) H.S. Harned and B.B. Owen "The Physical Chemistry of Electrolyte Solutions". Reinhold, New York. 3rd edition (1958)

9) J. Janz and R. Gordon. J. Am. Chem. Soc. 65, (1943,) 228.

10) J.L. Shereshefsky and C.P. Carter, J.A.C.S.72, (1950.)

11) R.G. Cameron, PhD. Thesis, University of Glasgow, (1974.)

12) L.C. Craig, Science 144, 1093 (1964)

13) S. Sourirajan, Ind. Eng. Chem. Fundamentals 2, 51 (1963)

14) S. Sourirajan. J. Applied Chem. (London) 14, 500 (1964)

15) E.J. Breton. O.S.W. Res. Dev. Progress Rept. 16 (1957).

16) C.E. Reid and J.R. Kuppes. J. App. Polymer Science 2, 264 (1959).

17) C.E. Reid and E.J. Breton. J. App. Polymer Science 1, 133 (1959)

18) K.S. Spiegler and C.P. Minnim. N.A.T.O. Advanced study Institute on "Charged Gels and Membranes" Forges-les-Eaux France (1973)

19) O. Kedem and G. Tanny, ibid.

20) C.R. Gardner and R. Paterson. J. Chem. Soc. (A) 1971. 2254.

APPENDIX (1)

Effect of pressure on chemical potential of Salt.

The chemical potential of salt can be written for a 1:1 salt

$$\mu_s = \mu_s^{\circ} + RT \ln a_s + P \hat{V}_{12}$$

where P is the pressure in Nm^2

μ_s is the chemical potential of salt in the standard state i.e. at 1 atmosphere.

$$a_s = a_1 a_2$$

$$= M + \gamma + . M - \gamma - = M_s^2 (\gamma \pm)^2$$

$$\therefore \ln a_s - 2 \log M_s \gamma \pm$$

Then $\mu_s = \mu_s^{\circ} + 2 \times 2.303 RT \text{ Log. } M_s \gamma \pm + P \hat{V}_{12}$

$\gamma \pm$ for 0.10M NaCl is 0.778

$\hat{V}_{12}$ for 0.10M NaCl is 17.61×10^{-6} m^3 mol.

Therefore at 1.0 atmosphere the chemical potential of salt is

$$\mu_s = \mu_s^{\circ} - 1.3 \times 10^4 + 1.75 \text{ J. mole}^{-1}$$

Therefore an applied pressure force will make a contribution of some 0.013% per atmosphere to the salt chemical potential.

Appendix (2)

Capacity Determination

Suppose that the equilibrating solution has a volume V cm^3, a concentration c $m.mol.cm^{-3}$ and a specific acitivity x_1 cpm/cm^3. Then the total activity is Vx_1 cpm. and the number of m.moles of the ion under study is cV m.moles.

Suppose the volume of the membrane is $\bar{V}$ cm^3 and the concentration of the counter-ion in the membrane is $\bar{\bar{c}}\bar{V}$ m. moles. Therefore, the total number of m. moles of counter-ion is $cV + \bar{\bar{c}}\bar{V}$

The fraction of the counter-ion in the solution is $\dfrac{cV}{(cV + \bar{\bar{c}}\bar{V})}$

Therefore, the fraction of total activity in the solution after equilibration is $\dfrac{cV}{(cV + \bar{\bar{c}}\bar{V})}$

The total activity in the solution is then

$$\frac{cV}{cV + \bar{\bar{c}}\bar{V}} Vx_1$$

and the specific activity in the solution is

$$\frac{cV}{cV + \bar{\bar{c}}\bar{V}} \cdot Vx_1 \cdot \frac{1}{V} \quad \text{i.e.} \quad \frac{cV}{cV + \bar{\bar{c}}\bar{V}} \cdot x_1$$

but the specific activity of the solution is measured as x_2

therefore,

$$x_2 = \frac{cV}{cV + \bar{\bar{c}}\bar{V}} \cdot x_1$$

giving

$$\bar{c} = \frac{cV}{\bar{V}} \left(\frac{x_1}{x_2} - 1 \right)$$

Thus the capacity of the membrane is obtained.

APPENDIX (3)

SUMMARY OF THE PROPERTIES OF POLYPENCO 'DELRIN'

Property	Value	Units
Mechanical		
Tensile strength	10,000	$lbs.in^{-2}$
Flexural Strength	14,000	$lbs.in^{-2}$
Thermal		
Melting Point	175	°C
Flammability	Slow burning	
Coefficient of Thermal conductivity	0.20	kcal/m.hr.°C
Electrical		
Dielectric Strength Short Term 0.5 mm (0.02 in) thick	16	kV/mm.
Volume Resistivity	10	ohm/cm
Chemical		
Resistant to	Solvents, weak acids and alkalis, lubricating oils and greases	
Not resistant to	Strong acids and alkalis, oxidising agents	
Miscellaneous		
Specific Gravity	1.4-1.42	

APPENDIX (4)

Proof that specific conductivity is independent of frame of reference.

Consider a pair or arbitrary reference frames R and S the relation between the flows of the ith constituent is

$$(J_i)_R = (J_i)_S + \bar{C}_i \; U_{SR} \qquad (A.4)$$

where $\bar{C}_i$ is the concentration in mole cm^{-3} and U_{sr} is the velocity of frame S with respect to frame R in $cm.sec.^{-1}$

$$\text{Now } (I)_R = Z_i(J_i)_R$$
$$(I)_S = Z_i(J_i)_S$$

Substitution of equation (A.4) in the $(I)_R$ expression yields

$$(I)_R = Z_i(J_i)_S + U_{SR} \; Z_i\bar{C}_i = (I)_R$$

because the U_{sr} term vanishes owing to electro neutrality, because S and R were arbitrary, I is independent of reference frame. Since $I = K\frac{-d\psi}{dx}$

$$K_R = K_S$$

and specific conductivity is reference frame independent

APPENDIX (5)

To calculate original concentration from dilute solution (NaCl)

C_1 is the concentration obtained for dilute solution whose conductance was measured.

$$m_1 = 1.002165 + 0.019765\ C_1 + 0.0002006\ C_1^2$$

$$m_2 = m_1 \times C_1$$

$$Wg = \frac{m_2 \times 58.4428 \times (\text{wt. of dilute sample})}{1000 + (m_2 \times 58.4428)}$$

$$m_3 = \frac{Wg \times 1000}{58.4428 \times (\text{wt. of concentrated solution} - Wg)}$$

$$C_2 = 0.99783 - 0.019529\ M_3 + 0.00039066\ M_3^2$$

$$C_{\text{original}} = m_3 \times C_2$$

APPENDIX (6)

SOLVENT FIXED MOBILITY COEFFICIENTS

Starting from equations 2.3

$$T\sigma = \sum_{i=1}^{4} J_i X_i \qquad (2.3)$$

and 2.13

$$\sum_{i=1}^{4} c_i X_i = 0 \qquad (2.13)$$

the latter equation can either be used to eliminate X_4 from equation (2.3) and so give the phenomenological equations appropriate to the membrane fixed frame of reference.

$$(J_1 - \frac{c_1}{c_4} J_4) = l_{11}X_1 + l_{12}X_2 + l_{13}X_3 \qquad (A.6.1a)$$

$$(J_2 - \frac{c_2}{c_4} J_4) = l_{21}X_1 + l_{22}X_2 + l_{23}X_3 \qquad (A.6.1b)$$

$$(J_3 - \frac{c_3}{c_4} J_4) = l_{31}X_1 + l_{32}X_2 = l_{33}X_3 \qquad (A.6.1c)$$

or alternatively eliminate X_3 and give the solvent fixed phenomenological equations

$$(J_1 - \frac{c_1}{c_3} J_3) = L_{11}X_1 + L_{12}X_2 + L_{14}X_4 \qquad (A.6.2a)$$

$$(J_2 - \frac{c_2}{c_3} J_3) = L_{21}X_1 + L_{22}X_2 + L_{24}X_4 \qquad (A.6.2b)$$

$$(J_4 - \frac{c_4}{c_3} J_3) = L_{41}X_1 + L_{42}X_2 + L_{44}X_4 \qquad (A.6.2c)$$

If X_3 is elinated from equations(A.6.1a-c.)using equation 2.13, and the terms collected, they may be rewritten

$$(J_1 - \frac{c_1}{c_4} J_4) = (l_{11} - \frac{c_1}{c_3} l_{13}) X_1 + (l_{12} - \frac{c_2}{c_3} l_{13}) X_2 - \frac{c_4}{c_3} l_{13} X_4 \quad (A.6.3a)$$

$$(J_2 - \frac{c_2}{c_4} J_4) = (l_{21} - \frac{c_1}{c_3} l_{23}) X_1 + (l_{22} - \frac{c_2}{c_3} l_{23}) X_2 - \frac{c_4}{c_3} l_{23} X_4 \quad (A.6.3b)$$

$$(J_3 - \frac{c_3}{c_4} J_4) = (l_{31} - \frac{c_1}{c_3} l_{33}) X_1 + (l_{32} - \frac{c_2}{c_3} l_{33}) X_2 - l_{33} \frac{c_4}{c_3} X_4 \quad (A.6.3c)$$

These equations may be made formally identical to equations (A.6.2a-c) by subtracting $\frac{c_1}{c_3}$ x equation A.6.3c. from equation A.6.3a, subtracting $\frac{c_2}{c_3}$ x equation A.6.3c from equation A.6.3b and finally multiplying equation A.6.3c all through by $-\frac{c_4}{c_3}$.

By equating coefficients in these resultant equations with those of equations A.3.2a-c the following expressions for L coefficients in terms of l coefficients are obtained.

$$L_{11} = l_{11} - 2. \frac{c_1}{c_3} l_{13} + \frac{c_1^2}{c_3^2} l_{33} \quad (A.6.4)$$

$$L_{12} = l_{12} - \frac{c_2}{c_3} l_{13} - \frac{c_1}{c_3} l_{23} + \frac{c_1 c_2}{c_3^2} l_{33} \quad (A.6.5.)$$

$$L_{22} = l_{22} - 2 \frac{c_2}{c_3} l_{23} + \frac{c_2^2}{c_3^2} l_{33} \quad (A.6.6)$$

$$L_{14} = \frac{c_1 c_4}{c_3^2} l_{33} - \frac{c_4}{c_3} l_{13} \quad (A.6.7)$$

$$L_{24} = \frac{c_2 c_4}{c_3^2} l_{33} - \frac{c_4}{c_3} l_{23} \quad (A.6.8.)$$

$$L_{44} = \frac{c_4^2}{c_3^2} l_{33} \quad (A.6.9)$$

Similarly

$$l_{11} = L_{11} - 2.\frac{c_1}{c_4} L_{14} + \frac{c_1^2}{c_4^2} L_{44} \qquad \text{(A.6.10)}$$

$$l_{12} = L_{12} - \frac{c_2}{c_4} L_{14} - \frac{c_1}{c_4} L_{24} + \frac{c_1 c_2}{c_4^2} L_{44} \qquad \text{(A.6.11)}$$

$$l_{22} = L_{22} - 2\ \frac{c_2}{c_4} L_{24} + \frac{c_2^2}{c_4} L_{14} \qquad \text{(A.6.13)}$$

$$l_{23} = \frac{c_2 c_3}{c_4^2} L_{44} - \frac{c_3}{c_4} L24 \qquad \text{(A.6.14)}$$

$$l_{33} = \frac{c_3^2}{c_4^2} L_{44} \qquad \text{(A.6.15)}$$